Structure and biosynthesis of fungal α-glucans

Christian Grün

Op de voorkant:
Schets van de ontwikkelingsstadia van de splijtgist *Schizosaccharomyces pombe*
Uit: Lindner, P. (1893) *Schizosaccharomyces pombe* n. sp., ein neuer Gährungserreger. *Wochenzeitschrift für Brauerei* **10,** 1298-1300.
Met dank aan Dr. F. Hochstenbach

CIP-GEGEVENS KONINKLIJKE BIBLIOTHEEK, DEN HAAG

Grün, Christian Hugo

Structure and biosynthesis of fungal α-glucans / Christian Hugo Grün. - Utrecht: Universiteit Utrecht, Faculteit Scheikunde.

Proefschrift Universiteit Utrecht. - Met lit. opg. - Met een samenvatting in het Nederlands.

ISBN 90-393-3300-9

Structure and biosynthesis of fungal α-glucans

Structuur en biosynthese van fungale α–glucanen

(Met een samenvatting in het Nederlands)

Proefschrift

ter verkrijging van de graad van doctor aan de Universiteit Utrecht
op gezag van de Rector Magnificus, Prof. Dr. W.H. Gispen,
ingevolge het besluit van het College voor Promoties
in het openbaar te verdedigen

op maandag 10 maart 2003 des middags te 16.15 uur

door

Christian Hugo Grün

geboren op 18 juni 1973, te Schweinfurt (Duitsland)

Promotores:	**Prof. Dr. J.F.G. Vliegenthart** en **Prof. Dr. J.P. Kamerling**
	Verbonden aan het Bijvoet Centrum van de Faculteit Scheikunde van de Universiteit Utrecht
Co-promotores:	**Dr. F. Hochstenbach**
	Verbonden aan het Academisch Medisch Centrum van de Universiteit van Amsterdam
	Dr. F.M. Klis
	Verbonden aan het Swammerdam Instituut voor Life Sciences van de Universiteit van Amsterdam

Het in dit proefschrift beschreven onderzoek werd mogelijk gemaakt met financiële steun van de Nederlandse Organisatie voor Wetenschappelijk Onderzoek (CW/ALW-NWO)

Wie viele Worte

Wie viele Worte in dem Buche stehn! Erinnern sollen sie! Als op Worte erinnern könnten!

Denn Worte sind schlechte Bergsteiger und schlechte Bergmänner. Sie holen nicht die Schätze von den Bergeshöhn und nicht die von den Bergestiefen.

Aber es gibt ein lebendiges Gedenken das über alles Erinnerungswerte sanft hinfuhr wie mit kosender Hand. Und wenn aus dieser Asche die Lohe aufsteigt, glühend und heiß, gewaltig und stark und Du hineinstarrst, wie vom magischen Zauber gebannt, dann —— Aber in dieses keusche Gedenken, da kann man sich nicht hineinschreiben mit ungeschickter Hand und grobem Handwerkszeug, das kann man nur in diese weißen, anspruchslosen Blätter.

Franz Kafka (1883-1924)

Contents

Abbreviations

1D, 2D	one-, two-dimensional
2AB	2-aminobenzamide
ags1$^+$	α-glucan synthase 1 (gene)
Ags1p	α-glucan synthase 1 protein
bgs1$^+$	β-glucan synthase 1 (gene)
chs1$^+$	chitin synthase 1 (gene)
CID	collision-induced dissociation
DMSO	dimethylsulfoxide
DP_n	number-average degree of polymerization
EDTA	ethylenediamine tetraacetate
EI	electron impact
ES	electrospray
f	furanose
Glc	glucose
GLC	gas-liquid chromatography
GTP	guanosine 5′-triphosphate
Hex	hexose
HPAEC	high-performance anion-exchange chromatography
HPSEC	high-performance size-exclusion chromatography
HSQC	hetronuclear single quantum coherence
Man	mannose
Mn	number-average molecular mass
MS	mass spectrometry
Mw	weight-average molecular mass
NMR	nuclear magnetic resonance
p	pyranose
OD_{595}	optical density at 595 nm
PAD	pulsed amperometric detection
PMAA	partially methylated alditol acetates
PMSF	phenylmethylsulfonyl fluoride
ppm	parts per million
RI	refractive index
SD	standard deviation
SDS	sodium dodecyl sulfate
SDS-PAGE	sodium dodecyl sulfate-polyacrylamide gel electrophoresis
SEC	size-exclusion chromatography
TLC	thin-layer chromatography
TOCSY	total correlation spectroscopy
UDP	uridine 5′-diphosphate
WEFT	water-eliminated Fourier transform
Xyl	xylose

Chapter 1

The fungal cell wall

Introduction

The variety of fungal species in nature is tremendous: 1.5 million species have been estimated to exist, of which approximately 70,000 have been described (Hawksworth, 1991). Briefly, a few general aspects of fungi will be discussed. Many fungi are important for life in that they live in symbiosis with plants or animals. Others live from plant materials, such as wood and leaf litter, or from dead animals and animal excrements. Therefore, they contribute significantly to the decomposition of organic material. A number of fungi are also of industrial importance, such as *Saccharomyces cerevisiae*, used for instance in brewing and bakery industries and for the production of heterologous proteins. Other fungi are used in food industry, such as the fruiting bodies of *Lentinus edodes* (shiitake), *Pleurotus ostreatus* (oyster mushroom), and the cultivated mushroom *Agaricus bisporus*. Unfortunately, a number of fungi causes devastating diseases in plants or animals. *Ophiostoma ulmi*, for example, causes the Dutch elm disease (Hintz, 1999), whereas *Cryphonectria parasitica* caused the chestnut blight, which brought the American chestnut population almost to extinction (Chasan, 1992). Fungi that can infect humans include *Candida albicans* (Mitchell, 1998), *Aspergillus fumigatus* (Latgé, 2001), and *Cryptococcus neoformans* (Thomas & Schwartz, 2001).

The cell wall is essential for fungal survival and its composition is unique to fungi, and therefore it forms an ideal target for the development of (novel) antifungal drugs. For this purpose, understanding of the cell-wall architecture as well as of the biochemical processes involved in cell-wall assembly are essential. Budding yeast *S. cerevisiae* and fission yeast *Schizosaccharomyces pombe* are unicellular fungi that have been used as model organisms to study eukaryotic processes, such as cell division and cell morphogenesis (Botstein *et al.*, 1997; Hayles & Nurse, 2001). Also fungus-specific aspects such as the assembly of the cell wall are preferably studied in these yeasts, because their genome sequences are known (Goffeau *et al.*, 1997; Wood *et al.*, 2002) and because of their genetic tractability.

Cell-wall architecture

The fungal cell is encapsulated by an extracellular matrix, the cell wall, which protects it from osmotic pressure and environmental stress, and determines cell shape. The cell wall has been described on one hand as a rigid layer of glycoproteins and polysaccharides, and on the other hand as a dynamic structure flexible enough to cope with cell growth. The cell walls of most fungi consist of five major components: (1→3)-β-glucan, (1→6)-β-glucan, (1→3)-α-glucan, chitin, and glycoproteins (**Fig. 1**). Of all fungi, the cell wall of *S. cerevisiae* has best been studied with regard to its structure and biosynthesis. It is composed of (1→3)-β-glucan, that forms an alkali-soluble fraction (20% of total cell wall) or a chitin-linked, alkali-insoluble fraction (35%). Furthermore, (1→6)-β-glucan (5%), chitin (2%), and mannoproteins (40%) are present (Klis *et al.*, 1997). Interestingly, this yeast lacks α-glucan. By using electron microscopy, it was shown that the cell-wall components are organized in a layered structure in which (1→3)-β-glucan forms densely interwoven microfibrils present as the innermost layer, followed by (1→6)-β-glucan and mannoproteins (Osumi, 1998; Cabib *et al.*, 1982). Most chitin, approximately 90%, is found in the region of the bud scars which remain after cell separation, whereas the remainder of the chitin is dispersed over the lateral walls. A covalent linkage between chitin and β-glucan was first suggested by Hartland *et al.* (1994), who based their conclusion on the insolubility of part of the β-glucan under alkaline conditions. Treatment with chitinase or disruption of the chitin synthase 3 gene led to solubilization of their preparation. Later, the covalent linkage between chitin, (1→3)-β-glucan, (1→6)-β-glucan and mannoproteins was demonstrated by the group of Cabib who digested cell walls with (1→3)-β-glucanase and chitinase and analyzed the products by chemical analyses methods, mass spectrometry, and NMR spectroscopy (Kollár *et al.*, 1995; Kollár *et al.*, 1997; Ovalle & Lipke, 1998). They concluded that the mannoproteins are attached to (1→6)-β-glucan via a glycosylphosphatidylinositol anchor. The (1→6)-β-glucan contains (1→3)-linked branches to which the reducing end of chitin may be connected via a (1→2) or (1→4) linkage. Finally, the reducing end of the (1→6)-β-glucan is linked to a non-reducing end of (1→3)-β-glucan through an as yet unknown linkage.

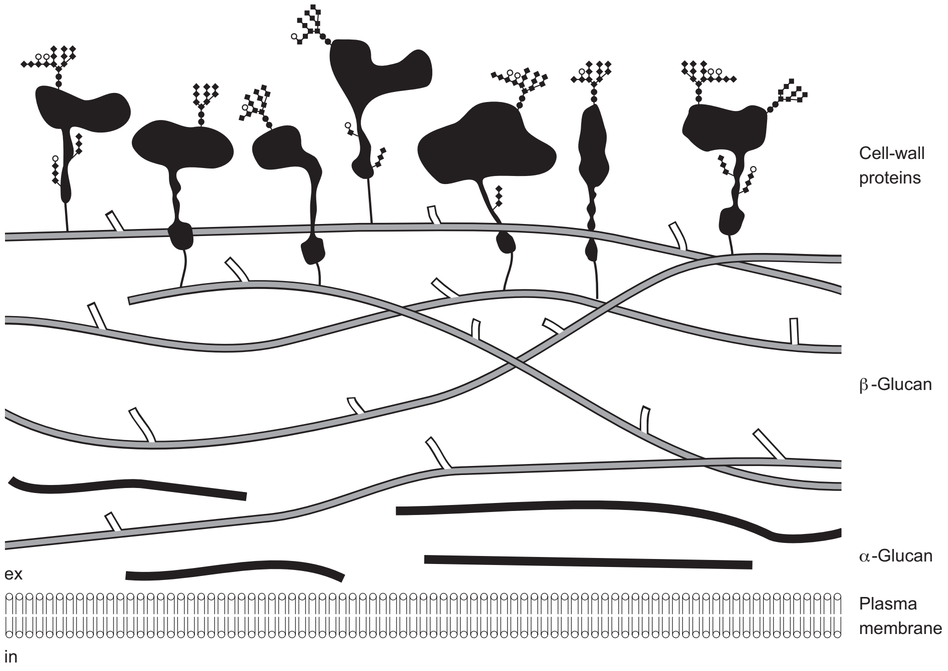

Fig. 1. Schematic representation of the fungal cell wall. The cell wall is composed of an outer layer of glycoproteins and inner layers of polysaccharides. Note that the composition of the cell wall (e.g., presence of α-glucan and chitin) varies between different fungal species.

A similar, layered cell-wall architecture was found in other fungi such as *C. albicans* (Chaffin *et al.*, 1998), *A. fumigatus* (Fontaine *et al.*, 2000), and fission yeast *S. pombe* (Kopecká *et al.*, 1995). Importantly, the cell walls of the latter two fungi differ from that of *S. cerevisiae* in that they contain galactomannan instead of mannan, and (1→3)-α-glucan (Bernard & Latgé, 2001; Manners & Meyer, 1977). Although it was shown that (1→3)-α-glucan forms a network of microfibrils in fission-yeast cell walls (Kopecká *et al.*, 1995), it is as yet unknown whether α-glucan is part of a β-glucan-chitin network.

Cell-wall polysaccharides

(1→3)-β-Glucan

Because of its predominant presence, (1→3)-β-glucan has best been studied of all fungal cell-wall polysaccharides with regard to chemical structure, physico-chemical properties, and biosynthesis. (1→3)-β-Glucan is present in the cell walls of almost all fungi, except of the hyphal walls of Zygomycetes (Barreto-Bergter & Gorin, 1983; Wessels & Sietsma, 1982; Bartnicki-García, 1968). The presence of β-glucan in the cell wall of *S. cerevisiae* has been established as early as 1950 (Bell & Northcote, 1950), but it took another sixteen years before its chemical structure was determined, namely a (1→3)-β-glucan with occasional (1→6)-linked branches (Manners & Patterson, 1966). The degree of polymerization was estimated to be approximately 1500 (Manners & Masson, 1969; Fleet & Manners, 1976). The glucan is only slightly crystalline in the lateral wall, which is probably due to branching (Kreger & Kopecká, 1975). Indeed, treatment of hyphal walls with hot 2% hydrochloric acid (HCl), which may have caused hydrolysis of intrachain glycosidic linkages and glycosidic linkages of branching points, resulted in an increase in crystallinity (Jelsma & Kreger, 1975). X-ray crystallography of HCl-treated (1→3)-β-glucan revealed that it forms a six-fold, parallel triple helix that is stabilized via 2-OH•••O-2 hydrogen bonds (Jelsma & Kreger, 1975; Chandrasekaran, 1997). Gawronski *et al.* (1999) investigated the solution structure of β-glucan by small-angle X-ray scattering and found that a β-glucan composed of a (1→3)-linked main chain with occasional branching at C-6 is composed of triple helices that tend to aggregate as trimers in aqueous solution. A β-glucan that consisted of a (1→3)-linked backbone with branches of only single glucose residues (1→6)-linked to the main chain consisted of a single triple helix (Gawronski *et al.*, 1999), indicating that the type of branching influences aggregation of individual β-glucan polymers.

(1→3)-β-Glucan synthase is a plasma-membrane localized enzyme that catalyzes the intracellular synthesis of (1→3)-β-glucan and that is thought to facilitate extrusion of the newly synthesized (1→3)-β-glucan through the plasma membrane into the extracellular space via a putative membrane-spanning pore (**Fig. 2A**) (Inoue *et al.*, 1996). Purifying (1→3)-β-glucan synthases were achieved by a technique called 'product entrapment'. Product entrapment is based on the affinity of the enzyme to its reaction product and has been successfully applied in the purification of many processive enzymes from crude cell membranes, such as chitin synthase (Kang *et al.*, 1984), cellulose synthase (Wong *et al.*, 1990), and glycogen synthase (Zhang *et al.*, 1993). Several groups demonstrated that also (1→3)-β-glucan synthases can be purified via product entrapment (Awald *et al.*, 1993; Inoue *et al.*, 1995; Kelly *et al.*, 1996). Two genes, each encoding a putative (1→3)-β-glucan synthase were cloned, called *FKS1* (*GSC1*) and *FKS2* (*GSC2*), of which the first is expressed during vegetative growth and the latter during sporulation (Douglas *et al.*, 1994a; Mazur *et al.*, 1995). However, disruption of either *FKS1* or *FKS2* did not result in a lethal phenotype during vegetative growth, but the double mutant was inviable (Inoue *et al.*, (1995), indicating that these genes can take over each other's function. *In vitro* studies showed that the glucan synthases require UDP-Glc as a donor and that activity is stimulated by the addition of GTP (Shematek *et al.*, 1980). Cabib *et al.* found that a small GTPase that is associated with (1→3)-β-glucan synthase is essential for synthase activity (Mol *et al.*, 1994). This GTPase was later identified as Rho1p. A temperature-sensitive *rho1* mutant was constructed that resulted in a decrease in (1→3)-β-glucan synthase activity (Yamochi *et al.*, 1994). The activity could be restored by the addition of purified or recombinant wild-type Rho1p (Drgonová *et al.*, 1996). This and other studies indicate that Rho1p is a regulatory subunit of Fks1p (Qadota *et al.*, 1996; Mazur & Baginsky, 1996).

Genes homologous to *FKS1* and *FKS2* are well conserved among other fungi, such as the human pathogenic yeasts *A. fumigatus* (Kelly *et al.*, 1996), *C. albicans* (Mio *et al.*, 1997), *C. neoformans* (Thompson *et al.*, 1999), and *Paracoccidioides brasiliensis* (Pereira *et al.*, 2000), and fission yeast *S. pombe* (Ishiguro *et al.*, 1997). In *S. pombe*, like in *S. cerevisiae*, a GTPase, Rho1p, was identified that is involved in (1→3)-β-glucan synthase activation and that regulates cell morphogenesis (Arellano *et al.*, 1996). (1→3)-β-Glucan synthase activity can be stimulated by GTP in most fungi studied, indicating that the stimulatory role of Rho1p is conserved. The only exceptions described to date are the Oomycetes *Phytophthora sojae* and *Achlya ambisexualis* that both do not display activation of (1→3)-β-glucan synthase upon addition of GTP (Antelo *et al.*, 1998).

As described above, (1→3)-β-glucan is a predominantly (1→3)-linked β-glucan containing approximately 3% of (1→6)-linked branches. Since (1→3)-β-glucan synthase is a plasma-membrane protein, it is likely that the branching occurs extracellularly rather than intracellularly. Hartland *et al.* (1991) have isolated a transglycosylase from the cell walls of *C. albicans* that may be involved in the branching of linear (1→3)-β-glucan. In an *in vitro* study, the authors showed that this transglycosylase cleaves laminaribiose from the reducing end of a linear (1→3)-β-glucan. The remaining (1→3)-β-glucan is then transferred to a second (1→3)-β-glucan where it is linked via a (1→6)-linked branch point, according to:

$$E + G_n \rightarrow E{\bullet}G_{n-2} + G_2$$
$$E{\bullet}G_{n-2} + G_n \rightarrow E + G_{2n-2}$$

were E = enzyme; G = substrate; n = degree of substitution

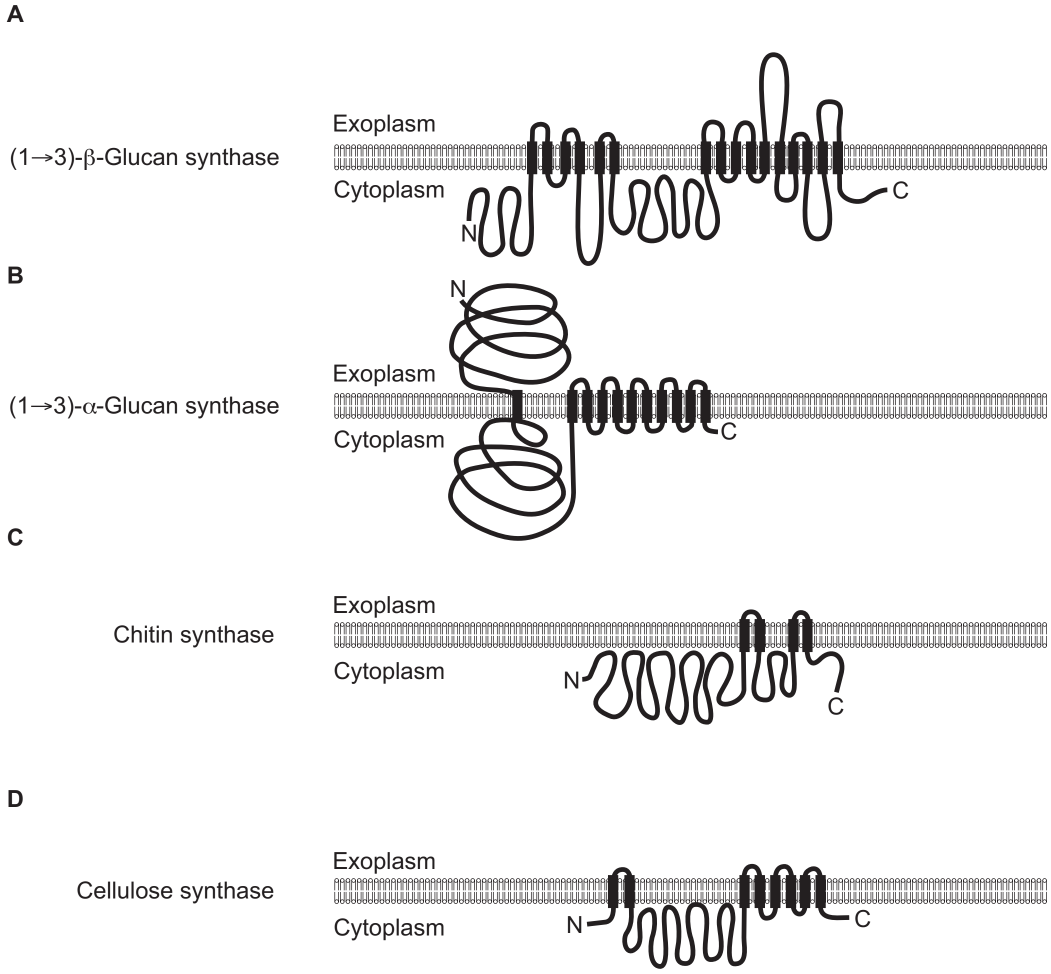

Fig. 2. Topology of a number of polysaccharide transmembrane synthases. (**A**) (1→3)-β-Glucan synthase Fks1p from *S. cerevisiae* (Kurtz & Rex, 2001); (**B)** (1→3)-α-glucan synthase Ags1p from *S. pombe* (Hochstenbach *et al.*, 1998); (**C**) chitin synthase Chs1p from *S. cerevisiae* (Bulawa *et al.*, 1986); (**D**) plant cellulose synthase I (Brown & Saxena, 2000). Enzyme topologies are based on hydropathy plots.

(1→6)-β-Glucan

A second type of β-glucan found in a large number of fungi is a highly-branched polysaccharide consisting of a (1→6)-linked backbone with (1→3)-linked side branches (Barreto-Bergter & Gorin, 1983). Depending on the fungal species, this polysaccharide is present in the cell wall from 5% ($^{w}/_{w}$) of total cell wall in *S. cerevisiae* to 20% in *C. albicans* (Klis *et al.*, 2001). In *S. cerevisiae*, it consists of on average 140 glucose residues and connects (1→3)-β-glucan and chitin with cell-wall proteins (Kollár *et al.*, 1997; Klis *et al.*, 1997; Kapteyn *et al.*, 1999). In an effort to identify genes that are involved in (1→6)-β-glucan synthesis, mutant *S. cerevisiae* strains were screened on decreased (1→6)-β-glucan levels. The screens involved the use of K1 killer toxin, which displays a lectin-like affinity for (1→6)-linked β-glucose that upon binding to the polysaccharide permeabilizes the plasma membrane and kills the yeast (Boone *et al.*, 1990). Mutant strains defective in (1→6)-β-glucan synthesis are K1 killer-toxin resistant, the so-called *kre* mutants, and by using these strains, genes associated with (1→6)-β-glucan biosynthesis can be identified (Shahinian & Bussey, 2000). Disruption of the *KRE5* gene, for example, led to an aberrant cell wall and very slow cell growth. Analysis of its cell wall showed that (1→6)-β-glucan was completely lacking in the *kre5*Δ null mutant. Based on *KRE5* sequence analysis and immunostaining, it was demonstrated that Kre5p is localized to the endoplasmic reticulum (Meaden *et al.*, 1990; Levinson *et al.*, 2002). The function of Kre5p remains unknown, but it has sequence similarity to UDP-glucose: glycoprotein glucosyltransferases, suggesting that it might be a glucosyltransferase involved in (1→6)-β-glucan synthesis (Parodi, 1999). Similarly, several other *KRE* genes have been identified in *S. cerevisiae*, but presently, gene(s) encoding a (1→6)-β-glucan synthase have as yet to be identified.

(1→3)-α-Glucan

Although absent in *S. cerevisiae* and *C. albicans*, (1→3)-α-glucan is found in a large number of fungi, mainly Ascomycetes and Basidiomycetes, where it is present at levels of 9 to 46% of the cell wall, which even reaches 88% in wall material of certain fruiting bodies (**Table I**). The chemical structure of α-glucan varies among the different fungi from polysaccharides consisting solely of (1→3)-linked α-glucose, to polysaccharides containing small percentages of (1→4)-linked residues, to nigeran-type polysaccharides in which alternating (1→3) and (1→4) linkages occur (**Table I**). Of the α-glucans consisting mainly of (1→3)-linked residues, degrees of polymerization vary between approximately 60 and 3500 (**Table I**). Crystallographic data show that (1→3)-α-glucan forms a two-fold single helix, which is stabilized by 2-OH•••O-4 hydrogen bonds (Jelsma & Kreger, 1979; Ogawa *et al.*, 1981). It has a sheet-like packing arrangement that is also observed for cellulose, suggesting that (1→3)-α-glucan is a structural polysaccharide (Chandrasekaran, 1997). However, crystals of good quality could only be obtained after chemical treatment of (1→3)-α-glucan with 2% hydrochloric acid at 60 °C (Jelsma & Kreger, 1979) or by per-*O*-acetylation prior to crystallization followed by deacetylation (Ogawa *et al.*, 1981).

Despite the large numbers of fungi that produce α-glucan, little is known about its function and its biosynthesis. In contrast to (1→3)-β-glucan, which is accepted to be essential for cell morphology and integrity, the function of α-glucan is controversial. In *Aspergillus nidulans*, for instance, complete inhibition of α-glucan synthase did not affect hyphal outgrowth, and it was suggested that in this fungus, α-glucan may function as a reserve carbohydrate (Zonneveld, 1973; Zonneveld, 1972). Similar results were obtained by inhibiting α-glucan synthase in regenerating protoplasts of *Schizophyllum commune* (Sietsma & Wessels, 1988). In contrast, Kopecká *et al.* (1995) showed that in fission yeast not only (1→3)-β-glucan, but also (1→3)-α-glucan may contribute to the rigidity of the cell. By using electron microscopy, the authors showed that α-glucan is present as a fibrillar layer, which is covered by layers of β-glucans. After removal of the β-glucans, the original cylindrical

Table I-A. Ascomycetous fungi whose cell walls contain (1→3)-α-glucan[1]

Species	Taxonomic class	Wall dry weight (%)	Type of linkage	DP[2]	References
Subphylum: Euascomycetes					
Acroscyphus sphaerophoroides	Lecanoromycetes		(1→3), (1→4) (2:3), (1→6) 6%		Takeda *et al.* (1972)
Alectoria sarmentosa	Lecanoromycetes		(1→3), (1→4) (11:9)		Takeda *et al.* (1972)
Alectoria sulcata	Lecanoromycetes		(1→3), (1→4) (11:9)		Takeda *et al.* (1972)
Aspergillus flavipes	Eurotiomycetes	16-32	(1→3)		Leal *et al.* (1992)
Aspergillus flavus	Eurotiomycetes		(1→3)		Seo *et al.* (1999)
Aspergillus fumigatus	Eurotiomycetes		(1→3)		Bernard & Latgé (2001)
Aspergillus nidulans	Eurotiomycetes	22	(1→3)		Borgia & Dodge (1992) Bull (1970) Polacheck & Rosenberger (1977)
Aspergillus niger var. unknown)	Eurotiomycetes	20-30	(1→3), some (1→4) (1→3), (1→4)	330-700	Bobbit *et al.* (1977) Hasegawa *et al.* (1969) Horisberger *et al.* (1972) Johnston (1965)
Aspergillus niger var. awamori	Eurotiomycetes	9	(1→3), some (1→4) (1→3), (1→4)		Bobbit *et al.* (1977)
Aspergillus ochraceus	Eurotiomycetes	16-32	(1→3)		Leal *et al.* (1992)
Blastomyces dermatiditis[3]	Eurotiomycetes	34.5	(1→3) (yeast form)		Hogan & Klein (1994) Kanetsuna & Carbonell (1971) Klein (1997)
Cetraria islandica	Lecanoromycetes		(1→3), (1→4) (55:45) (1→3), (1→4) (2:1)	35-50 12000	Peat *et al.* (1961) Fleming & Manners (1966) Olafsdottir *et al.* (1999)
Cetraria richardsonii	Lecanoromycetes		(1→3), (1→4) (11:9)		Nishikawa *et al.* (1969)
Cladosporium herbarum	Dothideomycetes	33	(1→3), (1→4) (1:2)		Miyazaki & Naoi (1974)
Elsinoe leucospila	Dothideomycetes		(1→4), (1→3) (5:2)		Misaki *et al.* (1978) Tsumuraya *et al.* (1978)
Eupenicillium crustaceum	Eurotiomycetes	16-32	(1→3)		Leal *et al.* (1992)
Evernia prunastri	Lecanoromycetes		(1→3), (1→4) (4:1 (1→3), (1→4) (3:2)	110-210 60-160	Stefanovich (1969) Takeda *et al.* (1972)
Fusarium oxysporum	Sordariomycetes		(1→3)		Schoffelmeer *et al.* (1999)
Fusicoccum amygdali	Dothideomycetes		(1→3), (1→4) (112:3)	600	Buck & Obaidah (1971) Obaidah & Buck (1971)
Histoplasma capsulatum[4]	Eurotiomycetes	46.5	(1→3) (yeast form)		Eissenberg *et al.* (1991) Eissenberg *et al.* (1996) Kanetsuna *et al.* (1974) Klimpel & Goldman (1988)
Histoplasma farciminosum[5]	Eurotiomycetes	13.5	(1→3) (yeast form)		San-Blas & Carbonell (1974)
Letharia vulpina	Lecanoromycetes		(1→3), (1→4) (11:9 and 3:2)		Iacomini *et al.* (1988)
Neurospora crassa	Sordariomycetes	14	(1→3), (1→4) (10%)		Cardemil & Pincheira (1979) Marshall *et al.* (1997)
Paracoccidioides brasiliensis	Eurotiomycetes	45	(1→3) (yeast form)		Kanetsuna & Carbonell (1970) San-Blas & San-Blas (1977) San-Blas & Vernet (1977) San-Blas *et al.* (1977) San-Blas *et al.* (1997)
Parmelia caperata	Lecanoromycetes		nigeran type[6]	100-130	Takeda *et al.* (1970)
Penicillium brevi-compactum	Eurotiomycetes	16-32	(1→3)		Leal *et al.* (1992)
Penicillium decumbens	Eurotiomycetes	16-32	(1→3)		Leal *et al.* (1992)
Penicillium expansum	Eurotiomycetes	26-43	(1→3)		Parra *et al.* (1994)

Ramalina celastri	Lecanoromycetes	28	(1→3), (1→4) (3:1)	1800	Stuelp *et al.* (1999)
Sphaerophorus globosus	Lecanoromycetes		(1→3), (1→4) (2:3), 6% (1→6)		Takeda *et al.* (1972)
Stereocaulon japonicum	Lecanoromycetes		(1→3), (1→4) (3:1)	64	Yokota & Shibata (1978) Yokota *et al.* (1979)
Stereocaulon pauschale	Lecanoromycetes		(1→3), (1→4) (4:1)	135	Hauan & Kjølberg (1971)
Subphylum: Archaeascomycetes					
Schizosaccharomyces pombe	Schizosaccharomycetales	28	(1→3), (1→4) (7%)	207	Bacon *et al.* (1968) Bush *et al.* (1974) Manners & Meyer (1977)

[1]Note that of the three major taxonomic groups, Euascomycetes, Archaeascomycetes, and Hemiascomycetes, so far α-glucans have not been identified in the Hemiascomycetes. [2]DP: degree of polymerization. [3]Anamorph of *Ajellomyces dermatitidis*. [4]Anamorph of *Ajellomyces capsulatus*. [5]Anamorph of *Ajellomyces capsulatus var. farciminosus*. [6]Nigeran is an α-glucan with alternating (1→3)-linked and (1→4)-linked α-Glc*p* residues.

Table I-B. Basidiomycetous fungi whose cell walls contain (1→3)-α-glucan[1]

Species	Taxonomic class	Wall dry weight (%)	Type of linkages	DP	References
Subphylum: Hymenomycetes					
Agrocybe cylindracea	Homobasidiomycetes		(1→3)	3500	Kiho *et al.* (1989) Yoshida *et al.* (1996)
Amanita muscaria	Homobasidiomycetes		(1→3)	260	Kiho *et al.* (1994) Yoshida *et al.* (1996)
Armillaria mellea	Homobasidiomycetes		(1→3), (1→4)		
			(1→3)		Sanchez Hernandez *et al.* (1993)
Coriolus versicolor	Homobasidiomycetes		(1→3), (1→4) (1:2)		Hirase *et al.* (1970)
Cryptococcus albidus	Heterobasidiomycetes		(1→3)		Bacon *et al.* (1968)
Cryptococcus neoformans	Heterobasidiomycetes	33	(1→3), (1→4) (3%)	85	James *et al.* (1990)
Cryptococcus terreus	Heterobasidiomycetes		(1→3)		Bacon *et al.* (1968)
Ganoderma lucidum	Homobasidiomycetes		(1→3)	1200	Chen *et al.* (1998a) Chen *et al.* (1998b)
Laetiporus sulphureus	Homobasidiomycetes	75-88	(1→3)		Jelsma & Kreger (1978) Jelsma & Kreger (1979) Takeo & Matsuzaki (1983)
Lentinus edodes	Homobasidiomycetes		(1→3), (1→4) (5.3:1); branched	600	Shida *et al.* (1978) Zhang *et al.* (1999) Zhang *et al.* (2000) Zhang *et al.* (2002)
Piptoporus betulinus[2]	Homobasidiomycetes	44-53	(1→3)	55-90	Jelsma & Kreger (1978) James & Cherniak (1990) Bacon (1968) Duff (1952)
Polyporus tumulosus	Homobasidiomycetes	15	(1→3)		Angyal *et al.* (1974) Ralph & Bender (1965)
Schizophyllum comune	Homobasidiomycetes	28	(1→3)		Siehr (1976) Sietsma & Wessels (1977) De Vries & Wessels (1975) Wessels *et al.* (1972)
Tremella mesenterica	Heterobasidiomycetes	25-38	(1→3)		Jelsma & Kreger (1978) Reid & Bartnicki-García (1976)

[1]Note that of the three major taxonomic groups, Urediniomycetes, Ustilaginomycetes, and Hymenomycetes, so far α-glucans have been identified only in the Hymenomycetes. [2]Formerly known as *Polyporus betulinus*.

shape of the cell was retained. Furthermore, for the dimorphic fungi *Histoplasma capsulatum*, *Blastomyces dermatitidis*, and *P. brasiliensis*, correlations between α-glucan levels and virulence were observed. These three fungi have α-glucan levels of approximately 35-45% of total cell-wall carbohydrates in their virulent yeast form, whereas in their non-virulent mycelial form, α-glucan was almost absent (Kanetsuna *et al.*, 1974; Hogan & Klein, 1994; San-Blas *et al.*, 1977). Additionally, a *H. capsulatum* yeast strain was isolated that showed no virulence towards mice. Analysis of its cell wall demonstrated that α-glucan was absent (Klimpel & Goldman, 1988), suggesting that cell-wall α-glucan might affect virulence (Kügler *et al.*, 2000).

Recently, a gene encoding an α-glucan synthase, *ags1*$^+$/*mok1*$^+$, was identified in fission yeast (Hochstenbach *et al.*, 1998; Katayama *et al.*, 1999). A hydropathy plot of the amino-acid sequence indicated an integral membrane protein consisting of three domains: a C-terminal multipass transmembrane domain, an intracellular domain, and an N-terminal extracellular domain (**Fig. 3**). A BLAST search revealed that the intracellular domain may act as a synthase, whereas the extracellular domain has sequence homology with amylases, and therefore might function as a transglycosylase (Hochstenbach *et al.*, 1998) (**Fig. 2B**). Importantly, a temperature-sensitive mutant with a point-mutation in the extracellular domain of Ags1p caused a three-fold decrease in α-glucan levels together with a rounded cell morphology when grown at a semi-permissive temperature. At a restrictive temperature cells lysed, indicating that α-glucan has an essential role in maintaining fission-yeast morphology (Hochstenbach *et al.*, 1998). With the completion of the genome project of fission yeast (Wood *et al.*, 2002), genes homologous to *ags1*$^+$ were identified, designated *mok11*$^+$, *mok12*$^+$, *mok13*$^+$, and *mok14*$^+$ (**Fig. 3**) (Hochstenbach *et al.*, 1998, Katayama *et al.* 1999). Their functions remain unknown, but disrupting each or all *mok*$^+$ genes did not lead to a noticeable phenotype in vegetatively-grown cells (Katayama *et al.*, 1999). By applying DNA-microarray analyses, Mata *et al.* (2002) showed that *ags1*$^+$ is downregulated during sporulation, whereas its homologs are upregulated. Together, these results indicate that *mok*$^+$ genes may be involved in the synthesis of the ascospore wall. α-Glucan synthases homologous to Ags1p are also found in other fungi such as the human pathogenic fungus *A. fumigatus*, which has two homologs (with Genbank accession numbers AAL18964 and AAL28129) that both possess the multidomain structure characteristic for the fission-yeast Ags1p (**Fig. 3**). Also in *C. neoformans*, *Neurospora crassa*, *S. commune*, and *Phanerochaete chrysosporium* genes homologous to fission-yeast *ags1*$^+$ were identified (**Fig. 3**).

Questions remain, however, regarding the molecular mechanism of α-glucan biosynthesis. It is unknown how the biosynthesis is initiated, what type of nucleotide is involved in chain elongation and how the synthesis is regulated. Latest studies indicate that a GTPase, Rho2p, may be involved in regulating α-glucan biosynthesis, since overexpression of Rho2p leads to increased levels of α-glucan (Hirata *et al.*, 1998; Calonge *et al.*, 2000).

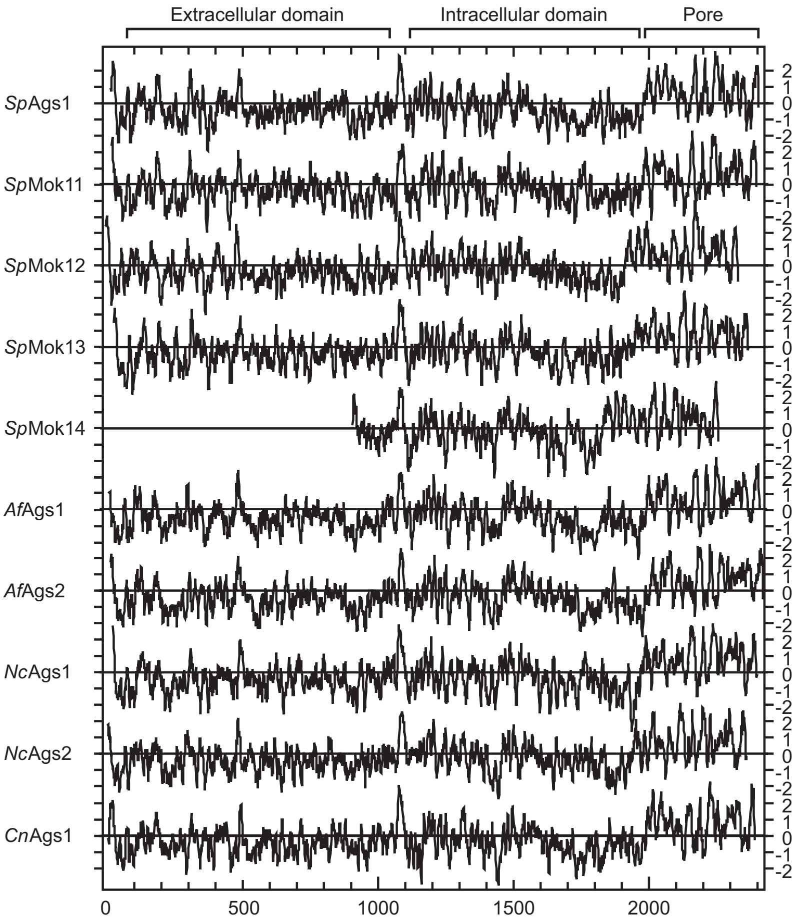

Fig. 3. Fungal α-glucan synthases display a multiple domain structure. Hydropathy plots were generated according to Kyte and Doolittle (1982). Note that the plot of *Cn*Ags1 is based on preliminary sequence data of strain B3501 (serotype D) obtained from The Institute for Genomic Research through the website at http://www.tigr.org. *Sp*: *Schizosaccharomyces pombe*; *Af*: *Aspergillus fumigatus*; *Nc*: *Neurospora crassa*; *Cn*: *Cryptococcus neoformans*.

Chitin

Chitin, a linear chain of (1→4)-β-*N*-acetyl-D-glucosamine residues, is present in many fungi as a cell-wall component at levels of up to 60% (Bartnicki-García, 1968). In *S. cerevisiae*, chitin is present at approximately 2% ($^{w}/_{w}$) of the total cell wall and is localized predominantly at the bud scars as a polysaccharide consisting of on average 190 *N*-acetylglucosamine residues, but is also dispersed in the lateral walls where it is covalently linked to (1→3)-β-glucan and (1→6)-β-glucan (Hartland *et al.*, 1994; Klis *et al.*, 2002). From X-ray crystallography studies, three crystalline forms are known, denoted α, β, and γ, of which the α-form is found in fungi (Wessels & Sietsma, 1982). α-Chitin forms a two-fold single helix that is stabilized by 3-OH•••O-5 hydrogen bonds. Its conformation is very similar to cellulose, which is consistent with its role as a structural polysaccharide (Chandrasekaran, 1997).

Chitin synthases are integral membrane proteins (**Fig. 2C**) that require UDP-*N*-acetylglucosamine as a donor. Three chitin synthases have been identified in *S. cerevisiae*. The significance of *CHS1* and *CHS2* for cell integrity has long been controversial. Based on gene-disruption experiments, the group of Cabib concluded that *CHS2* is essential for vegetative growth, whereas *CHS1* is not (Silverman *et al.*, 1988, Bulawa *et al.*, 1986). Studies by Bulawa and Osmond (1990), however, revealed that *chs2* null mutants are viable when grown in synthetic minimal medium and do not display a detectable deficiency in chitin. Therefore, a third chitin synthase, Chs3p, must be responsible for the observed chitin synthase activity. Cloning and disruption of the respective genes showed that Chs3p is responsible for chitin dispersed in the bud ring and the lateral wall, whereas Chs2p catalyzes the synthesis of chitin that forms the primary septum dividing the mother cell from the daughter cell (Shaw *et al.*, 1991; Cabib *et al.*, 1993). Importantly, a deletion of both Chs2p and Chs3p led to inviable cells (Shaw *et al.*, 1991). Chs1p was shown to act as a repair enzyme utilized at the end of cytokinesis (Valdivieso *et al.*, 1999).

Genes homologous to *CHS1* and *CHS2* have been identified in many other fungi, such as *C. albicans*, *A. nidulans*, *A. fumigatus*, and *S. pombe* (Munro & Gow, 2001; Arellano *et al.*, 2000; see Bowen *et al.*, 1992 for classification of a large number of fungal chitin synthases into three major groups). In fission yeast, two homologous genes were identified. Depletion or overexpression of $chs1^+$ did not lead to noticeable defects during vegetative growth, whereas ascospore formation was strongly affected, indicating that the gene is solely required for sporulation (Arellano *et al.*, 2000). The function of $chs2^+$ is unknown, but DNA-microarray analyses demonstrated that this gene, like $chs1^+$, is upregulated during meiosis (Mata *et al.*, 2002), and therefore may also display a function during sporulation. On the contrary, Sietsma and Wessels (1990) suggested that chitin may be synthesized also during vegetative growth. They showed that approximately 10% of the β-glucan isolated from vegetatively-grown fission yeast (strain CBS356) is insoluble under alkaline conditions, whereas chitinase or nitrous acid treatment led to fully alkali-soluble β-glucan. Furthermore, the authors were able to detect chitin-synthase activity during vegetative growth. When a fission-yeast strain with a disrupted chitin synthase was investigated, they found that the β-glucan was completely alkali-soluble (J.H. Sietsma, personal communication). These results suggested that chitin may be synthesized during vegetative growth. However, because the authors used a homothallic yeast strain (CBS356), which contains both h^+ and h^- cells, and because they harvested the yeast cells in the late exponential phase, it cannot be excluded that due to nutrient-depletion, mating and subsequent sporulation occurred, leading to activation of chitin synthases.

Glycogen and amylose

Amylose ((1→4)-α-glucan) and glycogen ((1→4)-α-glucan with (1→6)-linked branches) are polysaccharides found in many organisms, both bacteria and eukaryotes. Glycogen is generally considered to be a storage compound, providing carbon and energy. Also fungi such as *S. cerevisiae*, *S. pombe*, and *H. capsulatum* accumulate glycogen, which is degraded under nutrient-deprived conditions (Kane & Roth, 1974; Inoue & Shimoda, 1981; Garrison & Boyd, 1978). Glycogen synthesis has been studied extensively in mammals where it is initiated by a protein designated 'glycogenin'. This protein synthesizes short (1→4)-linked α-glucooligomers of four to eight residues from UDP-Glc that serve to prime glycogen synthesis by glycogen synthase (Alonso *et al.*, 1995; Whelan, 1998). In *S. cerevisiae* two genes encoding glycogen synthases, *GSY1* and *GSY2*, were identified (Farkas *et al.*, 1990; Farkas *et al.*, 1991). The synthases catalyze the addition of (1→4)-linked glucose residues from UDP-Glc to the non-reducing end of linear (1→4)-α-glucooligosaccharides (François & Parrou, 2001). Like in the mammalian counterpart, (1→4)-α-glucooligosaccharides are synthesized from UDP-Glc by yeast glycogenin, Ggl1p and Ggl2p, and act as a primer.

Genes homologous to *S. cerevisiae GSY* were found in the fungus *N. crassa*, but are absent from fission yeast *S. pombe* (Cid *et al.*, 2002; Hochstenbach *et al.*, 1998). In fission yeast, a glycogen-like material is accumulated during sporulation (Beltran *et al.*, 2000; Inoue & Shimoda, 1981). Genes containing sequence similarity to bacterial glycogen synthases were identified in fission yeast, namely *ags1*$^+$, *mok11*$^+$, *mok12*$^+$, *mok13*$^+$, and *mok14*$^+$ (Hochstenbach *et al.*, 1998; Katayama *et al.*, 1999). Surprisingly, studies indicate that Ags1p functions to synthesize (1→3)-α-glucan rather than (1→4)-α-glucan (Hochstenbach *et al.*, 1998; Katayama *et al.*, 1999). The functions of the *mok*$^+$ homologs still need to be determined.

Cellulose

Although cellulose, a (1→4)-β-glucan, is not found in fungi, recent discoveries concerning its biosynthesis led to new insights into polysaccharide synthesis. Cellulose biosynthesis has been studied thoroughly in bacteria and plants. *In vitro* studies indicated that cellulose synthesis is Mg^{2+} dependent and uses UDP-Glc as a donor (Gibeaut & Carpita, 1994). It was further reported that a primer consisting of (1→4)-linked β-glucose residues may be required for chain initiation (Blaschek *et al.*, 1983), but the actual need for a primer has long been controversial (Delmer & Amor, 1995). Recently, a breakthrough was achieved in the understanding of cellulose biosynthesis with the identification of sitosterol-β-glucoside as the primer for cellulose biosynthesis. In their paper, Peng *et al.* (2002) demonstrated that first a glucose residue is transferred onto a sitosterol molecule, forming sitosterol-β-glucoside. This molecule is then transferred to a glucosyltransferase, CesA-1, that upon addition of UDP-Glc, elongates the glucoside via (1→4)-linkages, forming a sitosterol-cellooligosaccharide. A membrane-bound cellulase subsequently liberates the cellooligosaccharide from the sitosterol, for use as a primer to initiate cellulose biosynthesis catalyzed by a second glucosyltransferase, CesA-2. No doubt, these findings will lead to new insights into the biosynthetic mechanisms of other polysaccharides (Read & Basic, 2002).

The fungal cell wall as a target for the development of fungicides

Infections caused by human pathogenic fungi threaten increasing numbers of patients with suppressed immune systems, such as patients undergoing organ transplants or chemotherapy, and patients infected with the human immunodeficiency virus. Some important pathogenic fungi include the dimorphic fungi *H. capsulatum*, *B. dermatitidis*, and *P. brasiliensis* that all are non-virulent in their mycelial form, but become pathogenic when in their yeast form (Kanetsuna *et al.*, 1974; Hogan & Klein, 1994; San-Blas *et al.*, 2002). *A. fumigatus* causes life-threatening mycosis, and due to the absence of adequate medication, death rates can reach up to 80% of infected patients (Beauvais & Latgé, 2001). *C. albicans*, on the contrary, is a dimorphic fungus that requires the ability to switch from a yeast form to a mycelial form for virulence (Lo *et al.*, 1997; Mitchell, 1998). Infections with *C. albicans* are common to immunosuppressed patients, but occasionally also healthy individuals are infected.

Current medication against fungal infections includes polyenes (fungicidal) and azoles (fungistatic) that both act on the plasma membrane of the fungal cell. The polyenes, such as amphotericin B, form complexes with membrane sterol, namely ergosterol, resulting in the formation of transmembrane pores that leak vital cellular ions, such as K^+ and Mg^{2+}. Since the polyenes also bind to mammalian cholesterol, toxicity is common (Georgopapadakou, 1998). A second drawback is the increasing fungal resistance to polyenes, that is based on alterations in fungal membrane lipids, and is found especially in *Fusarium* and *Trichosporon* species (Georgopapadakou, 1998). The second group of antifungals, the azoles, also act on fungal ergosterol, but rather than binding to it like the polyenes, it affects ergosterol biosynthesis by inhibiting a demethylation step catalyzed by cytochrome P-450$_{DM}$ leading to perturbation of the plasma membrane function (Georgopapadakou, 1998). The toxicity of azoles to humans is low, but since azoles are fungistatic rather than fungicidal, life-time medication is necessary. In addition, resistance is emerging in *Candida* species and in *C. neoformans* (Kelly *et al.*, 1996; Perea *et al.*, 2001; Cowen *et al.*, 2002; Georgopapadakou, 1998).

The fungal cell wall is unique among eukaryotes and therefore enzymes that are involved in its biosynthesis form ideal targets for the development of highly-specific antifungal drugs (reviewed in Kurtz & Rex, 2001). (1→3)-β-Glucan and chitin are cell-wall polymers that are both essential for cell viability and occur in most fungi. Accordingly, their synthases have been chosen for the development of novel cell-wall targeted fungicides (Georgopapadakou & Tkaz, 1995; Radding *et al.*, 1998; Onishi *et al.*, 2000; Ohyama *et al.*, 2000; Feldmesser *et al.*, 2000; De Pauw, 2000; Georgopapadakou, 2001; Kurtz & Rex, 2001). For example, polyoxins and nikkomycins inhibit chitin synthesis, whereas echinocandins, the related pneumocandins, and papulacandins inhibit (1→3)-β-glucan synthesis. Although the development of antifungals targeted against chitin synthesis stalled in the first phase of clinical development (Georgopapadakou, 2001), the echinocandin caspofungin inhibiting (1→3)-β-glucan synthesis has recently been approved for clinical use (Hussar, 2001; Ruhnke &

Maschmeyer, 2002).

Unfortunately, *C. neoformans* is not vulnerable towards inhibitors of (1→3)-β-glucan and chitin synthesis (Georgopapadakou, 2001). In addition, fungal strains resistant towards candins have already been identified in *C. albicans* and the model-yeast *S. cerevisiae* (Douglas *et al.*, 1994b; el-Sherbeini & Clemas, 1995; Kurtz *et al.*, 1996), indicating that the search for new targets has to continue. Other cell wall components that are potentially interesting targets for antifungals are (1→6)-β-glucan and (1→3)-α-glucan. The former is present in the cell wall only in minor amounts, but is an essential component for cell-wall rigidity since structural studies made clear that it interconnects mannoproteins with (1→3)-β-glucan and chitin. Also α-glucan has recently been shown to be essential for cell morphogenesis (Hochstenbach *et al.*, 1998) and therefore enzymes that are involved in the synthesis and assembly of (1→6)-β-glucan and (1→3)-α-glucan form interesting chemotherapeutic targets.

Aim and outline of the thesis

The fungal cell wall is a highly complex network of glycoproteins and polysaccharides. Enzymes that are involved in the synthesis and assembly of cell-wall components have gained increasing interest since they form ideal targets for the development of antifungal drugs. For this purpose, understanding the structure and biosynthesis of the individual cell-wall components is essential. The mechanism of how α-glucan is synthesized is barely understood and it is unknown whether this polysaccharide is covalently linked to other cell-wall components. The aim of this thesis is to obtain information on the biosynthesis of fungal cell-wall α-glucan by elucidating its chemical structure. As a first step, we make use of fission yeast *S. pombe* as a model organism, because mutants are available or engineerable and its genome sequence is known (Wood *et al.*, 2002). It was shown that fission-yeast α-glucan synthase, Ags1p, is a transmembrane protein, that may exert several discrete functions, such as the synthesis of α-glucan, the transport of this polysaccharide through the plasma membrane and the assembly or cross-linking to the cell-wall matrix (Hochstenbach *et al.*, 1998). To investigate the different functions of Ags1p, we study the chemical structures of α-glucan isolated from wild-type fission yeast as well as from a mutant that is defective in α-glucan biosynthesis.

In **Chapter 2**, the chemical structure of fission-yeast α-glucan is investigated. We show that fission-yeast α-glucan forms an individual fibrillar network that is not covalently linked to other cell-wall components such as β-glucan. By using a mutant that is defective in α-glucan biosynthesis, we propose that a single enzyme is involved in the synthesis and coupling of two α-glucan polymers and we speculate that a primer might be necessary for the initiation of α-glucan biosynthesis.

To identify the chemical structure of this speculative primer, we degrade the α-glucan by an (1→3)-α-glucanase and elucidate the chemical structure of the non-hydrolyzed material (**Chapter 3**). For this purpose, we purify and characterize an (1→3)-α-glucanase from *Trichoderma harzianum*, which is described in the **Supplementary data** at the end of Chapter 3. We demonstrate that the speculative primer is composed of (1→4)-α-glucooligomers with varying chain length.

In **Chapter 4**, the structure elucidation of three α-glucan fractions isolated from fission yeast ascospores is described. We show that the ascospore wall contains two mainly (1→3)-linked α-glucans that only differ in their degree of polymerization. Both α-glucans are composed fundamentally different from that of vegetatively-grown cells, indicating that a different biosynthetic mechanism may be involved. The third α-glucan fraction is composed solely of (1→4)-linked glucose residues. This fraction is ascribed to amylose, which may be a storage carbohydrate accumulated during sporulation.

In **Chapter 5**, we investigate whether the chemical structure of α-glucan is conserved among fungi. We determine the chemical structure of α-glucans from seven Ascomycetes and Basidiomycetes and find that in two species, the α-glucans are composed similar to that of fission-yeast cell walls, whereas the α-glucans from four fungi are composed similar to that of fission-yeast spore walls. The seventh fungus may contain both structural types. These results indicate that two biosynthetic mechanisms of α-glucan biosynthesis may be conserved in evolution.

The data obtained in this thesis are the result of a collaboration between a group involved in carbohydrate chemistry and molecular biologists. The combination of chemical analyses and molecular biology proved an extremely strong tool in unraveling the complex mechanisms that are involved in fungal α-glucan biosynthesis.

References

Alonso, M.D.; Lomako, J.; Lomako, W.M. & Whelan, W.J. (1995) A new look at the biogenesis of glycogen. *FASEB J.* **9,** 1126-1137.

Angyal, S.J.; Bender, J. & Ralph, B.J. (1974) Structure of polysaccharides from the *Polyporus tumulosus* cell wall. *Biochim. Biophys. Acta* **362,** 175-187.

Antelo, L.; Cosio, E.G.; Hertkorn, N. & Ebel, J. (1998) Partial purification of a GTP-insensitive (1→3)-β-glucan synthase from *Phytophtora sojae*. *FEBS Lett.* **433,** 191-195.

Arellano, M.; Cartagena-Lirola, H.; Nasser Hajibagheri, M.A.; Durán, A. & Valdivieso, M.H. (2000) Proper ascospore maturation requires the *chs1*$^{+}$ chitin synthase gene in *Schizosaccharomyces pombe*. *Mol. Microbiol.* **35,** 79-89.

Arellano, M.; Durán, A. & Perez P. (1996) Rho1 GTPase activates the (1→3)-β-D-glucan synthase and is involved in *Schizosaccharomyces pombe* morphogenesis. *EMBO J.* **15,** 4584- 4591.

Awald, P; Zugel, M.; Monks, C.; Frost, D. & Selitrennikoff, C.P. (1993) Purification of 1→3-β-glucan synthase from *Neurospora crassa* by product entrapment *Exp. Mycol.* **17,** 130-141.

Bacon, J.S.D.; Jones, D.; Farmer, V.C. & Webley, D.M. (1968) The occurrence of (1→3)-α-glucan in *Cryptococcus, Schizosaccharomyces* and *Polyporus* species, and its hydrolysis by a *Streptomyces* culture filtrate lysing cell walls of *Cryptococcus*. *Biochim. Biophys. Acta* **158,** 313-315.

Barreto-Bergter, E. & Gorin, P.A.J. (1983) Structural chemistry of polysaccharides from fungi and lichens. In: *Advances in carbohydrate chemistry and biochemistry*; Tipson, R.S. & Horton, D., Eds.; Academic Press: New York; Vol. 41; pp. 67-103.

Bartnicki-García, S. (1968) Cell wall chemistry, morphogenesis, and taxonomy of fungi. *Annu. Rev. Microbiol.* **22,** 87-108.

Beauvais, A. & Latgé, J.P. (2001) Membrane and cell wall targets in *Aspergillus fumigatus*. *Drug Resist. Updat.* **4,** 38-49.

Bell, D.J. & Northcote, D.H. (1950) The structure of a cell-wall polysaccharide of baker's yeast. *J. Chem. Soc.* 1944-1947.

Beltran, F.F.; Castillo, R.; Vicente-Soler, J.; Cansado, J. & Gacto, M. (2000) Role for trehalase during germination of spores in the fission yeast *Schizosaccharomyces pombe*. *FEMS Microbiol. Lett.* **193,** 117-121.

Bernard, M. & Latgé, J.P. (2001) *Aspergillus fumigatus* cell wall: composition and biosynthesis. *Med. Mycol.* **39 Suppl. 1,** 9-17.

Blaschek, W.; Haass, D.; Koehler, H.; Semler, U. & Franz, G. (1983) Demonstration of a β-1→4-primer glucan in cellulose-like glucan synthesized in vitro. *Z. Pflanzenphysiol.* **111,** 357-364.

Bobbit, T.F.; Nordin, J.H.; Roux, M.; Revol, J.F. & Marchessault, R.H. (1977) Distribution and conformation of crystalline nigeran in hyphal walls of *Aspergillus niger* and *Aspergillus awamori*. *J. Bacteriol.* **132,** 691-703.

Boone, C.; Sommer, S.S.; Hensel, A. & Bussey, H. (1990) Yeast *KRE* genes provide evidence for a pathway of cell wall β-glucan assembly. *J. Cell Biol.* **110,** 1833-1843.

Borgia, P.T. & Dodge, C.L. (1992) Characterization of *Aspergillus nidulans* mutants deficient in cell wall chitin or glucan. *J. Bacteriol.* **174,** 377-383.

Botstein, D.; Chervitz, S.A. & Cherry, J.M. (1997) Yeast as a model organism. *Science* **277,** 1259-1260.

Bowen, A.R.; Chen-Wu, J.L.; Momany, M.; Young, R.; Szaniszlo, P.J. & Robbins, P.W. (1992) Classification of fungal chitin synthases. *Proc. Natl. Acad. Sci. U S A* **89,** 519-523.

Brown Jr., R.M. & Saxena, I.M. (2000) Cellulose biosynthesis: a model for understanding the assembly of biopolymers. *Plant Physiol. Biochem.* **38,** 57-67.

Buck, K.W. & Obaidah, M.A. (1971) The composition of the cell wall of *Fusicoccum amygdali*. *Biochem. J.* **125,** 461-471.

Bull, A.T. (1970) Chemical composition of wild-type and mutant *Aspergillus nidulans* cell walls. The nature of polysaccharide and melanin constituents. *J. Gen. Microbiol.* **63,** 75-94.

Bulawa, C.E. & Osmond, B.C. (1990) Chitin synthase I and chitin synthase II are not required for chitin synthesis *in vivo* in *Saccharomyces cerevisiae*. *Proc. Natl. Acad. Sci. U S A* **87,** 7424-7428.

Bulawa, C.E.; Slater, M.; Cabib, E.; Au-Young, J.; Sburlati, A.; Adair, W.L. Jr. & Robbins, P.W. (1986) The *S. cerevisiae* structural gene for chitin synthase is not required for chitin synthesis *in vivo*. *Cell* **46,** 213-225.

Bush, D.A.; Horisberger, M., Horman, I. & Wursch, P. (1974) The wall structure of *Schizosaccharomyces pombe*. *J. Gen. Microbiol.* **81,** 199-206.

Cabib, E.; Mol, P.C.; Shaw, J.A. & Choi, W.J. (1993) Biosynthesis of cell wall and septum during yeast growth. *Arch. Med. Res.* **24,** 301-303.

Cabib, E.; Roberts, R. & Bowers, B. (1982) Synthesis of the yeast cell wall and its regulation. *Ann. Rev. Biochem.* **51,** 763-793.

Calonge, T.M.; Nakano, K.; Arellano, M.; Arai, R.; Katayama, S.; Toda, T.; Mabuchi, I. & Perez, P. (2000)

Schizosaccharomyces pombe Rho2p GTPase regulates cell wall α-glucan biosynthesis through the protein kinase Pck2p. *Mol. Biol. Cell.* **11,** 4393-4401.

Cardemil, L. & Pincheira, G. (1979) Characterization of the carbohydrate component of fraction I in the *Neurospora crassa* cell wall. *J. Bacteriol.* **137,** 1067-1072.

Chaffin, W.L.; López-Ribot, J.; Casanova, M.; Gozalbo, D. & Martínez, J.P. (1998) Cell wall and secreted proteins of *Candida albicans*: identification, function, and expression. *Microbiol. Mol. Biol. Rev.* **62,** 130-180.

Chandrasekaran, R. (1997) Molecular architecture of polysaccharide helices in oriented fibers. *Adv. Carbohydr. Chem. Biochem.* **52,** 311-439.

Chen, J.; Zhang, L.; Nakamura, Y. & Norisuye, T. (1998a) Viscosity behavior and chain conformation of a (1→3)-α-glucan from *Ganoderma lucidum*. *Polym. Bull.* **41,** 471-478.

Chen, J.; Zhou, J.; Zhang, L.; Nakamura, Y. & Norisuye, T. (1998b) Chemical structure of the water-insoluble polysaccharide isolated from the fruiting body of *Ganoderma lucidum*. *Polym. J.* **30,** 838-842.

Chasan, R. (1992) Chestnut blight - An end in sight? *Plant Cell* **4,** 1350-1352.

Cid, E.; Geremia, R.A.; Guinovarta, J.J. & Ferrer, J.C. (2002) Glycogen synthase: towards a minimum catalytic unit? *FEBS Lett.* **528,** 5-11.

Cowen, L.E.; Nantel, A.; Whiteway, M.S.; Thomas, D.Y.; Tessier, D.C.; Kohn, L.M. & Anderson, J.B. (2002) Population genomics of drug resistance in *Candida albicans*. *Proc. Natl. Acad. Sci. U S A* **99,** 9284-9289.

Delmer, D.P. & Amor, Y. (1995) Cellulose biosynthesis. *Plant Cell* **7,** 987-1000.

De Pauw, B.E. (2000) New antifungal agents and preparations. *Int. J. Antimicrob. Agents* **16,** 147-150.

Douglas, C.M. *et al.* (1994a) The *Saccharomyces cerevisiae FKS1* (*ETG1*) gene encodes an integral membrane protein which is a subunit of 1→3-β-D-glucan synthase. *Proc. Natl. Acad. Sci. U S A* **91,** 12907-12911.

Douglas, C.M.; Marrinan, J.A.; Li, W. & Kurtz, M.B. (1994b) A *Saccharomyces cerevisiae* mutant with echinocandin-resistant 1→3-β-D-glucan synthase. *J. Bacteriol.* **176,** 5686-5696.

Drgonová, J.; Drgon, T.; Tanaka, K.; Kollár, R.; Chen, G.C.; Ford, R.A.; Chan, C.S.; Takai, Y. & Cabib, E. (1996) Rho1p, a yeast protein at the interface between cell polarization and morphogenesis. *Science* **272,** 277-279.

Duff, R.B. (1952) The constitution of a glucosan from the fungus *Polyporus betulinus*. *J. Chem. Soc.* **III,** 2592-2594.

Eissenberg, L.G.; Poirier, S. & Goldman, W.E. (1996) Phenotypic variation and persistence of *Histoplasma capsulatum* yeasts in host cells. *Infect. Immun.* **64,** 5310-5314.

Eissenberg, L.G.; West, J.L.; Woods, J.P. & Goldman, W.E. (1991) Infection of P388D1 macrophages and respiratory epithelial cells by *Histoplasma capsulatum*: selection of avirulent variants and their potential role in persistent histoplasmosis. *Infect. Immun.* **59,** 1639-1646.

el-Sherbeini, M. & Clemas, J.A. (1995) Nikkomycin Z supersensitivity of an echinocandin-resistant mutant of *Saccharomyces cerevisiae*. *Antimicrob. Agents. Chemother.* **39,** 200-207.

Feldmesser, M.; Kress, Y.; Mednick, A. & Casadevall, A. (2000) The effect of the echinocandin analogue caspofungin on cell wall glucan synthesis by *Cryptococcus neoformans*. *J. Infect. Dis.* **182,** 1791-1795.

Fleet, G.H. & Manners, D.J. (1976) Isolation and composition of an alkali-soluble glucan from the cell walls of *Saccharomyces serevisiae*. *J. Gen. Microbiol.* **94,** 180-192.

Fleming, M. & Manners, D.J. (1966) *Biochem. J.* **100,** 24P.

Fontaine, T.; Simenel, C.; Dubreucq, G.; Adam, O.; Delepierre, M.; Lemoine, J.; Vorgias, C.E.; Diaquin, M. & Latgé, J.-P. (2000) Molecular organization of the alkali-insoluble fraction of *Aspergillus fumigatus* cell wall. *J. Biol. Chem.* **275,** 27594-25607.

François, J. & Parrou, J.L. (2001) Reserve carbohydrates metabolism in the yeast *Saccharomyces cerevisiae*. *FEMS Microbiol. Rev.* **25,** 125-145.

Gawronski, M.; Park, J.T.; Magee, A.S. & Conrad, H. (1999) Microfibrillar structure of PGG-glucan in aqueous solution as triple-helix aggregates by small angle X-ray scattering. *Biopolymers* **50,** 569-578.

Georgopapadakou, N.H. (1998) Antifungals: mechanism of action and resistance, established and novel drugs. *Curr. Opin. Microbiol.* **1,** 547-557.

Georgopapadakou, N.H. (2001) Update on antifungals targeted to the cell wall: focus on β-1→3-glucan synthase inhibitors. *Exp. Opin. Invest. Drugs* **10,** 269-280.

Georgopapadakou, N.H. & Tkacz, J.S. (1995) The fungal cell wall as a drug target. *Trends Microbiol.* **3,** 98-104.

Gibeaut, D.M. & Carpita, N.C. (1994) Biosynthesis of plant cell wall polysaccharides. *FASEB J.* **8,** 904-915.

Goffeau *et al.* (1997) The yeast genome directory. *Nature* **387,** (Suppl) 5-105.

Hartland, R.P.; Vermeulen, C.A.; Klis, F.M.; Sietsma, J.H. & Wessels, J.G. (1994) The linkage of (1→3)-β-glucan to chitin during cell wall assembly in *Saccharomyces cerevisiae*. *Yeast* **10,** 1591-1599.

Hasegawa, S.; Nordin, J.H. & Kirkwood, S. (1969) Enzymes that hydrolyze fungal cell wall polysaccharides. I. Purification and properties of an endo-α-D-(1→3)-glucanase from *Trichoderma*. *J. Biol. Chem.* **244,** 5460-5470.

Hauan, E. & Kjølberg, O. (1971) Studies on the polysaccharides of lichens. I. The structure of a water-soluble polysaccharide in *Stereocaulon paschale (L.) Fr*. *Acta Chem. Scand.* **25,** 2622-2628.

Hawksworth, D.L. (1991) The fungal dimension of biodiversity: magnitude, significance, and conservation. *Mycol. Res.* **95,** 641-655.

Hayles, J. & Nurse, P. (2001) A journey into space. *Nat. Rev. Mol. Cell. Biol.* **2,** 647-656.

Hirase, S.; Nakai, S. & Otsuka, S. (1970) *Proc. Japan. Cancer Assoc. 29th Annu. Meet.*, p. 227.

Hirata, D.; Nakano, K.; Fukui, M.; Takenaka, H.; Miyakawa, T. & Mabuchi, I. (1998) Genes that cause aberrant cell morphology by overexpression in fission yeast: a role of a small GTP-binding protein Rho2 in cell morphogenesis. *J. Cell. Sci.* **111,** 149-159.

Hintz, W.E. (1999) Sequence analysis of the chitin synthase A gene of the Dutch elm pathogen *Ophiostoma novo-ulmi* indicates a close association with the human pathogen *Sporothrix schenckii*. *Gene* **237,** 215-221.

Hochstenbach, F.; Klis, F.M.; Van Den Ende, H.; Van Donselaar, E. Peters, P.J. & Klausner, R.D. (1998) Identification of a putative α-glucan synthase essential for cell wall construction and morphogenesis in fission yeast. *Proc. Natl. Acad. Sci. U S A* **95,** 9161- 9166.

Hogan, L.H. & Klein, B.S. (1994) Altered expression of surface α-1→3-glucan in genetically related strains of *Blastomyces dermatitidis* that differ in virulence. *Infect. Immun.* **62,** 3543-3546.

Horisberger, M.; Lewis, B.A. & Smith, F. (1972) Structure of (1→3)-α-D-glucan (pseudonigeran) of *Aspergillus niger NNRL 326* cell wall. *Carbohydr. Res.* **23,** 183-188.

Hussar, D.A. (2001) New drugs of 2001. *J. Am. Pharm. Assoc.* **42,** 227-263.

Iacomini, M.; Gorin, P.A.J.; Baron, M.; Tulloch, A.P. & Mazurek, M. (1988) Novel D-glucans obtained by dimethyl sulfoxide extraction of the lichens *Letharia vulpina*, *Actinogrya muehlenbergii*, and an *Usnea* sp. *Carbohydr. Res.* **176,** 117-126.

Inoue, H. & Shimoda, C. (1981) Changes in trehalose content and trehalose activity during spore germination in fission yeast, *Schizosaccharomyces pombe*. *Arch. Microbiol.* **129,** 19- 22.

Inoue, S.B.; Qadota, H.; Arisawa, M.; Anraku, Y.; Watanabe, T. & Ohya, Y. (1996) Signaling toward yeast 1→3-β-glucan synthesis. *Cell Struct. Funct.* **21,** 395-402.

Inoue, S.B.; Takewaki, N.; Takasuka, T.; Mio, T.; Adachi, M.; Fujii, Y.; Miyamoto, C.; Arisawa, M.; Furuichi, Y. & Watanabe, T. (1995) Characterisation and gene cloning of 1→3-β-D-glucan synthase from *Saccharomyces cerevisiae*. *Eur. J. Biochem.* **231,** 845-854.

Ishiguro, J.; Saitou, A.; Durán, A. & Ribas, J.C. (1997) *cps1*$^{+}$, a *Schizosaccharomyces pombe* gene homolog of *Saccharomyces cerevisiae FKS* genes whose mutation confers hypersensitivity to cyclosporin A and papulacandin B. *J. Bacteriol.* **179,** 7653-7662.

James, P.G. & Cherniak, R. (1990) 4-Methylmorpholine N-oxide-methyl sulfoxide soluble glucan of *Piptoporus betulinus*. *Carbohydr. Res.* **206,** 167-172.

James, P.G.; Cherniak, R.; Jones, R.G. & Stortz, C.A. (1990) Cell-wall glucans of *Cryptococcus neoformans* Cap 67. *Carbohydr. Res.* **198,** 23-38.

Jelsma, J. & Kreger, D.R. (1975) Ultrastructural observations on (1→3)-β-D-glucan from fungal cell-walls. *Carbohydr. Res.* **43,** 200-203.

Jelsma, J. & Kreger, D.R. (1978) Observations on the cell-wall compositions of the bracket fungi *Laetiporus sulphureus* and *Piptoporus betulinus*. *Arch. Microbiol* **119,** 249-255.

Jelsma, J. & Kreger, D.R. (1979) Polymorphism in crystalline (1→3)-α-D-glucan from fungal cell-walls. *Carbohydr. Res.* **71,** 51-64.

Johnston, I.R. (1965) The partial acid hydrolysis of a highly dextrorotatory fragment of the cell wall of *Aspegillus niger*. *Biochem. J.* **96,** 659-664.

Kanetsuna, F. & Carbonell, L.M. (1970) Cell wall glucans of the yeast and mycelial forms of *Paracoccidioides brasiliensis*. *J. Bacteriol.* **101,** 675-680.

Kanetsuna, F. & Carbonell, L.M. (1971) Cell wall composition of the yeastlike and the mycelial forms of *Blastomyces dermatitidis*. *J. Bacteriol.* **106,** 946-948.

Kanetsuna, F. & Carbonell, L.M.; Gil, F. & Azuma, I. (1974) Chemical and ultrastructural studies on the cell walls of the yeastlike and mycelial forms of *Histoplasma capsulatum*. *Mycopathol. Mycol. Appl.* **54,** 1-13.

Kang, M.S.; Elango, N.; Mattia, E.; Au-Young, J.; Robbins, P.W. & Cabib, E. (1984) Isolation of chitin synthetase from *Saccharomyces cerevisiae* - Isolation of an enzyme by entrapment in the reaction product. *J. Biol. Chem.* **259,** 14966-14972.

Kapteyn, J.C.; Van Den Ende, H. & Klis, F.M. (1999) The contribution of cell wall proteins to the organization of the yeast cell wall. *Biochim. Biophys. Acta* **1426,** 373-383.

Katayama, S.; Hirata, D.; Arellano, M.; Pérez, P. & Toda T. (1999) Fission yeast α-glucan synthase mok1 requires the actin cytoskeleton to localize the sites of growth and plays an essential role in cell morphogenesis downstream of protein kinase C function. *J. Cell Biol.* **144,** 1173-1186.

Kelly, R.; Register, E.; Hsu, M.J.; Kurtz, M. & Nielsen, J. (1996) Isolation of a gene involved in 1→3-β-glucan synthesis in *Aspergillus nidulans* and purification of the corresponding protein. *J. Bacteriol.* **178,** 4381-4391.

Kiho, T.; Yoshida, I.; Katsuragawa, M.; Sakushima, M.; Usui, S. & Ukai, S. (1994) Polysaccharides in Fungi. XXXIV. A polysaccharide from the fruiting bodies of *Amanita muscaria* and the antitumor activity of its carboxymethylated product. *Biol. Pharm. Bull.* **17,** 1460-1462.

Kiho, T.; Yoshida, I.; Nagai, K. & Ukai, S. (1989) (1→3)-α-D-Glucan from an alkaline extract of *Agrocybe cylindracea*, and antitumor activity of its *O*-(carboxymethyl)ated derivatives. *Carbohydr. Res.* **189,** 273-279.

Klein, B.S. (1997) Role of cell surface molecules of *Blastomyces dermatitidis* in the pathogenesis and immunobiology of blastomycosis. *Semin. Respir. Infect.* **12,** 198-205.

Klimpel, K.R. & Goldman, W.E. (1988) Cell walls from avirulent variants of *Histoplasma capsulatum* lack α-(1→3)-glucan. *Infect. Immun.* **56,** 2997-3000.

Klis, F.M.; Caro, L.H.P.; Vossen, J.H.; Kapteyn, J.C.; Ram, A.F.J.; Montijn, R.C.; Van Berkel, M.A.A. & Van Den Ende, H. (1997) Identification and characterization of a major building block in the cell wall of *Saccharomyces cerevisiae*. *Biochem. Soc. Transactions* **25,** 856-860.

Klis, F.M.; de Groot, P. & Hellingwerf, K. (2001) Molecular organization of the cell wall of *Candida albicans*. *Med. Mycol.* **39 Suppl. 1,** 1-8.

Klis, F.; Mol, P.; Hellingwerf, K. & Brul, S. (2002) Dynamics of cell wall structure in *Saccharomyces cerevisiae*. *FEMS Microbiol. Rev.* **26,** 239-256.

Kollár, R.; Petráková, E.; Ashwell, G.; Robbins, P.W. & Cabib, E. (1995) Architecture of the yeast cell wall. The linkage between chitin and β-(1→3)-glucan. *J. Biol. Chem.* **270,** 1170- 1178.

Kollár, R.; Reinhold, B.B.; Petráková, E.; Yeh, H.J.C.; Ashwell, G.; Drgnová, J; Kapteyn, J.C.; Klis, F.M. & Cabib, E. (1997) Architecture of the yeast cell wall. β-(1→6)-Glucan interconnects mannoprotein, β-(1→3)-glucan, and chitin. *J. Biol. Chem.* **272,** 17762-17775.

Kopecká, M.; Fleet, G.H. & Phaff, H.J. (1995) Ultrastructure of the cell wall of *Schizosaccharomyces pombe* following treatment with various glucanases. *J. Struct. Biol.* **114,** 140-152.

Kreger, D.R. & Kopecká, M. (1975) On the nature and formation of the fibrillar nets produced by protoplasts of *Saccharomyces cerevisiae* in liquid media: an electronmicroscopic, X-ray diffraction and chemical study. *J. Gen. Microbiol.* **92,** 207-220.

Kurtz, M.B.; Abruzzo, G.; Flattery, A.; Bartizal, K.; Marrinan, J.A.; Li, W.; Milligan, J.; Nollstadt, K. & Douglas, C.M. (1996) Characterization of echinocandin-resistant mutants of *Candida albicans*: genetic, biochemical, and virulence studies. *Infect. Immun.* **64,** 3244-3251.

Kurtz, M.B. & Rex, J.H. (2001) Glucan synthase inhibitors as antifungal agents. *Adv. Protein. Chem.* **56,** 423-475.

Kyte, J. & Doolittle, R.F. (1982) A simple method for displaying the hydropathic character of a protein. *J. Mol. Biol.* **157,** 105-132.

Latgé, J.P. (2001) The pathobiology of *Aspergillus fumigatus*. *Trends Microbiol.* **9,** 382-389.

Leal, J.A.; Guerrero, C.; Gomez-Miranda, B.; Prieto, A. & Bernabe, M. (1992) Chemical and structural similarities in wall polysaccharides of some *Penicillium*, *Eupenicillium* and *Aspergillus* species. *FEMS Microbiol. Lett.* **69,** 165-168.

Levinson, J.N.; Shahinian, S.; Sdicu, A.M.; Tessier, D.C. & Bussey, H. (2002) Functional, comparative and cell biological analysis of *Saccharomyces cerevisiae* Kre5p. *Yeast* **19,** 1243-1259.

Lipke, P.N. & Ovalle, R. (1998) Cell wall architecture in yeast: new structure and new challanges. *J. Bacteriol.* **180,** 3735-3740.

Lo, H.J.; Köhler, J.R.; DiDomenico, B.; Loebenberg, D.; Cacciapuoti, A. & Fink, G.R. (1997) Nonfilamentous *C. albicans* mutants are avirulent. *Cell* **90,** 939-949.

Manners, D.J. & Masson, A.J. (1969) The structures of two glucans from yeast-cell walls. *FEBS Lett.* **4,** 122-124.

Manners, D.J. & Meyer, M.T. (1977) The molecular structures of some glucans from the cell wall of *Schizosaccharomyces pombe*. *Carbohydr. Res.* **57,** 189-203.

Manners, D.J. & Patterson, J.C. (1966) A re-examination of the molecular structure of yeast glucan. *Biochem. J.* **98,** 19-20c.

Marshall, M.; Gull, K. & Jeffries, P. (1997) Monoclonal antibodies as probes for fungal wall structure during morphogenesis. *Microbiology* **143,** 2255-2265.

Mata, J.; Lyne, R.; Burns, G. & Bähler, J. (2002) The transcriptional program of meiosis and sporulation in fission yeast. *Nature Genet.* **32,** 143-147.

Mazur, P. & Baginsky, W. (1996) In vitro activity of 1→3-β-D-glucan synthase requires the GTP-binding protein Rho1. *J. Biol. Chem.* **271,** 14604-14609.

Mazur, P.; Morin, N.; Baginsky, W.; el-Sherbeini, M.; Clemas, J.A.; Nielsen, J.B. & Foor, F. (1995) Differential expression and function of two homologous subunits of yeast 1→3-β-D-glucan synthase. *Mol. Cell. Biol.* **15,** 5671-5681.

Meaden, P.; Hill, K.; Wagner, J.; Slipetz, D.; Sommer, S.S. & Bussey, H. (1990) The yeast *KRE5* gene encodes a probable endoplasmic reticulum protein required for (1→6)-β-D-glucan synthesis and normal cell growth. *Mol. Cell. Biol.* **10,** 3013-3019.

Mio, T.; Adachi-Shimizu, M.; Tachibana, Y.; Tabuchi, H.; Inoue, S.B.; Yabe, T.; Yamada-Okabe, T.; Arisawa, M.; Watanabe, T. & Yamada-Okabe, H. (1997) Cloning of the *Candida albicans* homolog of *Saccharomyces cerevisiae GSC1/FKS1* and its involvement in β-1→3-glucan synthesis. *J. Bacteriol.* **179,** 4096-4105.

Misaki, A.; Tsumuraya, Y. & Takaya, S. (1978) *Agric. Biol. Chem.* **42,** 491-493.

Mitchell, A.P. (1998) Dimorphism and virulence in *Candida albicans*. *Curr. Opin. Microbiol.* **1,** 687-692.

Miyazaki, T. & Naoi, Y. (1974) Chemical structure of the water-soluble glucan from the cell wall of *Cladosporium herbarum*. Studies on fungal polysaccharide. XV. *Chem. Pharm. Bull.* **22,** 2058-2063.

Mizuno, M.; Morimoto, M.; Minato, K. & Tsuchida, H. (1998) Polysaccharides from *Agaricus blazei* stimulate lymphocyte T-cell subsets in mice. *Biosc. Biotechnol. Biochem.* **62,** 424-427.

Mol, P.C.; Park, H.M.; Mullins, J.T. & Cabib, E. (1994) A GTP-binding protein regulates the activity of (1→3)-β-glucan synthase, an enzyme directly involved in yeast cell wall morphogenesis. *J. Biol. Chem.* **269,** 31267-31274.

Munro, C.A. & Gow, N.A. (2001) Chitin synthesis in human pathogenic fungi. *Med. Mycol.* **39 Suppl. 1,** 41-53.

Nishikawa, Y.; Kobayashi, S.; Shibata, S.; Fukuoka, F. & Maekawa, S. (1969) *J. Jpn. Biochem. Soc.* **41,** 632.

Obaidah, M.A. & Buck, K.W. (1971) Characterization of two cell-wall polysaccharides from *Fusicoccum amygdali*. *Biochem. J.* **125,** 473-480.

Ogawa, K.; Okamura, K. & Sarko, A. (1981) Molecular and crystal structure of the regenerated form of (1→3)-α-D-glucan. *Int. J. Biol. Macromol.* **3,** 31-36.

Ohyama, T. *et al.* (2000) Arborcandins A, B, C, D, E and F, novel 1→3-β-glucan synthase inhibitors: production and biological activity. *J. Antibiot.* **53,** 1108-1116.

Olafsdottir, E.S.; Ingolfsdottir, K.; Barsett, H.; Smestad Paulsen, B.; Jurcic, K. & Wagner, H. (1999) Immunologically active (1→3)-(1→4)-α-D-glucan from *Cetraria islandica*. *Phytomed.* **6,** 33-39.

Onishi, J. *et al.* (2000) Discovery of novel antifungal (1→3)-β-D-glucan synthase inhibitors. *Antimicrob. Agents. Chemother.* **44,** 368-377.

Osumi, M. (1998) The ultrastructure of yeast: cell wall structure and formation. *Micron* **29,** 207- 233.

Parodi, A.J. (1999) Reglucosylation of glycoproteins and quality control of glycoprotein folding in the endoplasmic reticulum of yeast cells. *Biochim. Biophys. Acta.* **1426,** 287-295.

Parra, E.; Jimenez-Barbero; Bernabe, M.; Leal, J.A.; Prieto, A. & Gomez-Miranda, B. (1994) Structural investigation of two cell-wall polysaccharides of *Penicillium expansum* strains. *Carbohydr. Res.* **257,** 239-248.

Peat, S.; Whelan, W.J.; Turvey, J.R. & Morgan, K. (1961) The structure of isolichenin. *J. Chem. Soc.* 623-629.

Peng, L.; Kawagoe, Y.; Hogan, P. & Delmer, D. (2002) Sitosterol-β-glucoside as primer for cellulose synthesis in plants. *Science* **295,** 147-150.

Perea, S.; Lopez-Ribot, J.L.; Kirkpatrick, W.R.; McAtee, R.K.; Santillan, R.A.; Martinez, M.; Calabrese, D.; Sanglard, D. & Patterson, T.F. (2001) Prevalence of molecular mechanisms of resistance to azole antifungal agents in *Candida albicans* strains displaying high-level fluconazole resistance isolated from human immunodeficiency virus-infected patients. *Antimicrob. Agents Chemother.* **45,** 2676-2684.

Pereira, M.; Felipe, M.S.; Brígido, M.M.; Soares, C.M. & Azevedo, M.O. (2000) Molecular cloning and characterization of a glucan synthase gene from the human pathogenic fungus *Paracoccidioides brasiliensis*. *Yeast*, **16,** 451-462.

Polacheck, I. & Rosenberger, R.F. (1977) *Aspergillus nidulans* mutant lacking α-(1→3)-glucan, melanin, and cleistothecia. *J. Bacteriol.* **132,** 650-666.

Qadota, H.; Python, C.P.; Inoue, S.B.; Arisawa, M.; Anraku, Y.; Zheng, Y.; Watanabe, T.; Levin, D.E. & Ohya, Y. (1996) Identification of yeast Rho1p GTPase as a regulatory subunit of 1→3-β-glucan synthase. *Science* **272,** 279-281.

Radding, J.A.; Heidler, S.A. & Turner, W.W. (1998) Photoaffinity analog of the semisynthetic echinocandin LY303366: identification of echinocandin targets in *Candida albicans*. *Antimicrob. Agents. Chemother.* **42,** 1187-1194.

Ralph, B.J. & Bender, V.J. (1965) Isolation of two new polysaccharides from the cell wall of *Polyporus tumulosus*. *Chem. Ind.* 1181.

Read, S.M. & Bacic, T. (2002) Prime time for cellulose. *Science* **295,** 59-60.

Reid, I.D. & Bartnicki-García, S. (1976) Cell-wall composition and structure of yeast cells and conjugation tubes of *Tremella mesenterica*. *J. Gen. Microbiol.* **96,** 35-50.

Ruhnke, M. & Maschmeyer, G. (2002) Management of mycoses in patients with hematologic disease and cancer - review of the literature. *Eur. J. Med. Res.* **7,** 227-235.

San-Blas, G. & Carbonell, L.M. (1974) Chemical and ultrastructural studies on the cell walls of the yeastlike and mycelial forms of *Histoplasma farciminosum*. *J. Bacteriol.* **119,** 602-611.

San-Blas, G.; Nino-Vega, G. & Iturriaga, T. (2002) *Paracoccidioides brasiliensis* and paracoccidioidomycosis: Molecular approaches to morphogenesis, diagnosis, epidemiology, taxonomy and genetics. *Med. Mycol.* **40,** 225-242.

San-Blas, G.; Padrón, R.; Alamo, L. & San-Blas, F. (1997) Use of morphology index histograms to quantify populations of the fungal pathogen *Paracoccidioides brasiliensis*. *Microbiology* **143,** 197-202.

San-Blas, G. & San-Blas, F. (1977) *Paracoccidioides brasiliensis*: cell wall structure and virulence. A review. *Mycopathologia* **62,** 77-86.

San-Blas, G.; San-Blas, F.; Ormaechea, E. & Serrano, L.E. (1977) Cell wall analysis of an adenine-requiring mutant of the yeast-like form of *Paracoccidioides brasiliensis* strain IVIC Pb9. *Sabouraudia* **15,** 297-303.

San-Blas, G. & Vernet, D. (1977) Induction of the synthesis of cell wall α-1→3-glucan in the yeastlike form of *Paracoccidioides brasiliensis* strain IVIC Pb9 by fetal calf serum. *Infect. Immun.* **15,** 897-902.

Sanchez Hernandez, M.E.; Garcia Mendoza, C. & Novaes-Ledieu, M. (1993) Two different alkali-soluble α-glucans in hyphal walls of the basidiomycete *Armillaria mellea*. *Microbiologia* **9,** 34-42.

Schoffelmeer, E.A.; Klis, F.M.; Sietsma, J.H. & Cornelissen, B.J. (1999) The cell wall of *Fusarium oxysporum*. *Fungal Genet. Biol.* **27,** 275-282.

Seo, K.; Akiyoshi, H. & Ohnishi, Y. (1999) Alteration of cell wall composition leads to amphotericin B resistance in *Aspergillus flavus*. *Microbiol. Immunol.* **43,** 1017-1025.

Shahinian, S. & Bussey, H. (2000) β-1→6-Glucan synthesis in *Saccharomyces cerevisiae*. *Mol. Microbiol.* **35,** 477-489.

Shaw, J.A.; Mol, P.C.; Bowers, B.; Silverman, S.J.; Valdivieso, M.H.; Durán, A. & Cabib, E. (1991) The function of chitin synthases 2 and 3 in the *Saccharomyces cerevisiae* cell cycle. *J. Cell Biol.* **114,** 111-123.

Shematek, E.M.; Braatz, J.A. & Cabib, E. (1980) Biosynthesis of the yeast cell wall. I. Preparation and properties of β-(1→3)glucan synthetase. *J. Biol. Chem.* **255,** 888-894.

Shida, M.; Uchida, T. & Matsuda, K. (1978) A (1→3)-α-D-glucan isolated from the fruit bodies of *Lentinus edodes*. *Carbohydr. Res.* **60,** 117-127.

Siehr, D. (1976) *Can. J. Biochem.* Studies on the cell wall of *Schizophyllum commune*. Permethylation and enzymic hydrolysis. **54,** 130-136.

Sietsma, J.H. & Wessels, J.G.H. (1977) Chemical analysis of the hyphal wall of *Schizophyllum commune*. *Biochim. Biophys. Acta* **496,** 225-239.

Sietsma, J.H. & Wessels, J.G.H. (1988) Total inhibition of wall synthesis by 2-deoxyglucose and polyoxin D in protoplasts of *Schizophyllum commune*. *Acta Bot. Neerl.* **37,** 23-29.

Sietsma, J.H. & Wessels, J.G.H. (1990) The occurrence of glucosaminoglycan in the wall of *Schizosaccharomyces pombe*. *J. Gen. Microbiol.* **136,** 2261-2265.

Silverman, S.J.; Sburlati, A.; Slater, M.L. & Cabib, E. (1988) Chitin synthase 2 is essential for septum formation and cell division in *Saccharomyces cerevisiae*. *Proc. Natl. Acad. Sci. U S A* **85,** 4735-4739.

Stefanovich, V. (1969) The structure and the biological activities of sulfopolyglucans - I. The biological activity of sulfoevernan. *Life Sci. Part I* **8,** 1223-1233.

Stuelp, P.M.; Carneiro Leao, A.M.A.; Gorin, P.A.J. & Iacomini, M. (1999) The glucans of *Ramalina celastri*: relation with chemotypes of other lichens *Carbohydr. Polym.* **40,** 101-106.

Takeda, T.; Funatsu, M.; Shibata, S. & Fukuoka, F. (1972) Polysaccharides of lichens and fungi. V. Antitumour active polysaccharides of lichens of *Evernia*, *Acroscyphus* and *Alectoria* spp. *Chem. Pharm. Bull.* **20,** 2445-2449.

Takeda, T.; Nishikawa, Y. & Shibata, S. (1970) A new α-glucan from the lichen *Parmalia caperata (L.) Ach*. *Chem. Pharm. Bull.* **18,** 1074-1075.

Takeo, K. & Matsuzaki, S. (1983) A simple preparation of α- and β-nigerose octaacetate and β-nigerotriose hendecaacetate by the acetolysis of an alkali-soluble D-glucan from the fruit body of *Laetiporus sulphureus*. *Carbohydr. Res.* **113,** 281-289.

Thomas, I. & Schwartz, R.A. (2001) Cutaneous manifestations of systemic cryptococcosis in immunosupressed patients. *J. Med.* **32,** 259-566.

Thompson, J.R.; Douglas, C.M.; Li, W.; Jue, C.K.; Pramanik, B.; Yuan, X.; Rude, T.H.; Toffaletti, D.L.; Perfect, J.R. & Kurtz, M. (1999) A glucan synthase *FKS1* homolog in *Cryptococcus neoformans* is single copy and encodes an essential function. *J. Bacteriol.* **181,** 444-453.

Tsumuraya, Y.; Misaki, A.; Takaya, S. & Torii, M. (1978) A new fungal α-D-glucan, elsinan, elaborated by *Elsinoe leucospila*. *Carbohydr. Res.* **66,** 53-65.

Valdivieso, M.H.; Durán, A. & Roncero, C. (1999) Chitin synthases in yeast and fungi. *EXS* **87,** 55-69.

Vries, O.M.H. de & Wessels, J.G.H. (1975) Chemical analysis of cell wall regeneration and reversion of protoplasts from *Schizophyllum commune*. *Arch. Microbiol.* **102,** 209-218.

Wessels, J.G.H.; Kreger, D.R.; Marchant, R.; Regensburg, B.A. & Vries, O.M.H. de (1972) Chemical and morphological characterization of the hyphal wall surface of the basidiomycete *Schizophyllum commune*. *Biochim. Biophys. Acta* **273,** 346-358.

Wessels, J.G.H. & Sietsma, J.H. (1982) Fungal cell walls: a survey. In: *Encyclopedia of plant physiology*; Pirson, A. & Zimmermann, M.H., Eds.; Springer Verlag: Berlin; Vol. 13B, pp. 352-394.

Whelan, W.J. (1998) Pride and prejudice: the discovery of the primer for glycogen synthesis. *Protein Sci.* **7,** 2038-2041.

Wong, H.C. *et al.* (1990) Genetic organization of the cellulose synthase operon in *Acetobacter xylinum*. *Proc. Natl. Acad. Sci. U S A* **87,** 8130-8134.

Wood, V. *et al.* (2002) The genome sequence of *Schizosaccharomyces pombe*. *Nature* **415,** 871- 880.

Yamochi, W.; Tanaka, K.; Nonaka, H.; Maeda, A.; Musha T. & Takai, Y. (1994) Growth site localization of Rho1 small GTP-binding protein and its involvement in bud formation in *Saccharomyces cerevisiae*. *J. Cell Biol.* **125,** 1077-1093.

Yokota, I. & Shibata, S. (1978) A polysaccharide of the lichen, *Stereocaulon japonicum*. *Chem. Pharm. Bull.* **26,** 2668-2670.

Yokota, I., Shibata, S. & Saitô, H. (1979) A ^{13}C-n.m.r. analysis of linkages in lichen polysaccharides: an approach to chemical taxonomy of lichens. *Carbohydr. Res.* **69,** 252-258.

Yoshida, I.; Kiho, T.; Usui, S.; Sakushima, M. & Ukai, S. (1996) Polysaccharides in fungi. XXXVII. Immunomodulating activities of carboxymethylated derivatives of linear (1→3)-α-D-glucans extracted from the fruiting bodies of *Agrocybe cylindracea* and *Amanita muscaria*. *Biol. Pharm. Bull.* **19,** 114-121.

Zhang, P.; Zhang, L & Cheng, S. (1999) Chemical structure and molecular weights of α- (1→3)-D-glucan from *Lentinus edodes*. *Biosc. Biotechnol.Biochem.* **63,** 1197-1202.

Zhang, P.; Zhang, L. & Cheng, S. (2000) Effects of urea and sodium hydroxide on the molecular weight and conformation of α-(1→3)-D-glucan from *Lentinus edodes* in aqueous solution. *Carbohydr. Res.* **327,** 431-438.

Zhang, P.; Zhang, L. & Cheng, S. (2002) Solution properties of an α-(1→3)-D-glucan from *Lentinus edodes* and its sulfated derivatives. *Carbohydr. Res.* **337,** 155-160.

Zhang, W.; DePaoli-Roach, A.A. & Roach, P.J. (1993) Mechanisms of multisite phosphorylation and inactivation of rabbit muscle glycogen synthase *Arch. Biochem. Biophys.* **304,** 219-225.

Zonneveld, B.J.M. (1971) Biochemical analysis of the cell wall of *Aspergillus nidulans*. *Biochim. Biophys. Acta* **249,** 506-514.

Zonneveld, B.J.M. (1972) The significance of a α-1→3-glucan of the cell wall and α-1→3-glucanase for cleistothecium development. *Biochim. Biophys. Acta* **273,** 174-187.

Zonneveld, B.J.M. (1973) Inhibitory effect of 2-deoxyglucose on cell wall α-1→3-glucan synthesis and cleistothecium development in *Aspergillus nidulans*. *Dev. Biol.* **34,** 1-8.

Zonneveld, B.J.M. (1974) α-1→3 glucan synthesis correlated with α-1→3 glucanase synthesis, conidiation and fructification in morphogenetic mutants of *Aspergillus nidulans*. *J. Gen. Microbiol.* **81,** 445-451.

Zonneveld, B.J.M. (1975a) Sexual differentiation in *Aspergillus nidulans*: the requirement for manganese and its effect on α-1→3-glucan synthesis and degradation. *Arch. Microbiol.* **105,** 101-104.

Zonneveld, B.J.M. (1975b) Sexual differentiation in *Aspergillus nidulans*: the requirement for manganese and the correlation between phosphoglucomutase and the synthesis of reserve material. *Arch. Microbiol.* **105,** 105-108.

Zonneveld, B.J.M. (1976) The effect of glucose and manganese on adenosine-3′,5′-monophosphate levels during growth and differentiation of *Aspergillus nidulans*. *Arch. Microbiol.* **108,** 41-44.

Chapter 2

Synthesis of cell-wall α-glucan requires coupling of two (1→3)-α-glucan segments and affects fission-yeast morphogenesis

Christian H. Grün[1], Frans Hochstenbach[2], Bruno M. Humbel[3], Arie J. Verkleij[3], J. Hans Sietsma[4], Frans M. Klis[5], Johannis P. Kamerling[1], and Johannes F.G. Vliegenthart[1]

[1]*Bijvoet Center, Department of Bio-Organic Chemistry, Section of Glycoscience and Biocatalysis and* [3]*Department of Molecular Cell Biology, Institute for Biomembranes, Utrecht University;* [2]*Department of Biochemistry, Academic Medical Center, University of Amsterdam;* [4]*Laboratory for Molecular Biology of Plants, Groningen Biomolecular Sciences and Biotechnology Institute (GBB);* [5]*Swammerdam Institute for Life Sciences, University of Amsterdam*

Abstract

Morphology and structural integrity of fungal cells depend on cell-wall polysaccharides. The chemical structure and biosynthesis of two types of these polysaccharides, chitin and (1→3)-β-glucan, have been studied extensively, whereas little is known about α-glucan. Here, we describe the chemical structure of α-glucan isolated from wild-type and mutant cell walls of fission yeast. Wild-type α-glucan was found to consist of a single population of linear glucose polymers, approximately 260 residues in length. These glucose polymers were composed of two covalently-linked building blocks, each comprising a (1→3)-α-D-glucan segment of approximately 135 glucose residues with at its reducing end a small number of (1→4)-linked α-D-glucose residues. In contrast, α-glucan of an α-glucan synthase mutant with an aberrant cell morphology and with reduced α-glucan levels consisted of a single building block only. We propose that α-glucan biosynthesis involves an ordered series of events, in which two α-glucan building blocks are synthesized independently and then coupled to form mature cell-wall α-glucan that is essential for fission-yeast morphogenesis.

Introduction

Cell morphogenesis involves distinct molecular processes, such as establishment and maintenance of morphology. An excellent model eukaryote for studying cell morphogenesis is fission yeast, *Schizosaccharomyces pombe* (Lindner), because this unicellular yeast has a cylindrical rod-like morphology, many mutants are available or engineerable, and its complete genome sequence is known (Wood *et al.*, 2002). Fission-yeast cells establish their characteristic cell morphology by growing out from their cell ends in a linear polarized fashion. Mutants have been isolated that are unable to establish proper cell polarity: they fail to localize zones of growth properly and therefore display aberrant cell morphologies, such as bent, branched, or rounded morphologies (Hayles & Nurse, 2001).

A second aspect of cell morphogenesis is maintenance of cell morphology. After zones of growth have been localized, fission-yeast cells must assemble their extracellular cell wall correctly to maintain cell morphology. The cell wall of fungi (including fission yeast) consists of polysaccharides with associated glycoproteins, the polysaccharides being directly responsible for cell-wall rigidity. Disruption of the assembly process of cell-wall polysaccharides may lead to cell lysis. For instance, mutations in synthases for cell-wall polysaccharides can cause cells to swell or lyse (Ishiguro *et al.,* 1997; Hochstenbach *et al.*, 1998). Because most fungi possess similar structural polysaccharides, enzymes involved in their assembly form ideal targets for the development of new classes of drugs against pathogenic yeasts and other fungi.

The major polysaccharides present in most fungal cell walls are chitin, (1→3)-β-glucan, and (1→3)-α-glucan. Chitin and (1→3)-β-glucan have been generally accepted as polysaccharides that are indispensable for maintaining rigidity and structural integrity of fungal cells, and their respective chemical structures and assembly processes have been characterized in detail (Klis *et al.*, 2002). Furthermore, drugs were identified that inhibit their synthase activities, causing osmotic fragility or lysis of fungal cells (Georgopapadakou & Tkacz, 1995; Beauvais & Latgé, 2001). In contrast, the role of (1→3)-α-glucan is still controversial. For instance, a mutant of the fungus *Aspergillus nidulans* was isolated that lacked cell-wall α-glucan but showed normal hyphal growth, indicating that α-glucan is not an essential cell-wall component (Zonneveld, 1972). In addition, complete inhibition of α-glucan biosynthesis with 2-deoxyglucose in regenerating protoplasts of *A. nidulans* or *Schizophyllum commune* did not interfere with normal outgrowth of hyphae (Zonneveld, 1973; Sietsma and Wessels, 1988). On the other hand, for a number of pathogenic dimorphic fungi, a correlation was observed between α-glucan levels and virulence as follows. *Histoplasma capsulatum* in its virulent yeast form had α-glucan levels of approximately 46% of total cell-wall carbohydrates, whereas the non-virulent mycelial form lacked α-glucan (Kanetsuna *et al.*, 1974). When a *H. capsulatum* yeast strain was isolated that showed no virulence for mice, α-glucan levels proved to be absent (Klimpel & Goldman, 1988), suggesting that cell-wall α-glucan might affect virulence (Kügler *et al.*, 2000). A similar relationship between α-glucan levels and virulence was found for the dimorphic fungi, *Blastomyces dermatitidis* (Hogan & Klein, 1994), and *Paracoccidioides brasiliensis* (San-Blas *et al.*, 1977a). Interestingly, in the latter pathogen, a mutant with increased levels of α-glucan was also investigated that showed a higher degree of virulence than the wild-type strain (San-Blas *et al.*, 1977b).

Despite its potential relevance for virulence, little was known about the biosynthesis of cell-wall α-glucan. In fission yeast, α-glucan was identified by Bacon *et al.* (1968). Later, Bush *et al.* (1974) showed that the fission-yeast cell wall contained galactomannan (9-14% of total cell wall), β-glucan (42-55%), and α-glucan (28%). They also showed that their α-glucan fraction mainly consisted of (1→3)-linked α-glucose, with approximately 7% of (1→4)-glycosidic linkages. Whether these (1→4)-linkages are part of cell-wall α-glucan or represent contamination by intracellular glycogen had remained uncertain. More recently, we described a temperature-sensitive mutant, *ags1-1*^{ts}, with a point mutation in a gene responsible for α-glucan biosynthesis (Hochstenbach *et al.*, 1998). This mutant displayed a temperature-dependent cell morphology: at a permissive temperature of 19 °C, cells had a rod-like morphology similar to that of wild-type cells, whereas at a semi-permissive temperature of 34 °C, they were rounded, indicating that their cell walls had weakened. This change in cell morphology correlated with a threefold reduction in cell-wall α-glucan levels. Finally, at a restrictive temperature of 37 °C, *ags1-1*^{ts} cells lysed, demonstrating that α-glucan is essential for maintaining the integrity of fission-yeast cells.

Based on amino-acid sequence similarities, we proposed a model for the function of the putative α-glucan synthase, Ags1. In brief, we suggested that Ags1p consists of three domains: an intracellular domain for synthesis of α-glucan, a multipass transmembrane domain that might form a pore-like structure for transport of α-glucan across the plasma membrane, and an extracellular transglycosylase domain for linking or remodelling of α-glucan. This model provided a framework for addressing the molecular mechanism of α-glucan biosynthesis, in terms of chain initiation, elongation, and termination. For example, we wish to know whether a primer is used in chain initiation, how many glucose residues are added during chain elongation, and whether chain termination is subject to tight control.

Here, we focus on the chemical structure of α-glucan in fission yeast to gain insight into the molecular mechanism of its biosynthesis. By using high-performance size-exclusion chromatography (HPSEC) in combination with chemical analyses and NMR spectroscopy, we found that α-glucan of both wild-type cells and *ags1-1*^{ts} mutant cells with a rod-like morphology (grown at 19 °C) consisted of two building blocks. In contrast, α-glucan isolated from *ags1-1*^{ts} mutant cells with a rounded morphology (grown at 34 °C) consisted of a single building block only. These data suggest that the Ags1 protein is involved in the coupling of α-glucan building blocks. We conclude that both the synthase domain and the transglycosylase domain of the Ags1 protein are essential for α-glucan biosynthesis and speculate that both domains are suitable targets for the development of novel antifungal drugs.

Results

α-Glucan has an essential role in maintaining cell morphology

To gain insight into the role of α-glucan in cell morphogenesis, we took advantage of a mutant strain, *ags1-1*^{ts}, that is defective in the synthesis of α-glucan. When grown at the semi-permissive temperature of 34 °C, cells of this mutant strain, FH021, display a rounded morphology, osmotic sensitivity, and a threefold reduction in cell-wall α-glucan levels (Hochstenbach *et al.*, 1998). By using glass beads, we mechanically broke these rounded cells as well as rod-shaped cells of a matching wild-type strain, FH023, and visualized isolated cell walls by transmission electron microscopy. This lysis method preserved the typical rod-like morphology of wild-type cell walls and the rounded morphology of the mutant cells, distorted only by marks of glass bead impact (**Fig. 1, A** and **B**, see arrows).

To visualize the α-glucans of the cell walls, we specifically removed all cell-wall components except α-glucan, using the following mild isolation method that does not degrade its chemical structure. This method is based on the observation that the *S. pombe* cell wall lacks significant amounts of chitin and consists mainly of water-insoluble α-glucans and β-glucans, with associated glycoproteins. Digestion of the cell walls with Zymolyase, a purified mixture of β-glucanases and proteases, solubilizes the β-glucans and glycoproteins but keeps α-glucans intact. After Zymolyase digestion, the α-glucan fraction was isolated by centrifugation and the pellet fraction was extracted with a hot SDS solution to remove non-covalently linked material. This α-glucan preparation did not contain detectable β-glucans, as determined by NMR spectroscopy (see below). When analyzed by transmission electron microscopy, the α-glucan fraction of wild-type cell walls retained a rod-like morphology (**Fig. 1C**), whereas mutant cell walls disintegrated upon Zymolyase digestion (**Fig. 1D**). In both cases, the α-glucans retained a microfibrillar structure (**Fig. 1, C** and **D**, insets), indicating that this isolation method preserves their native structures. Together, these data demonstrate that wild-type α-glucan is essential for maintenance of the rod-like morphology of wild-type fission-yeast cells.

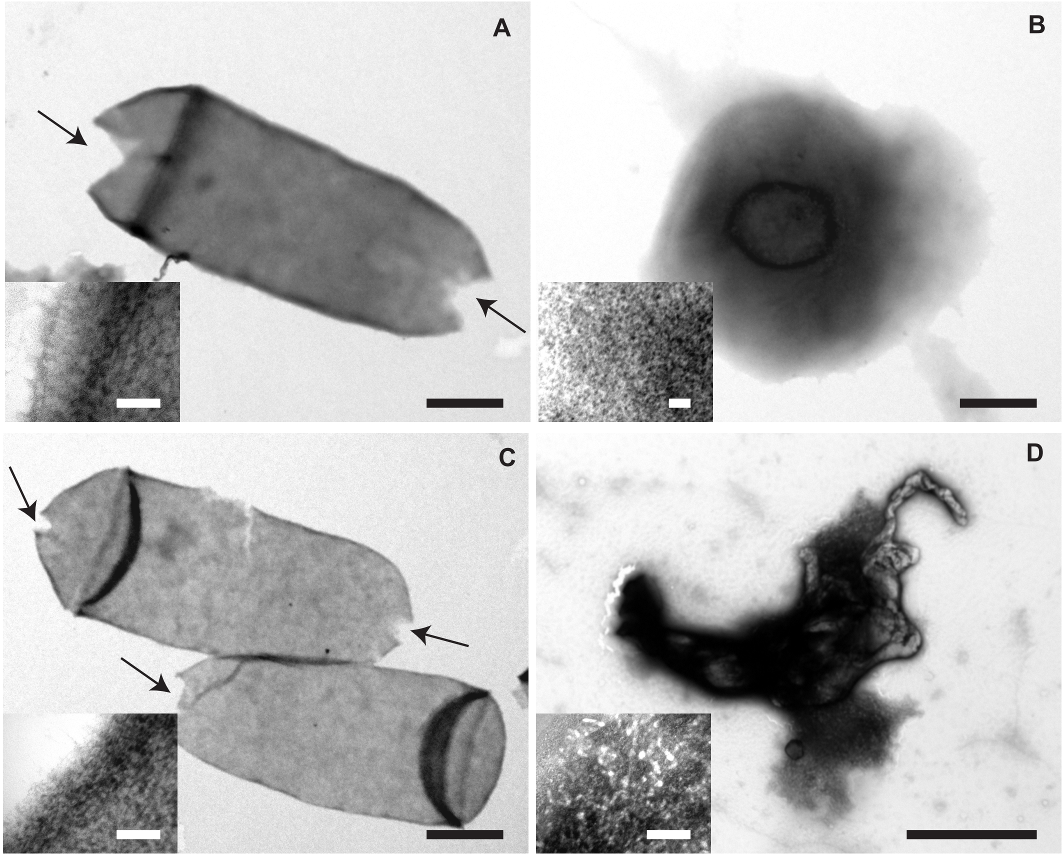

Fig. 1. α-Glucan of wild-type cell walls maintains a rod-like morphology, whereas α-glucan of rounded *ags1-1*^{ts} cells collapses after removal of β-glucan and glycoproteins. Electron micrographs of whole cell walls (**A**) and Zymolyase-treated cell walls (**C**) of wild-type strain FH023, and whole cell walls (**B**) and Zymolyase-treated cell walls (**D**) of *ags1-1*^{ts} mutant strain FH021 grown at 34 °C. Note that after the Zymolyase treatment, the wild-type cell walls maintained their rod-like morphology, whereas the mutant cell walls collapsed into loose fragments. Note also that lysis by using glass beads introduced only localized destruction (indicated by arrows), preserving most cell-wall polysaccharides. Bar represents 2 µm in the main micrographs and 100 nm in the insets.

α-Glucan consists of a single population of polymers

We wondered whether α-glucan is linked covalently to other cell-wall components, or whether it forms a separate population of molecules. To pursue this, we analyzed wild-type cell walls of strain FH023 by high-performance size-exclusion chromatography (HPSEC). Cell-wall preparations were dried completely, dissolved in dimethyl sulfoxide (DMSO), and analyzed on a calibrated mixed-bed column with a fractionation range of 0.2-2000 kDa. The size-exclusion chromatogram of whole wild-type cell walls shows three strongly overlapping peaks in the range of approximately 10-1000 kDa (**Fig. 2A**, profile I), suggesting that the *S. pombe* cell wall consists of three distinct populations of polymers. We then used HPSEC to analyze the α-glucan preparation isolated from wild-type cells (see above). Digestion of whole cell walls with Zymolyase reduced the chromatogram to a single, Gaussian-curved distribution, eluting at the same volume as the population of whole cell walls with the lowest molecular mass (**Fig. 2A**, profile II, see arrow). These data indicate that α-glucan consists of a single population of glucose polymers. Based on retention times, we infer that the cell-wall polymer population with the lowest molecular mass corresponds to α-glucan, indicating that it is not linked covalently to other polymers, such as β-glucans.

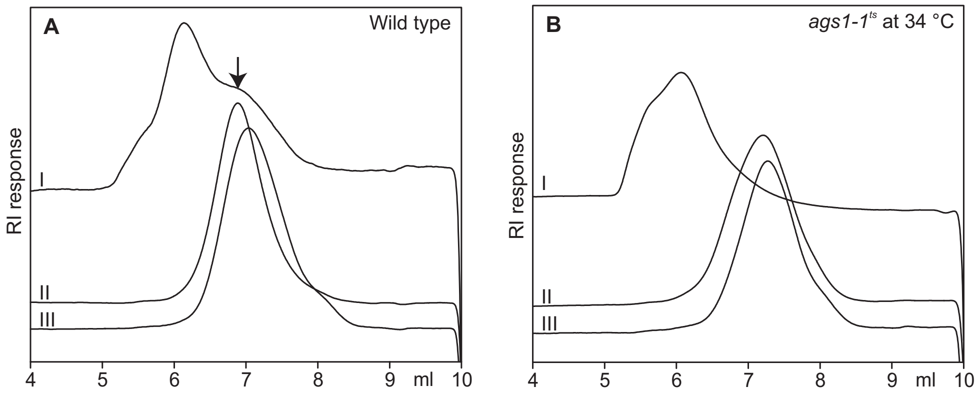

Fig. 2. Wild-type α-glucan is composed of two α-glucan segments, whereas mutant α-glucan is composed of only a single segment. Molecular mass distributions of untreated cell walls (**I**), Zymolyase-treated cell walls (**II**), Zymolyase-treated and Smith-degraded cell walls (**III**), isolated from wild-type strain FH023 (**A**), or *ags1-1*^{ts} mutant strain FH021 grown at 34 °C (**B**). Note that whole cell walls of wild-type cells reveal three DMSO-soluble polysaccharide populations, of which the population with the lowest molecular mass corresponds to α-glucan (marked by arrow). The relative intensity of this peak strongly decreased when growing the *ags1-1*^{ts} mutant at 34 °C, which is consistent with a threefold reduction in α-glucan levels. Smith degradation decreased the molecular mass distribution of α-glucan isolated from wild-type cells, but hardly affected the distribution of α-glucan isolated from *ags1-1*^{ts} mutant cells grown at 34 °C. Dried cell-wall preparations were dissolved in DMSO containing 3 mM sodium nitrate and their molecular mass distributions were analyzed by HPSEC on a calibrated mixed-bed column.

The discrete, Gaussian-curved nature of the α-glucan peak allowed the calculation of the molecular-mass distribution of the α-glucan population, yielding a number-average molecular mass (Mn) of 41.7 ± 5.7 kDa (mean ± SD; n = 3). This molecular mass is equivalent to a number-average degree of polymerization (DP_n) of 257 ± 35 (**Table I**). These data are in accordance with data obtained by Manners and Meyers (1977), reporting a DP_n of 207 for one of their α-glucan containing cell-wall fractions derived from *S. pombe* strain C-277.

Table I. Molecular mass averages and polydispersities of wild-type and mutant α-glucan

	Mn (kDa)	Mw (kDa)	Mw/Mn	DP_n
Wild type	41.7 ± 5.7	102.1 ± 9.5	2.47 ± 0.21	257 ± 35
Wild type, Smith degraded	22.5 ± 2.8	61.8 ± 8.4	2.75 ± 0.02	137 ± 18
ags1-1^{ts}	21.9 ± 0.7	63.5 ± 5.5	2.91 ± 0.31	135 ± 4
ags1-1^{ts}, Smith degraded	18.9 ± 2.2	50.4 ± 12.3	2.63 ± 0.33	116 ± 13

To assess the variation in α-glucan length, we determined the polydispersity of the α-glucan population. Polydispersities (weight-average molecular mass/Mn) of naturally occurring polysaccharides vary between 1.1 for alkali-soluble β-glucans from *Saccharomyces cerevisiae* (Williams *et al.*, 1994) to 35 for corn starch (Chuang, 1990). In α-glucan of strain FH023, we found a polydispersity of 2.38 ± 0.21, indicating a relatively narrow molecular-mass distribution. Together, these results show that in the *S. pombe* cell wall, α-glucan polymers consist of approximately 260 glucose residues. The length of these polymers is regulated tightly, suggesting that only a single α-glucan synthase system may be responsible for its biosynthesis.

α-Glucan consists of (1→3)-linked and (1→4)-linked glucose residues

The uniform nature of α-glucan enabled us to investigate its chemical structure. By using monosaccharide analysis including the determination of absolute configurations we found that D-glucose was almost the only monosaccharide present. Besides D-glucose, only variable trace amounts of mannose were found, while no *N*-acetyl glucosamine was detected. Linkage analysis showed that α-glucan consisted for 88.9 ± 1.0% (mean ± SD; n = 3) of (1→3)-linked glucose residues, with 9.0 ± 0.3% of (1→4)-linked residues (**Table II**). These data are in good agreement with the data of Bush and colleagues (1974), who observed approximately 7% of (1→4)-linked glucose residues in α-glucan of *S. pombe* strain, CBS351.

To independently verify our data from the chemical analyses and to determine the anomeric configuration of the constituents, we used one-dimensional ^{1}H-NMR and two-dimensional ^{1}H-^{13}C (HSQC) and ^{1}H-^{1}H (TOCSY) NMR spectroscopy. The ^{1}H-NMR and ^{13}C-NMR data are summarized in **Table III**. Two anomeric signals are present in the ^{1}H-NMR spectrum (**Fig. 3A**, horizontal axis), a signal of high intensity at 5.092 ppm

Table II. Linkage analysis of wild-type and mutant α-glucan

Residue	Molar amounts (%)	
	Wild type	*ags1-1*^{ts}
Glc*p*-(1→	1.1 [1]	2.6 [1]
→3)-Glc*p*-(1→	89.9	91.6
→4)-Glc*p*-(1→	9.0	5.8
→3,6)-Glc*p*-(1→ [2]	trace	trace
→3,4)-Glc*p*-(1→ [2]	trace	trace
→3,2)-Glc*p*-(1→ [2]	trace	trace

[1] Percentages of non-reducing ends appeared to be too high due to overlap with a contaminating compound.
[2] Using GLC-MS, variable traces of triple substituted glucose residues were detected, indicating undermethylation rather than branching points.

(denoted H-1_A) and one of low intensity at 5.139 ppm (denoted H-1_B). These signals indicate the presence of two distinct structural elements, denoted A and B, respectively. For the major constituent A, signals at 4.834, 4.435, and 4.128 ppm could be assigned to hydroxyl protons, because they do not produce cross-peaks in the HSQC spectrum (**Fig. 3A**, central panel). Using TOCSY, these signals were assigned to OH-4_A, OH-2_A, and OH-6_A, respectively (**Fig. 3B**). The absence of an OH-3_A hydroxyl signal in the ^{1}H-NMR spectrum together with a down-field shift of C-3_A at 82.7 ppm in the ^{13}C-NMR spectrum demonstrate that the major constituent A is (1→3)-linked. Because the $^3J_{1,2}$ coupling constant of 3.9 Hz and the low-field anomeric proton signal at 5.092 ppm are typical for an α-anomeric configuration, we conclude that the major constituent is (1→3)-linked α-glucan.

The minor constituent B also has an α-anomeric configuration, because of its low-field anomeric proton signal at 5.139 ppm and its $^3J_{1,2}$ coupling constant of 3.8 Hz (**Fig. 3A**, peak denoted H-1_B). In TOCSY and HSQC experiments, we identified C-4_B at a low-field chemical shift of 78.5 ppm, demonstrating that in constituent B, C-4 was involved in a glycosidic linkage. In addition, ^{13}C chemical shifts of all observed carbon atoms were found to be in good agreement with those obtained from amylose (data not shown). Together, these data demonstrate that the minor constituent is (1→4)-linked α-glucose. Signals corresponding to β-glucan were not detected by NMR spectroscopy (i.e., below the detection limit of 0.5%).

Although cell-wall α-glucan forms a single polymer population, as observed in HPSEC, we wished to exclude contamination by an independent but overlapping population of glycogen or amylose polymers. By staining cell lysates with iodine, we showed that glycogen and amylose contents were negligible in exponentially growing haploid cells, whereas they were easily detectable in sporulating diploids (data not shown). Furthermore, digestion with α-amylase or glucoamylase did not solubilize any detectable material (data not shown). These results indicate that the (1→4)-linked glucose residues form an integral part of cell-wall α-glucan molecules. In conclusion, our results show that fission-yeast α-glucan comprises a polysaccharide consisting mainly of (1→3)-linked α-glucose residues, with approximately 9% of (1→4)-linked α-glucose residues.

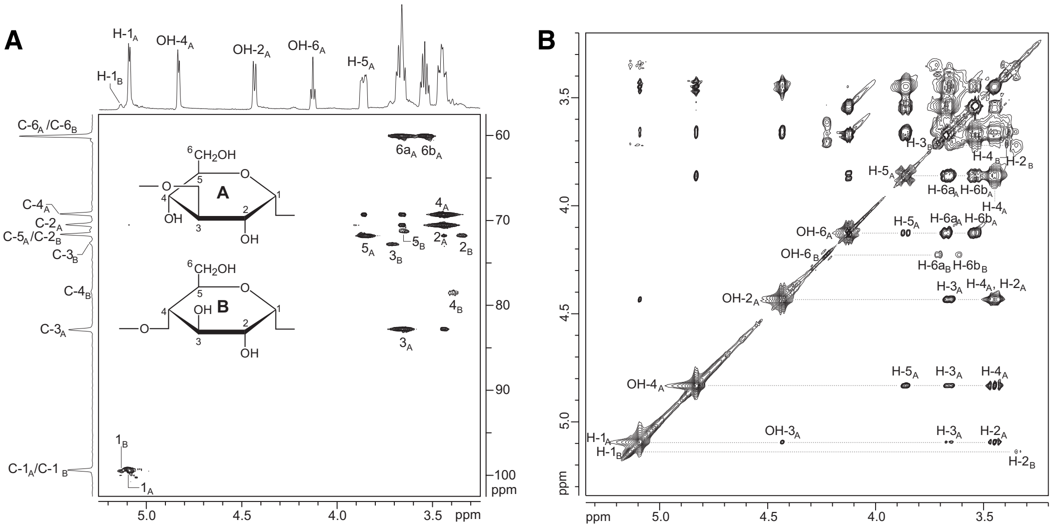

Fig. 3. α-Glucan consists of (1→3)-linked α-glucose residues with some (1→4)-linked residues. ^{1}H (horizontal axis), ^{13}C (vertical axis), and HSQC (**A**) and 50 ms TOCSY (**B**) NMR spectra of α-glucan from wild-type strain FH023. Samples were dissolved in DMSO-d_6 and the spectra were recorded at 500.08 MHz at 80 °C. The major constituent (denoted A) is (1→3)-linked α-glucose, whereas the minor constituent (denoted B) is (1→4)-linked α-glucose. Note that the down-field chemical shifts of C-3$_A$ and C-4$_B$ typify (1→3)-linked and (1→4)-linked glucose residues, respectively. Also note that the relative positions of the anomeric signals for both constituents (denoted H-1$_A$ and H-1$_B$) are typical for an α-anomeric configuration. Due to the obtained high signal-to-noise ratio required to study the minor constituent, long-range magnetization transfer signals of the major constituent were observed in the HSQC spectrum in addition to the single bond magnetization transfer signals. In fact, these 2-bond couplings facilitated the assignment of the spectrum.

Table III. Chemical shifts for α-glucan from *S. pombe* in DMSO-d_6 at 80 °C

Constituent **A** ((1→3)-α-Glc*p*)				Constituent **B** ((1→4)-α-Glc*p*)			
Proton	PPM	Carbon	PPM	Proton	PPM	Carbon	PPM
H-1	5.092	C-1	99.2	H-1	5.133	C-1	99.8
H-2	3.453	C-2	70.5	H-2	3.352	C-2	71.7
H-3	3.665	C-3	82.7	H-3	3.714	C-3	72.9
H-4	3.453	C-4	69.3	H-4	3.390	C-4	78.5
H-5	3.863	C-5	71.8	H-5	3.652	C-5	71.2
H-6a	3.669	C-6	60.0	H-6a	3.701	C-6	n.d. [1]
H-6b	3.541			H-6b	3.612		
OH-2	4.435			OH-2	n.d. [2]		
OH-4	4.83			OH-4	n.d. [2]		
OH-6	4.128			OH-6	4.231		

[1] The chemical shift corresponding to C-6$_B$ could not be determined due to overlap by C-6$_A$.

[2] Chemical shifts of OH-2$_B$ and OH-3$_B$ could not be determined. By analyzing a (1→4)-α-glucan preparation (amylose), these signals were found to occur around 5.1 ppm and therefore overlap with the H-1 signal of (1→3)-linked α-glucose.

α-Glucan is a linear polysaccharide consisting of two (1→3)-α-glucan segments

The (1→4)-linked residues must be embedded within linear polymers of (1→3)-linked residues, because no branching points could be detected in our linkage analysis (**Table II**). To determine whether the (1→4)-linked glucose residues were distributed randomly along the α-glucan chain or whether they were located at specific positions, we removed them selectively by periodate oxidation followed by acid hydrolysis (Smith degradation), and analyzed the remaining (1→3)-linked α-glucan by using HPSEC. If the (1→4)-linked glucose residues were distributed randomly, Smith degradation would result in a population of reaction products with a polydispersity increased significantly over that of native α-glucan, which was 2.38 ± 0.21. However, the Smith-degraded material eluted as a Gaussian-curved peak with a polydispersity of only 2.75 ± 0.02 (**Table I**), indicating that the (1→4)-linked residues must be located at specific positions.

To distinguish between the presence of (1→4)-linked residues at the reducing or non-reducing end and in the center, we measured the molecular mass of the reaction products. Smith-degraded α-glucan had an Mn of 22.5 ± 2.8 kDa (mean ± SD; n = 3) (**Fig. 2A**, profile III), which is equivalent to a DP_n of 137 ± 18 (**Table I**). Remarkably, this size is approximately half that of native α-glucan, which is 41.7 ± 5.7 kDa, equivalent to 257 ± 35 glucose residues (see above). Data indistinguishable from these on α-glucan of wild-type *S. pombe* strain FH023 were obtained for α-glucans of another wild-type strain, 972, and a nonsporulating diploid strain, FH058 (data not shown). Importantly, similar data were obtained for α-glucan of the *ags1-1*^{ts} mutant grown at the permissive temperature of 19 °C (not shown). These data show that Smith degradation divides wild-type α-glucan into two halves, demonstrating that there are (1→4)-linked glucose residues located in the center where they connect two segments of approximately 135 (1→3)-linked glucose residues.

(1→4)-linked α-glucose homooligosaccharide at the reducing end of α-glucan

Our results so far do not exclude the presence of additional (1→4)-linked glucose residues at the non-reducing or the reducing end. Treatment of the α-glucan preparation with glucoamylase, an *exo*-glucanase that hydrolyzes α-glycosidic (1→4)-linkages starting from the non-reducing end, did not result in release of glucose, providing no evidence for the presence of (1→4)-linked glucose residues at the non-reducing end of cell-wall α-glucan. To determine the type of linkage at the reducing end, we subjected α-glucan to controlled β-elimination, a chemical cleavage reaction, which occurs under alkaline conditions and which starts from the reducing end, progressing slowly towards the non-reducing end. β-Elimination can give detailed information on the type of linkages at the reducing end, because degradation products released into the medium are characteristic for the type of linkage. Specifically, isosaccharinic acids are formed from 4-substituted glucose at the reducing end, whereas metasaccharinic acids are formed from 3-substituted glucose at the reducing end (Kennedy & White, 1971; Whistler & BeMiller, 1958) (**Fig. 4**, reaction scheme).

As a reference for (1→4)-linked glucan, we incubated amylose in a saturated solution of calcium hydroxide for five days, and analyzed the hydrolysis products by GLC-MS after trimethylsilylation. In this analysis, both isosaccharinic acid isomers could be resolved as individual peaks of equal size (**Fig. 4A**, peaks I_a and I_b). As a reference for (1→3)-linked glucan, we used Smith-degraded cell-wall α-glucan or laminaran, a (1→3)-linked β-glucan. The released metasaccharinic acid isomers, however, could not be resolved individually, producing a single peak at a retention time identical to that of one of the isosaccharinic acid isomers (**Fig. 4B**, peak $II_{a,b}$, and data not shown). Thus, when we analyzed nigeran, an α-glucan with alternating (1→4)-linkages and (1→3)-linkages, we observed an equal mixture of isosaccharinic and metasaccharinic acids, eluting as two unequally-sized peaks (**Fig. 4C**, peaks I_a+$II_{a,b}$ and I_b).

We then carried out β-elimination of cell-wall α-glucan and analyzed the hydrolysis products at different time points. Immediately after the start of the reaction, no isosaccharinic or metasaccharinic acids were detected (**Fig. 4D**). However, after an incubation period of one day, we observed the release of both isosaccharinic acids and metasaccharinic acids in approximately equal amounts. This nearly equal ratio hardly changed in the course of five days (**Fig. 4E**). Linkage analysis showed that after a five-day incubation approximately 25 percent of the (1→4)-linked glucose residues had been hydrolyzed, whereas HPSEC analysis showed that the molecular mass distribution of the treated α-glucan had hardly changed (data not shown). Together, these data demonstrate that (1→4)-linked α-glucose residues are present at the reducing end.

The 4-substituted glucose residues at the reducing end of α-glucan may be part of a stretch of alternating (1→3)-linked and (1→4)-linked residues, or they may form a (1→4)-linked homooligosaccharide. To distinguish between these possibilities, we digested α-glucan with (1→3)-α-glucanase and analyzed individual reaction products. No alternating (1→3)-linked and (1→4)-linked residues were identified; instead, all reaction products that were characterized contained several sequential (1→4)-linked glucose residues (see Chapter 3). The release of metasaccharinic acids found here is explained by trace amounts of contaminating (1→3)-β-glucan that had not been removed completely by Zymolyase digestion and were not observed by NMR spectroscopy. Even very small amounts would largely influence our β-elimination results, especially since 3-substituted glucose residues are degraded approximately ten times faster than 4-substituted residues (Kennedy & White, 1979). Taken together, these data indicate that, in addition to the center, (1→4)-linked glucose residues occur at the reducing end of α-glucan. We interpret these data to mean that in *S. pombe*, cell-wall α-glucan is constructed from two building blocks, each composed of a linear (1→3)-α-glucan segment of approximately 135 residues containing some (1→4)-linked α-glucose residues at their reducing end.

ags1-1$^{\text{ts}}$ **mutant is unable to synthesize mature cell-wall α-glucan**

We next characterized the chemical structure of α-glucan present in low amounts in the cell walls of rounded *ags1-1*$^{\text{ts}}$ cells grown at 34 °C. Based on dry weights, we determined

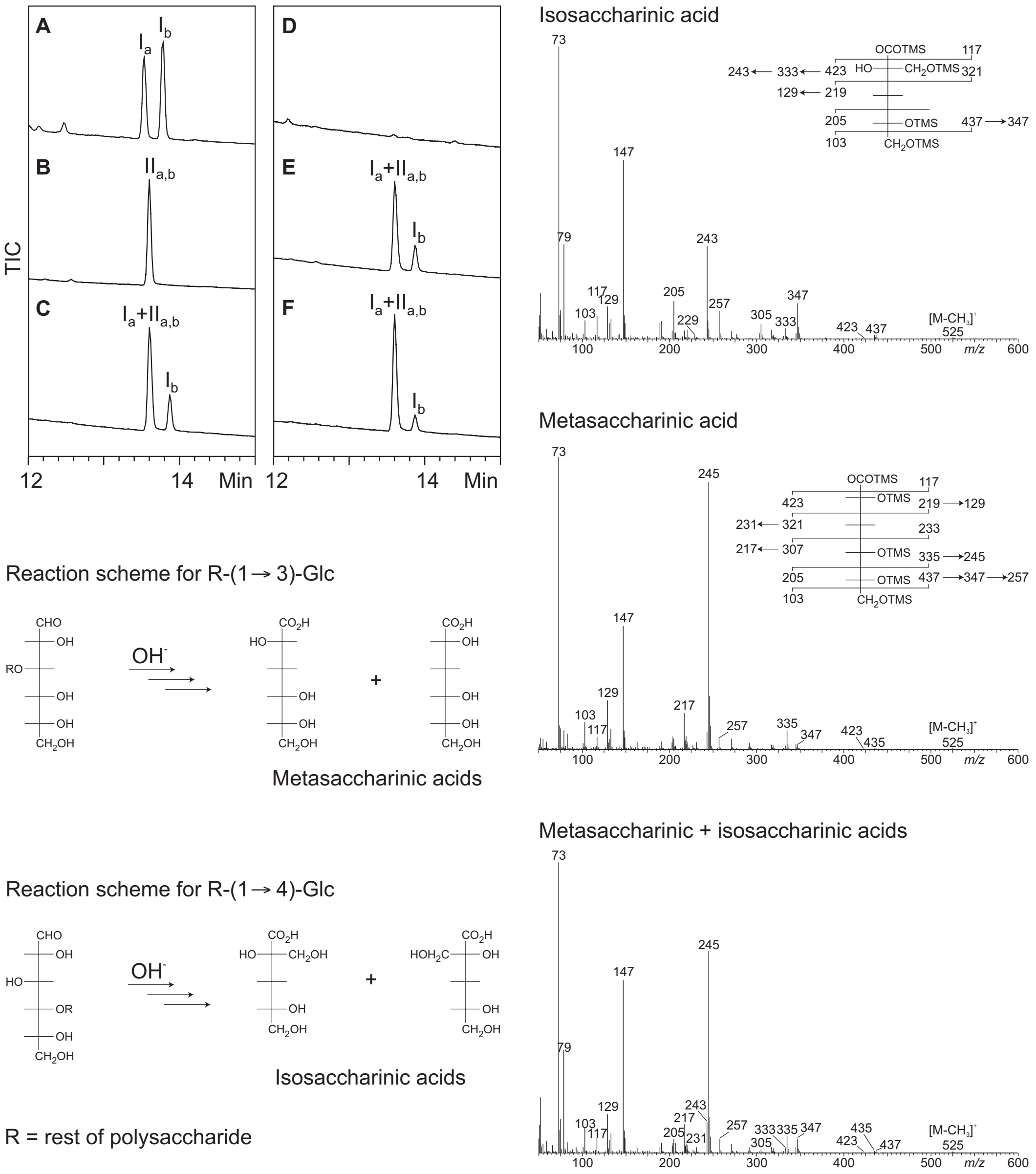

Fig. 4. α-Glucan of wild-type and mutant cell walls have (1→4)-linked glucose residues at their reducing ends. GLC chromatograms of β-elimination products of the following glucans: amylose ((1→4)-α-glucan) (**A**); Smith degraded *S. pombe* cell-wall α-glucan ((1→3)-α-glucan) (**B**); nigeran (α-glucan with alternating (1→3) and (1→4) linkages) (**C**); wild-type α-glucan at t = 0 (**D**), or after 5 days (**E**); α-glucan of *ags1-1*^{ts} mutant cells grown at 34 °C, after 5 days (**F**). Note that β-elimination of terminal 4-substituted glucose released two isosaccharinic acid isomers (denoted I_a and I_b; see also the reaction scheme below and the mass spectrum on the right), whereas β-elimination of terminal 3-substituted glucose released two metasaccharinic acid isomers (denoted $II_{a,b}$; see reaction scheme) that were not separated but identified by EI-MS (see mass spectrum on the right).

that α-glucan levels at 34 °C had decreased by a factor of 2.8, from 14.8% of whole cell walls at 19 °C to 5.3%. These data confirm our previous results using phenol-sulfuric acid measurements of cell-wall carbohydrate content (Hochstenbach *et al.*, 1998). Linkage analysis and ^{1}H-NMR spectroscopy showed that α-glucan of *ags1-1*^{ts} cell walls consisted mainly (91.6%) of (1→3)-linked α-glucose residues, with 5.8% of (1→4)-linked α-glucose residues (**Table III**), indicating that α-glucan of the *ags1-1*^{ts} mutant has a basic composition similar to that of wild-type α-glucan. However, when we analyzed its molecular-mass distribution, we made an unexpected observation. Although the HPSEC profile of the mutant α-glucan again showed a single, Gaussian-shaped peak, its Mn was calculated to be only 21.9 ± 0.7 kDa, which was equivalent to a DP_n of 135 ± 4 (**Fig. 2B**, profile II; **Table I**). This molecular mass is similar to that of Smith-degraded α-glucan, which was 22.5 ± 2.8 kDa equivalent to 137 ± 18 glucose residues (see above). The polydispersity of the mutant α-glucan was 2.91 ± 0.31, indicating a uniform population of polymers. Smith degradation slightly affected its characteristics, giving an Mn of 18.9 ± 2.2 kDa (equivalent to a DP_n of 116 ± 13 glucose residues), with a polydispersity of 2.63 ± 0.33 (**Fig. 2B**, profile III; **Table I**). Together, these results indicate that mutant α-glucan consists of a single (1→3)-α-glucan segment of approximately 120 residues with some (1→4)-linked glucose residues at one of its ends.

To determine whether these (1→4)-linked glucose residues are present at the non-reducing or reducing end, mutant α-glucan was subjected to glucoamylase digestion or β-elimination. Glucoamylase treatment did not result in the release of any glucose residues, providing no evidence for the presence of (1→4)-linked glucose residues at the non-reducing end. Next, we performed a β-elimination on mutant α-glucan in the same way as was done with wild-type α-glucan (see above). After five days of incubation, both isosaccharinic and metasaccharinic acids were released, as is evident from GLC-MS analysis of the trimethylsilylated products (**Fig. 4F**). Linkage analysis of the mutant α-glucan remaining after 5 days of incubation showed a 30% decrease in (1→4)-linked residues, while its HPSEC profile showed a slight shift in Mn from 22 to 18 kDa. These results demonstrate the presence of (1→4)-linked glucose residues at the reducing end of mutant α-glucan. In summary, our data show that in the cell wall of rounded *ags1-1*^{ts} cells, α-glucan was composed of only a single building block, namely a (1→3)-α-glucan segment of approximately 120 glucose residues, with some (1→4)-linked glucose residues attached to its reducing end. We conclude that *ags1-1*^{ts} mutant cells grown at a semi-permissive temperature are unable to couple α-glucan building blocks.

Discussion

Ags1p is involved in coupling α-glucan building blocks

Here we show that cell-wall α-glucan of vegetatively-grown fission-yeast cells consists of a single population of polysaccharides composed of two building blocks. In turn, each building block consists of a (1→3)-α-D-glucan segment of approximately 135 glucose residues with a number of (1→4)-linked α-D-glucose residues at its reducing end (**Fig. 5A**). Remarkably, cell-wall α-glucan of a mutant with a point mutation (G696S) in the extracellular domain of the α-glucan synthase, Ags1p, is composed of only a single building block (**Fig. 5A**), indicating that α-glucan building blocks could not be coupled in this mutant. To our knowledge, these results demonstrate for the first time that linear polysaccharides can be assembled by coupling of individual building blocks.

Model for α-glucan biosynthesis

To elucidate how the Ags1 protein may produce mature cell-wall α-glucan, we propose the following model (**Fig. 5B)**. First, the Ags1p intracellular domain synthesizes a first building block. This is then transported across the plasma membrane, perhaps via the Ags1p multipass transmembrane domain. Once transported, the Ags1p extracellular domain retains this first building block. Then, the same Ags1 protein initiates a second round of synthesis, and also transport the second building block across the plasma membrane. Finally, the Ags1p extracellular domain acts as a transglycosylase and couples both building blocks, thereby forming a mature cell-wall α-glucan molecule. This mature α-glucan molecule is then released into the cell-wall area, allowing synthesis of a following α-glucan molecule.

We speculate that the (1→4)-linked α-D-glucose residues at the reducing end of each α-glucan building block might constitute a primer for chain initiation (**Fig. 5B**, **step 1**). Biosynthesis of several polysaccharides requires an oligosaccharide primer for initiation, most notably the synthesis of streptococcal (1→3)-α-glucan, which requires a (1→6)-linked α-glucose primer (Germaine *et al.*, 1974), glycogen and starch (Smith, 1999), and cellulose (Peng *et al.*, 2002). Most importantly, the *Escherichia coli* glycogen synthase, GlgA, with which the intracellular domain of the Ags1 protein shares sequence similarity (Hochstenbach *et al.*, 1998), requires a (1→4)-linked α-glucose primer (Fox *et al.*, 1976). Based on the relative contribution of these residues to a mature α-glucan polymer, we predict that approximately twelve (1→4)-linked α-glucose residues are present in each postulated primer. These residues may form a (1→4)-linked α-glucose homooligosaccharide, as is used in glycogen biosynthesis.

In our model, we speculate that the postulated primer is elongated by the intracellular domain of Ags1p at its non-reducing end (**Fig. 5B**, **step 1**). We propose that chain elongation involves addition of glucose residues via (1→3)-linkages, consistent with the chemical structure of α-glucan. To test this hypothesis *in vitro*, biochemical assays need to be developed. First attempts to synthesize α-glucan *in vitro*, by using isolated cell membranes as a source of Ags1 synthase and UDP-glucose as a substrate, produced large quantities of (1→3)-β-glucan but no detectable α-glucan, as analyzed by ^{1}H NMR (unpublished results). Perhaps a primer is indeed required for α-glucan synthesis.

After chain termination, two newly-synthesized building blocks must be coupled to form mature α-glucan. We propose that the extracellular domain of the Ags1 protein is involved directly in the coupling of two building blocks (**Fig. 5B**, **step 2**). This domain shares sequence similarity with bacterial amylases that have been shown to function as transglycosylases (MacGregor *et al.*, 2001). These amylases can hydrolyze (1→4)-linked α-glucan oligosaccharides and transfer the newly generated reducing ends to the non-reducing ends of other α-glucan molecules.

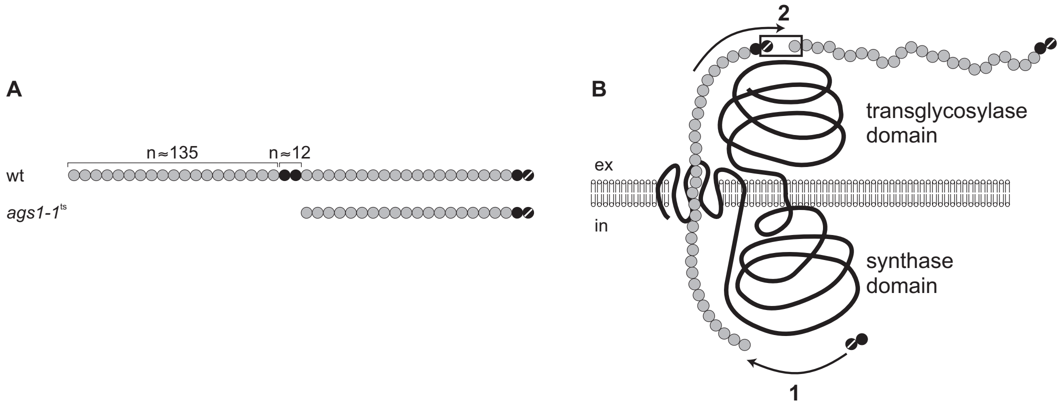

Fig. 5. Speculative model for synthesis and coupling of α-glucan by the Ags1 protein. Wild-type α-glucan consists of two building blocks, whereas mutant α-glucan is synthesized as a single building block (**A**). The model for the synthesis of α-glucan (**B**) proposes that the intracellular synthase domain of Ags1p synthesizes α-glucan by elongating a postulated primer at its non-reducing end, forming a building block (**1**). Subsequently, the extracellular transglycosylase domain of Ags1p couples two building blocks (**2**). Note that this coupling activity is absent from *ags1-1*^{ts} mutant cells grown at 34 °C, causing cell-wall deposition of only single α-glucan building blocks. Black circles: postulated (1→4)-linked primer; grey circles: (1→3)-linked segments; circles with a diagonal line indicate the reducing end.

ags1-1^{ts} mutant is unable in synthesizing mature α-glucan

Evidence corroborating our hypothesis that the Ags1 extracellular domain acts as a transglycosylase and couples α-glucan building blocks came from the analysis of the α-glucan structure of the *ags1-1*^{ts} mutant. We showed that the *ags1-1*^{ts} mutant had a temperature-dependent α-glucan structure correlating with its cell morphology. When grown at the permissive temperature of 19 °C, *ags1-1*^{ts} cells have a rod-like morphology comparable to that of wild-type cells, and possess a wild-type α-glucan structure. In contrast, when grown at the semi-permissive temperature of 34 °C, cells are rounded, and possess an α-glucan structure consisting of only a single building block. We infer from these data that at the semi-permissive temperature the point mutation in the extracellular domain of the Ags1 protein inhibits transglycosylase activity, such that the α-glucan building blocks cannot be coupled (**Fig. 5**).

In addition to the defect in α-glucan coupling, the *ags1-1*^{ts} mutant grown at the semi-permissive temperature had a defect in α-glucan biosynthesis, given the threefold reduction in α-glucan levels. We presume that this latter defect is caused by a decrease in

Ags1 protein levels at the plasma membrane. Katayama and colleagues (1999) observed that when their temperature-sensitive mutant with a mutation in the Ags1 protein (denoted Mok1p in their study) was grown at its semi-permissive temperature of 35.5 °C, mutant Ags1p was mislocalized to intracellular locations, depleting the plasma membrane of Ags1 protein. Which of these two events, the reduction in cell-wall α-glucan levels or the change in its structure, is directly responsible for the disorganization of cell-wall structure, the weakening of the cell wall, and the rounded cell morphology, remains unresolved. Nonetheless, our data clearly indicate that the Ags1 protein is involved in both synthesis and coupling of cell-wall α-glucan.

Ags1p as a potential target for antifungal drugs

Although compounds against fungal pathogens have been developed that inhibit synthesis of chitin and (1→3)-β-glucan, no inhibitors of cell-wall α-glucan synthesis have been identified as yet. Of the major fungal pathogens, *Candida albicans* lacks cell-wall α-glucan, and contains no homologs of the Ags1 protein. In contrast, other fungal pathogens, such as *Aspergillus fumigatus*, *Cryptococcus neoformans*, *H. capsulatum*, *P. brasiliensis*, *B. dermatitidis*, and *Coccidioides immitis*, contain cell-wall α-glucan. For *A. fumigatus*, two homologs (with Genbank accession numbers AAL18964 and AAL28129) of the *S. pombe* Ags1 protein have already been identified. They also possessed the multidomain structure characteristic for the *S. pombe* Ags1 protein, indicating that also their mechanism of action may have been conserved. Especially the α-glucan synthase of *Cryptococcus* has been notified as a potentially interesting target, because this pathogenic yeast is resistant against chitin and (1→3)-β-glucan synthase inhibitors (Georgopapadakou, 2001; Georgopapadakou & Tkacz, 1995). Our present data suggest that inhibition of either the synthase activity or the transglycosylase activity of the Ags1 protein may weaken fungal cell walls, rendering both domains targets suited for the development of novel antifungal drugs.

Materials and methods

Schizosaccharomyces pombe strains and cell culture

Strains FH021 (h^- *ags1-1*^{ts}) and FH023 (h^-) were described before (Hochstenbach *et al.*, 1998); strain FH058 (h^-/h^- ade6-M210/ade6-M216) was a spontaneous, nonsporulating derivative of diploid strain FH045 (h^+/h^- ade6-M210/ade6-M216). Strains FH023, FH058, and 972 (h^-) were grown in YEA medium at 28 °C, whereas strain FH021 was grown in YEA medium containing 1.2 M sorbitol at 19 °C or 34 °C for two days. The addition of sorbitol ensured that *ags1-1*^{ts} cells grown at 34 °C remained physically intact, while the two-day culture period ensured that virtually all cells displayed their proper morphology (Hochstenbach *et al.*, 1998).

Isolation of whole cell walls and cell-wall α-glucan

For whole cell-wall preparations, cells were grown in 1.5 L of the indicated medium to a final OD_{595} of 4, cooled in an ice-bath, collected by centrifugation, and washed twice in breaking buffer [5 mM sodium azide, 20 mM Tris-HCl, pH 7.6]. Cells were resuspended in breaking buffer and subjected to mechanical breakage in a Bead-Beater (BioSpec Products, Bartlesville, US) by using glass beads (0.45 mm diameter). Twelve rounds of one-minute homogenization were alternated with one-minute cooling periods, such that more than 95% of the cells had lysed. The cell lysate was collected and centrifuged. This and all subsequent centrifugation steps were carried out at 7500 × *g* at 4 °C for 20 min. After two washing steps in MilliQ-H_2O (Millipore), the pellet was resuspended in 200 ml of SDS-extraction buffer [40 mM 2-mercaptoethanol, 2% (w/v) SDS, 100 mM Na-EDTA, 50 mM Tris-HCl, pH 7.6], and incubated in a boiling waterbath for 20 min to remove cytosolic contaminants. The suspension was centrifuged, washed twice in MilliQ-H_2O, and stored in 5 mM sodium azide at 4 °C.

For α-glucan isolations, whole cell-wall preparations were resuspended in 200 ml of digestion buffer [5 mM sodium azide, 40 mM 2-mercaptoethanol, 50 mM citrate-phosphate, pH 5.3] containing 15 mg of Zymolyase-100T (Seikagaku), and incubated in a rotary shaker at 37 °C for at least 12 h. After centrifugation, the pellet was resuspended in breaking buffer, glass beads were added, and the cell-wall material was treated in a Mikro-Dismembrator (Braun) at 3000 rpm for 3 min to ensure that all cells had been broken. Then, Zymolyase digestion was repeated, followed by a final extraction with SDS. After two washing steps in MilliQ-H_2O, purified α-glucan was stored in 5 mM sodium azide at 4 °C.

Electron microscopy

Cell walls were adsorbed on Pioloform-carbon-coated copper grids and negatively stained with 1% (w/v) uranyl acetate. The ultrastructure was analyzed with a Technai 12 electron microscope (FEI / Electron Optics PD, Eindhoven, The Netherlands) at 120 kV acceleration voltage.

Monosaccharide and linkage analysis

For monosaccharide analysis, samples were subjected to methanolysis [1.0 M methanolic HCl, 24 h, 85 °C], followed by trimethylsilylation [5:1:1 (v/v/v) of pyridine/trimethylsilane/hexamethyldisilazane, 30 min, RT], and were analyzed by GLC and GLC-MS (Kamerling and Vliegenthart, 1989). Absolute configurations were determined by 2(-)-butanolysis (Gerwig *et al.*, 1978).

For linkage analysis, per-*O*-methylation was performed using the method of Hakomori (1964). Then, per-*O*-methylated polysaccharides were hydrolyzed in aqueous 90% (v/v) formic acid [1 h, 100 °C], followed by evaporation and incubation in 2 M trifluoroacetic acid [1 h, 120 °C]. Samples were reduced with excess $NaBD_4$ in 0.5 M NH_4OH for 90 min at RT, followed by acetylation with acetic acid anhydride [3 h, 120 °C].

GLC analyses were performed on a WCOT CP-SIL 5CB fused-silica capillary column (25 m × 0.32 mm) (Chrompack) using a CP 9002 gas chromatograph (Chrompack) and a temperature program of 140-240 °C at 4 °C/min. GLC-EI-MS of partially methylated alditol acetates was carried out on an MD800/8060 system (Fisons Instruments, Manchester, UK) equipped with a WCOT CP-SIL 5CB fused-silica capillary column (25 m × 0.25 mm) (Chrompack), also using a temperature program of 140-240 °C at 4 °C/min.

Nuclear magnetic resonance spectroscopy

All NMR spectra were recorded on a DRX500 spectrometer (Bruker). Samples were dissolved in 600 µl of 99.6% DMSO-d_6 and were analyzed at 80 °C. In one-dimensional ^{1}H-NMR experiments, residual water signals were suppressed by applying a WEFT pulse sequence. Two-dimensional ^{1}H-^{1}H total correlation spectroscopy (TOCSY) was carried out in the phase-sensitive mode using the States-TPPI method and using MLEV-17 mixing sequences of 10 to 50 ms. Spectral width was 3501 Hz in both dimensions; 512 experiments of 1024 data points were acquired with 32 scans per increment. In the sensitivity enhanced two-dimensional ^{1}H-^{13}C heteronuclear single quantum coherence (HSQC) experiment, Echo/Antiecho gradient selection with decoupling was used. Spectral widths were 1600 Hz and 10,000 Hz for the proton and the carbon dimensions, respectively, and 950 free-induction decays of 1024 data points were acquired using 128 scans per decay. Chemical shifts were expressed in ppm relative to internal DMSO (^{1}H, 2.505 ppm; ^{13}C, 39.6 ppm). Data were processed using in-house developed software.

Smith degradation

For the Smith degradation (Smith and Montgommery, 1956), polysaccharides were suspended in 15 mM sodium periodate at a concentration of approximately 2 mg per ml. The mixture was placed in the dark at 4 °C under continuous mixing. After 48 h, the reaction was stopped by adding ethylene glycol to a final concentration of 350 mM. Oxidized polysaccharides were reduced with an excess of $NaBH_4$ for 24 h. Then, excess borohydride was removed by the addition of acetic acid. The product was washed three times with water and hydrolyzed in 100 mM hydrochloric acid at RT during 8 h.

High-performance size-exclusion chromatography

The HPSEC system consisted of a Delta 600 pump (Waters) with a DRI 2410 refractive index detector (Waters). For the mobile phase, sodium nitrate was added to DMSO to a final concentration of 3 mM to reduce aggregation of polymers and to eliminate ionic strength effects (Chuang, 1990). The mobile phase was delivered at a flow-rate of 1.0 ml per min. A single PLgel 5 µm MIXED-C column (300 × 7.5 mm) (Polymer Laboratories) was connected in series with a PLgel 10 µm guard column (50 × 7.5 mm). Both columns were thermostated at 80 °C. The system was calibrated using pullulan narrow standards

(Standard P-82, Shodex) plus maltohexaose and glucose. Samples were lyophilized and then further dried overnight *in vacuo* over phosphorus pentoxide; then, they were dissolved in the mobile phase to a concentration of 2 mg/ml and filtered through 0.45 µm PTFE filters. Injection volumes of 100 µl were used. Data were processed using Millenium^{32} software (Waters).

Glucoamylase digestion

Glucoamylase (AMG L300) was a kind gift from AVEBE, Veendam, the Netherlands. Samples were digested for 24 h with 0.5 mass percent of glucoamylase at 57.5 °C and pH 4.3. Products were analyzed by thin-layer chromatography on Silica gel 60 F_{254} TLC plates (Merck), using 1-butanol-ethanol-water [3:2:2, v/v/v] as eluent. Carbohydrates were stained using orcinol-sulphuric acid.

β-Elimination

Alkaline degradation was carried out at RT in an oxygen-free saturated calcium hydroxide solution. After the time intervals indicated, samples were taken and centrifuged. Supernatants were neutralized by sparging with carbon dioxide, were evaporated to dryness under reduced pressure, were further dried *in vacuo* over phosphorus pentoxide, and were then trimethylsilylated. GLC-EI-MS analyses were performed as described for monosaccharide analysis. Residues were washed with water and prepared for analysis by linkage analysis or HPSEC. Reference compounds, amylose (Sigma), laminaran (Koch), and nigeran (Koch) were washed and lyophilized. (1→3)-α-glucan was prepared by performing Smith degradation on *S. pombe* cell-wall α-glucan, followed by partial hydrolysis in 2 M trifluoroacetic acid at 50 °C for 30 min to reinduce reducing termini.

Acknowledgements

The authors thank Dr. B.R. Leeflang for valuable discussion regarding the NMR experiments and J.D. Meeldijk for performing preliminary SEM experiments. F.H. was supported by a fellowship of Royal Netherlands Academy of Arts and Sciences, followed by a fellowship of the Dr. Anton Meelmeijer Fund.

References

Bacon, J.S.D.; Jones, D.; Farmer, V.C. & Webley, D.M. (1968) The occurrence of (1→3)-α-glucan in *Cryptococcus*, *Schizosaccharomyces* and *Polyporus* species, and its hydrolysis by a *Streptomyces* culture filtrate lysing cell walls of *Cryptococcus*. *Biochim. Biophys. Acta*, **158**, 313-315.

Beauvais, A. & Latgé, J.P. (2001) Membrane and cell wall targets in *Aspergillus fumigatus*. *Drug Resist. Updat.* **4**, 38-49.

Bush, D.A.; Horisberger, M.; Horman, I. & Wursch, P. (1974) The wall structure of *Schizosaccharomyces pombe*. *J.*

Gen. Microbiol., **81**, 199-206.

Chuang, J.-Y. (1990) Size exclusion chromatography of starch with dimethyl sulfoxide as the mobile phase: ionic-strength effect. *J. Appl. Polym. Sci.*, **45**, 227-242.

Fox, J.; Kawaguchi, K.; Greenberg, E. & Preiss, J. (1976) Biosynthesis of bacterial glycogen. Purification and properties of the *Escherichia coli* B ADPglucose:1→4-α-D-glucan 4-α-glucosyltransferase. *Biochemistry* **15,** 849-856.

Georgopapadakou, N.H. (2001) Update on antifungals targeted to the cell wall: focus on β-1→3-glucan synthase inhibitors. *Exp. Opin. Invest. Drugs*, **10**, 269-280.

Georgopapadakou, N.H. & Tkacz, J.S. (1995) The fungal cell wall as a drug target. *Trends Microbiol.*, **3**, 98-104.

Germaine, G.R.; Chludzinski, A.M. & Schachtele, C.F. (1974) *Streptococcus mutans* dextransucrase: requirement for primer dextran. *J. Bacteriol.* **120,** 287-294.

Gerwig, G.J.; Kamerling, J.P. & Vliegenthart, J.F.G. (1978) Determination of the D and L configuration of neutral monosaccharides by high-resolution capillary G.L.C. *Carbohydr. Res.*, **62**, 349-357.

Hakomori, S.-I. (1964) A rapid permethylation of glycolipid, and polysaccharide catalyzed by methylsulfinyl carbanion in dimethyl sulfoxide. *J. Biochem.*, **55**, 205-208.

Hayles, J. & Nurse, P. (2001) A journey into space. *Nat. Rev. Mol. Cell. Biol.*, **2**, 647-656.

Hochstenbach, F.; Klis, F.M.; Van Den Ende, H.; Van Donselaar, E.; Peters, P.J. & Klausner, R.D. (1998) Identification of a putative α-glucan synthase essential for cell wall construction and morphogenesis in fission yeast. *Proc. Natl. Acad. Sci. U S A*, **95**, 9161- 9166.

Hogan, L.H. & Klein, B.S. (1994) Altered expression of surface α-1→3-glucan in genetically related strains of *Blastomyces dermatitidis* that differ in virulence. *Infect. Immun.*, **62**, 3543- 3546.

Ishiguro, J.; Saitou, A.; Durán, A. & Ribas, J.C. (1997) *cps1+*, a *Schizosaccharomyces pombe* gene homolog of *Saccharomyces cerevisiae FKS* genes whose mutation confers hypersensitivity to cyclosporin A and papulacandin B. *J. Bacteriol.*, **179**, 7653-7662.

Kamerling, J.P. & Vliegenthart, J.F.G. (1989) Mass spectrometry. In Lawson, A.M. (ed.), *Clinical Biochemistry - Principles, Methods, Applications.* Walter de Gruyter, Berlin, Vol. 1, pp. 176-263.

Kanetsuna, F.; Carbonell, L.M.; Gil, F. & Azuma, I. (1974) Chemical and ultrastructural studies on the cell walls of the yeastlike and mycelial forms of *Histoplasma capsulatum*. *Mycopathol. Mycol. Appl.*, **54**, 1-13.

Katayama, S.; Hirata, D.; Arellano, M.; Pérez, P. & Toda, T. (1999) Fission yeast α-glucan synthase mok1 requires the actin cytoskeleton to localize the sites of growth and plays an essential role in cell morphogenesis downstream of protein kinase C function. *J. Cell Biol.*, **144**, 1173-1186.

Kennedy, J.F. & White, C.A. (1971) Polysaccharides. In Barton, D. & Ollis, W.D. (eds.), *Comprehensive Organic Chemistry.* Pergamon Press, Oxford, UK, Vol. 5, pp. 755-775.

Klimpel, K.R. & Goldman, W.E. (1988) Cell walls from avirulent variants of *Histoplasma capsulatum* lack α-(1→3)-glucan. *Infect. Immun.*, **56**, 2997-3000.

Klis, F.M.; Mol, P.; Hellingwerf, K. & Brul, S. (2002) Dynamics of cell wall structure in *Saccharomyces cerevisiae*. *FEMS Microbiol. Rev.* **26**, 239-256.

Kügler, S.; Schurtz Sebghati, T.; Groppe Eissenberg, L. & Goldman, W.E. (2000) Phenotypic variation and intracellular parasitism by *Histoplasma capsulatum*. *Proc. Natl. Acad. Sci.*, **97**, 8794-8798.

MacGregor, E.A.; Janecek, S. & Svensson, B. (2001) Relationship of sequence and structure to specificity in the α-amylase family of enzymes. *Biochim. Biophys. Acta*, **1546**,1-20.

Manners, D.J. & Meyer, M.T. (1977) The molecular structures of some glucans from the cell wall of *Schizosaccharomyces pombe*. *Carbohydr. Res.*, **57**, 189-203.

Peng, L.; Kawagoe, Y.; Hogan, P. & Delmer, D. (2002) Sitosterol-β-glucoside as primer for cellulose synthesis in plants. *Science*, **295**, 147-150.

San-Blas, G.; San-Blas, F. & Serrano, L.E. (1977a) Host-parasite relationships in the yeastlike form of *Paracoccidioides brasiliensis* strain IVIC Pb9. *Infect. Immun.*, **15**, 343-346.

San-Blas, G.; San-Blas, F.; Ormaechea, E. & Serrano, L.E. (1977b) Cell wall analysis of an adenine-requiring mutant of the yeast-like form of *Paracoccidioides brasiliensis* strain IVIC Pb9. *Sabouraudia*, **15**, 297-303.

Sietsma, J.H. & Wessels, J.G.H. (1988) Total inhibition of wall synthesis by 2-deoxyglucose and polyoxin D in protoplasts of *Schizophyllum commune*. *Acta Bot. Neerl.*, **37**, 23-29.

Smith, A.M. (1999) Making starch. *Curr. Opin. Plant. Biol.*, **2**, 223-229.

Smith, F. & Montgomery, R. (1956) End group analysis of polysaccharides. In Glick, D. (ed.), *Methods of biochemical analysis.* Interscience Publishers Inc., New York, Vol. 3, pp. 153-212.

Whistler, R.L. & BeMiller, J.N. (1958) Alkaline degradation of polysaccharides. In Wolfrom, M.L. & Tipson, R.S. (eds.), *Advances in carbohydrate chemistry and biochemistry.* Academic Press, New York, Vol. 13; pp. 289-329.

Williams, D.L.; Pretus, H.; Ensley, H.E. & Browder, I.W. (1994) Molecular weight analysis of a water-insoluble, yeast-derived (1→3)-β-D-glucan by organic-phase size-exclusion chromatography. *Carbohydr. Res.*, **253**, 293-298.

Wood, V. *et al.* (2002) The genome sequence of *Schizosaccharomyces pombe*. *Nature*, **415**, 871- 880.

Zonneveld, B.J. (1972) Morphogenesis in *Aspergillus nidulans*. The significance of a α-1→3-glucan of the cell wall and α-1→3-glucanase for cleistothecium development. *Biochim. Biophys. Acta.*, **273**, 174-187.

Zonneveld, B.J. (1973) Inhibitory effect of 2-deoxyglucose on cell wall α-1→3-glucan synthesis and cleistothecium development in *Aspergillus nidulans*. *Dev. Biol.*, **34**, 1-8.

Chapter 3

Identification of (1→4)-linked α-glucooligomers in cell-wall α-glucan of fission yeast

Christian H. Grün[1], Frans Hochstenbach[2], Frans M. Klis[3], Johannis P. Kamerling[1], and Johannes F.G. Vliegenthart[1]

[1]*Bijvoet Center, Department of Bio-Organic Chemistry, Section of Glycoscience and Biocatalysis, Utrecht University;* [2]*Department of Biochemistry, Academic Medical Center, University of Amsterdam;* [3]*Swammerdam Institute for Life Sciences, University of Amsterdam*

Abstract

The cell wall of fission yeast mainly consists of two types of polysaccharides, namely β-glucan and α-glucan. Previously, we have described the structure of fission-yeast α-glucan and concluded that it consists of two building blocks, each composed of a (1→3)-α-glucan segment of approximately 135 α-glucose residues linked to a short stretch containing (1→4)-linked residues. However, it remained unclear whether this stretch is a homooligosaccharide of (1→4)-linked α-glucose or whether it is composed of alternating (1→3)-linked and (1→4)-linked glucose residues. Here, we describe the chemical structure of the stretch containing (1→4)-linked glucose residues by digesting α-glucan with a (1→3)-α-glucanase preparation and the elucidation of the reaction products by nano-electrospray mass spectrometry. We identified two classes of oligosaccharides, namely one class comprising heterooligosaccharides consisting of a number of consecutive (1→4)-linked α-glucose residues linked to a number of (1→3)-linked α-glucose residues, and a second class consisting of consecutive (1→4)-linked α-glucose, only. We propose that the first class originates from the center part of the α-glucan, whereas the second class forms the reducing end. These data demonstrate that each (1→3)-α-glucan segment is covalently linked to a homooligomer of (1→4)-linked α-glucose residues.

Introduction

The cell wall of many fungi is composed of three types of polysaccharides, namely chitin, β-glucan and α-glucan. Although the first two types have been studied thoroughly, little is known about the chemical structure and biosynthesis of α-glucan. In fission yeast, *Schizosaccharomyces pombe*, α-glucan was identified by Bacon and co-workers (1968) and its chemical composition was determined by Bush and co-workers (1974), who concluded that it consisted mainly of (1→3)-linked α-glucose residues with some (1→4)-linked residues. Recently, we determined that these (1→4)-linked residues are an integral part of cell-wall α-glucan. We showed that α-glucan is a linear polysaccharide composed of two covalently coupled building blocks, each comprising a linear (1→3)-α-glucan segment of approximately 135 residues linked to a stretch containing a number of (1→4)-linked glucose residues. Importantly, α-glucan from a mutant that is defective in α-glucan synthesis consisted of a single building block, only (Chapter 2). We proposed a model for the biosynthesis of α-glucan in which we postulated that the (1→4)-linked glucose residues might form a primer molecule, necessary for the initiation of α-glucan synthesis.

The use of an oligosaccharide primer for polysaccharide biosynthesis is not unusual. For example, for the synthesis of (1→3)-α-glucan produced by *Streptococcus mutans*, a primer composed of (1→6)-linked α-glucose residues is required (Germaine *et al.*, 1974) and cellulose biosynthesis is initiated by a (1→4)-β-glucooligosaccharide (Peng *et al.*, 2002), whereas the synthesis of glycogen and starch requires a (1→4)-α-glucooligomer as a primer (Alonso *et al.*, 1995; Whelan, 1998; Smith, 1999). Importantly, *Escherichia coli* glycogen, with which the intracellular domain of fission yeast α-glucan synthase shares amino-acid sequence similarity (Hochstenbach *et al.*, 1998), requires a (1→4)-α-glucooligosaccharide for chain initiation (Fox *et al.*, 1976; Kawaguchi *et al.*, 1978). Therefore, we speculate that the (1→4)-linked glucose residues found in fission-yeast α-glucan may form a primer molecule. However, it remained unclear whether the putative primer consists of consecutive (1→4)-linked glucose residues or whether it is composed of mixed (1→3)-linked and (1→4)-linked residues.

Here, we elucidate the chemical structure of the putative primer for fission-yeast α-glucan biosynthesis by digesting cell-wall α-glucan with an *endo*-(1→3)-α-glucanase preparation. To elucidate the chemical structure of the digestion products, an analysis strategy is developed that is based on a method described by Angel *et al.* (1991), involving oxidation of the oligosaccharides by periodate followed by reduction and per-*O*-methylation, and mass spectrometric analysis. To discriminate between 3-substituted and 4-substituted reducing ends, reducing residues are derivatized with the fluorescent label 2-aminobenzamide (2-AB) prior to oxidation tandem. By sequencing the derivatized oligosaccharides using nano-electrospray tandem mass spectrometry (nanoES-MS^2), we demonstrate that the putative primer consists of consecutive (1→4)-linked α-glucose residues.

Results

Analysis method

To unambiguously discriminate between oligosaccharides containing (1→3)-linked and those containing (1→4)-linked hexoses, we developed a structural analysis method based on differences in chemical reactivity of these two types of linkage to periodate, which will oxidize residues with adjacent hydroxyl groups but will not affect other residues (Abdel-Akher *et al.*, 1952). In the case of →3)-Glc*p*-(1→ and →4)-Glc*p*-(1→ residues, only the latter will be oxidized, forming a polyaldehyde. This polyaldehyde is then reduced using sodium borodeuteride and per-*O*-methylated, resulting in a nominal mass of 208 amu, which is an increase of 4 atomic mass units (amu) per residue compared to →3)-Glc*p*-(1→ residues treated the same way (**Fig. 1**). To identify the type of linkage of the reducing end, oligosaccharides are derivatized prior to oxidation using the fluorescent label 2-aminobenzamide (2-AB). Upon oxidation, the label cleaves off in case of 4-substitution, whereas it remains linked to the oligosaccharide when 3-substituted (**Fig. 1**). According to the reaction schemes shown in **Fig. 1**, the nominal mass of an oxidized/reduced, and methylated →3)-Glc*p*-(1→[2AB] residue is 310 amu, whereas that of a →4)-Glc*p*-(1→[2AB] residue is 121 amu. Similarly, a Glc*p*-(1→ residue has a nominal mass of 179 amu. Thus, by measuring the molecular masses of oligosaccharides derived from (1→3)-α-glucanase-digested fission-yeast α-glucan following the structural analysis method, it is possible to determine the number of (1→3)-linked and (1→4)-linked glucose residues plus the type of glycosidic linkage of the reducing end, and by selecting ions for collision-induced dissociation (CID), information on the sequence can be obtained.

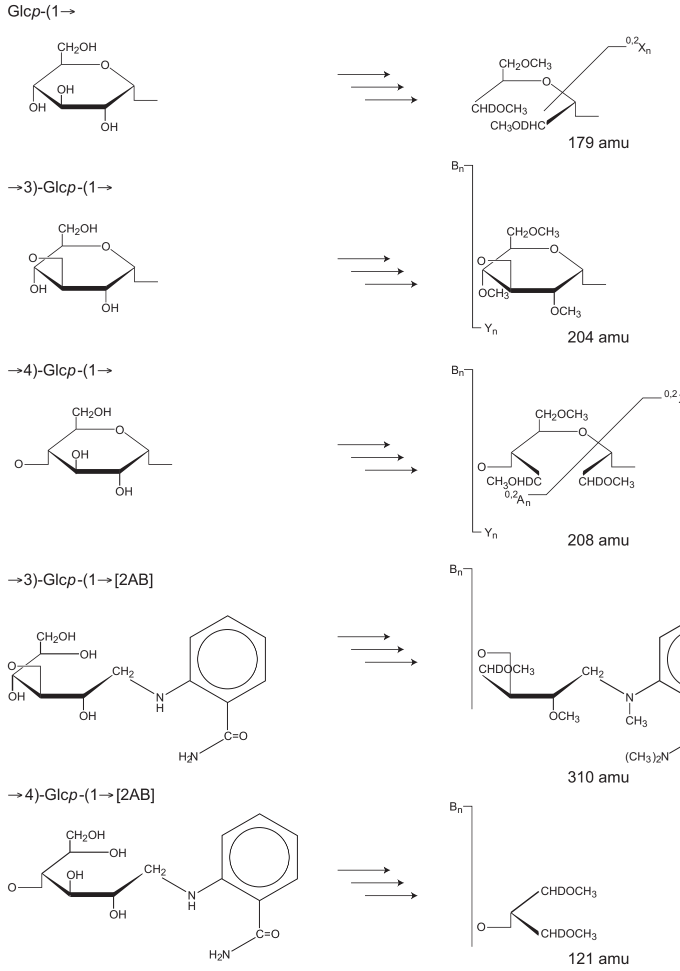

Fig. 1. Reaction scheme of periodate oxidation, reduction, and per-*O*-methylation on 3-substituted and 4-substituted glucose residues. Nominal masses of the reaction products are displayed next to theoretical fragmentation following the nomenclature of Domon and Costello (1988).

As model components to study our structural analysis method, we used laminaritetraose ((1→3)-β-glucotetraose) and maltotetraose ((1→4)-α-glucotetraose). Electrospray mass spectrometric analysis of the 2-AB-labeled and per-*O*-methylated laminaritetraose gave an ion at *m/z* 1047, representing a sodium-cationized, fully methylated tetrasaccharide that was derivatized at its reducing end (not shown). The nanoES mass spectrum of 2-AB-labeled laminaritetraose after periodate oxidation, reduction, and per-*O*-methylation showed a sodium-cationized ion at *m/z* 920 (not shown). Combining the theoretical masses of the different constituents with the measured *m/z* value, we surmise that the ion is composed of one Glc*p*-(1→ (179 amu), two →3)-Glc*p*-(1→ (2 × 204 amu), one →3)-Glc*p*-(1→[2AB] (310 amu), and a sodium ion (23 amu), giving a total of 920 amu. To determine its sequence, we selected this ion for collision-induced dissociation. The nanoES tandem mass spectrum showed a range of fragment ions that according to the nomenclature formulated by Domon and Costello (1988), corresponded mainly to B-type and Y-type ions (**Fig. 2**). The ion at *m/z* 799 corresponded to an $^{0,2}X_3$ ion, representing 'cross-ring fragmentation' of the non-reducing residue. The spectrum contained a series of Y_n (*m/z* 742, 538, and 334), B_n (*m/z* 609), and C_n ions (*m/z* 423 and 627), arising from the cleavage of each successive glycosidic linkage. The fragmentation scheme demonstrated that each intrachain residue was substituted at C-3 (**Fig. 2**). Furthermore, the mass spectrum showed that the 2-AB label remains attached, indicating that the reducing end was 3-substituted.

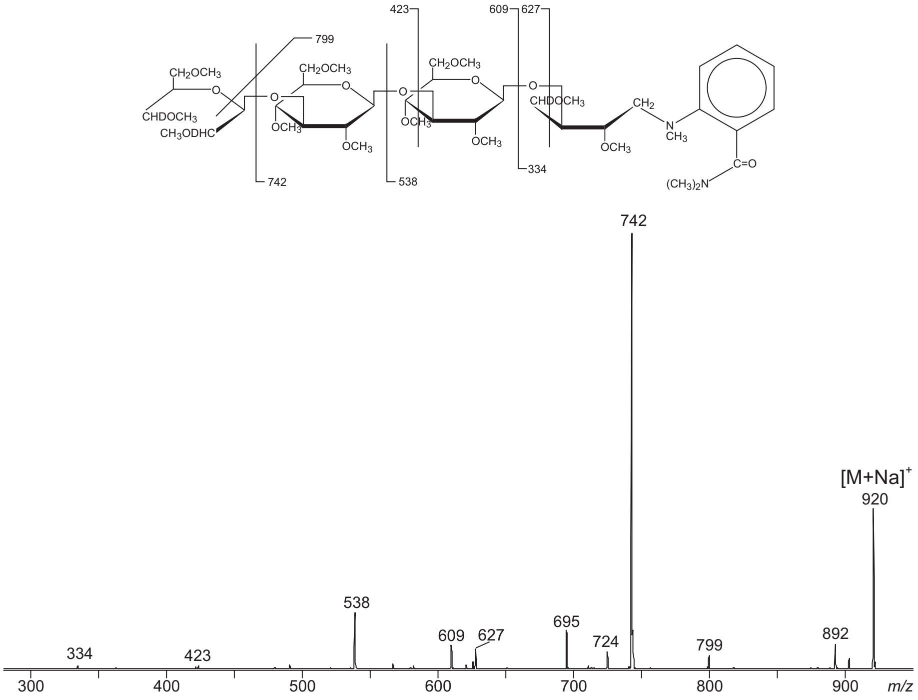

Fig. 2. Positive ion mode nanoES CID tandem mass spectrum of 2-AB labeled, periodate oxidized, and per-*O*-methylated laminaritetraose.

The nanoES mass spectrum of 2-AB-labeled, per-*O*-methylated maltotetraose showed an ion of high abundance at *m/z* 1047 that represented the fully-methylated compound (not shown). The 2-AB-labeled tetrasaccharide after oxidation, reduction, and per-*O*-methylation gave an ion at *m/z* 739, which corresponded to one Glc*p*-(1→ (179 amu), two

→4)-Glc*p*-(1→ (208 amu each), one 4)-Glc*p*-(1→[2AB] (121 amu) plus sodium. The nanoES tandem mass spectrum of the precursor ion at *m/z* 739 contained a series of Y_n and B_n ions at *m/z* 561, 353 and *m/z* 409, 617, respectively, arising from cleavage of each successive glycosidic linkage, as shown in the fragmentation scheme (**Fig. 3**). The fragmentation pattern showed that each intrachain residue had a nominal mass of 208 Da, representing oxidized (1→4)-linked glucose residues. In addition, $^{0,2}X_n$ ions at *m/z* 618 and 410 and $^{0,2}A_n$ ions at *m/z* 352 and 560 were observed that confirmed the proposed structure. As shown in the fragmentation scheme of **Fig. 3**, the oxidation of 4-substituted reducing ends resulted in the release of the 2-AB label, and therefore, could clearly be distinguished from 3-substituted reducing ends (compare **Fig. 3** with **Fig. 2**).

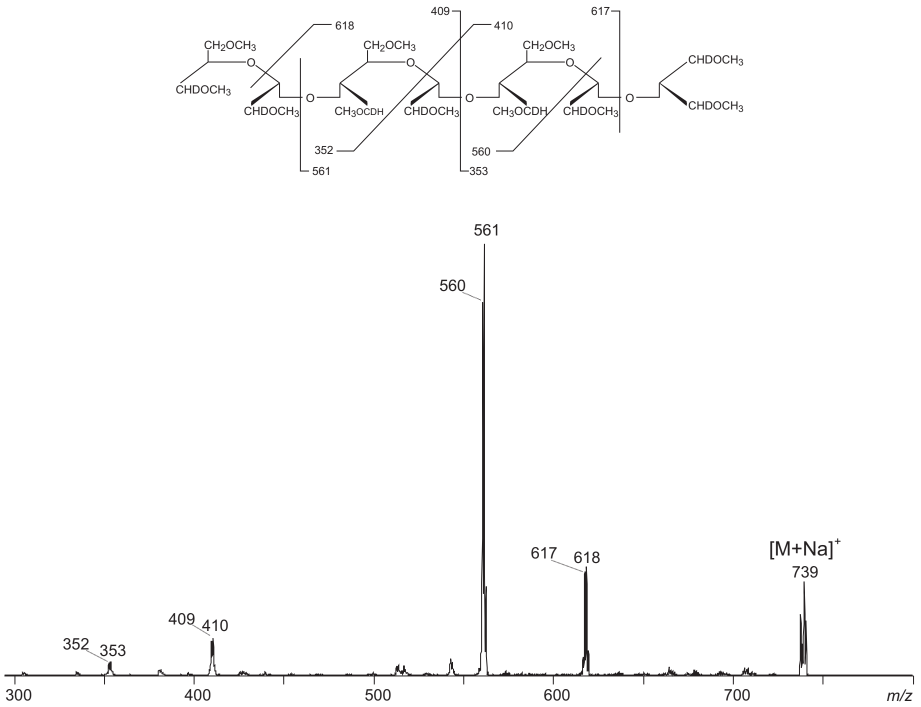

Fig. 3. Positive ion mode nanoES CID tandem mass spectrum of 2-AB labeled, periodate oxidized, and per-*O*-methylated maltotetraose.

Isolation and analysis of oligosaccharides derived from (1→3)-α-glucanase digestion

To elucidate the primary structure of cell-wall α-glucan from fission yeast (wild-type strain FH023), we digested 100 mg of α-glucan using a (1→3)-α-glucanase preparation. This glucanase has been isolated from a commercially available enzyme preparation of *Trichoderma harzianum*. It was shown that the enzyme has *endo*-catalytic activity and uses nigerotetraose as substrate to form nigerotriose and glucose (see Supplementary data at the end of this chapter). After desalting on Carbograph solid phase extraction columns, which in addition to desalting also removed monosaccharides, digestion products were fractionated on a Bio-Gel P4 column (**Fig 4**). Fractions **3** to **7** were further purified using high-performance anion-exchange chromatography (HPAEC) (**Fig. 5**).

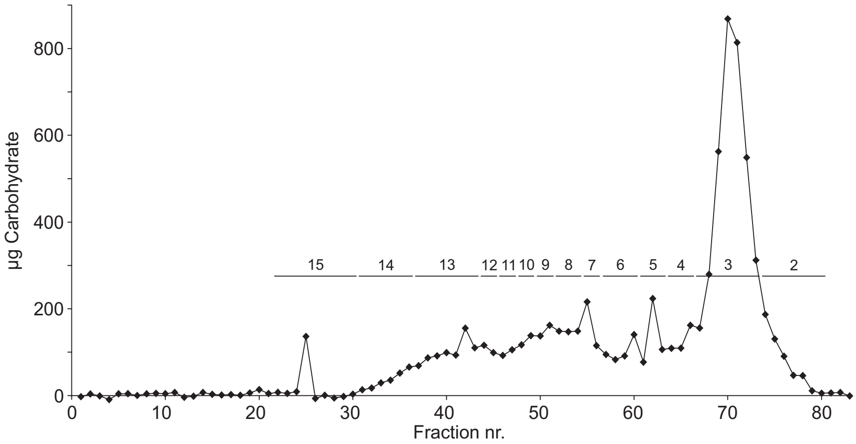

Fig. 4. Bio-Gel P4 size-exclusion chromatogram of *endo*-(1→3)-α-glucanase hydrolysis products of α-glucan from fission-yeast cell walls. Numbers indicate pooled fractions.

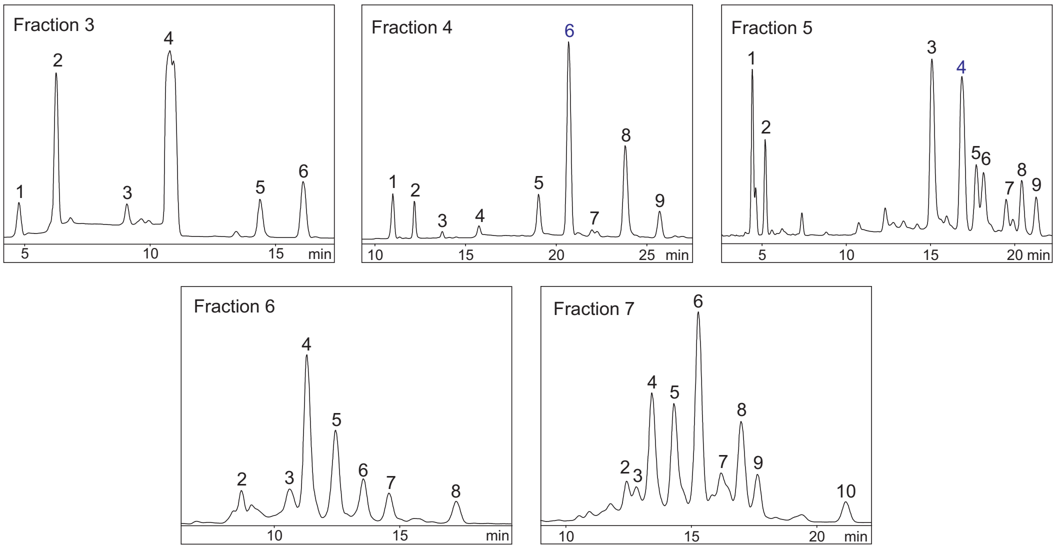

Fig. 5. Anion-exchange chromatograms of Bio-Gel P4 fractions 3-7 on a CarboPac PA1 column.

The HPAEC fractions were screened by ^{1}H-NMR spectroscopy for the presence of (1→3)-linked and (1→4)-linked α-Glc*p* residues. The anomeric protons of (1→3)-linked α-glucopyranose residues have chemical shifts around 5.36 ppm (**Fig. 6**, spectrum I), whereas the anomeric protons of (1→4)-linked residues are found around 5.40 ppm

(**Fig. 6**, spectrum II), allowing rapid identification of the types of linkages. Fractions that contained (1→4)-linked glucose residues were then derivatized at their reducing end with 2-AB. One part was directly per-*O*-methylated in order to determine its molecular mass, whereas another part underwent the oxidation procedure of periodate oxidation, reduction, and per-*O*-methylation prior to analysis by nanoES mass spectrometry.

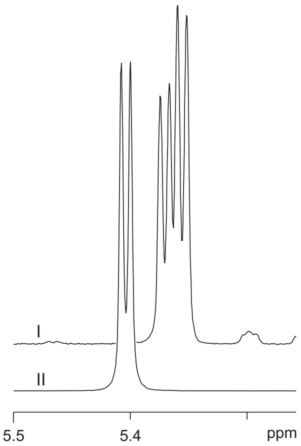

Fig. 6. Anomeric regions in the ^{1}H-NMR spectrum of nigerose (I) and maltose (II). Note that the anomeric proton of Glc*p*-(1→ in nigerose forms two doublets, which is due to the anomerization effect.

Fraction **3** — The HPAEC profile of fraction **3** showed six peaks of which subfraction **3.5** contained both (1→3)-linked and (1→4)-linked α-glucopyranose residues according to its ^{1}H-NMR spectrum (**Fig. 7A**). The mass spectrum of fraction **3.5** after 2-AB labeling and per-*O*-methylation showed an ion of high abundance at *m/z* 1047 representing fully per-*O*-methylated Hex$_4$ (not shown). In addition, an ion of low abundance was observed at *m/z* 843, representing fully per-*O*-methylated Hex$_3$, indicating a heterogeneous HPAEC fraction due to incomplete peak resolution for the oligosaccharides. After periodate oxidation, the mass of Hex$_4$ shifted to *m/z* 924 and hence may be composed of one Glc*p*-(1→, one →4)-Glc*p*-(1→, one →3)-Glc*p*-(1→, and one 3)-Glc*p*-(1→[2AB]. The nanoES tandem mass spectrum of precursor ion *m/z* 924 showed a range of fragment ions, of which Y$_3$ (*m/z* 746), Y$_2$ (*m/z* 538), and Y$_1$ (*m/z* 334) gave the full sequence of the tetrasaccharide as shown in the fragmentation scheme of **Fig. 7B**. The Y$_1$ ion clearly shows that the 2-AB label is still attached to the reducing end, demonstrating that the reducing residue is 3-substituted. According to the fragment ions, we conclude that the tetrasaccharide is Glc*p*-(1→4)-Glc*p*-(1→3)-Glc*p*-(1→3)-Glc*p* (**Table I**).

Fraction **4** — Fractionation of fraction **4** by HPAEC gave nine peaks that were analyzed by ^{1}H-NMR spectroscopy. Fractions **4.5** and **4.8** contained both (1→3)-linked and (1→4)-linked glucose residues, and were further analyzed by nanoES-MS. Analysis of fraction **4.5** by NMR spectroscopy and nanoES mass spectrometry showed that the major component is identical to that in fraction **3.5** (**Fig. 8**), which can be explained by incomplete separation of fractions **3** and **4** by Bio-Gel P4 size-exclusion chromatography.

The ^{1}H-NMR spectrum of fraction **4.8** showed anomeric signals of (1→4)-linked and (1→3)-linked Glc*p* (**Fig. 9A**). The mass spectrum of fraction **4.8** after 2-AB labeling and per-*O*-methylation showed predominantly two sodium-cationized pseudomolecular ions, an ion of high intensity at *m/z* 1251 that corresponds to a pentasaccharide and a low-intensity ion at *m/z* 1047 corresponding to a tetrasaccharide (not shown). Periodate oxidation followed by per-*O*-methylation gave a mass spectrum with ions at *m/z* 1128 and 1114, the latter indicating undermethylation (not shown). These *m/z* values showed that

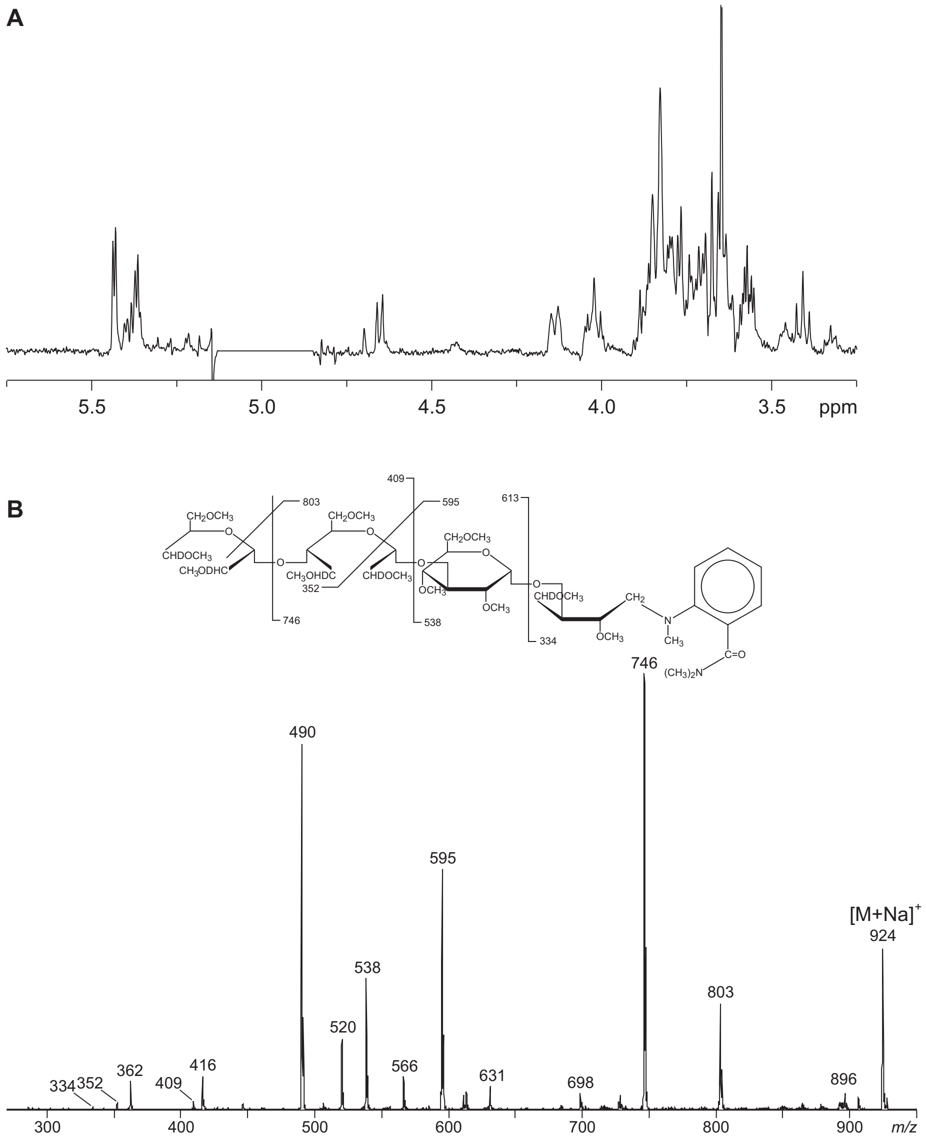

Fig. 7. Fraction **3.5** contains a tetrasaccharide with mixed (1→3)-linked and (1→4)-linked glucose residues. ^{1}H-NMR spectroscopy of HPAEC fraction **3.5** (**A**) and positive ion mode nanoES CID tandem mass spectrum of 2-AB labeled, periodate oxidized, and per-*O*-methylated HPAEC fraction **3.5**, *m/z* 924.

fraction **4.8** contained a pentasaccharide composed of one Glc*p*-(1→, one →4)-Glc*p*-(1→, two →3)-Glc*p*-(1→, and one 3)-Glc*p*-(1→[2AB]. In the nanoES tandem mass spectrum of the sodium-cationized precursor ion at *m/z* 1128, Y_n-, B_n-, and $^{1,2}X_n$-type ions were observed that gave the complete sequence of *m/z* 1128, namely Glc*p*-(1→4)-Glc*p*-(1→3)-Glc*p*-(1→3)-Glc*p*-(1→3)-Glc*p* (see fragmentation scheme in **Fig. 9B**, **Table I**).

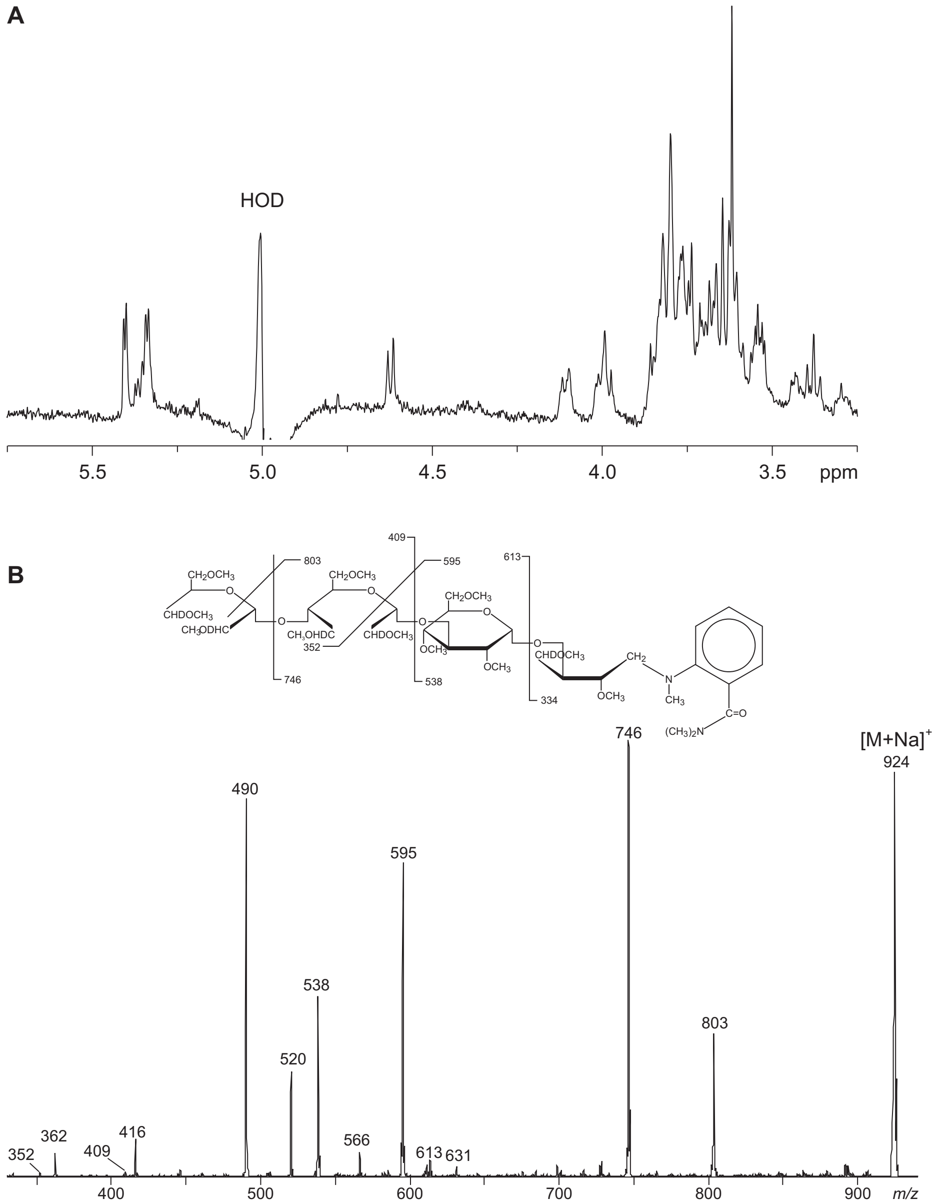

Fig. 8. Fraction **4.5** contains a tetrasaccharide with mixed (1→3)-linked and (1→4)-linked glucose residues. ^{1}H-NMR spectroscopy of HPAEC fraction **4.5** (**A**) and positive ion mode nanoES CID tandem mass spectrum of 2-AB labeled, periodate oxidized, and per-*O*-methylated HPAEC fraction **4.5**, *m/z* 924 (**B**).

Fraction **5** — The fractionation of Bio-Gel P4 fraction **5** by HPAEC gave nine subfractions (**Fig. 5**). Of these fractions, ^{1}H-NMR spectroscopy indicated that fractions **5.3**, **5.5**, **5.6**, and **5.8**, are composed of (1→4)-linked Glc*p* residues in addition to (1→3)-linked residues (**Fig. 10-12**). The mass spectrum obtained from the 2-AB labeled and per-*O*-methylated

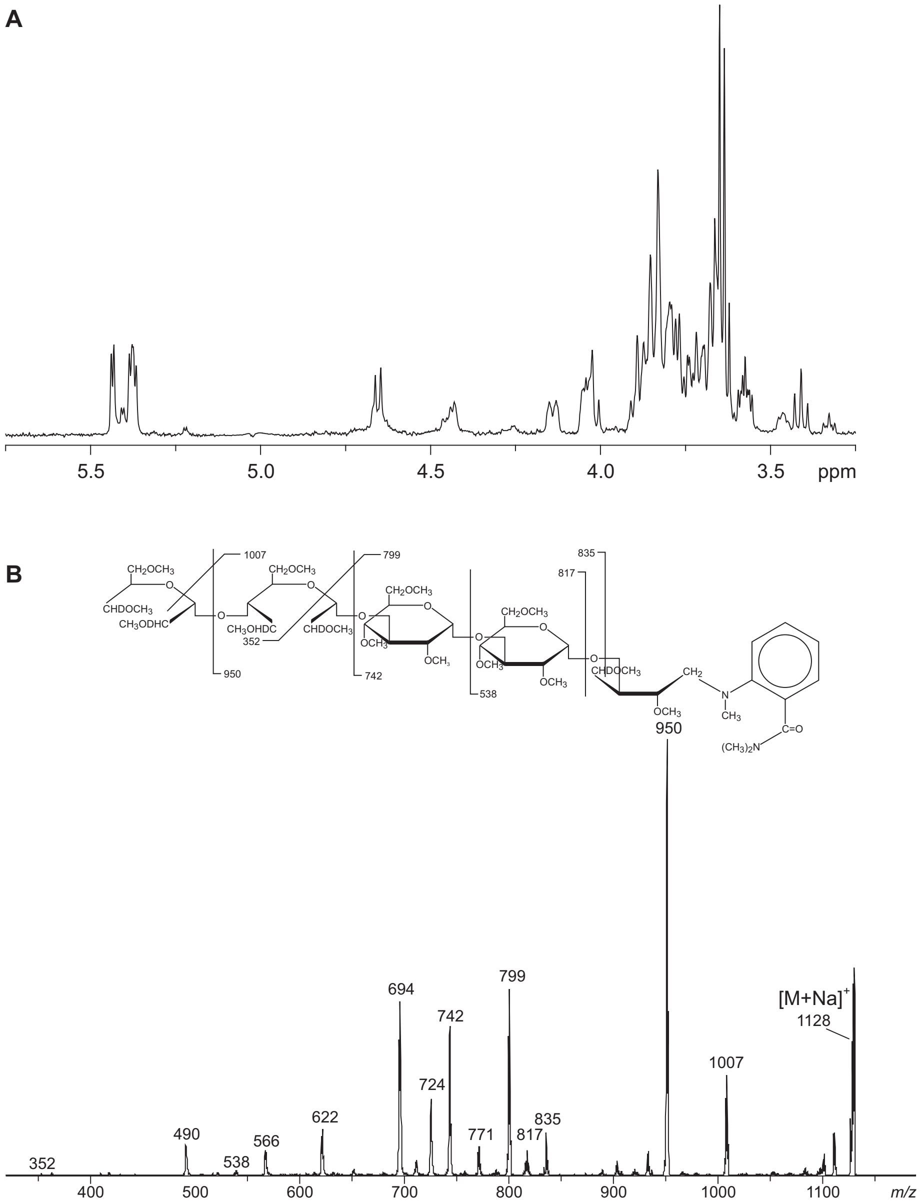

Fig. 9. Fraction **4.8** contains a pentasaccharide with mixed (1→3)-linked and (1→4)-linked glucose residues. ^{1}H-NMR spectroscopy of HPAEC fraction **4.8** (**A**) and positive ion mode nanoES CID tandem mass spectrum of 2-AB labeled, periodate oxidized, and per-*O*-methylated HPAEC fraction **4.8**, *m/z* 1128 (**B**). Note that when selecting *m/z* 1128 for MS^2, ratios between the isotopes of the pseudomolecular ion differed from natural abundance.

fraction **5.3** showed a major signal at *m/z* 1251, representing a fully methylated Hex$_5$. After applying the oxidation procedure, the mass spectrum showed an ion at *m/z* 1128, representing a sodium-cationized pseudomolecular pentasaccharide ion composed similarly to the major compound found in fraction **4.8** (not shown). The nanoES tandem mass spectrum of the precursor ion at *m/z* 1128 (**Fig. 10B**) gave a mass spectrum similar to that of fraction **4.8**, indicating that both structures are identical (**Table I**).

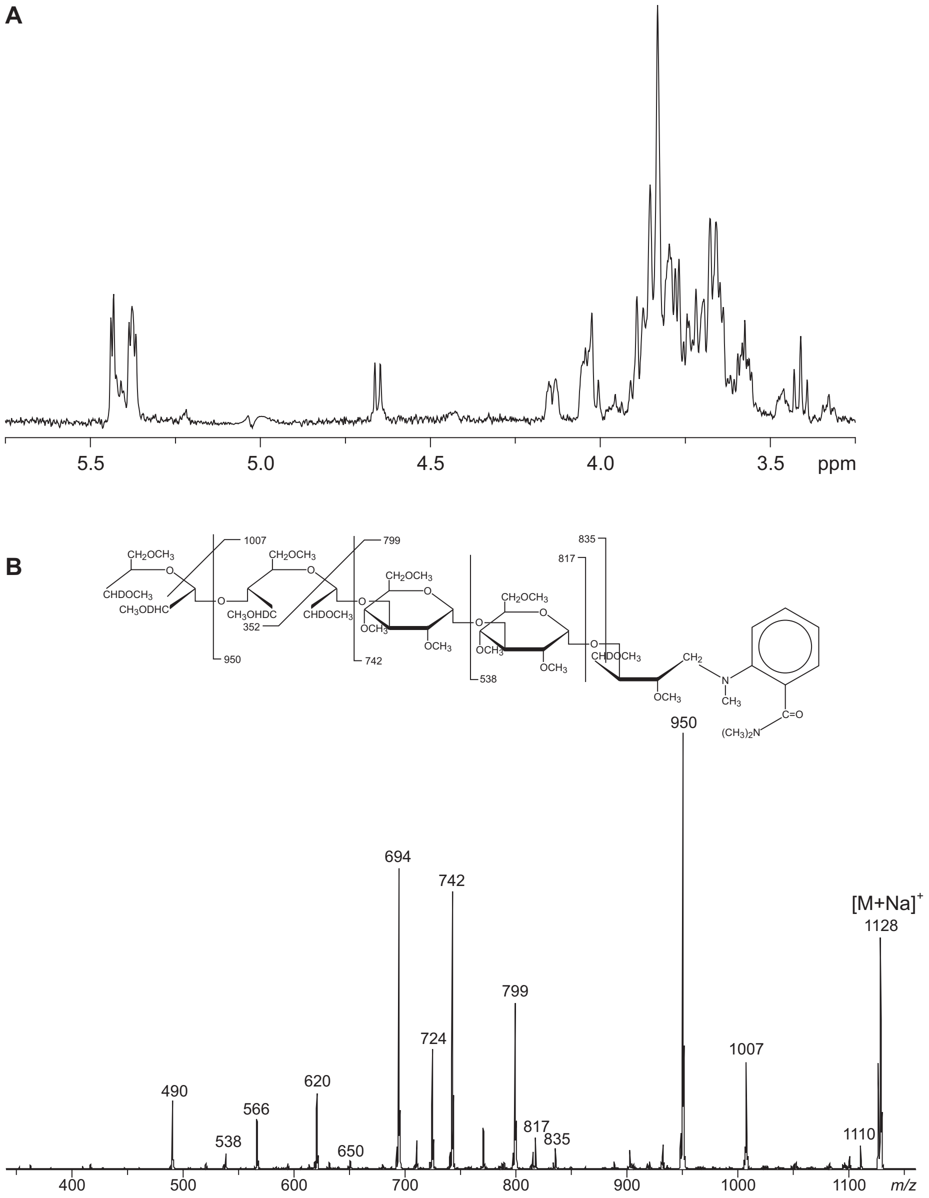

Fig. 10. Fraction **5.3** contains a pentasaccharide with mixed (1→3)-linked and (1→4)-linked glucose residues. ^{1}H-NMR spectroscopy of HPAEC fraction **5.3** (**A**) and positive ion mode nanoES CID tandem mass spectrum of 2-AB labeled, periodate oxidized, and per-*O*-methylated HPAEC fraction **5.3**, *m/z* 1128 (**B**).

The ^{1}H-NMR spectrum of fraction **5.5** indicated the presence of (1→4)-linked Glc*p* residues in addition to a small amount of (1→3)-linked residues (**Fig. 11A**). Mass-spectrometric analysis of per-*O*-methylated fraction **5.5** gave a low-intensity signal at *m/z* 1251, a medium-intensity signal at *m/z* 1455 and a signal of high intensity at *m/z* 1659, showing the presence of a mixture of sodium-cationized, fully-methylated penta-, hexa-, and heptasaccharides, respectively (not shown). The mass spectrum after applying the oxidation procedure showed a range of ions at *m/z* 986, 990, 1194, 1198, 1534, and 1548, of which the ion at *m/z* 1534 indicates undermethylation. Each of the ions was subsequently selected for collision-induced dissociation. In an effort to find the theoretical composition of the ion at *m/z* 990 according to the scheme in **Fig. 1**, we noticed that in the best fit (i.e., a pentasaccharide with (1→4)-linked residues, only), a mass difference of 43 amu occurred (namely *m/z* 990 vs. *m/z* 947), indicating underoxidation, which occurs when not all vicinal hydroxyl groups are oxidized. The tandem mass spectrum of the precursor ion at *m/z* 990 showed complete series of Y_n-, B_n-, and $^{1,2}X_n$-type ions, giving the full sequence of the pentasaccharide (**Fig. 11B**). The fragmentation pattern showed the loss of the 2-AB group from the reducing end after periodate oxidation, demonstrating a 4-substituted reducing end. A B_4 ion was identified at *m/z* 825, indicating that the underoxidation occurred at the reducing end (**Fig. 11B**). According to the fragmentation, we conclude that fraction **5.5** contained Glc*p*-(1→4)-Glc*p*-(1→4)-Glc*p*-(1→4)-Glc*p*-(1→4)-Glc*p* (**Table I**), which is in accordance with the NMR data.

Table I. *endo*-(1→3)-α-glucanase treatment of α-glucan from fission-yeast cell walls

HPAEC fraction	*m/z* [1] after per-*O*-methylation	*m/z* [1] after oxidation	Structure [2]	Origin
3.5	1047	924	○●◍⊘	Center
4.5	1047	924	○●◍⊘	Center
4.8	1251	1128	○●◍◍⊘	Center
5.3	1251	1128	○●◍◍⊘	Center
5.5	1251	990	○●●●⦸	Reducing end
	1455	1198	○●●●●⦸	Reducing end
	1659	1548	○●●●●⊘	Center
5.6	1455	1198	○●●●●⦸	Reducing end
5.8	1659	1406	○●●●●●⦸	Reducing end
6.3	1455	1198	○●●●●⦸	Reducing end
	1659			
6.4	1659	1198, 1402	○●●●●●⦸	Reducing end
	1863	1742	○●●●●●●⊘	Center
6.7	1455	1402	○◍●●●●⦸	Reducing end
7.5	1455, 1659, 1863	1818	○●●●●●●●⦸	Reducing end

[1] *m/z* ratios correspond to $[M + Na]^+$ ions.

[2] White spheres: non-reducing end; black spheres: (1→4)-linked residues; grey spheres: (1→3)-linked residues; reducing ends are marked with a diagonal line.

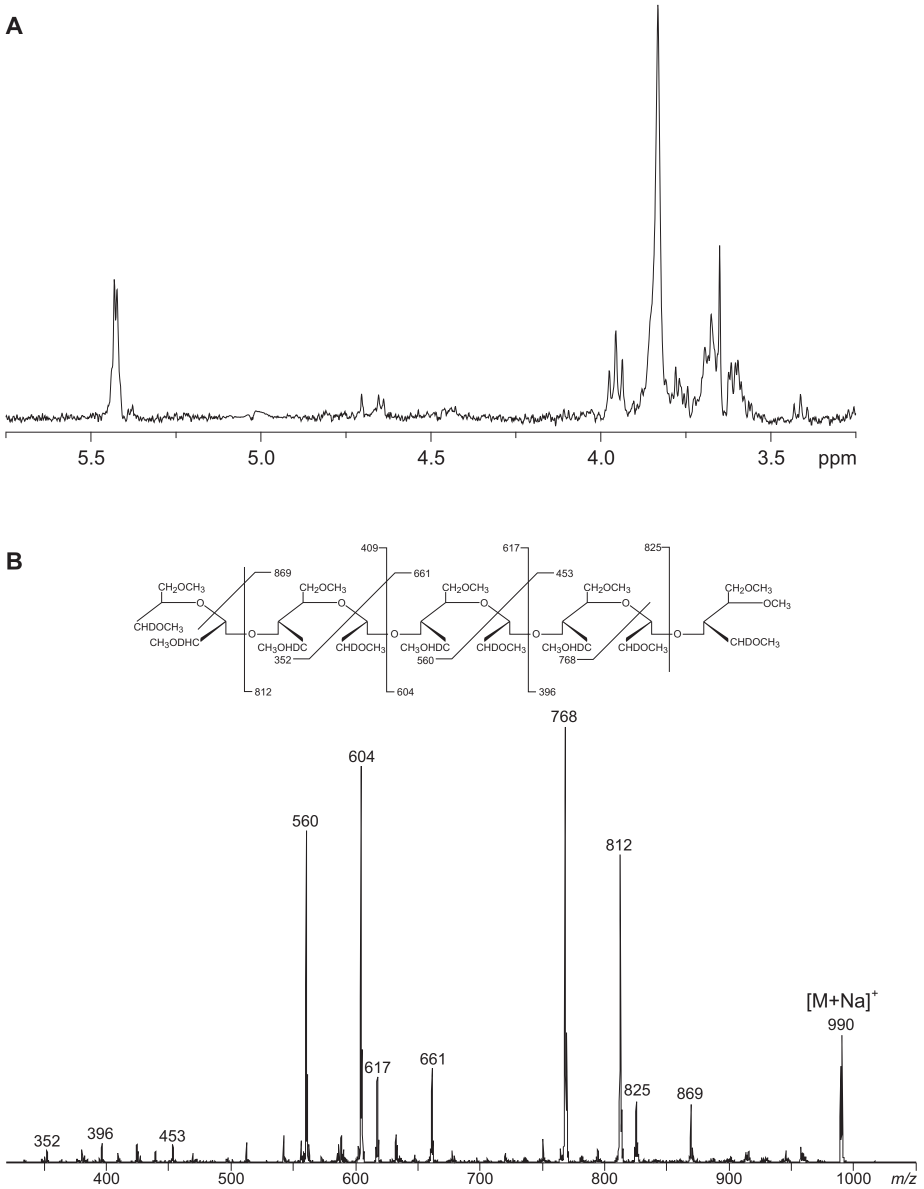

Fig. 11. Fraction **5.5** comprises a mixture of oligosaccharides. ^{1}H-NMR spectroscopy of HPAEC fraction **5.5** (**A**) and positive ion mode nanoES CID tandem mass spectrum of 2-AB labeled, periodate oxidized, and per-*O*-methylated HPAEC fraction **5.5**, *m/z* 990 (**B**), *m/z* 1198 (**C**), and *m/z* 1548 (**D**). Note that when selecting *m/z* 1198 for MS^2, besides the intended precursor ion, also isotopes of the *m/z* 1194 cluster were selected, resulting in a high-abundant ion at *m/z* 1196. This also explains the presence of fragment ions at *m/z* 1018, 974, 810, etc.

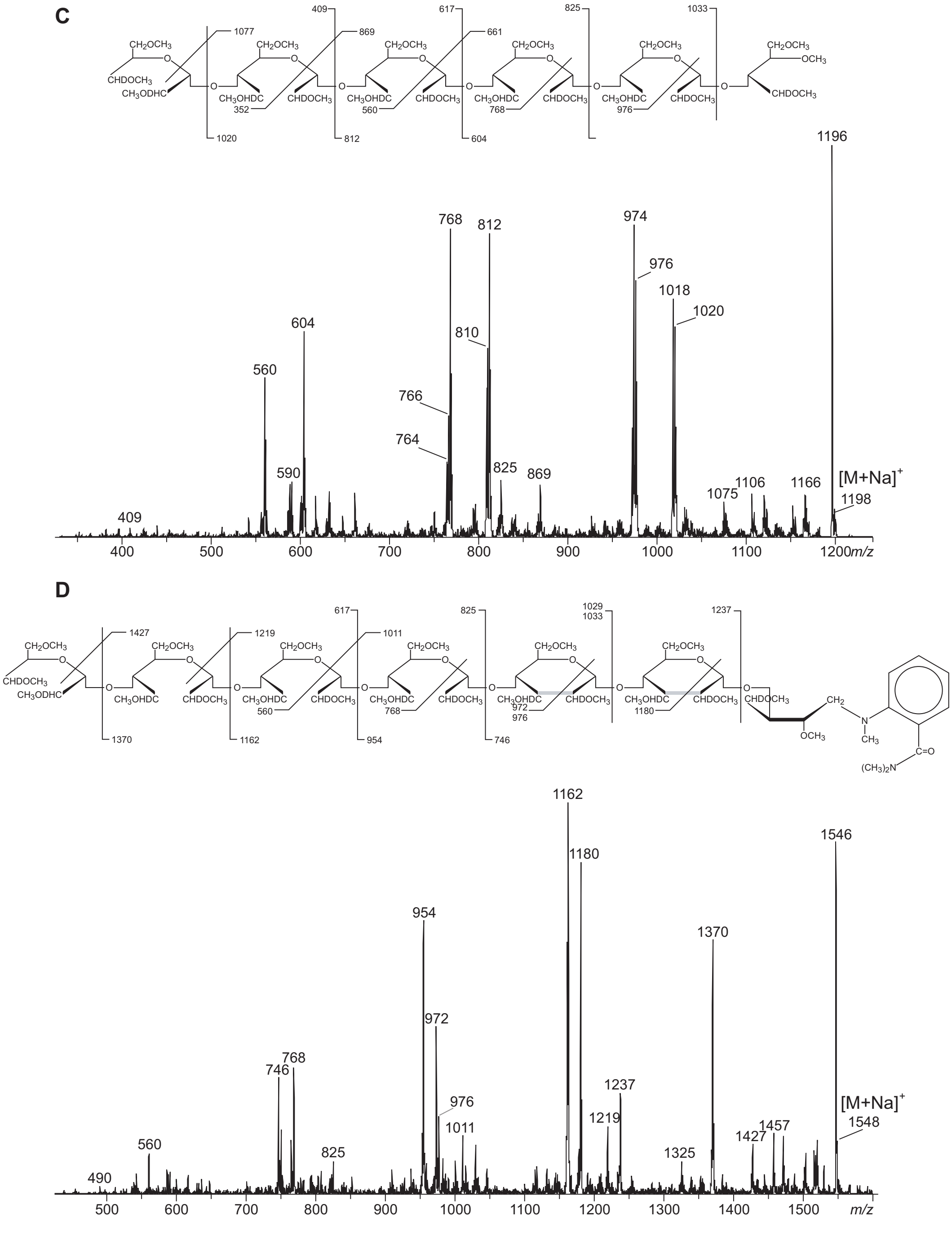

We then selected the ion at *m/z* 986 for collision-induced dissociation. Since this ion had a mass difference of 4 amu compared to the ion at *m/z* 990, it indicates the presence of either a (1→3)-linked residue, or underoxidation of a (1→4)-linked residue. In both cases a residue of 204 amu is found when analyzing the tandem mass spectrum. In the first case, it is likely that the (1→3)-linked residue is present at a specific location, whereas underoxidation may occur at virtually any residue. This was investigated by selecting the ion at *m/z* 986 for tandem mass spectrometric analysis, which gave a fragmentation pattern similar to that of the precursor ion at *m/z* 990, including $^{1,2}A_2$, $^{1,2}A_3$, $^{1,2}A_4$, $^{1,2}X_3$, $^{1,2}X_4$, and $^{1,2}X_5$ ions, giving the complete sequence of (1→4)-linked residues (not shown) indicating that underoxidation is more likely than the presence of an additional (1→3)-linked residue.

The next ion observed in the nanoES mass spectrum, at *m/z* 1198 was a hexasaccharide that may be composed entirely of (1→4)-linked glucose residues. The tandem mass spectrum of precursor ion *m/z* 1198 indeed showed that the hexasaccharide was composed of (1→4)-linked residues, only (**Fig. 11C**, **Table I**). Similar to the ion at *m/z* 990, this compound was also accompanied by an underoxidized form, observed at *m/z* 1194.

The ion at *m/z* 1548 was theoretically composed of one Glc*p*-(1→, four →4)-Glc*p*-(1→, one →3)-Glc*p*-(1→, and one →3)-Glc*p*-(1→[2AB]. The tandem mass spectrum (**Fig. 11D**) showed almost complete series of Y_n- and B_n-type fragment ions that, together with the presence of $^{1,2}A_n$-, and $^{1,2}X_n$-type ions at *m/z* 560, 768, 976 and *m/z* 1427, 1219, 1011, respectively, gave the complete sequence of the ion at *m/z* 1548 (see fragmentation scheme in **Fig. 11D**). According to the fragmentation scheme, the 2-AB label is still attached to the oligosaccharide, indicating 3-substituted reducing end (**Table I**). There may be a second (1→3)-linked residue, although the presence of ions at *m/z* 1237, 1180, 1029, and 972 suggest underoxidation (indicated as grey lines in **Fig. 11D**).

The mass spectrum of fraction **5.6** after 2-AB labeling and per-*O*-methylation showed an ion of high abundance at *m/z* 1455, together with ions of low abundances at *m/z* 1251 and *m/z* 1659, corresponding to sodium cationized pseudomolecular Hex_6, Hex_5, and Hex_7, respectively (not shown). The nanoES mass spectrum of fraction **5.6** after periodate oxidation showed predominantly an ion at *m/z* 1198 (not shown), and therefore, the fraction contained a hexasaccharide composed entirely of (1→4)-linked Glc*p* residues (**Table I**).

The last fraction in this series, fraction **5.8**, predominantly consisted of (1→4)-linked Glc*p* residues as determined by ^{1}H-NMR spectroscopy (**Fig. 12A**); (1→3)-linked residues were not detected. The mass spectrum showed an ion of high abundance at *m/z* 1659 next to an ion of low abundance at *m/z* 1455, analogous to sodium-cationized, fully per-*O*-methylated and 2-AB-derivatized Hex_7 and Hex_6, respectively (not shown). After applying the oxidation procedure, ions at *m/z* 1402, 1406, 1194, and 1198 were observed in the nanoES mass spectrum. Since the ions at *m/z* 1402 and 1194 presumably originated from underoxidation, we focused on the structures of the other ions. The mass of the pseudomolecular ion at *m/z* 1406 suggested that the main component in fraction **5.8** was a heptasaccharide composed of (1→4)-linked Glc*p* residues, only (**Table I**). This was confirmed by the nanoES tandem mass spectrometry (**Fig. 12B**) of the precursor ion at *m/z* 1406 that gave a fragmentation pattern corresponding with Glc*p*-(1→4)-Glc*p*-(1→4)-Glc*p*-(1→4)-Glc*p*-(1→4)-Glc*p*-(1→4)-Glc*p*-(1→4)-Glc*p*.

The ion at *m/z* 1198 differed 208 amu from the ion at *m/z* 1406, and therefore, must be a 2-AB-derivatized, oxidized, and fully per-*O*-methylated hexasaccharide consisting of (1→4)-linked glucose residues. These results show that fraction **5.8** contained two components, namely a heptasaccharide and a hexasaccharide that both are composed entirely of (1→4)-linked α-Glc*p* residues.

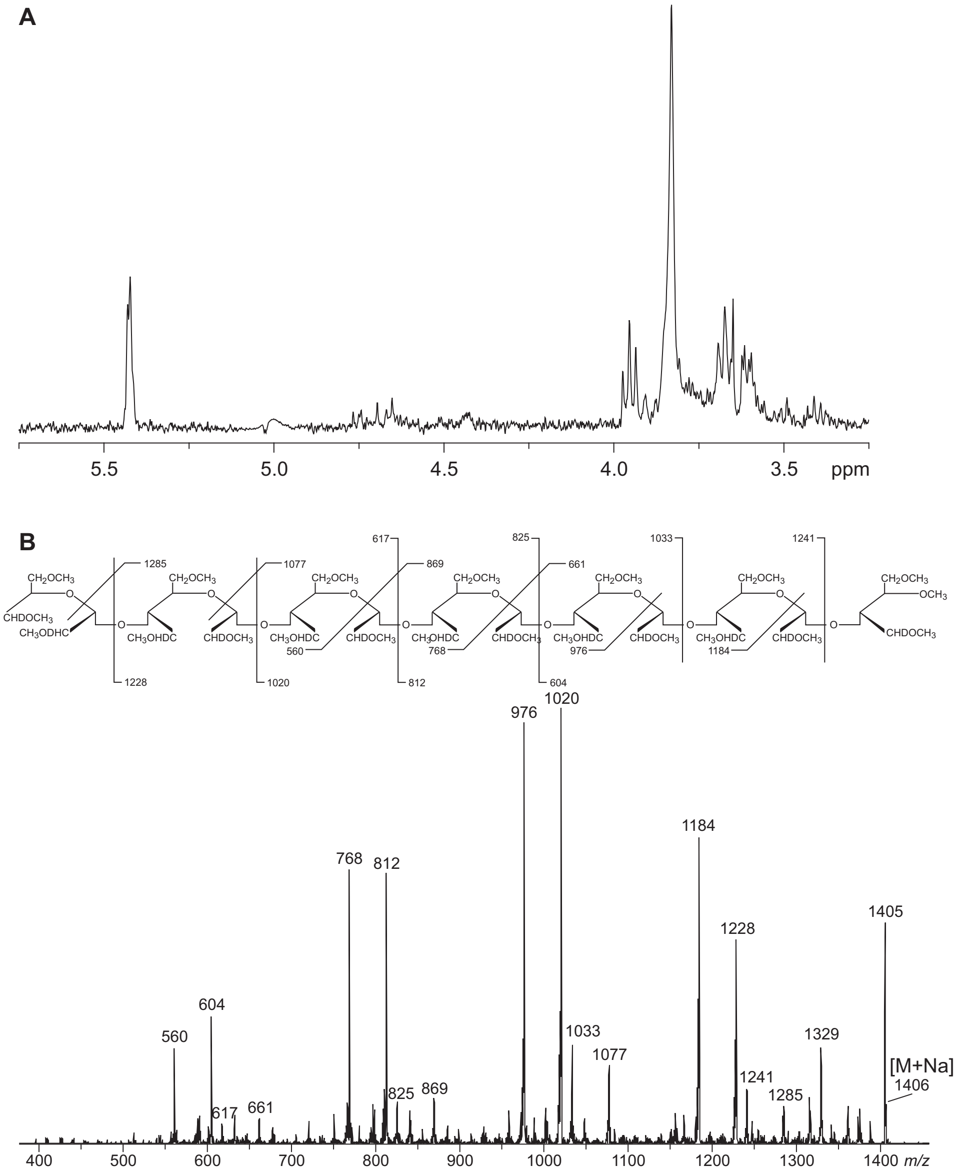

Fig. 12. Fraction **5.8** contains a heptasaccharide consisting of (1→4)-linked glucose residues. ^{1}H-NMR spectroscopy of HPAEC fraction **5.8** (**A**) and positive ion mode nanoES CID tandem mass spectrum of 2-AB labeled, periodate oxidized, and per-*O*-methylated HPAEC fraction **5.8**, *m/z* 1406 (**B**).

Fraction **6** — Fractioning Bio-Gel P4 fraction **6** by HPAEC gave approximately eight well resolved peaks (**Fig. 5**), of which fractions **6.3**, **6.4**, and **6.7** were analyzed further by nanoES-MS. The ^{1}H-NMR spectrum of fraction **6.3** showed two anomeric signals corresponding to (1→4)-linked and (1→3)-linked Glc*p* residues (**Fig. 13A**). The nanoES

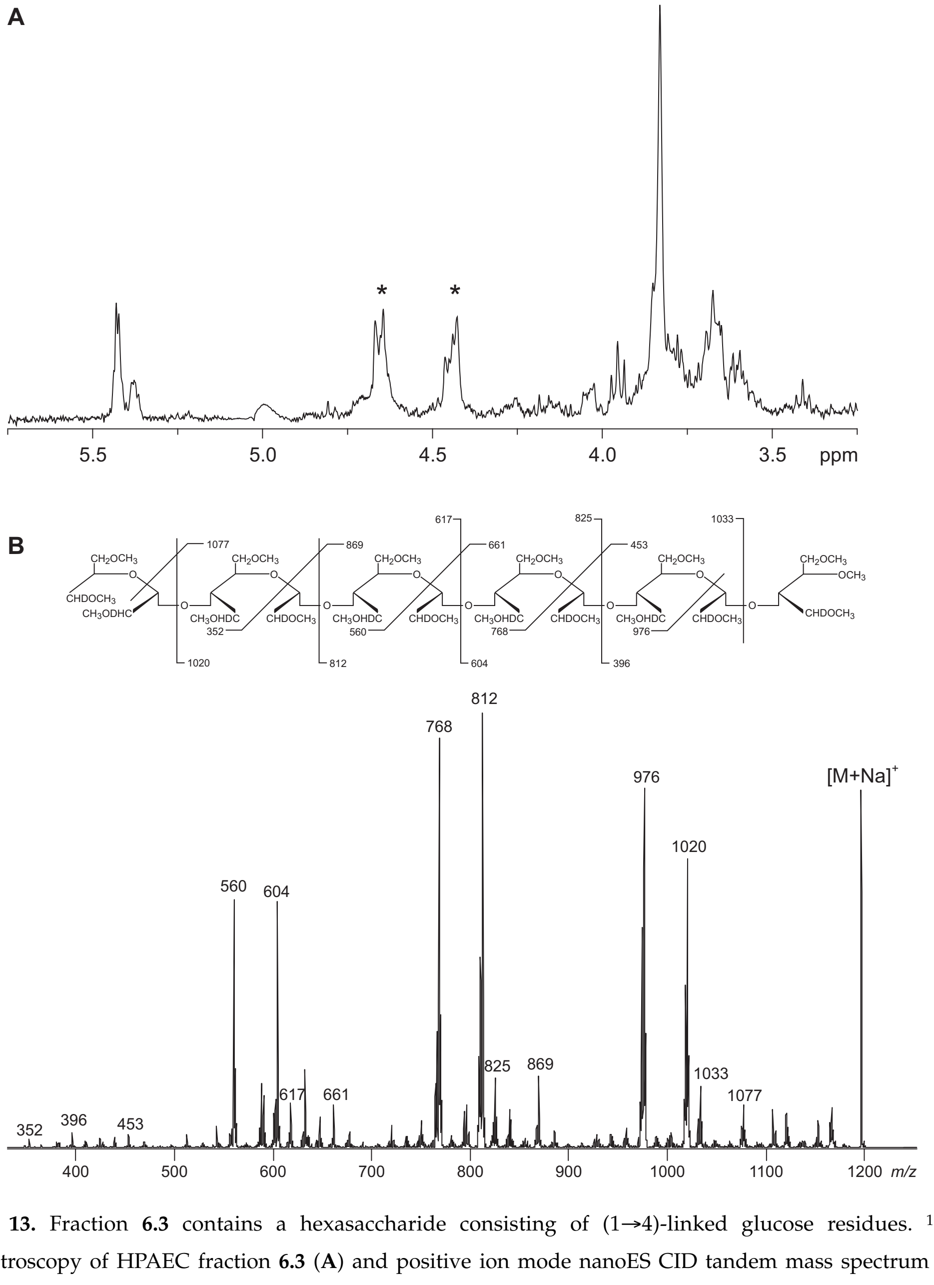

Fig. 13. Fraction **6.3** contains a hexasaccharide consisting of (1→4)-linked glucose residues. ^{1}H-NMR spectroscopy of HPAEC fraction **6.3** (**A**) and positive ion mode nanoES CID tandem mass spectrum of 2-AB labeled, periodate oxidized, and per-*O*-methylated HPAEC fraction **6.3**, *m/z* 1198 (**B**). NMR signals indicated with an asterisk (*) belong to an unknown contamination.

mass spectrum of the 2-AB labeled and per-*O*-methylated sample showed one signal of high abundance at *m/z* 1659, corresponding to a fully per-*O*-methylated heptasaccharide (not shown). In addition, a signal of medium abundance was detected at *m/z* 1455, which corresponded to a fully per-*O*-methylated hexasaccharide. The nanoES mass spectrum of fraction **6.3** after 2-AB labeling, oxidation/reduction and per-*O*-methylation gave two ions of high abundance at *m/z* 1194 and 1198, of which the latter corresponded to a hexasaccharide composed of (1→4)-linked glucose residues, only (not shown). This was confirmed by selecting the ion at *m/z* 1198 for tandem mass spectrometry (**Fig. 13B**, **Table I**). Tandem MS analysis of the ion at *m/z* 1194 showed that this ion originated from underoxidation (not shown). Importantly, a heptasaccharide was not identified, which is in contrast with the observations made for the MS analysis of the per-*O*-methylated sample, indicating that fraction **6.3** was slightly degraded due to overoxidation. Overoxidation is the degradation of 4-substituted reducing ends, that gradually processes towards the non-reducing end by hydrolyzing glycosidic linkages (Dyer, 1956). An erroneous calculation of the degree of polymerization can be the result, but by comparing the molecular masses before and after oxidation, overoxidation is readily noticed.

The ^{1}H-NMR spectrum of fraction **6.4** showed an anomeric signal corresponding to (1→4)-linked Glc*p* residues (**Fig. 14A**). MS analysis after 2-AB labeling and per-*O*-methylation gave an ion of high abundance at *m/z* 1863 and a signal of medium abundance at *m/z* 1659, corresponding to an octasaccharide and a heptasaccharide, respectively (not shown). The nanoES mass spectrum of fraction **6.4** undergoing the oxidation procedure showed ions at *m/z* 1194, 1198, 1398, 1402, and 1742 (not shown). Of these, the ion at *m/z* 1198 corresponded to a hexasaccharide consisting of (1→4)-linked glucose residues, only (**Fig. 14B**, **Table I**), whereas the ion at *m/z* 1194 originated from underoxidation (not shown). Both ions were probably formed by overoxidation of a (1→4)-linked heptasaccharide. Similarly, tandem mass spectrometry showed that the ions at *m/z* 1398 and 1402 corresponded to singly and doubly underoxidized (1→4)-linked heptasaccharides, respectively. When selecting the ion at *m/z* 1742 for collision-induced dissociation, we obtained a mass spectrum that corresponded to an octasaccharide with the 2-AB label still attached to the octasaccharide, indicating a 3-substituted reducing end (**Fig. 14C**, **Table I**). According to the fragmentation scheme, multiple-underoxidation may have occurred, and therefore, we presume that the ion at *m/z* 1742 is derived from Glc*p*-(1→4)-Glc*p*-(1→4)-Glc*p*-(1→4)-Glc*p*-(1→4)-Glc*p*-(1→4)-Glc*p*-(1→4)-Glc*p*-(1→3)-Glc*p*.

The ^{1}H-NMR spectrum obtained from fraction **6.7** showed two anomeric signals, corresponding to (1→4)-linked and (1→3)-linked Glc*p* residues (**Fig. 15A**). Analysis of this fraction after 2-AB labeling and per-*O*-methylation by nanoES-MS gave an ion at *m/z* 1455, indicating a fully methylated heptasaccharide (not shown). After periodate oxidation, reduction, and per-*O*-methylation, two ions were present in the mass spectrum at *m/z* 1398 and 1402 (not shown). The ion at *m/z* 1402 was selected for collision induced dissociation, which gave a fragmentation pattern consistent with a Glc*p*-(1→3)-Glc*p*-(1→4)-Glc*p*-(1→4)-Glc*p*-(1→4)-Glc*p*-(1→4)-Glc*p*-(1→4)-Glc*p* (**Fig. 15B**, **Table I**).

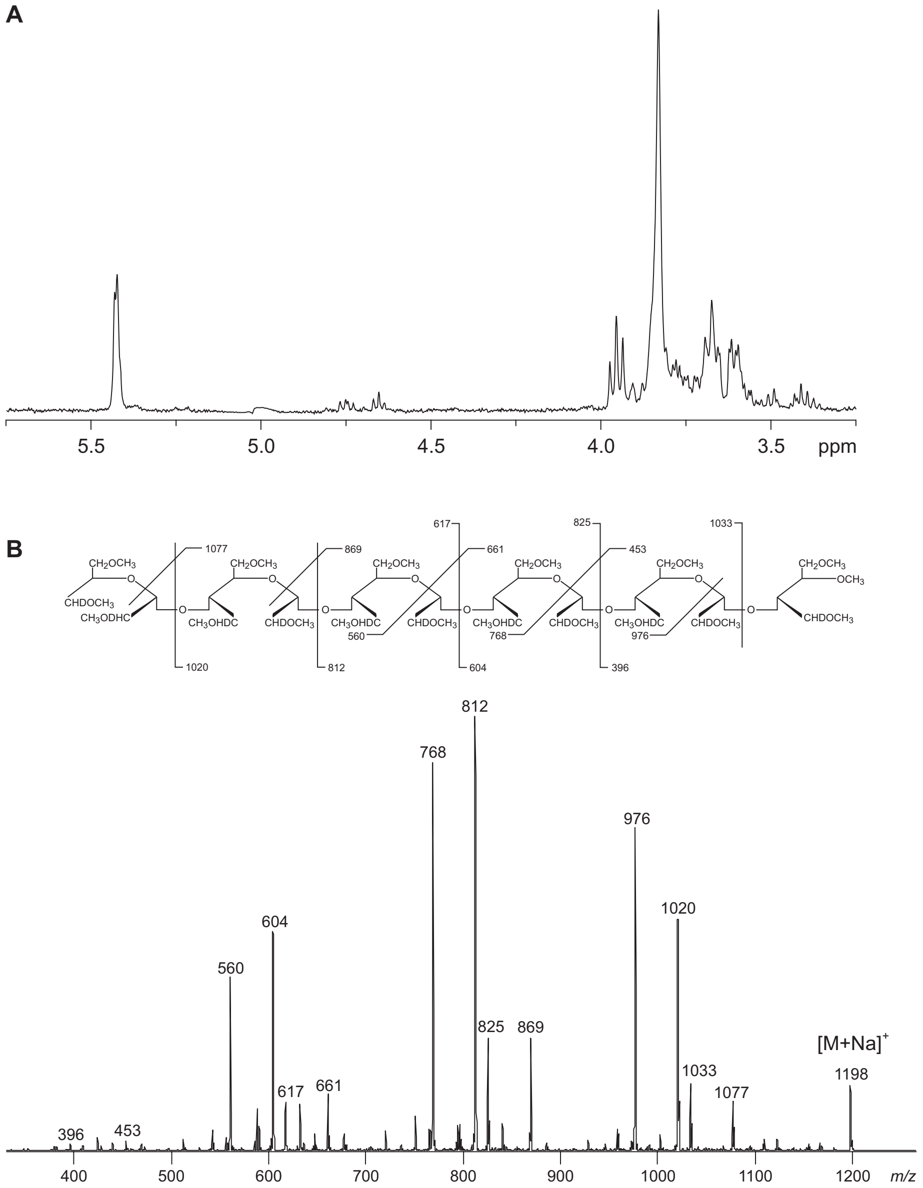

Fig. 14. Fraction **6.4** consists of a mixture of oligosaccharides. ^{1}H-NMR spectroscopy of HPAEC fraction **6.4** (**A**) and positive ion mode nanoES CID tandem mass spectrum of 2-AB labeled, periodate oxidized, and per-*O*-methylated HPAEC fraction **6.4**, *m/z* 1198 (**B**) and *m/z* 1742 (**C**). Linkages indicated in grey indicate possible underoxidation between C-2 and C-3.

Fraction **7** — HPAEC fractionation of Bio-Gel P4 fraction **7** gave ten major fractions (**Fig. 5**), of which ^{1}H-NMR analysis showed that fraction **7.5** contains both (1→4)-linked and (1→3)-linked α-Glc*p* (**Fig. 16A**). The positive ion mode ES mass spectrum obtained

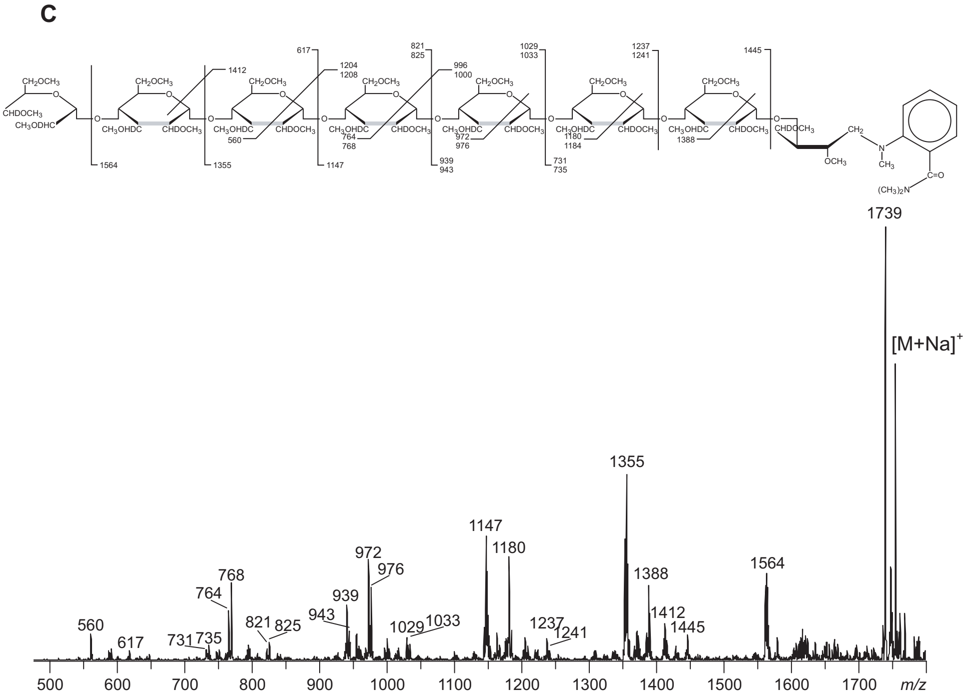

from per-*O*-methylated fraction **7.5** was of poor quality showing ions at *m/z* 1455, 1659, and 1863, representing a sodium-cationized, 2-AB labeled, and fully per-*O*-methylated hexasaccharide, heptasaccharide, and octasaccharide, respectively (not shown). The ES mass spectrum of this fraction after applying the oxidation procedure, also was of poor quality (not shown). An ion was observed at *m/z* 1818 that according to its mass-to-charge ratio may be composed of a nonasaccharide containing one Glc*p*-(1→, six →4)-Glc*p*-(1→, and one 4)-Glc*p* residues plus one →3)-Glc*p*-(1→ residue or one underoxidation. The ES tandem mass spectrum of this ion gave the complete sequence of the nonasaccharide, clearly indicating that a single underoxidation occurred (**Fig. 16B**, possible positions of underoxidation indicated by a grey line). Therefore, the fragmentation indicates that the nonasaccharide may be composed of (1→4)-linked glucose residues, only (**Table I**).

Due to the poor quality of the mass spectrum of fraction **7.5**, other ions than *m/z* 1818 could not be selected for collision-induced dissociation. Importantly, the nonasaccharide that we were able to identify by ES mass spectrometric analysis of the oxidized sample, was missing in the nanoES mass spectrum obtained from the per-*O*-methylated sample. This observation may be explained by the high mass-to-charge ratio of this ion, *m/z* 2076 for a single-charged pseudo-molecular ion, which exceeded the mass range of the mass spectrometer. Furthermore, ^{1}H-NMR spectrometry indicated the presence of some (1→3)-linkages. We assume that these residues were present as minor components that were overlooked, again due to the poor quality of the mass spectra.

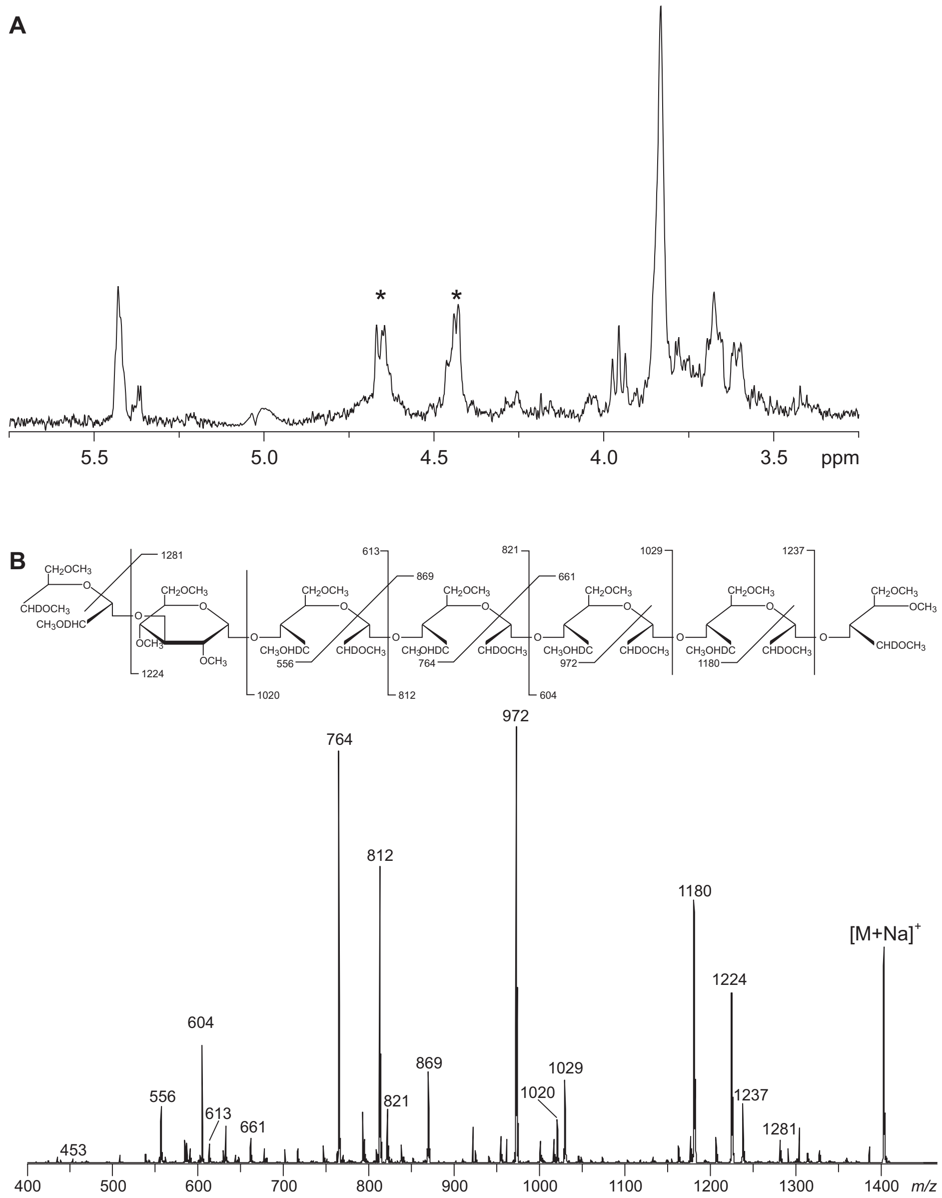

Fig. 15. Fraction **6.7** contains a heptasaccharide consisting of mixed (1→4)-linked and (1→3)-linked glucose residues. ^{1}H-NMR spectroscopy of HPAEC fraction **6.7** (**A**) and positive ion mode nanoES CID tandem mass spectrum of 2-AB labeled, periodate oxidized, and per-*O*-methylated HPAEC fraction **6.7**, *m/z* 1402 (**B**). NMR signals indicated with an asterisk (*) belong to an unknown contamination.

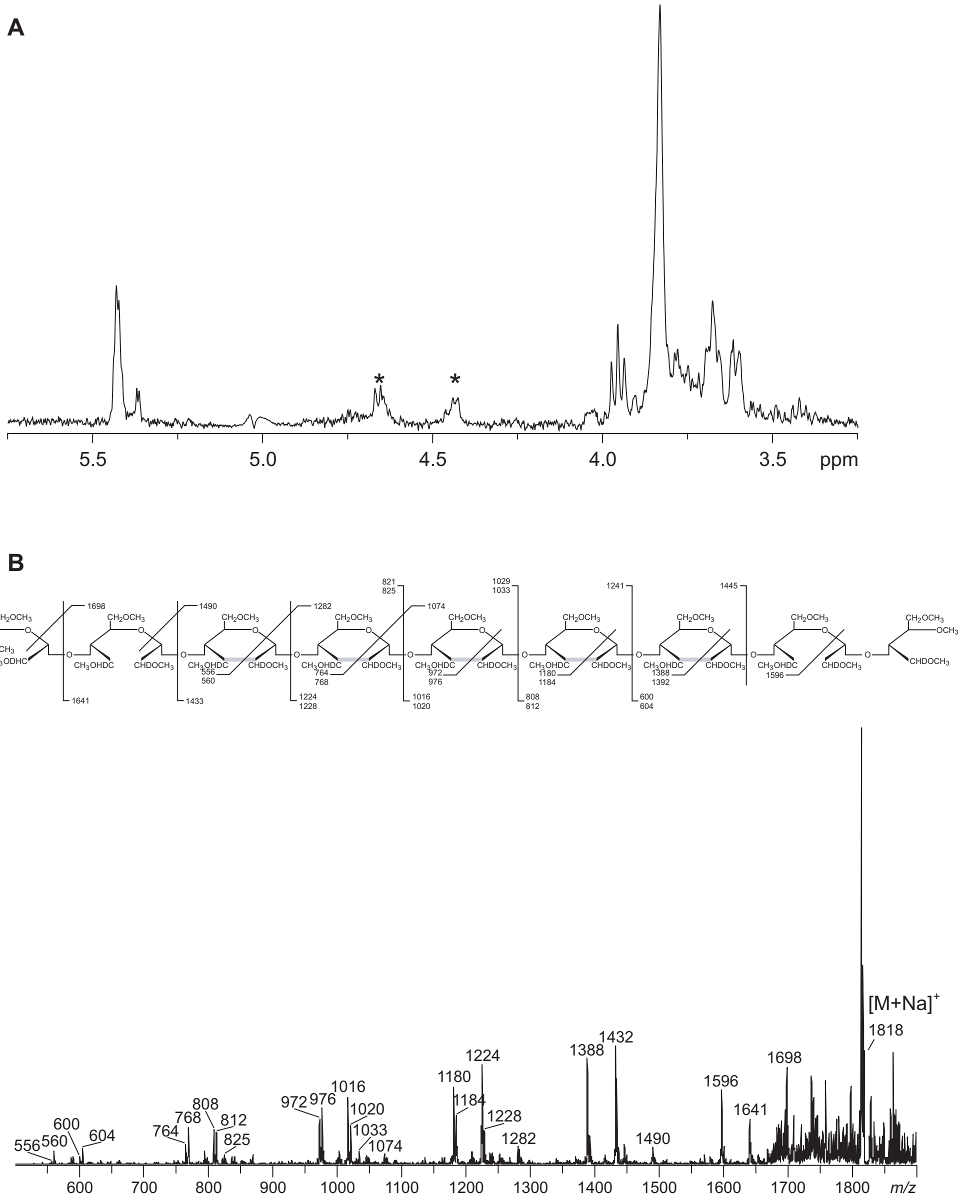

Fig. 16. Fraction **7.5** contains a nonasaccharide consisting of (1→4)-linked glucose residues. ^{1}H-NMR spectroscopy of HPAEC fraction **7.5** (**A**) and positive ion mode nanoES CID tandem mass spectrum of 2-AB labeled, periodate oxidized, and per-*O*-methylated HPAEC fraction **7.5**, *m/z* 1818 (**B**). NMR signals indicated with an asterisk (*) belong to an unknown contamination. Linkages indicated in grey indicate possible underoxidation between C-2 and C-3.

Discussion

Fission-yeast α-glucan

Here, we have characterized the stretches containing (1→4)-linked glucose residues present in cell-wall α-glucan of fission yeast after removing the (1→3)-linked glucose residues by *endo*-(1→3)-α-glucanase digestion. Analysis of the glucanase-resistant material showed that two classes of products were present. The first class comprises linear oligosaccharide structures composed of one or more consecutive (1→4)-linked α-glucose residues linked to an oligomer of two or more, (1→3)-linked glucose residues. Taking into consideration the catalytic mechanism of *T. harzianum* (see Supplemental data at the end of this chapter) together with our observation that fission-yeast α-glucan is resistant towards glucoamylase digestion (Chapter 2), we propose that this class of oligosaccharides originates from the intrachain region of α-glucan that links two (1→3)-α-glucan segments via a number of (1→4)-linked glucose residues (**Fig. 17**).

The second class consists of linear oligosaccharides that are composed exclusively of (1→4)-linked α-Glc*p* residues, or, in a single case, with a (1→3)-linked non-reducing end. Taking into consideration the catalytic mechanism of the (1→3)-α-glucanase preparation we assume that the second class of oligosaccharides was derived from the reducing end of the α-glucan polymer (**Fig. 17**). Previously, we showed that fission-yeast α-glucan is composed of two building blocks, each consisting of a (1→3)-α-glucan segment with a short stretch containing (1→4)-linked glucose residues. In the present study, we demonstrated that this stretch consists of oligomers of consecutive (1→4)-linked glucose residues.

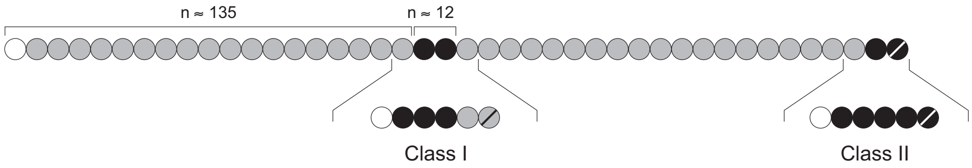

Fig. 17. Schematic representation of α-glucan from fission-yeast cell walls. Digestion of α-glucan with an *endo*-(1→3)-α-glucanase gave two classes of oligosaccharides, depending on whether they originated from the center part of the α-glucan molecule (Class I) or from the reducing end (Class II). White spheres: non-reducing end; black spheres: (1→4)-linked residues; grey spheres: (1→3)-linked residues; reducing ends are marked with a diagonal line.

Sequencing structurally closely related oligosaccharides

Complete structural elucidation of oligosaccharides containing chemically similar linkages by NMR spectroscopy is not always possible due to strong overlapping of signals. Linkage analysis gives quantitative information on the type of linkages (Lindberg, 1972), but the lack of sequence information and the relative high amounts that are needed necessitates the use of other methods. Mass spectrometry of per-*O*-acetylated or per-*O*-

methylated oligosaccharides is a highly sensitive technique that can be used for complete structural characterization of oligosaccharides (Dell & Morris, 2001; Dell *et al.*, 1997; Costello, 1997), but often relies on the presence of specific cross-ring fragmentation and the absence of others such that unambiguous determination of glycosidic linkages is not always possible. Our structural analysis method allowed us to rapidly sequence structurally closely related oligosaccharides. The method is based on differences in reactivity towards periodate in combination with nanoES mass spectrometry. We showed that this method can be used to unambiguously differentiate between (1→3)-linked and (1→4)-linked hexose residues. By using collision-induced dissociation, we were able to determine the sequences of oligosaccharides. Importantly, this method can be extended readily to other types of linkages, linear as well as branched oligosaccharides, and *N*-glycans derived from glycoproteins. Limitations encountered in this method include under- and overoxidation. Misinterpretation may be the result of underoxidation because (1→4)-linked residue may than have the same nominal mass as (1→3)-linked residues. However, since underoxidation occurs virtually randomly, this will be noticed readily. Overoxidation, on the other hand, leads to degradation of 4-substituted oligosaccharides starting from the reducing end and processing towards the non-reducing end (Dyer, 1956). Thus, the result may be an erroneous determination of the degree of polymerization of the molecule. Nonetheless, by comparing molecular masses of oligosaccharides before and after applying the oxidation procedure, overoxidation can be noticed easily and corrections can be made concerning the proposed structures.

A second limitation was encountered with a decrease in detection sensitivity with increasing molecular mass, which is common to carbohydrates. In addition to strong heterogeneity of high-molecular mass fractions, we were unable to obtain decent mass spectra of oligosaccharides with a degree of polymerization higher than approximately eight. Therefore, we only analyzed the first seven out of fifteen Bio-Gel P4 fractions. Although only a limited number of fractions were analyzed, we consider these fractions to be representative structures of the (1→4)-linked stretch present in fission-yeast α-glucan.

Finally, for the hydrolysis of α-glucan, we used an *endo*-(1→3)-α-glucanase preparation that was purified by binding to its substrate (see Supplementary data at the end of this chapter). Despite this substrate-specific purification, we cannot exclude the possibility of co-purification of contaminating enzymes, such as amylases, and although we could not determine such enzyme activity, we hydrolyzed fission-yeast α-glucan during a number of short 1-h incubations to minimize the chance of degradation with contaminating enzymes.

Concluding remarks

α-Glucan is present in the cell walls of many fungi at levels varying from 9 to 46%, depending on the fungal species. The basic chemical compositions of α-glucans from a number of fungal species have been elucidated, and interestingly, many α-glucans are composed similar to that of fission yeast. For instance, α-glucans from *Aspergillus* species, *Fusicoccum amygdali*, *Neurospora crassa*, and *Cryptococcus neoformans*, like fission-yeast α-glucan, consist mainly of (1→3)-linked α-Glc*p* residues with a small percentage of (1→4)-linked residues (Bobbit *et al.*, 1977; Buck & Obaidah, 1971; Obaidah & Buck, 1971; Cardemil & Pincheira, 1979; James *et al.* 1990). Furthermore, in *A. fumigatus*, *N. crassa*, and *C. neoformans*, homologs of *S. pombe* α-glucan synthase (Ags1p) have been identified. We therefore predict that also the chemical structure of fission-yeast α-glucan may be conserved among these and other fungi.

Materials and methods

Isolation of cell-wall α-glucan

Cells of strain FH023 (h^-) (Hochstenbach *et al.*, 1998) were grown in 12 L of YEA medium to a final OD_{595} of 4, cooled in an ice-bath, collected by centrifugation, and washed twice in breaking buffer [5 mM sodium azide, 20 mM Tris-HCl, pH 7.6]. Cells were resuspended in breaking buffer and subjected to mechanical breakage in a Malton-Gaulin, followed by a Bead-Beater (BioSpec Products, Bartlesville, US) by using glass beads (0.45 mm diameter). Twelve rounds of one-minute homogenization were alternated with one-minute cooling periods, such that more than 95% of the cells had lysed. The cell lysate was collected and centrifuged. This and all subsequent centrifugation steps were carried out at 7500 × at 4 °C for 20 min. After two washing steps in MilliQ-H_2O (Millipore), the pellet was resuspended in 200 ml of SDS-extraction buffer [40 mM 2-mercaptoethanol, 2% (w/v) SDS, 100 mM Na-EDTA, 50 mM Tris-HCl, pH 7.6], and incubated in a boiling waterbath for 20 min to remove cytosolic contaminants. The suspension was centrifuged, washed twice in MilliQ-H_2O, and stored in 5 mM sodium azide at 4 °C.

For α-glucan isolations, whole cell-wall preparations were resuspended in 200 ml of digestion buffer [5 mM sodium azide, 40 mM 2-mercaptoethanol, 50 mM citrate-phosphate, pH 5.3] containing 15 mg of Zymolyase-100T (Seikagaku), and incubated in a rotary shaker at 37 °C for at least 12 h. After centrifugation, the pellet was resuspended in breaking buffer, glass beads were added, and the cell-wall material was treated in a Mikro-Dismembrator (Braun) at 3000 rpm for 3 min to ensure that all cells had been broken. Then, Zymolyase digestion was repeated, followed by a final extraction with SDS. After two washing steps in MilliQ-H_2O, purified α-glucan was stored in 5 mM sodium azide at 4 °C.

Preparation and separation of α-glucan oligosaccharides

100 mg of α-glucan obtained from the cell walls of *S. pombe* wild-type strain FH023 was suspended in digestion buffer [50 mM NaOAc, pH 5.6, 5 mM NaN_3]. *endo*-(1→3)-α-glucanase (purified from an enzyme preparation from *Trichoderma harzianum* (Novozym, Sigma) via adsorption chromatography) was added and the reaction mixture was

incubated at 37 °C during 1 h. Glucanase digestion was repeated several times using fresh buffer and enzyme. Collected supernatants were desalted by solid-phase extraction using Carbograph SPE columns (Alltech Associates) using the procedure described by Packer *et al.* (1998), which also separates monosaccharides from oligosaccharides. Products were applied on a thermostated Bio-Gel P4 size-exclusion column (1.6 × 90 cm, 55 °C) (BioRad) and eluted with water at a flow-rate of 4.8 ml/h. Carbohydrates in the eluate were quantitatively determined by the phenol-sulfuric acid assay (Dubois *et al.*, 1956). Fractions of 2.0 ml were collected and appropriate fractions were pooled and further purified by HPAEC.

High-performance anion-exchange chromatography

HPAEC was performed on a Dionex DX 500 system equipped with a GP 40 gradient pump and an ED 40 electrochemical detector (Dionex Corporation). A 4 × 250 mm Carbopac PA-1 column was used for analytical HPAEC. Appropriate linear gradients were applied for each component using 100 mM NaOH and 500 mM NaOAc in 100 mM NaOH as eluents. A flow rate of 1.0 ml/min was used. Purification of Bio-Gel P4 fractions was performed on a semi-preparative 9 × 250 mm Carbopac PA-1 column using the same eluents at a flow rate of 4.0 ml/min. Fractions were desalted using Carbograph SPE columns, followed by evaporation of the solvent *in vacuo*.

Nuclear magnetic resonance spectroscopy

^{1}H-NMR spectra were recorded on a Bruker DRX500 spectrometer (Bijvoet Center, Department of NMR Spectroscopy) at 27 °C. Samples were dissolved in 600 µl 99.9% D_2O. The residual HOD signal was suppressed by applying a WEFT pulse sequence (Hård *et al.*, 1992). Chemical shifts were referred to internal acetate (^{1}H: 1.908 ppm). Data were processed using in house developed software.

2-AB labeling, periodate oxidation, and methylation

Oligosaccharides were labeled at their reducing ends with 2-aminobenzamide (2-AB) according to Bigge *et al.* (1995). To the dried oligosaccharides, 5 µl of a solution of 2-AB (23.6 mg) and sodium cyanoborohydride (31.75 mg) in DMSO/acetic acid 7:3, (500 µl) was added. The reaction was carried out at 65 °C for 2 h after which the samples were cleaned-up on Whatman QM-A chromatography paper. Reactants were removed by rinsing with acetonitrile (1 ml) and 4% water in acetonitrile (6 × 1 ml). Labeled products were eluted with water (4 × 0.5 ml).

Periodate oxidation of labeled oligosaccharides was basically performed as described by Angel *et al.* (1991). Briefly, 2-AB labeled oligosaccharides were dissolved in 50 mM sodium acetate (pH 5.5) containing 8 mM sodium periodate. Samples were stirred in the dark at 4 °C during 24 h. The pH was adjusted to 7.0 by addition of NaOH. $NaBD_4$ was added and incubation was continued during 24 h at 4 °C. Excess of $NaBD_4$ was removed by adjusting the pH to 4.5 with acetic acid. Boric acid was co-evaporated with methanol under reduced pressure. The reduced products were acetylated in acetic anhydride/pyridine during 30 min at 70 °C. After concentration to dryness, acetylated products were extracted by chloroform from water. The dried products were methylated according to Ciucanu and Kerek (1984).

Mass spectrometry

Experiments were performed on an LC-Q ion trap mass spectrometer (Thermoquest/ Finnigan) equipped with a nanoES sample probe (Protana). 2-AB labeled, oxidized/reduced, and per-*O*-methylated samples were dissolved in methanol/water (7:3) to a concentration of approximately 10 to 30 pmol/µl. For each experiment, 2 µl were loaded into the gold-coated glass capillary. The capillary temperature was set to 180 °C. Spectra were taken in the positive ion mode with a spray voltage of 1.5 kV and a varying capillary voltage of 31.5 to 46.0 V.

References

Abdel-Akher, M.; Hamilton, J.K.; Montgommery, R. & Smith, F. (1952) A new procedure for the determination of the fine structure of polysaccharides. *J. Am. Chem. Soc.* **74,** 4970-4971.

Alonso, M.D.; Lomako, J.; Lomako, W.M. & Whelan, W.J. (1995) A new look at the biogenesis of glycogen. *FASEB J.* **9,** 1126-1137.

Angel, A.S.; Lipniunas, P.; Erlansson, K. & Nilsson, B. (1991) A procedure for the analysis by mass spectrometry of the structure of oligosaccharides from high-mannose glycoproteins. *Carbohydr. Res.* **221,** 17-35.

Bacon, J.S.D.; Jones, D.; Farmer, V.C. & Webley, D.M. (1968) The occurrence of (1→3)-α-glucan in *Cryptococcus*, *Schizosaccharomyces* and *Polyporus* species, and its hydrolysis by a *Streptomyces* culture filtrate lysing cell walls of *Cryptococcus*. *Biochim. Biophys. Acta* **158,** 313-315.

Bigge, J.C.; Patel, T.P.; Bruce, J.A.; Goulding, P.N.; Charles, S.M. & Parekh, R.B. (1995) Nonselective and efficient fluorescent labeling of glycans using 2-amino benzamide and anthranilic acid. *Anal. Biochem.* **230,** 229-238.

Bobbit, T.F.; Nordin, J.H.; Roux, M.; Revol, J.F. & Marchessault, R.H. (1977) Distribution and conformation of crystalline nigeran in hyphal walls of *Aspergillus niger* and *Aspergillus awamori*. *J. Bacteriol.* **132,** 691-703.

Buck, K.W. & Obaidah, M.A. (1971) The composition of the cell wall of *Fusicoccum amygdali*. *Biochem. J.* **125,** 461-471.

Bush, D.A.; Horisberger, M.; Horman, I. & Wursch, P. (1974) The wall structure of *Schizosaccharomyces pombe*. *J. Gen. Microbiol.* **81,** 199-206.

Cardemil, L. & Pincheira, G. (1979) Characterization of the carbohydrate component of fraction I in the *Neurospora crassa* cell wall. *J. Bacteriol.* **137,** 1067-1072.

Ciucanu, I. & Kerek, F. (1984) A simple and rapid method for the permethylation of carbohydrates. *Carbohydr. Res.* **131,** 209-217.

Costello, C.E. (1997) Time, life...and mass spectrometry. New techniques to address biological questions. *Biophys. Chem.* **68,** 173-188.

Dell, A. & Morris, H.R. (2001) Glycoprotein structure determination by mass spectrometry. *Science* **291,** 2351-2356.

Dell, A.; Morris, H.R.; Panico, M.; Haslam, S.M.; Easton, R. & Khoo, K.-H. (1997) Trends in mass spectrometry of carbohydrates and glycoconjugates. *Carbohydr. Eur.* **17,** 10-16.

Domon, B. & Costello, C.E. (1988) A systematic nomenclature for carbohydrate fragmentation in FAB-MS/MS spectra of glycoconjugates. *Glycoconj. J.* **5,** 379-409.

Dubois, M.; Gilles, K.A.; Hamilton, J.K.; Rebers, P.A. & Smith, F. (1956) Colorimetric method for the determination of sugars and related substances. *Anal. Chem.* **28,** 350-356.

Dyer, J.R. (1956) Use of periodate oxidation in biochemical analysis. In: *Methods of biochemical analysis*; Glick, D., Ed.; Vol. 3, Interscience Publishers Inc.: New York, pp. 111-152.

Fox, J.; Kawaguchi, K.; Greenberg, E. & Preiss, J. (1976) Biosynthesis of bacterial glycogen. Purification and properties of the *Escherichia coli B* ADPglucose:1→4-α-D-glucan 4-α-glucosyltransferase. *Biochemistry* **15,** 849-856.

Fuglsang, C.C.; Berka, R.M.; Wahleithner, J.A.; Kauppinen, S.; Shuster, J.R.; Rasmussen, G. Halkier, T.; Dalboge, H. & Henrissat, B. (2000) Biochemical analysis of recombinant fungal mutanases. A new family of α1→3-glucanases with novel carbohydrate-binding domains. *J. Biol. Chem.* **275,** 2009-2018.

Germaine, G.R.; Chludzinski, A.M. & Schachtele, C.F. (1974) *Streptococcus mutans* dextransucrase: requirement for primer dextran. *J. Bacteriol.* **120,** 287-294.

Hård, K; Van Zadelhoff, G.; Moonen, P.; Kamerling, J.P. & Vliegenthart, J.F.G. (1992) The Asn-linked carbohydrate chains of human Tamm-Horsfall glycoprotein of one male. Novel sulfated and novel *N*-acetylgalactosamine-containing *N*-linked carbohydrate chains. *Eur. J. Biochem.* **209,** 895-915.

Hochstenbach, F.; Klis, F.M.; Van Den Ende, H.; Van Donselaar, E. Peters, P.J. & Klausner, R.D. (1998) Identification of a putative α-glucan synthase essential for cell wall construction and morphogenesis in fission yeast. *Proc. Natl. Acad. Sci. U S A* **95,** 9161-9166.

James, P.G.; Cherniak, R.; Jones, R.G. & Stortz, C.A. (1990) Cell-wall glucans of *Cryptococcus neoformans* Cap 67. *Carbohydr. Res.* **198,** 23-38.

Kawaguchi, K.; Fox, J.; Holmes, E.; Boyer, C. & Preiss, J. (1978) *De novo* synthesis of *Escherichia coli* glycogen is due to primer associated with glycogen synthase and activation by branching enzyme. *Arch. Biochem. Biophys.* **190,** 385-397.

Lindberg, B. (1972) Methylation analysis of polysaccharides. In: *Methods in enzymology*; Ginsburg, V., Ed.; Academic Press: New York and London; Vol. 28; pp. 178-195.

Obaidah, M.A. & Buck, K.W. (1971) Characterization of two cell-wall polysaccharides from *Fusicoccum amygdali*. *Biochem. J.* **125,** 473-480.

Packer, N.H.; Lawson, M.A.; Jardine, D.R. & Redmond, J.W. (1998) A general approach to desalting oligosaccharides released from glycoproteins. *Glycocon. J.* **15,** 737-747.

Peng, L.; Kawagoe, Y.; Hogan, P. & Delmer, D. (2002) Sitosterol-β-glucoside as primer for cellulose synthesis in plants. *Science* **295,** 147-150.

Smith, A.M. (1999) Making starch. *Curr. Opin. Plant. Biol.* **2,** 223-229.

Whelan, W.J. (1998) Pride and prejudice: the discovery of the primer for glycogen synthesis. *Protein Sci.* **7,** 2038-201.

Supplementary data

Catalytic mechanism of (1→3)-α-glucanase from *Trichoderma harzianum*

Christian H. Grün[1], Alexander A. Nieuwland[1], Frans Hochstenbach[2], Nick Dekker[2], Frans M. Klis[3], Johannis P. Kamerling[1], and Johannes F.G. Vliegenthart[1]

[1]*Bijvoet Center, Department of Bio-Organic Chemistry, Section of Glycoscience and Biocatalysis, Utrecht University;* [2]*Department of Biochemistry, Academic Medical Center, University of Amsterdam;* [3]*Swammerdam Institute for Life Sciences, University of Amsterdam*

Abstract

(1→3)-α-Glucanases are glycosidases that catalyze the hydrolysis of (1→3)-α-glycosidic linkages. Glycosidases obtained in a pure form are invaluable tools for studying the chemical structures of carbohydrates. Here, we characterize the catalytic mechanism of (1→3)-α-glucanase isolated from the fungus *Trichoderma harzianum*. Defined nigerooligosaccharide substrates were obtained by acid hydrolysis of (1→3)-α-glucan followed by size-exclusion and high-performance anion-exchange chromatography (HPAEC). The action pattern was investigated by analyzing digest products by HPAEC. By labeling the substrate at its reducing end, we showed that the enzyme possesses *endo*-catalytic activity. Furthermore, we showed that nigerotetraose is the minimal substrate that is readily hydrolyzed. Enzymatic hydrolysis of (1→3)-α-glucan yielded mostly glucose, indicating repetitive attack by the enzyme. Using NMR spectroscopy, we showed that the enzyme hydrolyzes the substrate with inversion of the anomeric configuration. We propose a model for the catalytic mechanism of *endo*-(1→3)-α-glucanase from *T. harzianum* in which the enzyme attacks an intrachain glycosidic linkage of the polysaccharide substrate, and after initial hydrolysis proceeds in the direction of the non-reducing end, releasing β-glucose residues. The hydrolysis continues until the substrate is reduced to a trisaccharide, which is subsequently released into the medium.

Introduction

(1→3)-α-Glucanases represent a group of enzymes that hydrolyze (1→3)-α-glycosidic linkages. The (1→3)-α-glucanase from the mycopathogenic fungus *Trichoderma harzianum* was first described by Guggenheim and Haller (1972) and its nucleotide sequence was analyzed by Fuglsang *et al.* (2000). The results of Fuglsang and colleagues indicate that the COOH-terminal domain of the enzyme constitutes a substrate-binding domain, whereas the NH_2-terminal domain represents the catalytic domain. Interestingly, the enzyme shows sequence similarity with two open reading frames (ORFs) in fission-yeast *Schizosaccharomyces pombe*, suggesting that these ORFs encode enzymes with similar functions (Fuglsang *et al.*, 2000). Furthermore, the authors assigned the enzyme to a new gene family of glycosidases and carbohydrate-binding proteins.

Although the overall binding properties of the enzyme towards insoluble (1→3)-α-glucan have been described, little is known about its hydrolytic mechanism. For instance, nothing is known about the minimum substrate and whether it attacks the substrate at the non-reducing end, displaying *exo*-catalytic activity, or whether intrachain glycosidic linkages are hydrolyzed and therefore has *endo*-catalytic activity. A fundamental question is whether the enzymatic action hydrolyzes the glycosidic linkage with retention or with inversion of the anomeric configuration. α-Amylases, on the one hand, are *endo*-(1→4)-α-glucanases releasing products with α-anomeric configurations and therefore retain the anomeric configuration of the substrate. Two carboxylic acids are involved, of which one attacks the anomeric carbon of the substrate. A second carboxylic acid is involved in protonation of the glycosidic oxygen followed by deprotonation of a water molecule, thus retaining the original conformation (Ly & Withers, 1999). β-Amylases, on the other hand, are *exo*-(1→4)-α-glucanases releasing disaccharides (maltose units) of which the reducing glucose has a β-anomeric configuration, and therefore are called inverting glycosidases. Inverting glycosidases bind to the substrate via a single carboxylic acid, whereas the second carboxylic acid is directly involved in deprotonating a water molecule (Ly & Withers, 1999). This one-step reaction results in the inversion of the anomeric configuration.

Here, we describe the hydrolytic action of a purified (1→3)-α-glucanase from *T. harzianum*. By using (1→3)-α-glucan as well as defined nigerooligosaccharide substrates, we show that the (1→3)-α-glucanase has *endo*-catalytic activity that hydrolyzes glycosidic linkages with inversion of the anomeric configuration. We further show that the enzyme is able to attack the substrate repetitively after initial attack, progressing towards the non-reducing end, releasing glucose residues.

Results

Isolation of (1→3)-α-glucanase

(1→3)-α-Glucanase was purified from a commercially-available enzyme preparation (Novozym) by adsorption chromatography. This method is based on binding of (1→3)-α-glucanase to its substrate (1→3)-α-glucan at 4 °C, at which temperature the catalytic activity is low. After a washing step, (1→3)-α-glucanase was eluted by addition of ethylene glycol. The purified enzyme preparation resolved as a single band in non-reducing sodium dodecyl sulfate-polyacrylamide gel electrophoresis (SDS-PAGE), migrating at a molecular mass of 80 kDa as visualized by silver staining. When run under reducing conditions, two additional, weakly stained bands were observed with molecular masses of approximately 50 and 30 kDa, indicating that a small portion of the purified enzyme was degraded proteolytically (**Fig. 1**). We conclude that adsorption chromatography achieved purification of the (1→3)-α-glucanase to chromatographic homogeneity.

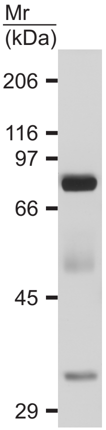

Fig. 1. Reducing SDS-PAGE of α-(1→3)-glucanase from *T. harzianum* after adsorption chromatography gave a major band at 80 kDa. Two weak bands at 30 kDa and 50 kDa indicate proteolytic degradation.

Glucose is the main hydrolysis product

To determine the main hydrolysis products of (1→3)-α-glucanase from *T. harzianum*, (1→3)-α-glucan from the fruiting bodies of *Pleurotus ostreatus* was incubated with the purified enzyme. After selected time intervals, samples were taken and analyzed by high-performance anion-exchange chromatography (HPAEC). At t = 0, hydrolysis products were virtually absent (**Fig. 2**). The HPAEC profile of the sample taken after an incubation time of 10 min showed two peaks, corresponding to glucose and nigerotriose in the molar ratio of 7.5 : 1 (**Fig. 2**). Increasing the incubation time to 0.5 h, led to a gradual increase of these products. In addition, we noticed peaks corresponding to nigerose and to higher oligosaccharides, albeit of lower intensity. Remarkably, a peak corresponding to nigerotetraose was almost absent, indicating that this oligosaccharide is a good substrate and, when formed, is further hydrolyzed. This was confirmed by using a purified nigerotetraose as a substrate, which was rapidly hydrolyzed to nigerotriose and glucose (not shown). The accumulation of high amounts of trisaccharide relative to disaccharide suggests that nigerotriose is not a good substrate, and therefore, hydrolysis is slow. This observation was confirmed by using purified nigerotriose as a substrate, which was hydrolyzed very slowly compared to nigerotetraose (not shown). In conclusion, (1→3)-α-glucanase from *T. harzianum* uses nigerotetraose efficiently as minimum substrate and hydrolyzes (1→3)-α-glucan with glucose as major product.

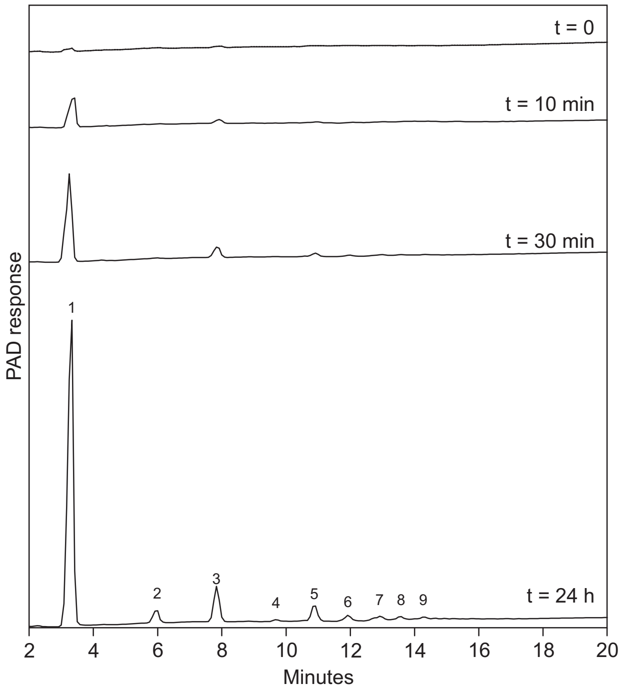

Fig. 2. Glucose is the main hydrolysis product of (1→3)-α-glucanase acting on (1→3)-α-glucan. HPAEC analysis of degradation products taken after specified time intervals. Numbers refer to the degree of polymerization.

The enzyme shows *endo*-catalytic activity

To determine whether the (1→3)-α-glucanase hydrolyzes the substrate starting from its non-reducing end (*exo*-catalytic activity) or whether it hydrolyzes intrachain glycosidic linkages (*endo*-catalytic activity), we labeled nigerooligosaccharides by reduction with sodium borohydrate and used these as a substrate for (1→3)-α-glucanase digestion.

We observed that the reduction of the nigerooligosaccharides affected enzyme activity in that nigerotetraitol was not hydrolyzed (not shown). Applying this labeling procedure, nigeropentaitol became the minimum substrate. HPAEC analysis showed that nigeropentaitol in the absence of enzyme eluted as a single peak after approximately 8.1 min (**Fig. 3** upper panel). After hydrolysis with (1→3)-α-glucanase during 24 hours, this peak vanished completely, and instead, four peaks eluted that corresponded to nigeroitol, glucose, nigerose and nigerotriose (**Fig. 3**, lower panel). These results indicate that nigeropentaitol is hydrolyzed forming nigerotriose and nigeroitol. In a secondary, slower step, the trisaccharide is partly digested forming nigerose and glucose (see previous paragraph). The absence of nigerotetraitol clearly indicates that *exo*-catalytic activity is absent. Thus, these findings demonstrate that the (1→3)-α-glucanase hydrolyzes intrachain glycosidic linkages, and therefore, possesses *endo*-catalytic activity.

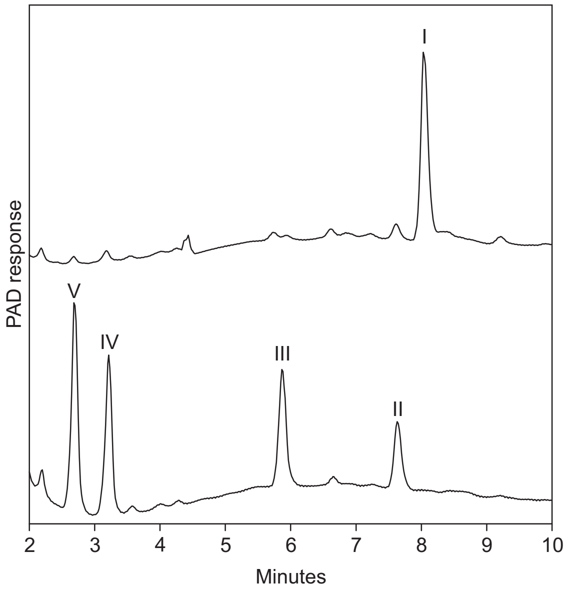

Fig. 3. (1→3)-α-Glucanase from *T. harzianum* possesses *endo*-catalytic activity. Nigeropentaitol is hydrolyzed between the second and third residue (counting from the reducing end). Peak annotation as referred to standards: I, nigeropentaitol; II, nigerotriose; III, nigerose, IV, glucose; V, nigeroitol. Upper panel: t = 0; lower panel: t = 24 h.

The enzyme hydrolyzes (1→3)-α-glycosidic linkages with inversion of configuration

To determine the anomeric configuration of the (1→3)-α-glucanase products, we incubated water-soluble, carboxymethylated (1→3)-α-glucan with enzyme and analyzed the products by ^{1}H-NMR spectroscopy. In **Fig. 4A**, the ^{1}H-NMR spectrum of an equilibrium mixture of α-Glc*p* and β-Glc*p* is shown (signals that are specific for the anomeric configuration are marked). The ^{1}H-NMR spectrum of carboxymethylated (1→3)-α-glucan only showed signals that were assigned to (1→3)-linked α-Glc*p* residues, originating from the carboxymethylated polysaccharide, whereas signals corresponding to free glucose were absent (**Fig 4B**). Importantly, this spectrum was essentially the same as the spectrum immediately taken after addition of (1→3)-α-glucanase (not shown). After 10 min digestion at 37 °C, signals corresponding to β-Glc*p* were clearly visible, whereas α-Glc*p* signals were absent (**Fig. 4C**). To induce mutarotation, the pH was increased by adding ammonium hydroxide, after which signals corresponding to α-Glc*p* appeared in addition to β-Glc*p* (**Fig. 4D**). These results demonstrate that (1→3)-α-glucanase from *T. harzianum* liberates β-Glc*p* during hydrolysis of (1→3)-α-glucan, and therefore acts with inversion of the anomeric configuration, indicating that hydrolysis of (1→3)-α-glycosidic linkages occurs via a one-step reaction (Ly & Withers, 1999).

Discussion

Proposed catalytic mechanism

In this study, we isolated a (1→3)-α-glucanase from a commercially-available enzyme preparation obtained from *T. harzianum* and analyzed its catalytic mechanism. It was shown that the enzyme could be isolated via adsorption chromatography. This purification method is substrate-specific, and contaminating proteins were not detected when running an SDS-PAGE. In addition, competing enzyme activity, such as amylase activity, could not be detected (not shown). Also the activity of a second (1→3)-α-glucanase, such as an *exo*-(1→3)-α-glucanase was lacking, indicating that a pure enzyme preparation was obtained by substrate-binding.

We demonstrated that the (1→3)-α-glucanase has *endo*-catalytic activity, hydrolyzing intrachain (1→3)-α-glycosidic linkages. Remarkably, β-Glc*p* is the major product formed by the hydrolysis of (1→3)-α-glucan, suggesting that the enzyme displays repetitive attacks. Enzymes that attack repetitively remain linked to their substrate after initial attack and transfer the substrate along its active site. Considering a repetitive-attack mechanism for (1→3)-α-glucanase from *T. harzianum*, we propose a model in which the enzyme first binds to the substrate (**Fig. 5**, **step 1**) and hydrolyzes an intrachain glycosidic linkage, after which only one part of the substrate dissociates and is released into the medium, whereas the other part remains bound to the substrate binding site of the enzyme (**Fig. 5**, **step 2**). The residual substrate then shifts to the catalytic site for repetitive attack (**Fig. 5**, **step 3**). By shifting just a single glucose residue, multiple glucose residues

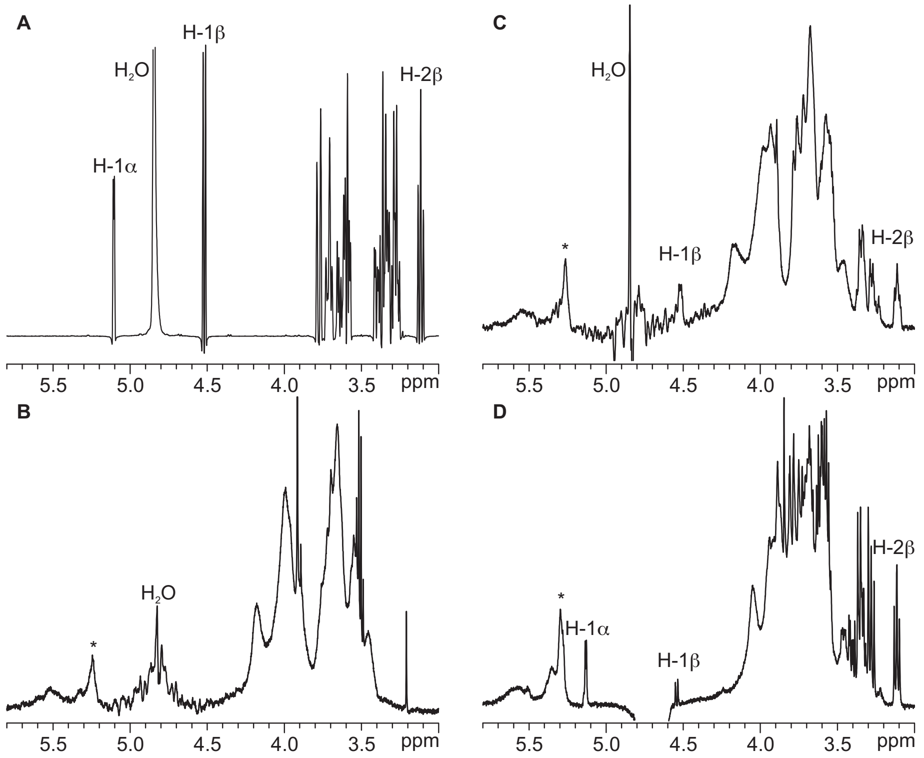

Fig. 4. The hydrolase cleaves glycosidic linkages with inversion of anomeric configuration. The ^{1}H-NMR spectrum of glucose shows α-anomeric and β-anomeric signals in the ratio 4:6 (**A**). Carboxymethylated (1→3)-α-glucan from *Laetiporus sulphureus* (**B**). Carboxymethylated α-glucan after 10 min digestion with (1→3)-α-glucanase (**C**). Same as in **C** after addition of ammonium hydroxide (**D**). Signals marked with an asterisk (*) are anomeric signals of the carboxymethylated (1→3)-α-glucan. Signals marked with H_2O indicate the water signal.

are released before dissociation occurs. This continuous hydrolysis may terminate when the substrate reaches a trisaccharide, which is a poor substrate (**Fig. 5**, **step 4**), and is consequently released (**Fig. 5**, **step 5**). Repetitive attack is common to β-amylases, which bind to (1→4)-α-glucan and liberate multiple β-maltose units. A number of α-amylases, such as porcine pancreatic α-amylase, also display repetitive attack following the initial random attack (Robyt & French, 1970; French, 1981). Since repetitive attack is a highly effective way for hydrolyzing substrates into glucose, it is likely that parasitic fungi like *T. harzianum* produce glycosidases that can convert carbohydrates according to this mechanism.

Considering the catalytic mechanism, we predict that nigerotetraose hydrolyzes to glucose and nigerotriose (**Fig. 6A**), which is consistent with our model. Similarly, nigeropentaitol is, as predicted, hydrolyzed into nigeroitol and nigerotriose (**Fig. 6B**).

Consequently, if a substrate were used containing (1→4)-linked residues followed by a number of sequentially (1→3)-linked residues, we predict that the reaction is initiated by hydrolyzing an intrachain (1→3)-α-glycosidic linkage, for instance adjacent to the (1→4)-linked residue, releasing oligosaccharides composed entirely of (1→4)-linked glucose residues (**Fig. 6C**). These findings fit well with our previous results after (1→3)-α-glucanase digestion of fission-yeast α-glucan, which is a (1→3)-α-glucan containing approximately 9% of (1→4)-linked residues (see Chapter 3).

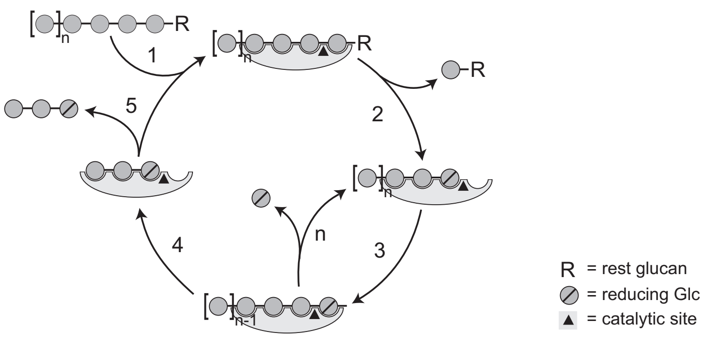

Fig. 5. Proposed catalytic mechanism of *endo*-(1→3)-α-glucanase from *T. harzianum*. The enzyme binds to the substrate (**1**), hydrolyzes an interior glycosidic linkage, and releases part of the substrate (**2**). The other part is transferred across the catalytic part of the enzyme, releasing glucose units (**3**). This process continues until a trisaccharide remains (**4**), which is subsequently released into the medium (**5**).

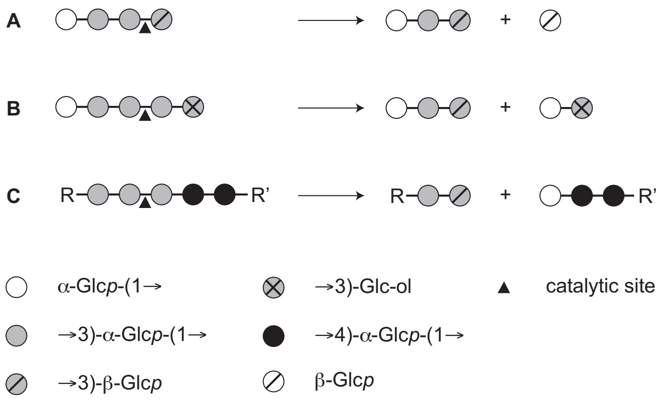

Fig. 6. Schematic representation of the hydrolysis of different substrates by (1→3)-α-glucanase from *T. harzianum*.

Importantly, the hydrolysis products and therefore the catalytic mechanism of *T. harzianum* (1→3)-α-glucanase is very similar to an *endo*-(1→3)-α-glucanase from *Cladosporium resinae* (*Amorphotheca resinae*) (Walker & Hare, 1977). This enzyme, like α-glucanase from *T. harzianum*, has *endo*-catalytic activity and is able to attack the (1→3)-α-glucan substrate repetitively after initial attack. Similar as reported in the present study, the main hydrolysis product is β-glucose, indicating that (1→3)-α-glycosidic linkages are hydrolyzed with inversion of the anomeric configuration. However, unlike the glucanase described in the present study, the (1→3)-α-glucanase from *C. resinae* uses nigerotriose as minimum substrate, converting it to nigerose and glucose. Nigerose is not a good substrate, and consequently, is hydrolyzed at very low rate.

In fission yeast *S. pombe*, a gene was identified that shows sequence homology with the catalytic domain of (1→3)-α-glucanase from *T. harzianum* (Fuglsang *et al.*, 2000). Interestingly, the C-terminal substrate-binding domain is missing. This *S. pombe* homolog may give some clue on the function of the substrate-binding domain of *T. harzianum* (1→3)-α-glucanase and its ability of repetitive attack.

Materials and methods

Purification of (1→3)-α-glucanase by adsorption chromatography

To pretreat Novozym, 50 mg of Novozym (Sigma) was diluted in 1 ml of 50 mM Tris-HCl, pH 7.6 containing 1 mM phenylmethylsulfonyl fluoride (PMSF) and 10 l of protease inhibitor cocktail (Sigma P-8215) at RT. In a partial purification step, the solution was run over a DEAE ion exchange chromatography column (Pharmacia 17-0500-01) equilibrated with 50 mM Tris- HCl, pH 7.6 at RT, and flowthrough fractions containing (1→3)-α-glucanase activity were pooled. Then, the buffer was exchanged for 5 mM sodium azide, 50 mM sodium acetate, pH5.6 (Buffer A), using a PD10 gel filtration column (Amersham Pharmacia 17-0851-01), and 0.85 mM PMSF and 10 l of protease inhibitor cocktail was added.

To reprecipitate (1→3)-α-glucan, 20 mg of (1→3)-α-glucan (*Pleurotus ostreatus*) was dissolved in 10 ml of 10 M HCl and incubated at 37 °C for 15 min. Then, 40 ml of ice-cold 1.25 M sodium acetate, 1.25 M NaOH was added and the mixture was neutralized by addition of 10 M NaOH. After an overnight incubation, the precipitated (1→3)-α-glucan was washed three times in ice-cold Buffer A.

For adsorption, the pretreated Novozym was incubated with reprecipitated (1→3)-α-glucan in Buffer B (Buffer A containing 10% (v/v) ethylene glycol and 1 M NaCl) on an end-over-end tumbler at 4 °C for 45 min. Then, the complex of (1→3)-α-glucanase and (1→3)-α-glucan was centrifuged at 5000 rpm (2040 × g) at 4 °C for 2 min and washed three times with ice- cold buffer B. For elution of (1→3)-α-glucanase, the complex was incubated in 1 ml of 80% $(^{v}/_{v})$ ethylene glycol in Buffer A at RT for 5 min. Then, the suspension was centrifuged at 14000 rpm (16000 × g) at RT for 2 min and the supernatant, which contained the (1→3)-α-glucanase, was collected. Finally, ethylene glycol was removed by gel filtration over a PD-10 column equilibrated with buffer A.

α-Glucan preparations

Fruiting bodies of *Pleurotus ostreatus* were obtained from a supermarket in Amsterdam, The Netherlands, and those of *Laetiporus sulphureus* were obtained from an infected tree in a park in Amsterdam. Approximately 300 g (fresh weight) of mushrooms were cut into cubes of approximately 1 cm^3 and finely minced in 100 mM EDTA, 50 mM Tris, pH 7.6 in a blender for 2 min at maximum speed. After addition of 2% (w/v) of SDS and 40 mM of 2-mercaptoethanol, cytosolic contaminants were extracted by boiled for 15 min. Wall material was isolated by centrifugation at 3222 × g for 10 min and washed in water. After repeating the mincing and extraction steps, wall material was resuspended in ice-cold 2 mM NaBH4, 2 M KOH and stirred at 4 °C for 30 min. Insoluble material was removed by centrifugation at 10,651 × g for 20 min. To isolate the alkali-soluble, water-insoluble fraction, acetic acid was added to the alkali-soluble supernatant under constant stirring until the pH was 6. The water-insoluble fraction was allowed to precipitate overnight at 4 °C under gentle stirring and was collected by centrifugation at 4500 × g for 15 min. To remove (1→3)-β-glucan, the pellet was resuspended in 5 mM sodium azide, 40 mM 2-mercaptoethanol, 50 mM citrate-phosphate buffer, pH 5.3 containing 45 mg of Zymolyase-100T (Seikagaku). After an overnight-incubation in a rotary shaker at 200 rpm at 37 °C, the insoluble fraction was collected by centrifugation at 4500 × g for 15 min and was washed twice with water. After repeating the alkali-extraction and Zymolyase digestion, the material was extracted with SDS and 2-mercaptoethanol as described and washed in 5 mM sodium azide.

O-(carboxy)methylation of α-glucan from *L. sulphureus* was performed as described by Kiho *et al.* (1989).

Enzymatic degradation

All experiments were carried out in 50 mM sodium acetate [pH 5.5] containing 5 mM sodium azide at 37 °C. Samples were desalted using Carbograph SPE solid phase extraction columns (Alltech) according to Packer *et al.* (1998).

High-performance anion-exchange chromatography

The high-performance anion-exchange chromatography (HPAEC) system consisted of a Dionex DX 500 equipped with a GP 40 gradient pump, an ED 40 Electrochemical detector, and a CarboPac PA1 (9 × 250 mm) column. Appropriate linear gradients were applied for each component using 100 mM NaOH and 500 mM NaOAc in 100 mM NaOH as eluents at a flow rate of 4.0 ml/min.

Partial acid hydrolysis

A suspension of 100 mg of (1→3)-α-glucan from the fruiting bodies of *Laetiporus sulphureus* in 98% formic acid was heated at 100 °C for 10 min. After evaporation of the acid under a stream of nitrogen, hydrolysis was continued by addition of 0.5 M trifluoroacetic acid and heating at 100 °C for 12 min, then the clear solution was lyophilized.

Size-exclusion chromatography

Products obtained after acid hydrolysis were separated on a Bio-Gel P2 column (1.5 × 96 cm, Biorad) to separate oligosccharides with a maximum degree of polymerization (DP) of four. The column was thermostated at 58 °C. Oligosaccharides were eluted with ammonium bicarbonate (5 mM) and the eluent was monitored using a Differential Refractometer Bischoff. Oligosaccharides with a DP larger than four were fractionated on a Bio-Gel P4 column of similar size using the same eluent. Oligosaccharides were further purified to homogeneity by HPAEC.

Labeling of the reducing end

Samples were dissolved in 0.5 M ammonium hydroxide and reduced by adding sodium borohydride at RT during 4 hours. Excess of borohydride was removed by addition of 10% ($^{v}/_{v}$) acetic acid. Boric acid was removed by co-evaporation from methanol under reduced pressure.

^{1}H-NMR spectroscopy

Samples were dissolved in 50 mM sodium acetate [pH 5.5] containing 5 mM sodium azide and 10% deuterium oxide. Spectra were recorded at 500.13 MHz on a Bruker DRX500 at 10 °C. At this temperature, the proton signal corresponding to water is situated exactly between the two anomeric signals of glucose, and therefore, suppression of the water signal will not disturb signals corresponding to glucose. Chemical shifts were referred to internal acetone (^{1}H: 2.225 ppm).

References

French, D. (1981) Amylases: enzymatic mechanisms. *Basic Life Sci.* **18,** 151-182.

Fuglsang, C.C.; Berka, R.M.; Wahleithner, J.A.; Kauppinen, S.; Shuster, J.R.; Rasmussen, G. Halkier, T.; Dalboge, H. & Henrissat, B. (2000) Biochemical analysis of recombinant fungal mutanases. A new family of α–1,3-glucanases with novel carbohydrate-binding domains. *J. Biol. Chem.* **275,** 2009-2018.

Guggenheim, B. & Haller, R. (1972) Purification and properties of an α-(1→3) glucanohydrolase from *Trichoderma harzianum*. *J. Dent. Res.* **51,** 394-402.

Kiho, T.; Yoshida, I.; Nagai, K. & Ukai, S. (1989) (1→3)-α-D-Glucan from an alkaline extract of *Agrocybe cylindracea*, and antitumor activity of its *O*-(carboxymethyl)ated derivatives. *Carbohydr. Res.* **189,** 273- 279.

Ly, H.D. & Withers, S.G. (1999) Mutagenesis of glycosidases. *Annu. Rev. Biochem.* **68,** 487-522.

Packer, N.H.; Lawson, M.A.; Jardine, D.R. & Redmond, J.W. (1998) A general approach to desalting oligosaccharides released from glycoproteins. *Glycocon. J.* **15,** 737-747.

Robyt, J.F. & French, D. (1970) Multiple attack and polarity of action of porcine pancreatic α-amylase. *Arch. Biochem. Biophys.* **138,** 662-670.

Walker, G.J. & Hare, M.D. (1977) Metabolism of the polysaccharides of human dental plaque. Part II. Purification and properties of *Cladosporium resinae* (1→3)-α-D-glucanase, and the enzymic hydrolysis of glucans synthesised by extracellular D-glucosyltransferases of oral streptococci. *Carbohydr. Res.* **58,** 415-432.

Chapter 4

Spore-wall α-glucan of fission yeast is not assembled from building blocks but rather consists of a single (1→3)-α-glucan polymer

Christian H. Grün[1], Frans Hochstenbach[2], Frans M. Klis[3], Johannis P. Kamerling[1], and Johannes F.G. Vliegenthart[1]

[1]*Bijvoet Center, Department of Bio-Organic Chemistry, Section of Glycoscience and Biocatalysis, Utrecht University;* [2]*Department of Biochemistry, Academic Medical Center, University of Amsterdam;* [3]*Swammerdam Institute for Life Sciences, University of Amsterdam*

Abstract

Under conditions of nitrogen starvation, diploid fission-yeast cells undergo meiosis followed by sporulation. During sporulation, individual nuclei are surrounded by a double layer of membranes, called the forespore membranes. In between these membranes, the spore wall is formed. In contrast to vegetative growth where the existing cell wall is extended, spore walls are formed *de novo*. Although it is known that spore walls of fission yeast contain chitin and β-glucan, the presence of α-glucan has not been demonstrated. Here, we identify (1→3)-α-glucan as a major constituent of fission-yeast spore walls. Upon extracting spore walls with dimethyl sulfoxide, we obtained, in addition to an amylose-like polysaccharide, two distinct linear (1→3)-α-glucan populations consisting of approximately 480 and 680 glucose residues, respectively. Importantly, their chemical structures differed fundamentally from (1→3)-α-glucan from vegetative cell walls in that it was not composed of two covalently-linked building blocks (dimeric structure), but instead consisted of a monomer of (1→3)-linked α-glucose residues. This finding is consistent with DNA-microarray analyses that showed that the synthase for cell-wall α-glucan, Ags1p, is downregulated during sporulation, whereas Ags1p homologs are upregulated. Taken together, we propose that an α-glucan synthase other than Ags1p is responsible for the *de novo* biosynthesis of α-glucan in spore walls.

Introduction

Fission yeast, *Schizosaccharomyces pombe* (Lindner), undergoes a haplontic life cycle when grown under nutrient-rich conditions. Under conditions of nutritional stress (i.e., nitrogen starvation), sexual differentiation occurs in which haploid cells of opposite mating types fuse, forming diploid cells that undergo meiosis and sporulation. Three major meiotic phases can be distinguished. During the early, premeiotic S phase, chromosome pairing and recombination takes place. During the middle phase, the first (M I) and second (M II) meiotic division occur, forming four haploid nuclei within the cell wall of the original cell, called the ascus. During the late phase, each nucleus is surrounded by a double layer of membranes, called the forespore membranes. In between these membrane layers, the spore wall is formed. This spore wall, like the cell wall of haploid cells, consists mainly of polysaccharides and glycoproteins. The spore wall ensures structural integrity, regulates cell permeability, and resists environmental stresses. However, in contrast to vegetative growth, in which the cell wall extends, spore walls are created entirely *de novo*.

In *Saccharomyces cerevisiae*, cell-wall as well as spore-wall architecture are well-studied. In vegetatively-grown *S. cerevisiae* cells, cell-walls are composed of (1→6)-β-glucan and (1→3)-β-glucan layers followed by a layer of mannoproteins (Klis *et al.*, 1997; Klis, 1994), whereas spore walls contain two additional surface layers, namely a carbohydrate layer consisting of chitosan and an outermost layer consisting of dityrosine polymers (Briza *et al.* 1988; Briza *et al.* 1986). This implies that the biochemistry of spore-wall formation and also the genes involved differ from those of cell-wall formation. In fission yeast, meiotic expression of 99.3% of the approximately 4,900 known genes was followed using DNA microarrays (Mata *et al.*, 2002). Mata and co-workers demonstrated that during meiosis and sporulation more than 50% of the genome is regulated. More specifically, they found that 1,033 genes were upregulated at least four-fold. Among these are several genes with known or putative functions in spore-wall construction. For instance, a gene encoding a (1→3)-β-glucan synthase, *bgs2*$^{+}$, which is dispensable for cell-wall formation in vegetatively growing cells, is essential for the assembly of spore walls (Liu *et al.*, 2000; Martín *et al.*, 2000). Furthermore, two chitin synthase homologs *chs1*$^{+}$ and *chs2*$^{+}$ were identified in fission yeast, of which *chs1*$^{+}$ is required for proper spore maturation (Arellano *et al.*, 2000). The function of *chs2*$^{+}$ remains unknown, but is probably also required for sporulation as this gene is strongly upregulated during meiosis (Mata *et al.*, 2002).

α-Glucan is a major polysaccharide constituent in the fission-yeast cell wall and its synthase has recently been identified (Hochstenbach *et al.*, 1998). This α-glucan is composed of two building blocks, each comprising a (1→3)-α-glucan segment of approximately 135 residues with a small number of (1→4)-linked α-glucose residues attached to its reducing end (see Chapter 2). Importantly, the gene encoding the α-glucan synthase, *ags1*$^{+}$, is downregulated during meiosis, whereas four homologous genes (*mok11*$^{+}$, *mok12*$^{+}$, *mok13*$^{+}$, and *mok14*$^{+}$) are upregulated (Mata *et al.*, 2002). Together with the fact that these genes could be deleted without forming a noticeable phenotype in the vegetative growth phase (Katayama *et al.*, 1999), this indicates that the genes do not possess an essential function during vegetative growth but may be involved in sporulation. However, thus far, no (1→3)-α-glucan was identified in spore walls of fission yeast.

Here, we identify two different populations of (1→3)-α-glucan in fission-yeast spore walls and describe their chemical structures. By using high-performance size-exclusion chromatography in combination with chemical analyses and NMR spectroscopy, we show that both spore-wall (1→3)-α-glucans are composed of single, linear (1→3)-α-glucan polymers. The significant differences in chemical structures between α-glucan of cell walls and of spore walls together with the regulation patterns of genes encoding putative α-glucan synthases suggest that an α-glucan synthase different from Ags1p may be involved in its biosynthesis.

Results

Composition of spore walls

To determine the chemical composition of spore walls, we physically lysed fission-yeast spores and collected spore walls by centrifugation. Quantitative monosaccharide analysis of whole spore walls revealed the presence of glucose, mannose and galactose in the molar ratio of 92.2 : 4.8 : 3.0 in addition to traces of *N*-acetylglucosamine. Cell walls were then dried completely and extracted with dimethyl sulfoxide (DMSO). The molecular mass distribution of the extract was determined by high-performance size-exclusion chromatography (HPSEC). The size-exclusion profile showed two overlapping peaks with a number-average molecular mass (Mn) of 22.2 kDa and a polydispersity (Mw/Mn) of 5.87 (**Fig. 1A**, **Table I**). The heterogeneous nature of the spore walls was also apparent in the 1D ^{1}H-NMR spectrum, which showed two H-1α signals at 5.146 ppm ($^3J_{1,2}$ 4.0 Hz) and 5.093 ($^3J_{1,2}$ 3.7 Hz), and a H-1β signal at 4.544 ppm ($^3J_{1,2}$ 7.8 Hz) in a relative abundance of 4:1:1 (**Fig. 2A**). Based on the monosaccharide composition, we infer that these signals correspond to glucose residues, indicating that the DMSO extract of fission-yeast spore walls contains three major polysaccharides, namely two α-glucans and one β-glucan.

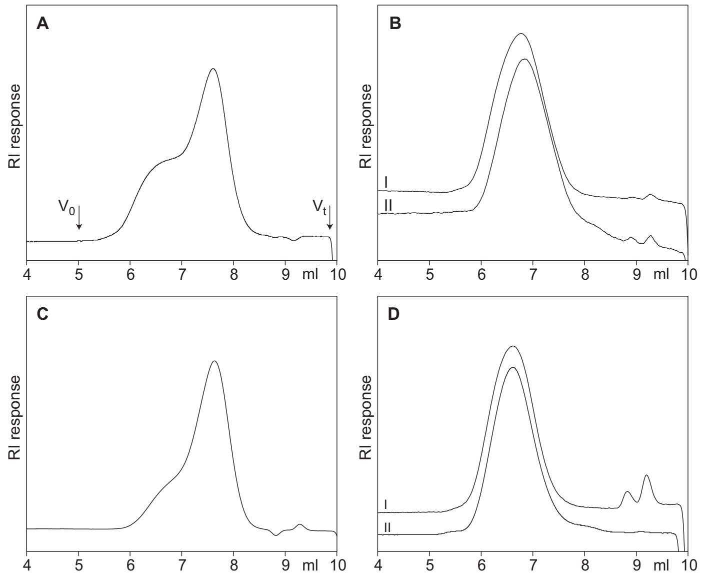

Fig. 1. Molecular mass distributions of whole spore polysaccharides (**A**), **P I** ((1→3)-α-glucan) untreated (**I**) and Smith degraded (**II**) (**B**), **P II** ((1→4)-α-glucan) (**C**), and **P III** ((1→3)-α-glucan) untreated (**I**) and Smith degraded (**II**) (**D**). Dried polysaccharide preparations were dissolved in DMSO containing 3 mM sodium nitrate and their molecular mass distributions were analyzed by HPSEC on a calibrated mixed-bed column.

Table I. Molecular-mass averages and polydispersities of spore components

	Mn (kDa)	Mw (kDa)	Mw/Mn	DP_n
Whole spore walls	22.2	130.1	6.45	137
P I	77.8	196.3	2.52	480
P I, Smith degraded	55.9	139.4	2.50	345
P II	16.5	55.7	3.36	102
P III	109.7	256.4	2.33	677
P III, Smith degraded	96.2	200.5	2.08	594

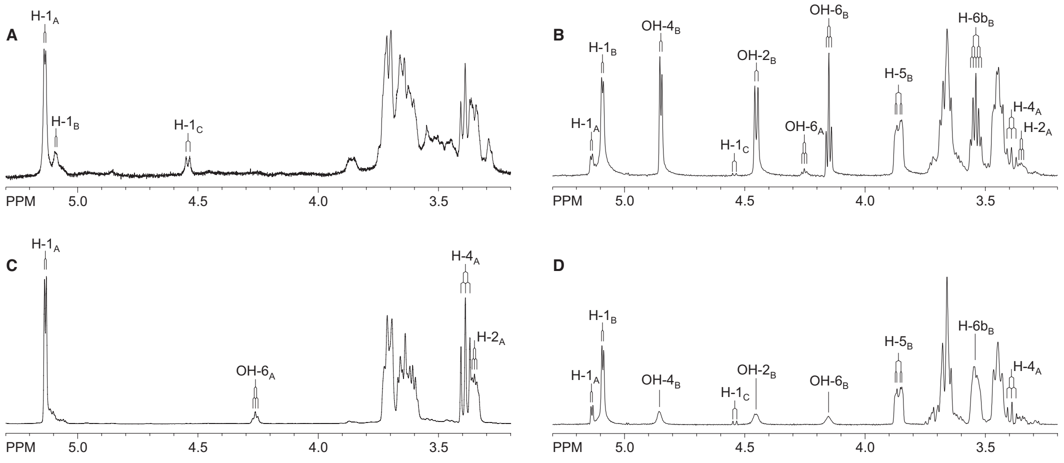

Fig. 2. The DMSO extract of spore polysaccharides consists of two α-glucans and one β-glucan. ^{1}H-NMR spectra of whole spore polysaccharides (**A**), **P I** (**B**), **P II** (**C**), and **P III** (**D**). Constituent A represents (1→4)-linked α-Glc*p*, B represents (1→3)-linked α-Glc*p*, and C represents (1→3)-linked β-Glc*p* (see text for assignment). The numbers refer to the corresponding carbon atom as assigned by 2D NMR spectroscopy. Samples were dissolved in DMSO-d_6 and spectra were recorded at 500.08 MHz at 80 °C.

Fractionation of spore walls

To investigate the chemical structures of the α-glucans, we separated the major spore wall components into three different fractions (**Fig. 3**, denoted **P I**, **P II**, and **P III**). Spore walls were digested with Zymolyase, which solubilized approximately 80% of the β-glucan as was shown by ^{1}H NMR (data not shown). Monosaccharide analysis of the Zymolyase-resistant material showed that glucose was the only monosaccharide constituent, indicating that in addition to (1→3)-β-glucan, also the mannose, galactose, and *N*-acetylglucosamine constituents were liberated. Since the enzyme used to hydrolyze (1→3)-β-glucan also contains proteases, we suppose that the monosaccharides other than glucose constituted protein-linked glycans. Spore walls were then dissolved in DMSO and two polysaccharide fractions were obtained by precipitation. A first fraction precipitated after addition of ethanol to a final volume of 40%, yielding **P I**, which comprised 30% ($^w/_w$) of the Zymolyase-resistant cell wall. A second fraction was obtained by precipitation at 60% of ethanol (**P II**, 56% ($^w/_w$) of the Zymolyase-resistant cell wall). The homogeneity of the preparations was investigated by ^{1}H-NMR spectroscopy. The extraction procedure was repeated for **P I** until a near homogeneous preparation was obtained. The DMSO-insoluble residue could be dissolved completely in 1 M sodium hydroxide, and a polysaccharide fraction precipitated upon neutralization that was collected by centrifugation (**P III**, 14% ($^w/_w$) of the Zymolyase-resistant cell wall). Addition of three volumes of ethanol to the supernatant did not result in precipitation of additional material, indicating that the supernatant was devoid of polysaccharides.

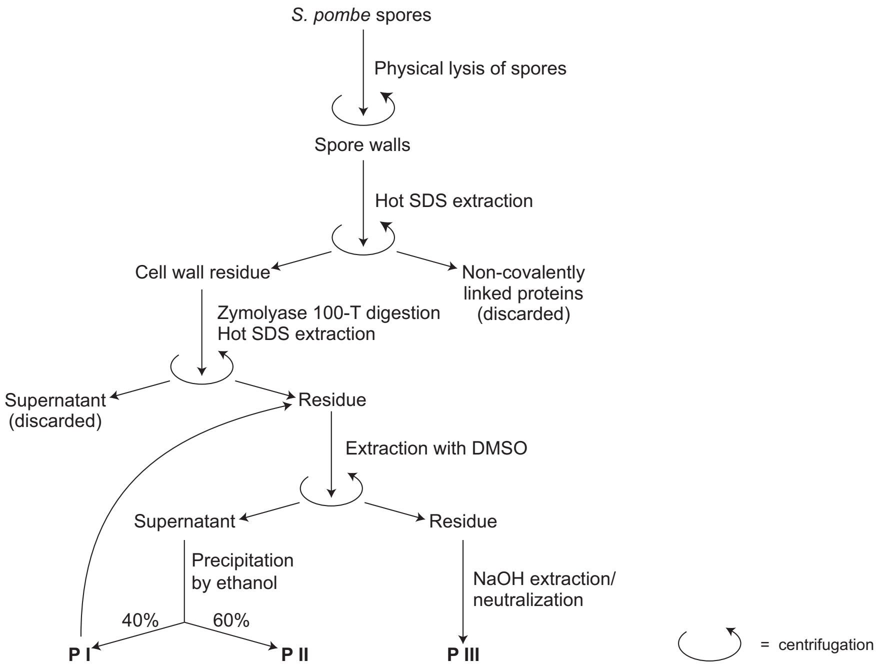

Fig. 3. Schematic representation for the isolation and fractionation of spore α-glucans.

P I consists mainly of (1→3)-α-D-glucan

To characterize the **P I** fraction, monosaccharide analysis together with the determination of the absolute configuration showed that **P I** consisted entirely of D-glucose. Linkage analysis demonstrated the presence of (1→3)-linked residues as a main constituent together with 12.6% (1→4)-linkages (**Table II**). Triple substituted residues were not observed, indicating that branching points are not present.

Table II. Linkage analysis of spore α-glucans

Residue	Molar amounts (%)		
	P I	**P II**	**P III**
Glc*p*-(1→	-	1.1	-
→3)-Glc*p*-(1→	87.4	1.6	91.6
→4)-Glc*p*-(1→	12.6	97.3	8.4

In the 1D ^{1}H-NMR spectrum of **P I** (**Fig. 2B**) H-1α signals at 5.138 ppm (denoted H-1_A) and 5.092 ppm (denoted H-1_B) are present in the relative intensity of 1:10, in addition to a low-intensity H-1β signal at 4.544 ppm (denoted H-1_C), indicating the presence of three constituents denoted A, B, and C. For the major constituent B, proton signals at 4.849, 4.453, and 4.139 ppm were observed, which did not produce cross-peaks in the 2D ^{1}H-^{13}C HSQC spectrum (**Fig. 4A**), demonstrating that these signals represent slowly-exchanging hydroxyl groups. By using 2D ^{1}H-^{1}H TOCSY (**Fig. 4B**), the hydroxyl signals could be assigned to OH-4$_B$, OH-2$_B$, and OH-6$_B$, respectively. 2D NMR spectroscopy (TOCSY and HSQC) allowed the assignment of all proton and carbon resonances of constituent B (**Table III**). The low-field shift of C-3$_B$ at 83.0 ppm together with the absence of an OH-3$_B$ and the small $^3J_{1,2}$ coupling constant demonstrate that the major constituent of **P I** consists of (1→3)-linked α-glucopyranose residues.

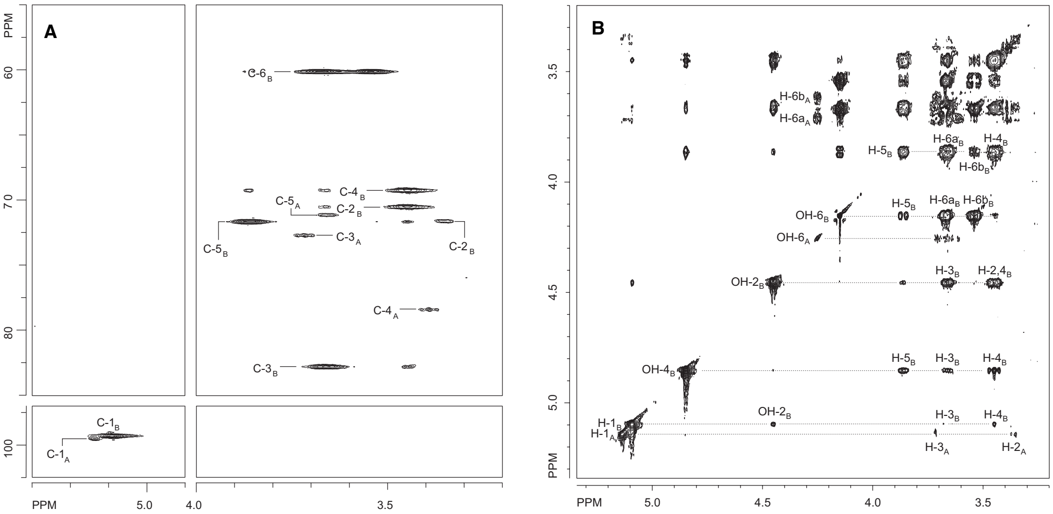

Fig. 4. Fraction **P I** consists of (1→3)-linked α-glucopyranose residues with some (1→4)-linked residues. ^{1}H-^{13}C HSQC spectrum (**A**) and ^{1}H-^{1}H TOCSY spectrum (50 ms mixing time) (**B**). The major constituent (denoted B) represents (1→3)-linked α-Glc*p*, whereas the minor constituent (denoted A) represents (1→4)-linked α-Glc*p*. C-1$_B$ means a cross-peak between H-1 and C-1 of constituent B in the HSQC spectrum. Cross-peaks belonging to the same scalar coupling network are indicated along a dotted line starting from the corresponding diagonal peak in the TOCSY spectrum. Note that the down-field shifts of C-3$_B$ and C-4$_A$ are typical for (1→3)-linked and (1→4)-linked residues, respectively. Note also that OH-2$_B$, OH-4$_B$, OH-6$_B$, and OH-6$_A$ give cross-peaks in the TOCSY spectrum, whereas these cross-peaks are absent in the HSCQ spectrum. Samples were dissolved in DMSO-d_6 and spectra were recorded at 500.08 MHz at 80 °C.

The constituent of medium intensity, A, has an anomeric signal at 5.138 ppm (**Fig. 2B**, denoted H-1$_A$). The low-field shift together with the small $^3J_{1,2}$ coupling constant of 3.9 Hz indicates an α-anomeric configuration. The assignments of proton and carbon signals as obtained by the TOCSY and HSQC spectra are displayed in **Table III**. The low-field chemical shift of C-4$_A$ at 78.5 ppm demonstrates that constituent A represents (1→4)-linked α-D-glucopyranose residues (**Fig. 5**). ^{1}H and ^{13}C chemical shifts are in good agreement with experimental data obtained from a (1→4)-α-glucan, amylose (not shown).

Table III. Proton and carbon chemical shifts of **P I**

Constituent **A** ((1→4)-α-Glc*p*)				Constituent **B** ((1→3)-α-Glc*p*)			
Proton	PPM	Carbon	PPM	Proton	PPM	Carbon	PPM
H-1	5.138	C-1	99.6	H-1	5.092	C-1	99.4
H-2	3.353	C-2	71.7	H-2	3.449	C-2	70.7
H-3	3.715	C-3	72.8	H-3	3.660	C-3	83.0
H-4	3.390	C-4	78.5	H-4	3.449	C-4	69.3
H-5	3.660	C-5	71.2	H-5	3.863	C-5	71.7
H-6a	4.252	C-6	n.d.	H-6a	3.671	C-6	60.2
H-6b	3.608			H-6b	3.540		
OH-2	n.d.			OH-2	4.453		
OH-4	n.d.			OH-4	4.849		
OH-6	4.253			OH-6	4.139		

n.d. = not detected

Constituent C is present at very low intensity and only the anomeric proton was observed in the ^{1}H-NMR spectrum (**Fig. 2B**). Due to its low abundance, cross-peaks were not observed in the TOCSY and HSQC spectra, making allocation difficult. Nevertheless, this signal was observed also in the ^{1}H-NMR spectrum of whole spore walls (**Fig. 2A**) and its intensity decreased fourfold by Zymolyase digestion. Therefore, we assume that constituent C represents a (1→3)-β-glucan. Indeed, NMR analysis of a (1→3)-β-glucan (laminaran) demonstrated that the anomeric proton has a chemical shift and coupling constant similar to constituent C (not shown).

Together, our results indicate that **P I** comprises a mixture of polysaccharides consisting mainly of a linear (1→3)-α-D-glucan, with approximately 10% (1→4)-linked α-D-glucose residues. Based on our results, we cannot exclude the possibility that the (1→4)-linked glucose residues form a contaminating component, namely of **P II** (see below). In addition, small amounts of (1→3)-linked β-glucose residues are present, indicating (1→3)-β-glucan contamination.

To determine the molecular mass distribution of **P I**, the preparation was dried, dissolved in DMSO and analyzed by high-performance size-exclusion chromatography (HPSEC) on a calibrated column. P I eluted as a single peak at the same volume as the high molecular mass population in **Fig. 1A** (**Fig. 1B**, profile I). The polysaccharide had an Mn of 77.8 kDa, which corresponds to a number-average degree of polymerization (DP_n) of 480. The polydispersity of 2.52 was significantly lower than that of whole spore extracts, which was 5.87.

We wondered whether the (1→4)-linked glucose residues are covalently linked to the (1→3)-linked main constituent, and if so, whether they are distributed randomly throughout the polysaccharide or whether they are located at specific regions. To pursue this, we selectively removed the (1→4)-linked residues by periodate oxidation followed by mild acid hydrolysis (Smith degradation), and analyzed the remaining (1→3)-α-glucan by HPSEC. In the case of a random distribution, a rapid decrease in molecular mass together with an increased polydispersity may be expected. However, the Smith degraded polysaccharide eluted as a Gaussian-curved peak with an Mn of 55.9 kDa (DP_n 378), which is a decrease of approximately 28% compared to the native sample. Importantly, the polydispersity (2.50) remained unchanged (**Fig. 1C**, profile II; **Table I**). These results indicate that the (1→3)-linked main constituent is not interspersed with (1→4)-linkages, but that the (1→4)-linked residues either form a contaminating component or are located near or at one of the termini of the (1→3)-linked main chain.

P II comprises two types of amylose

Similar to fraction **P I**, we determined the chemical structure of fraction **P II**. Monosaccharide analysis together with the determination of the absolute configuration demonstrated D-glucose as the sole monosaccharide constituent of **P II**. Linkage analysis showed (1→4)-linked glucopyranose residues to be the main constituent in addition to small amounts (~1%) of (1→3)-linked residues and terminal Glc. Triple substituted residues indicating branching could not be detected, and therefore we assume that **P II** consists of a linear polysaccharide (**Table II**).

The 1D ^{1}H-NMR spectrum (**Fig. 2C**) showed a H-1α signal at 5.146 ppm. A signal of low intensity was observed at 4.263 ppm that represents OH-6, because it is a slowly-exchanging triplet, does not form cross-peaks in the HSQC spectrum (**Fig. 5A**), and forms cross-peaks with the H-6a/b protons in the TOCSY spectrum (**Fig. 5B**). Proton and carbon chemical shifts were assigned using TOCSY and HSQC experiments (**Table IV**) The down-field shift of C-4 at 78.5 ppm indicates 4-substitution, which is consistent with the chemical analysis data. From these data we conclude that **P II** consists of a linear (1→4)-α-D-glucan. The absence of 6-substituted and 4,6-disubstituted residues indicates that the (1→4)-α-D-glucan represents amylose rather than glycogen.

Table IV. Proton and carbon chemical shifts of **P II** ((1→4)-α-Glc*p*)

Proton	PPM	Carbon	PPM
H-1	5.146	C-1	99.7
H-2	3.35	C-2	71.7
H-3	3.714	C-3	72.9
H-4	3.39	C-4	78.5
H-5	3.652	C-5	71.2
H-6a	3.701	C-6	60.2
H-6b	3.612		
OH-2	n.d.		
OH-4	n.d.		
OH-6	4.263		

n.d. = not detected

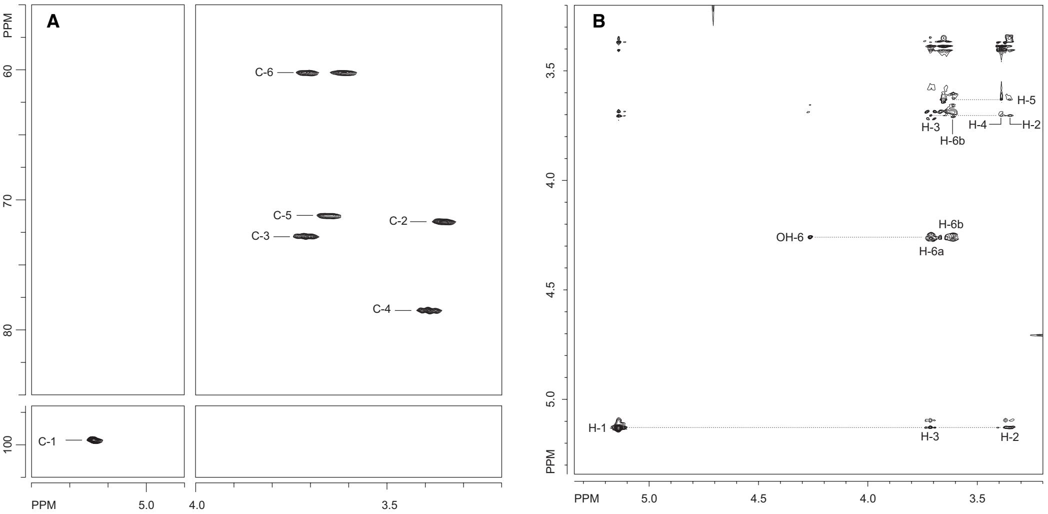

Fig. 5. Fraction **P II** consists of (1→4)-linked α-glucopyranose residues. ^{1}H-^{13}C HSQC spectrum (**A**) and ^{1}H-^{1}H TOCSY spectrum (50 ms mixing time) (**B**). C-1 means a cross-peak between H-1 and C-1 in the HSQC spectrum. Cross-peaks belonging to the same scalar coupling network are indicated along a dotted line starting from the corresponding diagonal peak in the TOCSY spectrum. Note that the down-field shifts of C-4 typify 4-substituted residues. Note also that OH-6 gives cross-peaks in the TOCSY spectrum, whereas these cross-peaks are absent in the HSCQ spectrum. Samples were dissolved in DMSO-d_6 and spectra were recorded at 500.08 MHz at 80 °C.

The HPSEC profile of **P II** showed two overlapping peaks with a combined Mn of 16.5 kDa, which corresponds to a DP of 102 (**Fig. 1C**, **Table I**). The profile was very similar to that of whole spore wall extracts, albeit with a lower polydispersity, namely 3.30 rather than 5.87. Since chemical analysis and NMR data demonstrated that (1→4)-α-D-glucan was virtually the sole component of **P II** (apart from traces of (1→3)-linked glucose residues), we conclude that both peaks represent amylose. Taken together, the results demonstrate that **P II** comprises two different amylose populations.

P III contains a second (1→3)-α-glucan fraction

After extraction of the DMSO-insoluble residue with cold sodium hydroxide solution, fraction **P III** was obtained by neutralization (14% $^w/_w$ of total spore carbohydrates). This fraction, to our surprise, was readily soluble in DMSO, and could therefore be analyzed by using the same methods as for fractions **P I** and **P II**. Monosaccharide analysis gave glucose as only monosaccharide constituent. These glucose residues were mainly (1→3)-linked (91.6%) in addition to 8.4% (1→4)-linked residues (**Table II**). The 1D ^{1}H-NMR spectrum of **P III** was virtually indistinguishable from **P I** in that both spectra contained signals corresponding to (1→4)-linked and (1→3)-linked α-Glc*p*, and (1→3)-linked β-Glc*p* (**Fig. 2D**). HPSEC analysis showed that **P III** consisted of a single population of polymers with an Mn of 109.7 kDa (DP 677) and a polydispersity of 2.33 (**Fig. 1D**, profile I; **Table I**), demonstrating that the average degree of polymerization of **P III** was significantly higher than that of **P I**, which was approximately 480. These results indicate that **P III** comprises a second population of α-glucans consisting mainly of (1→3)-linked α-glucose residues. Removal of the (1→4)-linked residues by Smith degradation did not significantly affect the molecular mass distribution of **P III** (**Fig. 1D**, profile II), demonstrating that in the case of a covalent linkage between the (1→3)-α-glucan backbone and the (1→4)-linked residues, the latter must be located at the reducing or non-reducing end.

Discussion

Spore α-glucan

In this study, we elucidated the chemical structures of the major types of water-insoluble α-glucan from isolated walls of *S. pombe* spores. We showed that the DMSO-extract of the wall contains (1→3)-α-D-glucan (**P I**) and (1→4)-α-D-glucan (**P II**). As amylose is known to accumulate in spore walls, it is very well possible that spore-wall preparations become contaminated with amylose-containing granula of cytoplasmic origin. We assume therefore that the presence of (1→4)-α-glucan (**P II**) in our preparations is due to cytoplasmic contamination. The DMSO-insoluble material, accounting for approximately 14% ($^{w}/_{w}$) of the Zymolyase-resistant spore wall fraction, contains a second (1→3)-α-glucan that could be obtained via alkaline extraction (**P III**). Structural characterization of the α-glucans revealed that both (1→3)-α-D-glucan fractions, **P I** and **P III**, are linear polysaccharides consisting mainly of (1→3)-linked α-D-Glc*p* residues in addition to approximately 10% (1→4)-linkages. The two fractions have similar chemical composition, but differ in degree of polymerization, namely approximately 480 for **P I** and 680 for **P III**. Despite their different solubility characteristics, we cannot exclude that **P I** and **P III** initially form one population and that the differences in solubility may be attributed to their molecular masses or crystallinity.

In addition to the (1→3)-linked Glc*p*, both fractions contain a small percentage of (1→4)-linked Glc*p* residues that may originate from contamination by **P II**, which is a linear (1→4)-α-glucan. Alternatively, in the case of a covalent linkage between the (1→3)-α-glucan and the (1→4)-linked residues, these residues must be located at or near the reducing or non-reducing end of the α-glucan because removing the (1→4) linkages by Smith degradation did not result in a strong decrease of the molecular mass of the α-glucan. This means that the chemical structures of spore-wall (1→3)-α-glucans are significantly different from (1→3)-α-glucan of vegetatively-grown cells, which broke in two halves after Smith degradation, indicating that it is composed of two similarly-sized (1→3)-α-glucan segments that were covalently-linked via a number of (1→4)-linked α-glucose residues (see Chapter 2).

Homologs of Ags1p may synthesize spore-wall (1→3)-α-glucan

The differences in the chemical structures of α-glucan from vegetatively-grown cells and from spores suggest that the biosynthesis of (1→3)-α-glucan in vegetatively growing cells and in sporulating cells is different. We speculate that during sporulation an α-glucan synthase different from Ags1p may be involved in (1→3)-α-glucan synthesis. This is consistent with the findings of Mata *et al.* (2002) who showed by DNA-microarray analysis that *ags1*$^+$ is downregulated during meiosis, whereas the *ags1*$^+$ homologs *mok11*$^+$, *mok12*$^+$, *mok13*$^+$, and *mok14*$^+$ are upregulated, suggesting that one (or more) of the *mok*$^+$ homologs may be essential for (1→3)-α-glucan biosynthesis during sporulation. The Mok proteins also have a similar multidomain structure as found in Ags1p. The only exception is Mok14p in which the extracellular domain is missing. Previously we proposed a mechanism of cell-wall α-glucan biosynthesis, in which the extracellular domain may function as a transglycosylase that couples two α-glucan building blocks (Chapter 2). Considering the chemical structure of spore-wall α-glucan, the question regarding the function of the extracellular domain of the Mokp homologs arose. We wondered whether the catalytic site in these homologs is conserved. Svensson (1994) showed that in fungal and plant α-amylases, three regions are involved in hydrolytic activity. In *Aspergillus orizae* α-glucosidase (TAKA), the first region includes Glu_{230}, which is regarded as a general acid catalyst and constitutes one of the three invariant carboxylic acid residues at the catalytic site. The other regions include Asp_{206}, that acts as a nucleofile, and Asp_{297}. Sequence alignment of TAKA with Ags1p showed that the three regions were conserved. Importantly, these regions were also conserved in Mok11p, Mok12p, and Mok13p. Presently, we have no explanation for the different mechanisms of α-glucan biosynthesis in vegetatively growing cells and in sporulating cells, and whether the extracellular domain is catalytically active in the Mokp homologs remains to be investigated.

Materials and Methods

Isolation of spore walls and α-glucans

Diploid cells of strain FH045 (h^+/h^- ade6-210/ade6-216) were grown at 28 °C in 1 L of a chemically defined medium, EMM, in the presence of a high concentration of nitrogen (10 g/L of ammonium chloride) to prevent sporulation (Moreno *et al.*, 1991). Then, the cells were washed and incubated at 28 °C in EMM without ammonium chloride to induce sporulation. After four days, the cell culture was centrifuged at 3300 × g. To digest (1→3)-β-glucan of contaminating ascus walls, the cell pellet was resuspended in 5 mM sodium azide, 40 mM 2-mercaptoethanol, 50 mM citrate-phosphate buffer, pH 5.3 containing 45 mg of Zymolyase-100T (Seikagaku). After an overnight-incubation in a rotary shaker at 200 rpm at 37 °C, spores were collected by centrifugation at 3300 × g for 15 min and resuspended in water. Then, the cell suspension was layered on top of 5 mM sodium azide, 8% sucrose, 90% Percoll and centrifuged at 10,000 × g. Spores were able to enter the sucrose-Percoll layer and pellet, whereas cell debris (including asci remnants) remained in the water fraction. The pellet fraction was resuspended and subjected to mechanical breakage by addition of glass beads (0.45 mm diameter) using a Mikro-Dismembrator (B. Braun Biotech International). Subsequently, spore walls were extracted with SDS and treated with Zymolyase as described (Chapter 2).

To isolate α-glucans, Zymolyase-resistant spore walls were lyophilized and further dried *in vacuo* over phosphorus pentoxide, and were dissolved in DMSO to a concentration of approximately 4 mg/ml by heating at 80 °C. DMSO-soluble polysaccharides were obtained by centrifugation at 10,000 × g for 10 min. This extraction procedure was repeated twice. α-Glucans were precipitated from the combined supernatants by addition of ethanol to a final concentration of 40% (fraction **P I**) or 60% (fraction **P II**) with intermediate collection of the fractions by centrifugation at 10,000 × g for 10 min. Fraction **P I** was washed twice with ethanol and three times with water, whereas fraction **P II** was washed three times with ethanol. Fraction **P I** was further purified by repeating the dissolution-precipitation procedure. Fraction **P III** was obtained by suspending the dried DMSO-insoluble spore-wall fraction in 1 M NaOH for 10 min at RT. The supernatant was collected by centrifugation at 16,000 × g for 10 min and fraction **P III** was obtained by addition of 1 M acetic acid to pH 6 at 4 °C. The precipitate was collected by centrifugation at 10,000 × g for 10 min and the pallet was washed thoroughly with water.

Monosaccharide analysis and linkage analysis

For monosaccharide analysis, samples were subjected to methanolysis [1.0 M methanolic HCl, 24 h, 85 °C], followed by trimethylsilylation [5:1:1 pyiridine/chloro-trimethylsilane/hexamethyldisilazane, 30 min, RT], and were analyzed by GLC and GLC-IE-MS (Kamerling and Vliegenthart, 1989). Absolute configurations were determined by butanolysis (Gerwig *et al.*, 1978).

For linkage analysis, per-*O*-methylation was performed using the method of Hakomori (1964). Then, per-*O*-methylated polysaccharides were hydrolyzed in aqueous 90% (v/v) formic acid [1 h, 100 °C], followed by evaporation and treatment with 2 M trifluoroacetic acid [1 h, 120 °C]. Samples were reduced with excess $NaBD_4$ in 0.5 M NH_4OH for 90 min at RT, followed by acetylation with acetic acid anhydride [3 h, 120 °C].

GLC analyses were performed on a WCOT CP-SIL 5CB fused-silica capillary column (25 m × 0.32 mm) (Chrompack) using a CP 9002 gas chromatograph (Chrompack) and a temperature program of 140-240 °C at 4 °C/min. GLC-EI-MS of partially methylated alditol acetates was carried out on an MD800/8060 system (Fisons Instruments, Manchester, UK) equipped with a WCOT CP-SIL 5CB fused-silica capillary column (25 m × 0.25 mm) (Chrompack), using the same temperature program.

Size-exclusion chromatography

The HPSEC system consisted of a Delta 600 pump (Waters) with a DRI 2410 refractive index detector (Waters). For the mobile phase, sodium nitrate was added to DMSO to a final concentration of 3 mM to reduce aggregation of polymers and to eliminate ionic strength effects (Chuang, 1990). It was delivered at a flow-rate of 1.0 ml per min. A single PLgel 5 µm MIXED-C column (300 × 7.5 mm) (Polymer Laboratories) was connected in series with a PLgel 10 µm guard column (50 × 7.5 mm). Both columns were thermostated at 80 °C. The system was calibrated using pullulan narrow standards (Standard P-82, Shodex) plus maltohexaose and glucose. Samples were lyophilized and then further dried overnight *in vacuo* over phosphorus pentoxide, dissolved in the mobile phase to a concentration of 2 mg/ml, and filtered through 0.45 µm PTFE filters. Injection volumes of 100 µl were used. Data were processed using Millenium^{32} software (Waters). Number-average molecular mass (Mn) and weight-average molecular mass (Mw) were determined by dividing each HPSEC profile into a number of virtual time slices, n_i, each corresponding to a certain molecular mass M_i that is obtained by calibrating the column. From these values, Mn and Mw can be calculated according to:

$$\mathrm{Mn} = \frac{\sum_i n_i \mathrm{M}_i}{\sum_i n_i} \quad \text{and} \quad \mathrm{Mw} = \frac{\sum_i n_i \mathrm{M}_i^2}{\sum_i n_i \mathrm{M}_i} \quad .$$

The polydispersity is given by the ratio of the weight to the number-average molecular mass (Mw/Mn) and is a measure of the breadth of the molecular mass distribution.

Nuclear magnetic resonance

All NMR spectra were recorded on a DRX500 spectrometer (Bruker). Samples were dissolved in 600 µl of 99.6% DMSO-*d6* and were analyzed at 80 °C. Residual water signals were suppressed by applying a WEFT pulse sequence in 1D ^{1}H NMR experiments (Hård *et al.*, 1992). 10 ms and 50 ms 2D ^{1}H-^{1}H total correlation spectroscopy (TOCSY) was carried out in the phase-sensitive mode using the States-TPPI method and the MLEV-17 sequence for mixing. The sensitivity enhanced 2D ^{1}H-^{13}C heteronuclear single quantum coherence (HSQC) experiment used Echo/Antiecho gradient selection with decoupling. Chemical shifts are expressed in ppm relative to internal DMSO (^{1}H, 2.505 ppm; ^{13}C, 39.6 ppm). Data were processed using in-house developed software.

Smith degradation

For Smith degradation (Smith & Montgommery, 1956), polysaccharide samples were suspended in 15 mM sodium periodate at a concentration of approximately 2 mg per ml. The mixture was placed in the dark at 4 °C under continuous mixing. After 48 h, the reaction was stopped by adding ethylene glycol to a final concentration of 350 mM. Oxidized polysaccharides were reduced with an excess of $NaBH_4$ during 24 h. Then, excess borohydride was removed by the addition of acetic acid. The product was washed three times with water and hydrolyzed in 100 mM hydrochloric acid at RT during 8 h.

References

Arellano, M.; Cartagena-Lirola, H.; Nasser Hajibagheri, M.A.; Durán, A. & Valdivieso, M.H. (2000) Proper spore maturation requires the *chs1*$^+$ chitin synthase gene in *Schizosaccharomyces pombe. Mol. Microbiol.* **35,** 79-89.

Beltran, F.F.; Castillo, R.; Vicente-Soler, J.; Cansado, J. & Gacto, M. (2000) Role for trehalase during germination of spores in the fission yeast *Schizosaccharomyces pombe. FEMS Microbiol. Lett.* **193,** 117-121.

Briza, P.; Ellinger, A.; Winkler, G. & Breitenbach, M. (1988) Chemical composition of the yeast spore wall. The second outer layer consists of chitosan. *J. Biol. Chem.* **263,** 11569-11574.

Briza, P.; Winkler, G.; Kalchhauser, H. & Breitenbach, M. (1986) Dityrosine is a prominent component of the yeast spore wall. A proof of its structure. *J. Biol. Chem.* **261,** 4288-4294.

Cardemil, L. & Pincheira, G. (1979) Characterization of the carbohydrate component of fraction I in the *Neurospora crassa cell wall. J. Bacteriol.* **137,** 1067-1072.

Chuang, J.-Y. (1990) Size exclusion chromatography of starch with dimethyl sulfoxide as the mobile phase: ionic-strength effect. *J. Appl. Polym. Sci.* **45,** 227-242.

Gerwig, G.J.; Kamerling, J.P. & Vliegenthart, J.F.G. (1978) Determination of the D and L configuration of neutral monosaccharides by high-resolution capillary G.L.C. *Carbohydr. Res.* **62,** 349-357.

Hakomori, S.-I. (1964) A rapid permethylation of glycolipid, and polysaccharide catalyzed by methylsulfinyl carbanion in dimethyl sulfoxide. *J. Biochem.* **55,** 205-208.

Hård, K; Van Zadelhoff, G.; Moonen, P.; Kamerling, J.P. & Vliegenthart, J.F.G. (1992) The Asn-linked carbohydrate chains of human Tamm-Horsfall glycoprotein of one male. Novel sulfated and novel *N*-acetylgalactosamine-containing *N*-linked carbohydrate chains. *Eur. J. Biochem.* **209,** 895-915.

Hochstenbach, F.; Klis, F.M.; Van Den Ende, H.; Van Donselaar, E. Peters, P.J. & Klausner, R.D. (1998) Identification of a putative α-glucan synthase essential for cell wall construction and morphogenesis in fission yeast. *Proc. Natl. Acad. Sci. U S A* **95,** 9161-9166.

Inoue, H. & Shimoda, C. (1981) Changes in trehalose content and trehalose activity during spore germination in fission yeast, *Schizosaccharomyces pombe. Arch. Microbiol.* **129,** 19-22.

James, P.G.; Cherniak, R.; Jones, R.G. & Stortz, C.A. (1990) Cell-wall glucans of *Cryptococcus neoformans* Cap 67. *Carbohydr. Res.* **198,** 23-38.

Kamerling, J.P. & Vliegenthart, J.F.G. (1989) Mass spectrometry. In Lawson, A.M. (ed.), *Clinical Biochemistry - Principles, Methods, Applications.* Walter de Gruyter, Berlin, Vol. 1, pp. 176-263.

Katayama, S.; Hirata, D.; Arellano, M.; Pérez, P. & Toda T. (1999) Fission yeast α-glucan synthase *mok1* requires the actin cytoskeleton to localize the sites of growth and plays an essential role in cell morphogenesis downstream of protein kinase C function. *J. Cell Biol.* **144,** 1173-1186.

Klis, F.M.; Caro, L.H.P.; Vossen, J.H.; Kapteyn, J.C.; Ram, A.F.J.; Montijn, R.C.; Van Berkel, M.A.A. & Van Den Ende, H. (1997) Identification and characterization of a major building block in the cell wall of *Saccharomyces cerevisiae. Biochem. Soc. Transactions* **25,** 856-860.

Klis, F.M. (1994) Review: cell wall assembly in yeast. *Yeast* **10,** 851-569.

Liu, J.; Tang, X.; Wang, H. & Balasubramanian, M. (2000) *Bgs2*p, a 1,3-β-glucan synthase subunit, is essential for maturation of spore wall in *Schizosaccharomyces pombe. FEBS Lett.* **478,** 105-108.

Martín, V.; Ribas, J.C.; Carnero, E.; Durán, A. & Sánchez, Y. (2000) *bgs2*$^+$, a sporulation-specific glucan synthase homologue is required for proper spore wall maturation in fission yeast. *Mol. Microbiol.* **38,** 308-321.

Mata, J.; Lyne, R.; Burns, G. & Bähler, J. (2002) The transcriptional program of meiosis and sporulation in fission yeast. *Nature Genet.* **32,** 143-147.

Moreno, S.; Klar, A. & Nurse, P. (1991) Molecular genetic analysis of fission yeast *Schizosaccharomyces pombe*. *Methods. Enzymol.*; **194,** 795-823.

Smith, F. & Montgomery, R. (1956) End group analysis of polysaccharides. In Glick, D. (ed.), *Methods of biochemical analysis*. Interscience Publishers Inc., New York, Vol. 3, pp. 153-212.

Svensson B. (1994) Protein engineering in the α-amylase family: catalytic mechanism, substrate specificity, and stability. *Plant Mol. Biol.* **25,** 141-157.

Chapter 5

Evidence for two conserved mechanisms of cell-wall α-glucan biosynthesis in fungi

Christian H. Grün[1], Frans Hochstenbach[2], J. Hans Sietsma[3], Frans M. Klis[4], Johannis P. Kamerling[1], and Johannes F.G. Vliegenthart[1]

[1]*Bijvoet Center, Department of Bio-Organic Chemistry, Section of Glycoscience and Biocatalysis, Utrecht University;* [2]*Department of Biochemistry, Academic Medical Center, University of Amsterdam;* [3]*Laboratory for Molecular Biology of Plants, Groningen Biomolecular Sciences and Biotechnology Institute (GBB), University of Groningen;* [4]*Swammerdam Institute for Life Sciences, University of Amsterdam*

Abstract

The cell wall of most fungi is composed of glycoproteins, β-glucan, chitin and α-glucan. Previously, we showed that in the cell wall of the ascomycetous fission yeast *Schizosaccharomyces pombe*, α-glucan displays a dimeric structure that is composed of two covalently-linked building blocks, each consisting of a linear (1→3)-α-glucan segment with a small number of (1→4)-linked residues at its reducing end, indicating a two-step biosynthetic mechanism. In contrast, the structure of α-glucan in spore walls consists of a single (1→3)-α-glucan monomer, suggesting an alternative, single-step biosynthetic mechanism. Here, we examine the chemical structures of α-glucans from the cell walls of seven ascomycetous and basidiomycetous species. We found that the α-glucans from the cell walls of *Lentinus edodes* and *Cryptococcus neoformans* Cap67, similar to α-glucan from fission-yeast cell walls, occur as dimeric structures, whereas the α-glucans from *Pleurotus ostreatus*, *Piptoporus betulinus*, *Neurospora crassa*, and *Schizophyllum commune* occur as monomeric structures. Interestingly, the fruiting bodies of *Laetiporus sulphureus* contain both structures of α-glucan. We conclude that for the biosynthesis of fungal α-glucan, both one-step and two-step biosynthetic mechanisms are conserved in evolution.

Introduction

Fungal cell morphology and integrity depend on cell-wall polysaccharides. The cell wall of most fungi consists mainly of glycoproteins and four types of polymers, namely (1→3)-β-glucan, (1→6)-β-glucan, chitin, and (1→3)-α-glucan. Disruption of enzymes involved in cell-wall synthesis may cause cell lysis. For instance, mutations in (1→3)-β-glucan and (1→3)-α-glucan synthases may lead to cell swelling or cell lysis (Ishiguro *et al.* 1997; Hochstenbach *et al.* 1998). Because most fungi possess similar structural polysaccharides, the enzymes involved in their assembly form ideal targets for the development of novel antifungal drugs (Georgopapadakou & Tkaz, 1995; Radding *et al.*, 1998; Onishi *et al.*, 2000; Ohyama *et al.*, 2000; Feldmesser *et al.*, 2000; De Pauw, 2000; Georgopapadakou, 2001; Kurtz & Rex, 2001).

Recently, we have identified a putative (1→3)-α-glucan synthase, Ags1p, in fission yeast *Schizosaccharomyces pombe* (Hochstenbach *et al.*, 1998). Based on its hydropathy plot and amino-acid sequence similarities, we identified three Ags1p domains, namely an intracellular synthase domain, a C-terminal multipass transmembrane domain and an N-terminal extracellular domain that might act as a transglycosylase (Hochstenbach *et al.*, 1998). By examining the chemical structures of α-glucan from cell walls of wild-type cells as well as from a (1→3)-α-glucan synthase mutant that showed an aberrant cell morphology, we proposed a model for the mechanism of action of Ags1p (Chapter 2). In short, we found that fission-yeast α-glucan is composed of two (1→3)-α-glucan polymers that were covalently linked via a short stretch of (1→4)-linked residues. The α-glucan from the mutant strain, however, was composed of only a single α-glucan monomer, indicating that Ags1p is essential for both the synthesis and coupling of α-glucan building blocks, and therefore displaying a two-step biosynthetic mechanism.

In fission yeast, four genes homologous to *ags1*$^+$, namely *mok11*$^+$, *mok12*$^+$, *mok13*$^+$, and *mok14*$^+$, were identified that can be depleted without forming a noticeable phenotype (Hochstenbach *et al.*, 1998; Katayama *et al.*, 1999). Based on DNA-microarray analyses, Mata *et al.* (2002) showed that *ags1*$^+$ was downregulated, whereas the *mok*$^+$ homologs were upregulated during meiosis, indicating that these genes may encode α-glucan synthases required for spore-wall formation. Indeed, recently we have identified two (1→3)-α-glucans in fission-yeast spore walls (see Chapter 4). Importantly, unlike α-glucan from cell walls of vegetatively-grown cells, spore-wall α-glucans are composed of single (1→3)-α-glucan monomers, indicating a one-step biosynthetic mechanism.

α-Glucan synthases homologous to fission-yeast Ags1p have been identified in the fungi *Aspergillus fumigatus* (with Genbank accession numbers AAL18964 and AAL28129), *Neurospora crassa* (with protein identification numbers NCU02478.1 and NCU08132.1), *Schizophyllum commune* (H.A.B. Wösten, personal communication) and *Cryptococcus neoformans*. Interestingly, these homologous enzymes also have a similar multidomain structure as Ags1p. Therefore, we wondered whether also the reaction products of these synthases may be conserved, and thus, whether their α-glucan structures are similar to cell-wall or spore-wall α-glucan of fission yeast.

Here we examine the chemical structures of cell-wall α-glucans from seven fungal species and compare the chemical structures with those of α-glucans from fission-yeast cell walls and spore walls. By using high-performance size-exclusion chromatography (HPSEC) in combination with chemical analysis and NMR spectroscopy, we found that in two out of seven fungi an α-glucan is present as dimers similar to cell-wall α-glucan from fission yeast, indicating a two-component biosynthetic mechanism. In four species the α-glucan is present as monomers similar to α-glucan from fission-yeast spore walls, indicating a one-component biosynthetic mechanism. One species, *Laetiporus sulphureus*, bears both structures. These one-component and two-component biosynthetic mechanisms have been found in both Ascomycetes and Basidiomycetes, indicating that both mechanisms are conserved in evolution.

Results

α-Glucan isolation

To investigate whether the chemical structures of α-glucans differ between different fungal species, we have analyzed the chemical structures of α-glucan preparations from seven different fungal species. The α-glucans were obtained by alkaline extraction of cell walls, hyphal walls or fruiting bodies, followed by precipitation. The homogeneity of the samples was determined by chemical analyses and by ^{1}H-NMR spectroscopy. Contaminations by other polysaccharides did not exceed 10-15% of the total preparation.

Neurospora crassa

To study the chemical structure of an α-glucan from a mycelial Ascomycete, we isolated an α-glucan from *N. crassa* cell walls, strain FGSC987, which were extracted with 1 M sodium hydroxide. The alkali-soluble material gave a precipitate upon neutralization, accounting for 8.3% of total cell-wall material (dry weight). This is slightly lower than the α-glucan-containing fraction reported by Cardemil and Pinchera (1979), which was 14% of total cell walls in their RL-3-8A strain. Monosaccharide analysis demonstrated that the preparation consisted mainly of glucose. Mannose was present in trace amounts, only. By determining the type of linkage, we found in addition to (1→3)-linked glucose, approximately 5.3% (1→4)-linked glucose residues (**Table II**). Some disubstituted residues were detected, that were assigned to undermethylation as non-reducing ends were lacking.

^{1}H-NMR analysis gave a spectrum that is similar to the spectrum of *S. pombe* α-glucan, and therefore, corresponds to a (1→3)-α-glucan (**Fig. 1**). In addition, we observed signals at 5.14 and 4.55 ppm, which could be assigned to (1→4)-linked α-Glc*p* and (1→3)-linked β-Glc*p* (17%), respectively. Furthermore, signals were present at 4.89, 4.31, and 4.25 ppm, which have chemical shifts similar to those reported for the hydroxyl-signals of (1→3)-linked β-Glc*p* (Ensley *et al.*, 1994). These data indicate that the preparation obtained by sodium-hydroxide extraction of *N. crassa* mainly consists of a (1→3)-α-glucan.

To determine the molecular mass distribution of the α-glucan, the preparation was analyzed by high-performance size-exclusion chromatography (HPSEC) on a calibrated column. The profile showed a main population with a shoulder of high-molecular mass (**Fig. 2**), which is probably due to the (1→3)-β-glucan contamination. The preparation had an Mn of 42.8 kDa (DP_n 246), which corresponds to a number-average degree of polymerization (DP_n) of 246. This is similar to that of cell-wall α-glucan of fission yeast (**Table III**). The polydispersity, however, was 7.71, indicating a rather broad molecular mass distribution.

To determine whether the α-glucan is composed as a monomer or a dimer, we treated the α-glucan with periodate followed by acid hydrolysis (Smith degradation), which affects vicinal hydroxyl groups such as in (1→2)-linked, (1→4)-linked, and (1→6)-linked hexoses, but not in (1→3)-linked hexoses. In the case of a dimeric structure, the molecular mass will be half of that of the native α-glucan, whereas in case of a monomeric structure, the molecular mass distribution will remain unaltered (**Fig. 2**, compare HPSEC profiles of cell-wall and spore-wall α-glucan of *S. pombe*). HPSEC analysis of the Smith-degraded α-glucan preparation from *N. crassa* showed that the number-average degree of polymerization hardly changed (**Fig. 2**, **Table III**), indicating that the (1→4)-linked glucose residues were not interspersed in the α-glucan molecule. However, the shoulder that was observed in the molecular mass profile of the native material disappeared, indicating degradation of a contaminating polysaccharide. The HPSEC results indicate that similar to the α-glucan from fission-yeast spore walls, *N. crassa* α-glucan occurs as a monomer.

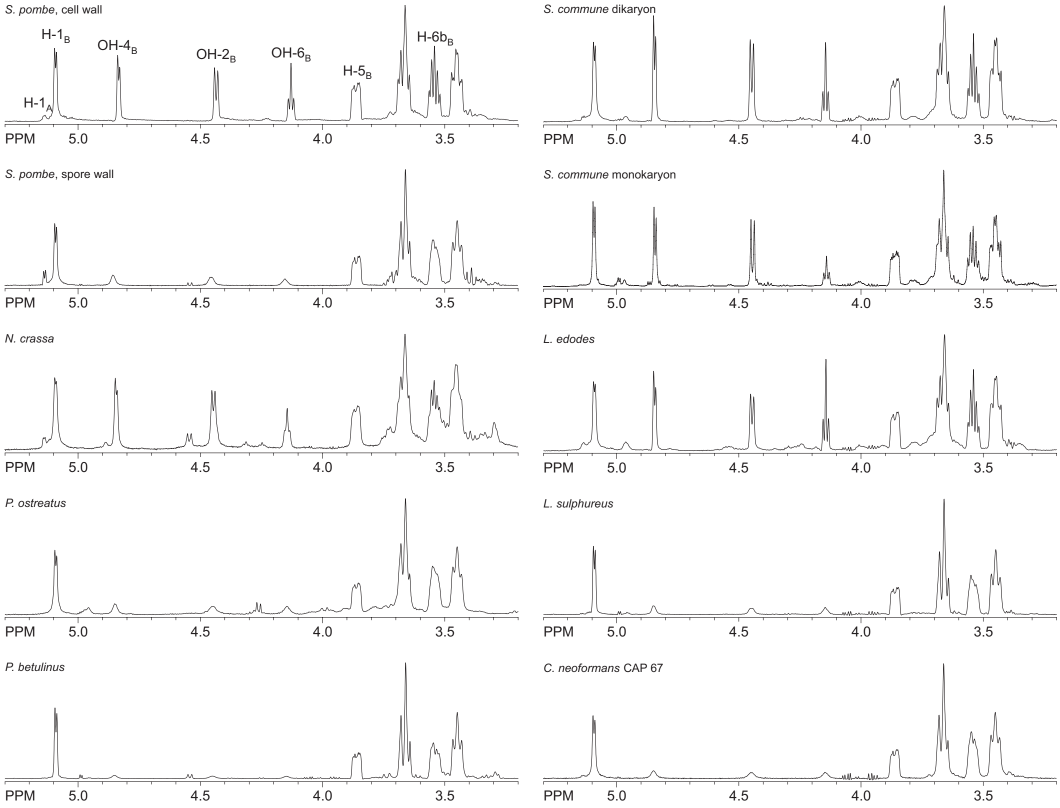

Fig. 1. ^{1}H-NMR spectra of α-glucans from *S. pombe* cell walls, *S. pombe* spore walls, *N. crassa*, *P. ostreatus*, *P. betulinus*, *S. commune* dikaryon, *S. commune* monokaryon, *L. edodes*, *L. sulphureus*, and *C. neoformans* Cap67. Samples were dissolved in DMSO-d_6 and spectra were recorded at 500.08 MHz at 80 °C. See text for details.

Pleurotus ostreatus

Fruiting bodies of basidiomycetous *P. ostreatus* (oyster mushroom) are easily available because they are widely used in food industry. The alkali extraction of the fruiting bodies gave a polysaccharide preparation that upon monosaccharide analysis predominantly consisted of glucose (**Table I**). In addition to glucose, mannose (5.8%) and xylose (8.3%) was found, which are probably part of a xylomannan contamination. Linkage analysis demonstrated that the major part of the glucose is (1→3)-linked in addition to some disubstituted Glc (**Table II**). The percentage of disubstituted residues varied between independent experiments, indicating undermethylation rather than branching points. In addition, we identified 3-substituted Man, 3,4-disubstituted Man, 2-substituted, and non-reducing Xyl. (1→4)-Linked glucose residues were not detected.

In the ^{1}H-NMR spectrum of the α-glucan from *P. ostreatus*, H-1α signals at 5.091 and 4.958 ppm and a H-1β signal at 4.261 ppm were observed in the relative intensities of 77:13:10, indicating the presence of three different constituents (**Fig. 1**). The two minor constituents were not further identified, but may represent the xylomannan contamination. The chemical shifts of the major constituent, including the slowly-exchanging hydroxyl signals at 4.85, 4.45, and 4.15 ppm, resemble those of (1→3)-α-glucan from *S. pombe* (**Fig. 1**). Signals corresponding to (1→3)-linked β-Glc*p* (anomeric proton around 4.54 ppm) or (1→4)-linked α-Glc*p* (around 5.14 ppm) were not detected (i.e., below the detection limit of 0.5%).

Determination of the molecular mass distribution by HPSEC showed that the α-glucan preparation eluted as two strongly overlapping populations, indicating that the cell walls of the fruiting bodies of *P. ostreatus* contained two different α-glucan populations (**Fig. 2**). The number-average molecular mass (Mn) of the combined populations was 70.8 ± 9.5 kDa (mean ± SD; n = 3), which corresponds to a number-average degree of polymerization (DP_n) of 437 ± 59 (**Table III**). The polydispersity (Mw/Mn) was 8.34 ± 2.05, indicating a relatively broad molecular mass distribution compared to fission-yeast α-glucan from cell walls or spore walls, which was 2.41 and 2.33, respectively (**Table III**). The HPSEC analysis of Smith-degraded glucan gave an Mn of 62.4 ± 7.5 kDa (DP_n of 385 ± 46), which is similar to that of the native α-glucan, indicating that *P. ostreatus* α-glucan is composed of a monomer.

Piptoporus betulinus

The Basidiomycete *P. betulinus* is a fruiting-body bearing fungus that infects dying birch trees and is regarded as a wood-rot fungus (Rösecke *et al.*, 2000). Monosaccharide analysis of an α-glucan preparation obtained from the fruiting bodies of *P. betulinus* demonstrated that the preparation consisted almost entirely of glucose (**Table I**). Linkage analysis indicated that the glucose residues are mostly (1→3)-linked with only a small percentage of (1→4)-linkages (**Table II**). Triple-substituted residues were detected as trace amounts only, indicating that these may originate from undermethylation rather than from branching points. ^{1}H-NMR spectroscopy (**Fig. 1**) demonstrated that the major constituent is (1→3)-linked α-Glc*p*. In addition to signals corresponding to (1→3)-linked α-Glc*p*, signals of low intensity were identified at 5.15 and 4.54 ppm, that were assigned to anomeric protons of (1→4)-linked α-Glc*p* and (1→3)-linked β-Glc*p*, respectively.

We then determined the molecular mass distribution of the α-glucan using HPSEC. The preparation eluted as two strongly overlapping populations. The Mn of the combined populations was 11.4 ± 0.9 kDa, which corresponds to a DP_n of 71 ± 5 (**Table III**). This is in good agreement with the data of James and Cherniak (1990) who found an estimated molecular mass of 15 kDa for their α-glucan preparation. The polydispersity was 2.33 ± 0.30, which indicates a relatively narrow molecular mass distribution, similar to that of fission-yeast α-glucan (**Table III**). To determine whether the α-glucan is composed as a monomer or as a dimer, we performed Smith degradation and analyzed the products by HPSEC, resulting in a profile that was almost indistinguishable from that of the native polysaccharide, indicating that the polysaccharide is resistant to periodate (**Fig 2**). Also the calculated Mn and polydispersity are similar to those of the native polysaccharide

(**Table III**), demonstrating that the α-glucan from the fruiting bodies of *P. betulinus* is composed as a monomer.

Table I. Monosaccharide analysis of α-glucan preparations

Species	Glc	Man	Xyl
N. crassa	100	trace	-
P. ostreatus	86.8	6.2	7.0
P. betulinus	98.8	1.2	trace
S. commune dikaryon	89.7	10.3	trace
S. commune monokaryon	87.0	12.0	1.0
L. edodes	83.5	11.4	5.0
L. sulphureus	96.2	2.3	1.5
C. neoformans	100	-	-

Table II. Linkage analysis of α-glucans

Residue	Molar amounts (%)							
	N. crassa	*P. ostreatus*	*P. betulinus*	*S. commune* dikaryon	*S. commune* monokaryon	*L. edodes*	*L. sulphureus*	*C. neoformans*
Xyl*f*-(1→	-	4.5	trace	trace	trace	2.6	trace	-
→2)-Xyl*f*-(1→	-	1.5	-	-	-	-	-	
Glc*p*-(1→	-	-	-[1]	-	-[1]	-	-	-
→3)-Glc*p*-(1→	88.9	82.0	93.9	80.3	80.2	68.3	92.1	94.1
→4)-Glc*p*-(1→	5.3	-[3]	2.9[2]	16.3[2]	15.3[2]	18.2[2]	2.8[2]	3.9
→3)-Man*p*-(1→	-	2.6[3]						-
→3,4)-Glc*p*-(1→	2.5	-	trace	2.2	2.4	3.5	1.6	0.7
→3,4)-Man*p*-(1→	-	1.0	-	-	-	0.8	1.2	-
→2,3)-Glc*p*-(1→	1.1	3.9	0.9	trace	trace	5.3	0.7	trace
→3,6)-Glc*p*-(1→	2.3	4.5	2.3	1.2	2.1	1.3	1.6	1.3

[1] Percentages of non-reducing ends could not be determined due to overlap with a contaminating compound.

[2] →4)-Glc*p*-(1→ and →3)-Man*p*-(1→ have identical retention times on GLC and therefore their individual contribution could not be determined.

[3] In accordance with note 2, the presence of small amounts of →4)-Glc*p*-(1→ in the α-glucan preparation from *P. ostreatus* cannot be excluded.

Schizophyllum commune

S. commune is a Basidiomycete which cell walls have been extensively studied and which is especially used as a model organism to study cell-wall hydrophobins in filamentous fungi (Van Wetter *et al.*, 2000; Szaniszlo *et al.*, 1985; Sietsma & Wessels, 1977). An alkali extract from the hyphal walls of a dikaryon of *S. commune* (strain 4-39 × 4-40) yielded a preparation that upon monosaccharide analysis consisted for approximately 90% of glucose and 10% of mannose (**Table I**). Xylose was present in trace amounts only. Linkage analysis indicated that the glucose residues are mainly (1→3)-linked in addition to (1→4)-linked and 3,6-disubstituted glucose residues (**Table II**). The analysis further gave (1→3)-linked and 3,4-disubstituted mannose. Importantly, the partially methylated alditol acetates (PMAA) of (1→4)-linked Glc*p* and (1→3)-linked Man*p* have identical elution times on Glc, and therefore their individual contributions could not be determined. ^{1}H-NMR spectroscopy confirmed the presence of (1→3)-linked α-Glc*p* as the main constituent in addition to a small percentage (8%) of (1→4)-linked α-Glc*p* (**Fig. 1**).

When analyzed by HPSEC, the sample eluted as a single, Gaussian-curved distribution, indicating that a single population of α-glucan polymers is present in the hyphal walls of *S. commune* (**Fig. 2**). The Mn was 49.6 ± 1.7 kDa (DP_n 306 ± 11) and the polydispersity was 3.96 ± 0.20 (**Table III**). When removing the (1→4)-linked residues residues by Smith degradation and analysing the product by HPSEC, we observed that the molecular mass distribution did not change significantly (**Fig. 2**, **Table III**), indicating that the α-glucan is composed of a monomer.

Similarly, we analyzed an α-glucan preparation from monokaryon strain 4-39. We showed that the α-glucans from the two strains had a similar chemical composition (**Tables I** and **II**, **Fig. 1**). When determining its molecular mass distribution, however, we found an Mn of only 9.7 kDa (DP_n 60), which is approximately one fifth of that of the α-glucan from the dikaryon (**Table III**). Removal of the (1→4)-linked residues by Smith degradation did not affect its molecular mass distribution, indicating that the α-glucans isolated from both strains are composed as monomers.

Lentinus edodes

The edible fungus *L. edodes* (shiitake) produces fruiting bodies that upon alkali extraction gave a polysaccharide fraction. Monosaccharide analysis of this preparation gave glucose (83.5%), mannose (11.4%) and xylose (5,0%), indicating that this preparation, like the α-glucan from *P. ostreatus*, is contaminated with a xylomannan (**Table I**). Linkage analysis showed that (1→3)-linked Glc*p* is the main constituent (**Table II**), in addition to (1→4)-linked Glc*p* and (1→3)-linked Man*p*. We also identified some disubstituted Glc*p* residues, but since non-reducing glucose was lacking, these indicate undermethylation rather than branching points.

To confirm the chemical analysis data, we analyzed the preparation by ^{1}H-NMR spectroscopy. The spectrum of *L. edodes* α-glucan is almost identical to that of the α-glucan preparation from *S. commune* (**Fig. 1**). Integrating the α-Glc*p* signals gave a ratio of 88:12

for (1→3)-linked and (1→4)-linked α-Glc*p*, respectively. These data demonstrate that the α-glucan part of the preparation consists of approximately 12% (1→4)-linked α-Glc*p* residues in addition to approximately 88% (1→3)-linked α-Glc*p* residues.

To assess whether the α-glucan is a monomer or a dimer, we removed the (1→4)-linked residues by Smith degradation and analyzed the native as well as the degraded preparation by HPSEC. The native α-glucan eluted as a single peak with a near Gaussian distribution with an Mn of 96.9 ± 19.2 kDa, which corresponds to a DP_n of 598 ± 119 (**Fig. 2**; **Table III**). The polydispersity of 4.98 ± 0.76 indicates a relatively broad molecular mass distribution. These data are in good agreement with the data of Zhang and co-workers (1999) who found an Mn of 96 to 118 kDa, depending on the analytical conditions. Interestingly, after removal of the (1→4)-linked residues by Smith degradation, the Mn decreased to 49.3 ± 13.1 (DP_n 304 ± 81), which is approximately half the size of the untreated α-glucan. These results indicate that the α-glucan is composed as a dimer in which two linear (1→3)-linked α-glucan segments of approximately 300 glucose residues are coupled via a number of (1→4)-linked glucose residues. Shida *et al.* (1979) also investigated the chemical structure of α-glucan from *L. edodes*. By using low-pressure SEC, they noticed a slight shift in elution time after Smith degradation and concluded that the (1→4)-linked residues must be located at or near the reducing or non-reducing end. By using high-performance SEC on a calibrated column, we showed that Smith degradation caused bisection of the glucan.

Laetiporus sulphureus

L. sulphureus is a parasitic fungus that infects a large number of tree species. The sulfur-colored fruiting bodies are normally formed several years after the initial infection. Harvested fruiting bodies were extracted with potassium hydroxide that gave a precipitation upon neutralization. The precipitate was incubated with Zymolyase to hydrolyze (1→3)-β-glucan and the Zymolyase-resistant material was analyzed. The monosaccharide composition of the α-glucan preparation from *L. suphureus* is similar to the preparations from *L. edodes* and *P. ostreatus*, albeit with a lower mannose and xylose content (2.3 and 1.5%, respectively) (**Table I**). Linkage analysis indicated that the preparation is mainly composed of (1→3)-linked Glc*p* with a small percentage of (1→4)-linked Glc*p*, (1→3)-linked Man*p*, non-reducing Xyl*f*, and 3,4-disubstituted Man*p* (**Table II**). The low percentage of Man and Xyl is clearly visible in the ^{1}H-NMR spectrum showing a decrease in the signals at 4.96 and 4.26 ppm when compared to that of *L. edodes* (**Fig. 1**). The ^{1}H-NMR spectrum further confirms the presence of (1→4)-linked α-Glc*p* in addition to the major constituent of (1→3)-linked α-Glc*p* in the ratio of 96:4.

To determine the molecular mass distribution, we analyzed the α-glucan by HPSEC. The glucan eluted as two overlapping peaks, indicating that the cell walls of the fruiting bodies of *L. sulphureus* contain two different α-glucan populations (**Fig. 2**). Due to the strong overlap of the two populations, we were not able to determine an accurate molecular mass distribution of each individual population, and therefore, the analysis was limited to the combined populations. We then removed the (1→4)-linked glucose residues by Smith degradation and determined the molecular mass distribution of the reaction product. Comparing the two HPSEC profiles showed that only the high-molecular mass population was affected by Smith degradation, whereas the low-molecular mass population remained unaltered (**Fig. 2**), resulting in a decrease in polydispersity from 16.3 ± 3.9 to 11.3 ± 2.2 (**Table III**). These results indicate that the fruiting bodies of *L. sulphureus* contain two α-glucan populations that differ in molecular mass, of which the high-molecular mass population may occur as a dimer, whereas the low-molecular mass distribution is a monomer.

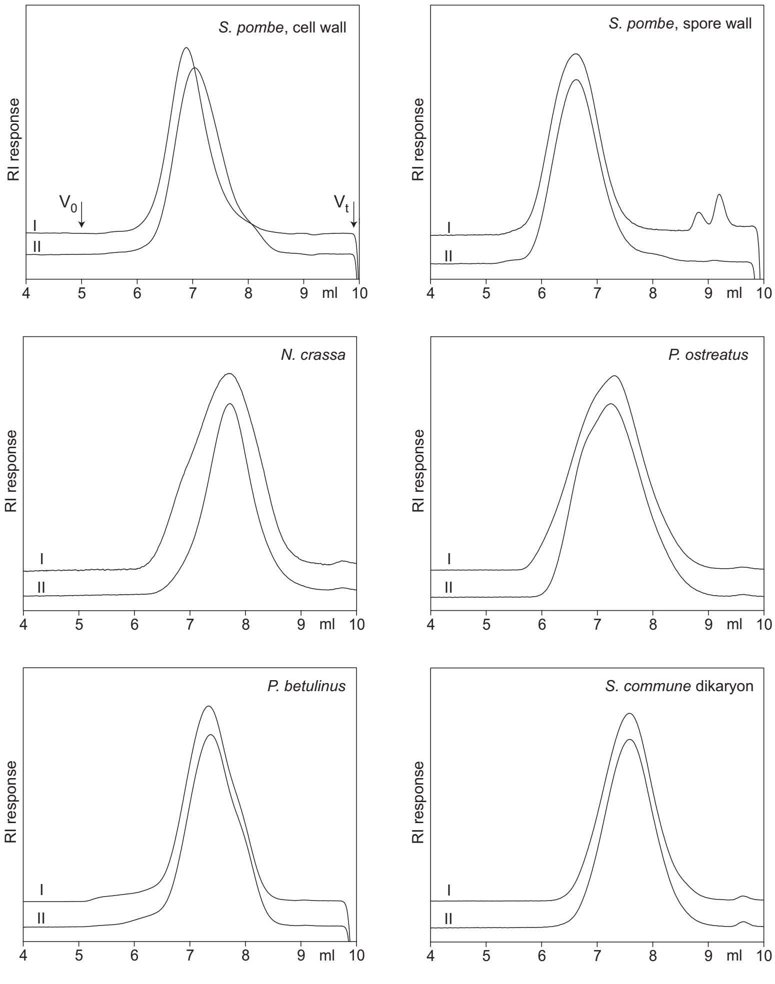

Fig. 2. Molecular mass distributions of untreated (**I**) and Smith-degraded (**II**) α-glucans from *S. pombe* cell walls, *S. pombe* spore walls, *N. crassa*, *P. ostreatus*, *P. betulinus*, *S. commune* dikaryon, *S. commune* monokaryon, *L. edodes*, *L. sulphureus*, and *C. neoformans* Cap67. Samples were dissolved in DMSO and analyzed on a calibrated HPSEC system. Note that the α-glucans from *S. pombe* and *P. betulinus* were analyzed on a PLgel MIXED-C column, whereas the other samples were analyzed on a PLgel MIXED-B column.

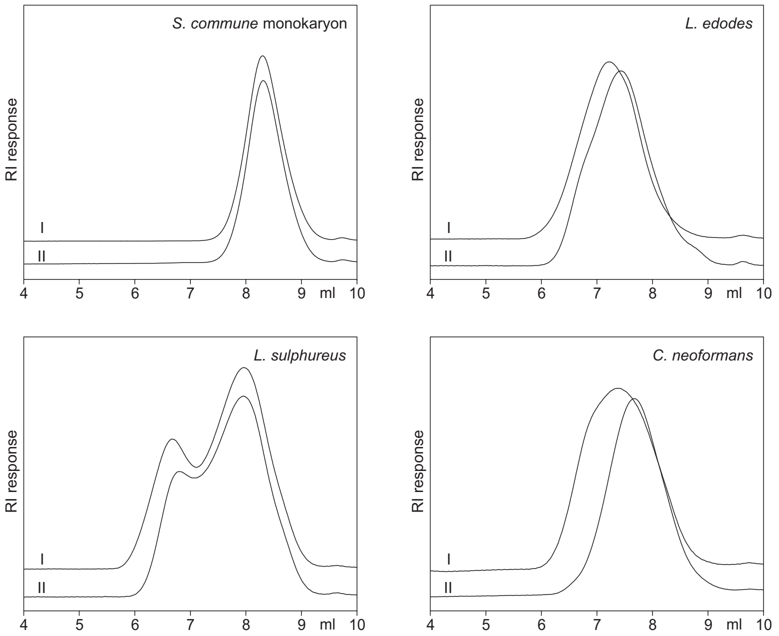

Table III. Molecular mass averages and polydispersities of α-glucans

	Mn (kDa)	Mw (kDa)	Mw/Mn	DP_n
S. pombe, cell wall	41.7 ± 5.7 [1]	102.1 ± 9.5	2.47 ± 0.21	275 ± 35
S. pombe, cell wall, Smith[2]	22.5 ± 2.8	61.8 ± 8.4	2.75 ± 0.02	137 ± 18
S. pombe, spore wall	110	256	2.33	677
S. pombe, spore wall, Smith	96.2	200.5	2.0	594
P. ostreatus	70.8 ± 9.5	580 ± 127	8.34 ± 2.05	437 ± 59
P. ostreatus, Smith	62.4 ± 7.5	425 ± 79	6.83 ± 1.13	385 ± 46
P. betulinus	11.4 ± 0.9	26.8 ± 4.1	2.33 ± 0.30	71 ± 5
P. betulinus, Smith	11.3 ± 1.2	27.0 ± 2.0	2.42 ± 0.29	70 ± 7
N. crassa	42.8	330	7.71	264
N. crassa, Smith	38.0	175	4.60	235
S. commune dikaryon	49.6 ± 1.7	196 ± 4.1	3.96 ± 0.20	306 ± 11
S. commune dikaryon, Smith	45.1 ± 4.0	162 ± 21.3	3.59 ± 0.41	278 ± 24
S. commune monokaryon	9.7	22.2	2.30	60
S. commune monokaryon, Smith	9.6	21.2	2.20	59
L. edodes	93.2 ± 15.4	479 ± 64	5.26 ± 1.11	576 ± 95
L. edodes, Smith	49.4 ± 8.3	213 ± 54	4.33 ± 0.20	305 ± 51
L. sulphureus	20.8 ± 1.8 [3]	332 ± 61 [3]	16.3 ± 3.9 [3]	n.d.
L. sulphureus, Smith	20.4 ± 1.2 [3]	230 ± 42 [3]	11.3 ± 2.2 [3]	n.d.
C. neoformans Cap67	62.3	543.6	8.72	385
C. neoformans Cap67, Smith	33.6	200.4	5.97	207

[1] Mean ± SD; n = 3.

[2] Smith = Smith degraded.

[3] Note that these are average values of two poorly-resolved α-glucan populations.

***Cryptococcus neoformans* Cap67**

C. neoformans is a potent human pathogenic fungus that can infect the central nervous system causing cryptococcal meningitis in immunocompromised patients (Hull & Heitman, 2002). α-Glucan synthase of *C. neoformans* has been notified as a potentially interesting target for the development of novel antifungal drugs (Georgopapadakou, 2001). To study cell-wall α-glucan from *C. neoformans*, we made use of an acapsular strain, Cap67. Extraction of the cell walls by 1 M NaOH gave a precipitate upon neutralization that counted for 40% ($^{w}/_{w}$) of the total cell wall, which is in accordance with data obtained by James *et al.* (1990). Monosaccharide analysis showed that the preparation consisted entirely of glucose (**Table I**). Linkage analysis showed that the glucose residues were mainly (1→3) linked in addition to approximately 3.9% (1→4) linkages (**Table II**). Analysis by ^{1}H-NMR spectroscopy showed that all glucose residues have an α-anomeric configurations (**Fig. 1**). The most abundant anomeric signal at 5.093 ppm could be assigned to (1→3)-linked α-Glc*p*, whereas a signal of low intensity present at 5.145 ppm indicates (1→4)-linked α-Glc*p*, which is consistent with the chemical analyses.

To assess whether the α-glucan is composed of a monomer or a dimer, we determined its molecular mass distribution by HPSEC before and after Smith degradation. The native α-glucan eluted as a single peak with an Mn of 62.3 kDa (DP_n 385) and a polydispersity of 8.72, indicating a relatively broad distribution (**Fig. 2**, **Table III**). The Mn of 62.3 kDa is significantly higher than that reported by James and co-workers (1990), who reported a molecular mass of only 14 kDa obtained by size-exclusion chromatography. This may be the result of a different extraction procedure used for isolating α-glucan, namely a 30-min extraction with 60% 4-methylmorpholine *N*-oxide at 120 °C, whereas in the present study, a 5-min extraction with 1 M NaOH at RT was used. After removing the (1→4)-linked residues by Smith degradation, the α-glucan had an Mn of 33.6 kDa (DP_n 207), which is approximately half of that of native α-glucan (**Fig. 2**, **Table III**). These data demonstrate that *C. neoformans* Cap67 α-glucan is composed as a dimer.

Discussion

In this study, we have elucidated the chemical structures of cell-wall α-glucans from seven fungal species. The α-glucans were composed mainly of (1→3)-linked α-glucose residues in addition to a small percentage of (1→4)-linked residues. By determining the molecular mass distributions of the native α-glucans and of the α-glucans after Smith degradation, we showed that the α-glucans of *L. edodes* and *C. neoformans* Cap67 are composed of two similarly-sized (1→3)-α-glucan segments that were covalently coupled via a number of (1→4)-linked residues and therefore occur as a binary structure, whereas α-glucans from *P. ostreatus*, *P. betulinus*, *N. crassa*, and *S. commune* occur as a single structure. The fruiting bodies of *L. sulphureus* appear to possess both structural forms of α-glucan.

Previously, we have elucidated the chemical structures of α-glucans from fission-yeast cell walls and from spore walls. We demonstrated that cell-wall α-glucan is composed of two covalently-linked building blocks, each consisting of a (1→3)-α-glucan segment of approximately 135 glucose residues with at its reducing end a small number of (1→4)-linked α-glucose residues (see Chapters 2 and 3). We further concluded that during vegetative growth a single enzyme, namely Ags1p, may be responsible for both the synthesis and the coupling of the (1→3)-α-glucan segments. In contrast, spore-wall α-glucan consisted of single (1→3)-α-glucan polymers of approximately 500-700 glucose residues (see Chapter 4). These results indicate that two different mechanisms for α-glucan biosynthesis can occur in the same organism. Based on the findings of Mata and co-workers (2002), who showed that *ags1*$^+$ is downregulated during meiosis, whereas the homologous *mok*$^+$ genes are upregulated, we assume that one (or several) of the homologous *mok*$^+$ genes is responsible for the synthesis of spore-wall α-glucan. Genes homologous to fission-yeast *ags1*$^+$ were identified, among others, in *N. crassa*, *C. neoformans*, and *S. commune*, that also possess the multidomain structure characteristic for the fission-yeast Ags1p. Of these, we showed that the α-glucan from *N. crassa* and *S. commune* have a chemical structure similar to that of fission-yeast spore walls, whereas the α-glucan from *C. neoformans* resembles that of fission-yeast cell walls. Our present results indicate that both mechanisms of α-glucan biosynthesis may be conserved in both Ascomycetes and Basidiomycetes.

In our previous study, we speculated that the extracellular domain of fission-yeast Ags1p functions as a transglycosylase that couples two (1→3)-glucan building blocks to form mature α-glucan. Although this extracellular domain is conserved in fission-yeast *mok*$^+$ homologs (with the exception of *mok14*$^+$) and in α-glucan synthases from the above-mentioned fungal species, neither spore-wall α-glucan from fission yeast nor the α-glucans from *N. crassa* and *S. commune* occur as a binary structure. We therefore speculate that this extracellular domain may not only have a catalytic function by coupling two α-glucan building blocks, but may also be needed for the deposition of α-glucan in the fungal cell wall, perhaps functioning as a lectin. Hydrolases such as chitinases have been shown to have lectin-like properties after eliminating its catalytic function (Renkema *et al.*, 1998), and it is conceivable that a dual function may also be present in fungal α-glucan synthases.

A further point of discussion is the degree of polymerization of the α-glucans from different fungi. We found that of α-glucans that are composed of a monomer, the DP_n varies from approximately 60 to over 600, indicating that despite sequence homology of the α-glucan synthases, regulation of chain elongation varies tremendously between fungal species. Also in α-glucans that are composed of a dimer, the polysaccharides do not possess a uniform length, but rather vary from 275 to approximately 600 glucose residues. How α-glucan biosynthesis is regulated is presently unknown and, therefore, an explanation on the heterogeneity between the different fungal α-glucans cannot be given. Importantly, of the α-glucans that are composed as a dimeric structure, the polydispersity did not increase after Smith degradation, indicating that each building block is similarly sized.

In conclusion, by analyzing cell-wall α-glucans from a number of fungi, we identified that α-glucan can be composed as a monomer or a dimer. These structures are found in both Ascomycetes and Basidiomycetes, indicating that the two biosynthetic mechanisms that were initially identified in fission yeast *S. pombe* are conserved in evolution.

Materials and Methods

Isolation of α-glucans

Fruiting bodies of *P. ostreatus* and *L. edodes* were obtained from a supermarket in Amsterdam, The Netherlands, and those of *L. sulphureus* were obtained from an infected tree in a park in Amsterdam. Approximately 300 g (fresh weight) of mushrooms were cut into cubes of approximately 1 cm^3 and finely minced in 100 mM EDTA, 50 mM Tris, pH 7.6 in a blender for 2 min at maximum speed. After addition of 2% (w/v) of SDS and 40 mM of 2-mercaptoethanol, cytosolic contaminants were extracted by boiling for 15 min. Wall material was isolated by centrifugation at 3222 × g for 10 min and washed in water. After repeating the mincing and extraction steps, wall material was resuspended in ice-cold 2 mM NaBH4, 2 N KOH and stirred at 4 °C for 30 min. Insoluble material was removed by centrifugation at 10,651 × g for 20 min. To isolate the alkali-soluble, water-insoluble fraction, acetic acid was added to the alkali-soluble supernatant under constant stirring until the pH was 6. The water-insoluble fraction was allowed to precipitate overnight at 4 °C under gentle stirring and was collected by centrifugation at 4500 × g for 15 min. To remove (1→3)-β-glucan, the pellet was resuspended in 5 mM sodium azide, 40 mM 2-mercaptoethanol, 50 mM citrate-phosphate buffer, pH 5.3 containing 45 mg of Zymolyase-100T (Seikagaku). After an overnight-incubation in a rotary shaker at 200 rpm at 37 °C, the insoluble fraction was collected by centrifugation at 4500 × g for 15 min and was washed twice with water. After repeating the alkali-extraction and Zymolyase digestion, the material was extracted with SDS and 2-mercaptoethanol as described and washed in 5 mM sodium azide.

Cryptococcus neoformans Cap67 cells (strain CBS7931, acapsular, serotype D) were grown in 1.5 L of YPD medium (1% (w/v) yeast extract, 2% (w/v) peptone, 2% (w/v) glucose) to an OD_{595} of approximately 4, which is equivalent to 10 g wet weight of cells per L. Cell walls were prepared as described (Chapter 2).

N. crassa and *C. neoformans* Cap67 cell walls were suspended in 1 M NaOH for 5 min after at RT which solid material was removed by centrifugation at 10,000 × g for 10 min. This extraction procedure was repeated twice by resuspending the pallet in 1 M NaOH; supernatants were pooled. To isolate the alkali-soluble, water-insoluble fraction, acetic acid was added to the alkali-soluble supernatant under constant mixing until the pH was 6. The water-insoluble fraction was allowed to precipitate during 48 h at 4 °C and was collected by centrifugation at 10,000 × g for 5 min.

A dikaryon of *S. commune* was constituted by mating monokaryon strains 4-39 (*MAT*A41 *MAT*B41) (CBS 341.81) and 4-40 (*MAT*A43 *MAT*B43) (CBS 340.81) and was grown as described (Sietsma *et al.*, 1977). Collected mycelia of dikaryon 4-39 × 4-40 and of monokarion 4-39 were washed and were fragmented by passing them through an X-press (Biotec, Stockholm, Sweden). Cell-walls were isolated by centrifugation [3,000 × g] and washing of the pallet until a clear supernatant was obtained. The pallet was resuspended in Tris buffer [0.1 M, pH 7.0] containing 2% SDS, and were extracted by boiling for 1 h. Wall material was isolated by centrifugation and washed three times in water. α-Glucan was obtained by extraction of the wall material with 1 M KOH during 20 min at 60 °C, followed by centrifugation. The supernatant was collected and acetic acid was added until the pH was 5. The water-insoluble fraction was allowed to precipitate overnight at 4 °C and was collected by centrifugation followed by washing of the pallet in water.

α-Glucan from the fruiting bodies of *P. betulinus* was a kind gift of Prof. J.R. Clamp, Bristol, UK.

Monosaccharide analysis and linkage analysis

For monosaccharide analysis, samples were subjected to methanolysis [1.0 M methanolic HCl, 24 h, 85 °C], followed by trimethylsilylation [5:1:1 pyiridine/chlorotrimethylsilane/hexamethyldisilazane, 30 min, RT], and were analyzed by GLC and GLC-IE-MS (Kamerling and Vliegenthart, 1989).

For linkage analysis, per-*O*-methylation was performed using the method of Hakomori (1964). Then, per-*O*-methylated polysaccharides were hydrolyzed in aqueous 90% (v/v) formic acid [1 h, 100 °C], followed by evaporation and treatment with 2 M trifluoroacetic acid [1 h, 120 °C]. Samples were reduced with excess $NaBD_4$ in 0.5 M NH_4OH for 90 min at RT, followed by acetylation with acetic acid anhydride [3 h, 120 °C].

GLC analyses were performed on a WCOT CP-SIL 5CB fused-silica capillary column (25 m × 0.32 mm) (Chrompack) using a CP 9002 gas chromatograph (Chrompack) and a temperature program of 140- 240 °C at 4 °C/min. GLC-EI-MS of partially methylated alditol acetates was carried out on an MD800/8060 system (Fisons Instruments, Manchester, UK) equipped with a WCOT CP-SIL 5CB fused-silica capillary column (25 m × 0.25 mm) (Chrompack), using the same temperature program.

Size-exclusion chromatography

The HPSEC system consisted of a Delta 600 pump (Waters) with a DRI 2410 refractive index detector (Waters). For the mobile phase, sodium nitrate was added to DMSO to a final concentration of 3 mM to reduce aggregation of polymers and to eliminate ionic strength effects (Chuang, 1990). The flow-rate was 1.0 ml per min. A single PLgel 10 µm MIXED-B or PLgel 5 µm MIXED-C column (300 × 7.5 mm) (Polymer Laboratories) was connected in series with a PLgel 10 µm guard column (50 × 7.5 mm). The columns were thermostated at 80 °C. The system was calibrated using pullulan narrow standards

(Standard P-82, Shodex) plus maltopentaose and glucose. Samples were lyophilized and further dried overnight *in vacuo* over phosphorus pentoxide, then dissolved in the mobile phase to a concentration of 2 mg/ml, and filtered through 0.45 m PTFE filters. Injection volumes of 100 µl were used. Data were processed using Millenium^{32} software (Waters). Number-average molecular mass (Mn) and weight-average molecular mass (Mw) were determined by dividing each HPSEC profile into a number of virtual time slices, n_i, each corresponding to a certain molecular mass M_i that is obtained by calibrating the column. From these values, Mn and Mw can be calculated according to:

$$\mathrm{Mn} = \frac{\sum_i n_i \mathrm{M}_i}{\sum_i n_i} \quad \text{and} \quad \mathrm{Mw} = \frac{\sum_i n_i \mathrm{M}_i^2}{\sum_i n_i \mathrm{M}_i} \quad .$$

The polydispersity is given by the ratio of the weight to the number-average molecular mass (Mw/Mn) and is a measure of the breadth of the molecular mass distribution.

Nuclear magnetic resonance

All ^{1}H-NMR spectra were recorded on a DRX500 spectrometer (Bruker). Samples were dissolved in 600 µl of 99.6% DMSO-*d6* and were analyzed at 80 °C. Residual water signals were suppressed by applying a WEFT pulse sequence (Hård *et al.*, 1992). Chemical shifts are expressed in ppm relative to internal DMSO (^{1}H, 2.505 ppm; ^{13}C, 39.6 ppm). Data were processed using in-house developed software.

Smith degradation

For Smith degradation (Smith and Montgommery, 1956), polysaccharide samples were suspended in 15 mM sodium periodate at a concentration of approximately 2 mg per ml. The mixture was placed in the dark at 4 °C under continuous mixing. After 48 h, the reaction was stopped by adding ethylene glycol to a final concentration of 350 mM. Oxidized polysaccharides were reduced with an excess of $NaBH_4$ during 24 h. Then, excess borohydride was removed by the addition of acetic acid. The product was washed three times with water and hydrolyzed in 100 mM hydrochloric acid at RT during 8 h.

References

Cardemil, L. & Pincheira, G. (1979) Characterization of the carbohydrate component of fraction I in the *Neurospora crassa* cell wall. *J. Bacteriol.* **137,** 1067-1072.

Chuang, J.-Y. (1990) Size exclusion chromatography of starch with dimethyl sulfoxide as the mobile phase: ionic-strength effect. *J. Appl. Polym. Sci.* **45,** 227-242.

Ensley, H.E.; Tobias, B.; Pretus, H.A.; McNamee, R.B.; Jones, E.L.; Browder, I.W. & Williams, D.L. (1994) NMR spectral analysis of a water-insoluble (1→3)-β-D-glucan isolated from *Saccharomyces cerevisiae*. *Carbohydr. Res.* **258,** 307-311.

Feldmesser, M.; Kress, Y.; Mednick, A. & Casadevall, A. (2000) The effect of the echinocandin analogue caspofungin on cell wall glucan synthesis by *Cryptococcus neoformans*. *J. Infect. Dis.* **182,** 1791-1795.

Georgopapadakou, N.H. (2001) Update on antifungals targeted to the cell wall: focus on β-1,3-glucan synthase inhibitors. *Exp. Opin. Invest. Drugs* **10,** 269-280.

Georgopapadakou, N.H. & Tkacz, J.S. (1995) The fungal cell wall as a drug target. *Trends Microbiol.* **3,** 98-104.

Hakomori, S.-I. (1964) A rapid permethylation of glycolipid, and polysaccharide catalyzed by methylsulfinyl carbanion in dimethyl sulfoxide. *J. Biochem.* **55,** 205-208.

Hård, K; Van Zadelhoff, G.; Moonen, P.; Kamerling, J.P. & Vliegenthart, J.F.G. (1992) The Asn-linked carbohydrate chains of human Tamm-Horsfall glycoprotein of one male. Novel sulfated and novel *N*-acetylgalactosamine-containing *N*-linked carbohydrate chains. *Eur. J. Biochem.* **209,** 895-915.

Hochstenbach, F.; Klis, F.M.; Van Den Ende, H.; Van Donselaar, E. Peters, P.J. & Klausner, R.D. (1998) Identification of a putative α-glucan synthase essential for cell wall construction and morphogenesis in fission yeast. *Proc. Natl. Acad. Sci. U S A* **95,** 9161-9166.

Hull, C.M. & Heitman, J. (2002) Genetics of *Cryptococcus neoformans*. *Annu. Rev. Genet.* **36,** 557-615.

Ishiguro, J.; Shimada, S.; Gabriel, M. & Kopecká, M. (2001) Characterization of a fission yeast mutant which displays defects in cell wall integrity and cytokinesis. *Genes Genet. Syst.* **76,** 257-269.

James, P.G. & Cherniak, R. (1990) 4-Methylmorpholine *N*-oxide-methyl sulfoxide soluble glucan of *Piptoporus betulinus*. *Carbohydr. Res.* **206,** 167-172.

James, P.G.; Cherniak, R.; Jones, R.G. & Stortz, C.A. (1990) Cell-wall glucans of *Cryptococcus neoformans* Cap67. *Carbohydr. Res.* **198,** 23-38.

Kamerling, J.P. & Vliegenthart, J.F.G. (1989) Mass spectrometry. In Lawson, A.M. (ed.), *Clinical Biochemistry - Principles, Methods, Applications.* Walter de Gruyter, Berlin, Vol. 1, pp. 176-263.

Katayama, S.; Hirata, D.; Arellano, M.; Pérez, P. & Toda T. (1999) Fission yeast α-glucan synthase *mok1* requires the actin cytoskeleton to localize the sites of growth and plays an essential role in cell morphogenesis downstream of protein kinase C function. *J. Cell Biol.* **144,** 1173-1186.

Kurtz, M.B. & Rex, J.H. (2001) Glucan synthase inhibitors as antifungal agents. *Adv. Protein. Chem.* **56,** 423-475.

Mata, J.; Lyne, R.; Burns, G. & Bähler, J. (2002) The transcriptional program of meiosis and sporulation in fission yeast. *Nature Genet.* **32,** 143-147.

Ohyama, T. *et al.* (2000) Arborcandins A, B, C, D, E and F, novel 1,3-β-glucan synthase inhibitors: production and biological activity. *J. Antibiot.* **53,** 1108-1116.

Onishi, J. *et al.* (2000) Discovery of novel antifungal (1→3)-β-D-glucan synthase inhibitors. *Antimicrob. Agents. Chemother.* **44,** 368-377.

De Pauw, B.E. (2000) New antifungal agents and preparations. *Int. J. Antimicrob. Agents* **16,** 147-150.

Radding, J.A.; Heidler, S.A. & Turner, W.W. (1998) Photoaffinity analog of the semisynthetic echinocandin LY303366: identification of echinocandin targets in *Candida albicans*. *Antimicrob. Agents. Chemother.* **42,** 1187-1194.

Renkema, G.H.; Boot, R.G.; Au, F.L.; Donker-Koopman, W.E.; Strijland, A.; Muijsers, A.O.; Hrebicek, M. & Aerts, J.M.F.G. (1998) Chitotriosidase, a chitinase, and the 39-kDa human cartilage glycoprotein, a chitin-binding lectin, are homologues of family 18 glycosyl hydrolases secreted by human macrophages. *Eur. J. Biochem.* **251,** 504-509.

Rösecke, J.; Pietsch, M. & König, W.A. (2000) Volatile constituents of wood-rotting Basidiomycetes.

Phytochemistry **54,** 747-750.

Sietsma, J.H.; Rast, D. & Wessels, J.G.H. (1977) The effect of carbon dioxide on fruiting and on the degradation of a cell wall glucan in *Schizophyllum commune*. *J. Gen. Microbiol.* **102,** 385-389.

Sietsma, J.H. & Wessels, J.G.H. (1977) Chemical analysis of the hyphal wall of *Schizophyllum commune*. *Biochim. Biophys. Acta* **496,** 225-239.

Shida, M.; Uchida, T. & Matsuda, K. (1978) A (1→3)-α-D-glucan isolated from the fruit bodies of *Lentinus edodes*. *Carbohydr. Res.* **60,** 117-127.

Smith, F. & Montgomery, R. (1956) End group analysis of polysaccharides. In Glick, D. (ed.), *Methods of biochemical analysis.* Interscience Publishers Inc., New York, Vol. 3, pp. 153-212.

Szaniszlo P.J., Kang M.S. & Cabib E. (1985) Stimulation of β-(1→3)-glucan synthetase of various fungi by nucleoside triphosphates: generalized regulatory mechanism for cell wall biosynthesis. *J. Bacteriol.* **161,** 1188-1194.

Van Wetter, M.A.; Wösten, H.A.B.; Sietsma, J.H. & Wessels, J.G.H. (2000) Hydrophobin gene expression affects hyphal wall composition in Schizophyllum commune. *Fungal. Genet. Biol.* **31,** 99-104.

Zhang, P.; Zhang, L. & Cheng, S. (1999) Chemical structure and molecular weights of α-(1→3)-D-glucan from *Lentinus edodes*. *Biosc. Biotechnol.Biochem.* **63,** 1197-1202.

Summary

In **Chapter 1**, an overview on fungal cell-wall architecture and polysaccharide biosynthesis is given. Fungal cell morphology and integrity depend on a cell-surrounding wall, which is composed of glycoproteins and polysaccharides. Disrupting enzymes that are involved in cell-wall biosynthesis may lead to inviable cells. The fungal cell wall is unique among eukaryotes and therefore it forms an ideal target for the development of novel antifungal drugs. For the development of polysaccharide-targeted fungicides, understanding of the chemical structure and biosynthesis of cell-wall polysaccharides is essential. The cell wall of most fungi consists of three major polysaccharides, namely chitin, (1→3)-β-glucan and α-glucan. Although the first two types have been studied extensively, little is known about the chemical structure and biosynthesis of α-glucan. In this thesis, the chemical structure of α-glucans from a number of fungal species are elucidated. The data are used to obtain insight into the mechanisms of α-glucan biosynthesis.

In **Chapter 2**, the chemical structure of α-glucan from the cell walls of fission yeast *Schizosaccharomyces pombe* is described. A mild procedure was used for the isolation of cell-wall α-glucan using enzymatic degradation of cell-wall glycoproteins and (1→3)-β-glucan. The integrity of the cell-wall before and after enzyme treatment was investigated using transmission electron microscopy (TEM). By using a combination of chemical analyses techniques, ^{1}H-NMR spectroscopy, and high-performance size-exclusion chromatography (HPSEC), the α-glucan was found to consist of a single population of linear glucose polymers, approximately 260 residues in length. It was shown that the α-glucan was not covalently linked to other cell-wall constituents, such as chitin or (1→3)-β-glucan. Furthermore, the α-glucan was found to be composed of two covalently-linked building blocks, each comprising a (1→3)-α-glucan segment of approximately 135 glucose residues with at its reducing end a small number of (1→4)-linked α-glucose residues. In contrast, α-glucan of an α-glucan synthase mutant with aberrant cell morphology consisted of a single building block, only. A model for the biosynthesis of fission-yeast α-glucan was proposed in which a single enzyme is involved in the synthesis and coupling of two α-glucan building blocks, displaying a two-step biosynthetic mechanism.

In **Chapter 3**, the chemical structure of the (1→4)-linked moiety in fission-yeast α-glucan was investigated by digesting α-glucan with a purified (1→3)-α-glucanase. The digestion products were fractionated by low-pressure size-exclusion chromatography (Bio-Gel P4) followed by high-performance anion-exchange chromatography (HPAEC). The fractions were then analyzed by nano-electrospray mass spectrometry (nanoES-MS). Prior to nanoES-MS analysis, samples were derivatized with a fluorescent label and oxidized using sodium periodate. This procedure enabled the complete sequencing of the digestion products, showing that two classes of polysaccharides were present, namely one class comprising heterooligosaccharides consisting of a number of consecutive (1→4)-linked α-glucose residues linked to a number of (1→3)-linked α-glucose residues, and a second class consisting of consecutive (1→4)-linked α-glucose, only. It was proposed that the first class originates from the center part of fission-yeast α-glucan, whereas the second class forms the reducing end. In the **Supplementary data**, the isolation and catalytic mechanism of the (1→3)-α-glucanase is described. It was shown that the enzyme possesses *endo*-catalytic activity and is able to perform repetitive attack after initial random attack.

In **Chapter 4**, the elucidation of the chemical structure of α-glucan from fission-yeast spore walls is described. It was found that the chemical structure of spore-wall α-glucan differed fundamentally from cell-wall α-glucan in that it was not composed of two covalently linked building blocks (dimeric structure), but instead consisted of a single polymer (monomeric structure) of (1→3)-linked α-glucose residues, indicating a different, one-step biosynthetic mechanism.

In **Chapter 5**, the chemical structures of α-glucans from seven Ascomycetes and Basidiomycetes were investigated in to determine whether the two mechanisms for α-glucan biosynthesis are conserved in evolution. It was shown that the α-glucans from the cell walls of the Basidiomycetes *Lentinus edodes* and *Cryptococcus neoformans* Cap67, similar to α-glucan from fission-yeast cell walls, occur as dimeric structures, whereas the

α-glucans from the Ascomycete *Neurospora crassa* and the Basidiomycetes *Pleurotus ostreatus*, *Piptoporus betulinus*, and *Schizophyllum commune* occur as monomeric structures. Interestingly, the fruiting bodies of *Laetiporus sulphureus* contain both structures of α-glucan. It was concluded that for the biosynthesis of fungal α-glucan, both one-step and two-step biosynthetic mechanisms are conserved in evolution.

Samenvatting

Inleiding

Schimmels komen in de natuur in een enorme verscheidenheid voor: naar schatting 1,5 miljoen soorten, waarvan tot nu toe slechts ongeveer 70.000 zijn beschreven. Onder schimmels worden zowel ééncelligen (gisten), filamenteuzen als vruchtlichaam-dragenden (paddestoelen) verstaan. Veel schimmels hebben een essentiële functie voor de biodiversiteit doordat zij in symbiose leven met planten of doordat zij het primaire organisme vormen voor de afbraak van plantaardig en dierlijk materiaal. Een aantal schimmels is van belang voor de (voedsel-)industrie, zoals *Saccharomyces cerevisiae*, een gist die gebruikt wordt voor bakkerijproducten en voor de brouwerij, de vruchtlichamen van *Agaricus bisporus* (champignon), *Lentinus edodes* (Shii-take) en *Pleurotus ostreatus* (oesterzwam), en de schimmeldraden van *Fusarium venenatum* die zeer eiwitrijk zijn en daardoor een ideale vleesvervanger vormen (Quorn). Andere schimmels kunnen echter desastreuze gevolgen hebben voor het welzijn van planten en dieren. *Ophiostoma ulmi* bijvoorbeeld, veroorzaakt de iepziekte die, indien remedies uitblijven, tot een volledige uitroeiing van alle iepen in het noordelijke halfrond kan leiden. De vernietigende kracht van pathogene schimmels is reeds bekend van de schimmel *Cryphonectria parasitica* die met name de Amerikaanse kastanje infecteert. Deze schimmel is voor het eerst rond 1900 in Noord-Amerika opgedoken en heeft in 40 jaar tijd 3,5 miljard bomen geïnfecteerd waardoor praktisch de volledige populatie Amerikaanse kastanje is vernietigd. Een aantal schimmels kan infecties bij mensen veroorzaken, dit zijn de humaan pathogene schimmels. In het algemeen treden schimmelinfecties op bij patiënten met een verlaagde of onderdrukte weerstand, zoals patiënten die lijden aan het humane immuno-deficiëntie virus (HIV) of patiënten die chemotherapie of orgaantransplantatie ondergaan. Tot de bekendste humaan pathogene schimmels behoren *Candida albicans*, *Cryptococcus neoformans* en *Aspergillus fumigatus*. Voornamelijk de twee laatstgenoemden zijn gevreesd als ‘ziekenhuisschimmel’ en kunnen zware infecties veroorzaken zoals hersenvliesontsteking, niet zelden met de dood tot gevolg. De traditionele bestrijding van schimmelinfecties bij mensen is voornamelijk gebaseerd op het verstoren van de functie van de plasmamembraan die de gehele schimmel-cel omgeeft. De plasmamembraan is opgebouwd uit vetzuren, waarvan net als bij dierlijke cellen, sterolen een belangrijke bouwsteen vormen. Door ofwel aan de sterolen te binden (*polyenen*) ofwel de biosynthese van sterolen te verstoren (*azolen*), wordt de levensvatbaarheid van de schimmel belemmerd. Het gebruik van *polyenen* is echter niet zonder risico voor de patiënt doordat zij niet enkel binden aan fungaal sterol, maar ook aan humaan cholesterol. De *azolen* zijn weliswaar specifiek gericht op de biosynthese van fungaal sterol, maar ze kunnen slechts de groei van de schimmel stoppen, zonder dat de schimmel geheel uitgeroeid wordt. Het gevolg hiervan is dat de patiënt levenslange medicatie moet ondergaan. Een bijkomend nadeel van *polyenen* en *azolen* is de opkomende resistentie van schimmels tegen deze stoffen.

De meest recente ontwikkelingen op het gebied van de fungiciden richt zich op de biosynthese van de fungale celwand. Schimmels bezitten naast een plasmamembraan nog een celwand die de plasmamembraan omsluit (zie **Fig. 1** op p. 11 voor een schematische weergave). Deze celwand bestaat uit geglycosyleerde eiwitten en uit een vlechtwerk van polysachariden die samen zorgen voor de mechanische stabiliteit van de cel en bescherming bieden tegen invloeden uit de omgeving. Zodoende is de celwand essentieel voor de levensvatbaarheid van de schimmel. De compositie van de celwand is uniek voor schimmels en daardoor vormen de enzymen die betrokken zijn bij de celwand-biosynthese een ideaal doelwit voor de ontwikkeling van schimmel-specifieke fungiciden. Voor de ontwikkeling van fungiciden gericht op enzymen die betrokken zijn bij de assemblage van celwand polysachariden, is het begrijpen van de mechanismen die betrokken zijn bij de biosynthese van de polysachariden van uiterst belang.

Één van de polysachariden die een belangrijke celwand component is voor vele schimmels is α–glucan. Het α-glucan bestaat uit lange ketens van aan elkaar gekoppelde glucose-eenheden, afhankelijk van de schimmelsoort variërend van 60 tot meer dan 3500 glucose moleculen. Echter, weinig is bekend over de structuur en de biosynthese van fungaal α-glucan. Om het mechanisme van de biosynthese van α-glucan te kunnen begrijpen, is het van fundamenteel belang dat de chemische structuur van dit polysacharide bekend is. In dit proefschrift zijn de chemische structuren van α-glucanen geïsoleerd uit de celwanden van een aantal schimmelsoorten beschreven. De resultaten van het onderzoek zijn gebruikt om inzicht te krijgen in de processen die ten grondslag liggen aan de biosynthese van α-glucan.

Resultaten beschreven in dit proefschrift

Hoofdstuk 1 omvat een samenvatting van de literatuur die handelt over de architectuur van de fungale celwand en de structuur en biosynthese van celwand polysachariden. Het bestuderen van de literatuur leert ons bijvoorbeeld de samenhang tussen structuur en functie van enzymen die betrokken zijn bij celwand biosynthese. Zo blijkt dat veel van deze enzymen zogenaamde transmembraan eiwitten zijn, waarbij een katalytisch (polysacharide-synthetiserend) domein binnen de membraan zit terwijl een ander domein door de membraan is geweven en een soort porie-functie vervult waardoor de gesynthetiseerde polysacharide door de membraan zou kunnen worden gebracht. In het geval van enzymen die betrokken zijn bij de α-glucan synthese, bevindt zich bovendien een domein van het eiwit aan de buitenkant van de membraan (zie **Fig. 2** op p. 14).

Hoofdstuk 2 behandelt de chemische structuur van α-glucan geïsoleerd uit de celwanden van de splijtgist *Schizosaccharomyces pombe*. Deze gist (waarvan een tekening de kaft van dit proefschrift siert) is in het in dit proefschrift beschreven onderzoek als model organisme gebruikt. Analyse van de chemische structuur van het α-glucan wees uit dat het niet gekoppeld is aan andere celwand componenten, zoals geglycosyleerde eiwitten of andere polysachariden, maar een losstaande populatie vormt. Door het α-glucan chemisch te behandelen en het onbehandelde alsmede het behandelde α-glucan te analyseren, is gebleken dat het α-glucan feitelijk opgebouwd is uit twee identieke polysacharide-ketens, elk bestaande uit ongeveer 135 glucose eenheden. Het α-glucan van een splijtgist-stam waarbij een mutatie is aangebracht in het buitenste domein van het enzym verantwoordelijk voor α-glucan synthese, bleek uit slechts een enkele polysacharide-keten van ongeveer 135 glucose eenheden te bestaan. Deze resultaten geven aan dat één enkel enzym betrokken is bij zowel de synthese van de afzonderlijke α-glucan ketens als de koppeling van deze ketens en ze suggereren dat het buitenste domein deze koppelfunctie heeft.

Één van de conclusies die getrokken kon worden uit de resultaten beschreven in hoofdstuk 2, was de mogelijkheid dat een korte keten van glucose-eenheden (oligosacharide) als een soort initiator voor de biosynthese van α-glucan zou kunnen dienen. In **hoofdstuk 3** wordt de chemische structuur beschreven van dit oligosacharide. Dit is gedaan door α-glucan eerst enzymatisch af te breken om vervolgens de producten te zuiveren en te analyseren. Voor deze experimenten moest een enzym worden gezuiverd, waarvan de zuivering alsmede de karakterisering in het **supplement** behorende tot hoofdstuk 3 is beschreven.

Één van de karakteristieken van schimmels is de mogelijkheid tot het vormen van sporen op het moment dat de voedingsbron dreigt te verdwijnen. De sporen hebben als eigenschap dat ze zijn opgewassen tegen invloeden uit de omgeving en ze kunnen zowel mechanische als chemische stress doorstaan. Zodra de sporen een nieuwe voedingsbron vinden, vormen ze weer normale, vegetatief groeiende schimmelcellen. Net als schimmelcellen, zijn ook sporen omgeven door een wand, de sporenwand. Uit onderzoek uitgevoerd op bakkersgist *S. cerevisiae* is gebleken dat de sporenwand qua samenstelling weliswaar lijkt op die van de celwand, maar er zijn ook duidelijke verschillen geconstateerd. In **hoofdstuk 4** is gekeken naar de samenstelling van de sporenwand van splijtgist. De interesse ging hierbij in het bijzonder uit naar de aanwezigheid van α-glucan, daar deze component nog niet eerder in gistsporen is aangetoond. Het is gebleken dat de sporenwanden inderdaad grote hoeveelheden α-glucan bezitten. Analyse van de chemische structuur leerde dat het α-glucan, anders dan in celwanden, niet is opgebouwd uit twee aan elkaar gekoppelde polysacharide ketens, maar bestaat uit één enkele keten. Deze resultaten gaven aan dat de biosynthese van α-glucan tijdens sporulatie verschilt van die tijdens vegetatieve groei.

Om een idee te krijgen of de twee mechanismen voor de biosynthese van α-glucan geconserveerd zijn in evolutie, is een aantal schimmels geselecteerd dat onderdeel uitmaakt van twee verschillende taxonomische groepen, namelijk de Ascomyceten en de Basidiomyceten (**hoofdstuk 5**). Uit deze schimmels zijn α-glucanen geïsoleerd waarvan sommigen, zoals die van de humaan pathogene gist *C. neoformans*, bleken te bestaan uit twee aan elkaar gekoppelde polysacharide ketens, vergelijkbaar met het α-glucan uit celwanden van splijtgist. Andere schimmels hadden juist een α-glucan dat opgebouwd was uit een enkele polysacharide keten en dus een structuur had vergelijkbaar met die uit sporenwanden van splijtgist. Uit het onderzoek bleek verder dat geen correlatie bestond tussen de gevonden opbouw van het α-glucan en de taxonomische groep waartoe de desbetreffende schimmel behoorde, hetgeen aangeeft dat beide mechanismen voor de biosynthese van fungaal α-glucan geconserveerd zijn in evolutie.

De resultaten beschreven in dit proefschrift geven fundamentele antwoorden op de vraag hoe fungaal α-glucan wordt gesynthetiseerd. Het verstoren van α-glucaan synthese heeft desastreuze gevolgen voor de levensvatbaarheid van de schimmel en zodoende vormt het een ideaal doelwit voor de ontwikkeling van nieuwe fungiciden.

Dankwoord

Bij deze wil ik iedereen bedanken die aan de totstandkoming van dit proefschrift heeft bijgedragen.

Op het moment dat ik deze woorden schrijf, realiseer ik mij dat ik twee personen met deze wel erg summiere dankbetuiging ernstig tekort doe. Frans Hochstenbach en Frans Klis, in willekeurige volgorde, jullie waren er altijd als ik de nieuwste resultaten wilde bediscussiëren. Uit het verre Amsterdam, nee, niet zozeer qua afstand, maar meer uit het oogpunt van wetenschappelijke achtergrond, wisten jullie beiden de koolhydraatchemie die ik jullie presenteerde met een verassend gemak te digesteren. Frans K., door jou heb ik mogen kennismaken met de wereld van de mycologie en ik vond het meer dan logisch dat jij niet alleen de coördinatie over het gehele project had, maar dat je ook mijn co-promotor werd. Je hebt op een adequate wijze voor gezorgd dat in de verschillende hoofdstukken die dit proefschrift vormen niet alleen de chemie klopte, maar dat elk hoofdstuk ook nog 'biologisch verantwoord' werd.

Frans H., ik heb jou leren kennen als een gedreven wetenschapper met een wel bijzonder aanstekelijk enthousiasme voor het onderzoek. Het doorlopen van het promotietraject is er één van vallen en opstaan. Belangrijk hierbij is dat het weer opstaan vergemakkelijkt wordt en jij was degene die in een periode van vier jaar steeds de helpende hand toestak door juist als het wat minder ging mij de nodige schouderklopjes te geven. Jij hebt hiermee laten zien dat je naast een excellente wetenschapper tevens een goede leidinggevende bent. De vele zondagen die we bij elkaar kwamen in het AMC zal ik niet snel vergeten. De discussies die we met regelmaat hebben gevoerd, hebben mij tot nadenken gebracht en hebben daardoor een enorme impact gehad op mijn wetenschappelijke ontwikkeling. Ik wens jou alle succes met de voortzetting van het α-glucan project.

Curriculum vitae

De auteur van dit proefschrift werd geboren op 18 juni 1973 te Schweinfurt, Duitsland. Na het behalen van het HAVO-diploma in 1991 aan het Christelijk Lyceum te Zeist, werd in 1993 het VWO-diploma behaald aan dezelfde instelling. In september 1993 begon hij aan de studie Scheikunde aan de Universiteit Utrecht. Tijdens deze studie werd een bijvak Beleid en Management aan het Centrum voor Beleid en Management en een hoofdvak Massaspectrometrie (Dr. J.E. Thomas-Oates, Prof. Dr. J. Haverkamp) gevolgd, waarbij een deel van het onderzoek in het Unilever Research Laboratorium, Vlaardingen (Dr. P.J.W. Schuyl, Prof. Dr. J. Haverkamp) werd verricht. Naast zijn studie was hij actief als vrijwilliger bij de Chemiewinkel Utrecht. Na het behalen van zijn doctoraal examen in juli 1998, was hij van augustus 1998 tot november 2002 als Onderzoeker in Opleiding verbonden aan de sectie Bio-Organische Chemie van het Bijvoet Centrum (Prof. Dr. J.P. Kamerling en Prof. Dr. J.F.G. Vliegenthart), waar het in dit proefschrift beschreven onderzoek werd verricht. Tijdens deze onderzoeksperiode nam hij deel aan de ‘FEBS - Advanced Course on Glycoconjugates’ in Lille, Frankrijk (1998) en de ‘6th European Training Course on Carbohydrates’ in Debrecen, Hongarije (2000). Onderdelen van de in dit proefschrift beschreven resultaten werden gepresenteerd tijdens onder meer het ‘20th International Carbohydrate Symposium’ in Hamburg, Duitsland (2000) en het ‘XVI International Symposium on Glycoconjugates’ in Den Haag (2001).